

**Degradation of skin elastin in ageing and disease:  
An *ex vivo* quantitative proteomic approach**

Dissertation

zur Erlangung des  
Doktorgrades der Naturwissenschaften (Dr. rer. nat.)

der  
Naturwissenschaftlichen Fakultät I – Biowissenschaften –

der Martin-Luther-Universität  
Halle-Wittenberg,

vorgelegt

von Frau Angela Cristina Mora Huertas  
geb. am 04. März 1980 in Guateque, Kolumbien

Gutachter:

1. Prof. Dr. Dr. Reinhard. Neubert
2. Prof. Dr. Dierk Scheel
3. Assoc. Prof. Dr. Laurent Duca

Halle (Saale), 26.09.2017

*To my family*

# Acknowledgments

Thank God for blessing each moment in my life and most of all for allowing me to achieve this goal.

First of all, I would like to show my deepest gratitude to Dr. Andrea Heinz. Her timely guidance, constructive criticism and scientific approach have helped me in a great extent to finish this work. Thanking you is not enough, but it is the best way to pay tribute to a person whose endless support, kind and understanding spirit played a key role throughout this process.

I am also very grateful to Dr. Christian Schmelzer for accepting me as a member of his research group and introducing me to the fascinating topic of the elastin and the mass spectrometry. It has been delightful to broaden my knowledge around your kindness, expertise and help.

Special thanks to Prof. Dr. Reinhard Neubert for the opportunity of doing my doctoral project in the AG Biopharmazie and for his permanent assistance with the administrative issues.

On the part of Leibniz Institute for Plant Biochemistry of Halle; I would like to thank Dr. Wolfgang Hoehenwarter for providing the 'Progenesis Q.I' software as well as Miss Petra Majovsky for her measurements with the Orbitrap Q Exactive Mass Spectrometer. I would like to acknowledge the Martin Luther University Halle-Wittenberg team, specially Dr. Frank Heyroth for his thoughtful help with scanning electron microscopy on the Interdisciplinary Center for Materials Science and Prof. Dr. Johannes Wohlrab from the Department of Dermatology and Venereology for the supplying the skin biopsies samples.

My thanks and appreciations also to my colleagues Jing, Christoph and Tobias, who have willingly helped me out in innumerable ways; to Angelica Avila for her hard work and enthusiasm during our lab time; and to Frau Manuela Woigk for her assistance in daily lab work.

## Acknowledgments

Thanks to the Universidad Nacional de Colombia in Bogota for giving me the opportunity to foster my academic development and to the Department of Pharmacy's professors for your kind support.

I would like to express my deepest gratitude to my mentors, Prof. Noralba Sierra, Roberto Pinzon and Luis F. Ospina for their wisdom, knowledge, trust and care.

Thanks to Colombian Institutions: Departamento Administrativo de Ciencia, Tecnología e Innovación (Colciencias) and Fundación para el Futuro de Colombia (Colfuturo) for the funding sources and its management.

On my family's side, my deepest gratitude to my parents, Elisenia and Rafael; your teaching, love, and encouragement made it possible. To my siblings Neyla, Claudia, Ricardo and particularly to Rafael and his family, Luisa, Catalina and Sergio, for all the love and support received. Also to Karen and Tulia for your kind encouragement, as well as my uncles, aunts and cousins.

My special thanks to Martin for his patience and support during this writing time, and for encouraging me to strive towards my goal. Thanks for all the special moments that we have shared.

My extended hug and warm thanks to my friends here in Germany, specially to Alejandra, Hina, Marisol, Yenny, Efrem, Elkin, Julio, Mauricio and Walter for their support, care, advice and for making my stay in Germany homey and comfortable. Special thanks to my friends in Colombia, particularly to Carolina, Martha, Sandra and Yoshie; your encouragement, enthusiasm and friendship made this journey easier.

Finally, I want to express my deepest gratitude to my Uncle Tito for showing me that it is possible to achieve this dream and for lightening my way when the dark times arrived.

# Table of Contents

Acknowledgments.....	I
Table of Contents.....	III
List of Acronyms .....	VII
List of Figures.....	IX
List of Tables .....	XII
Abstract .....	XIII
1 Theoretical Background.....	1
1.1 Human skin and extracellular matrix.....	1
1.2 Elastic fibres .....	3
1.2.1 Structure of elastic fibres.....	3
1.2.2 Elastogenesis .....	4
1.2.3 Tropoelastin and elastin structure .....	6
1.2.4 Structural role of some tropoelastin domains .....	10
1.2.5 Degradation of elastic fibres.....	11
1.2.6 Bioactive peptides.....	12
1.2.7 Elastic fibres in aging and skin diseases.....	15
1.3 Mass spectrometry in proteomics.....	17
1.3.1 Instrumentation.....	17
1.3.2 Identification approaches.....	21
1.3.3 Quantification approaches .....	22
2 Aim .....	26
3 Material and Methods .....	27
3.1 Materials .....	27
3.1.1 Chemicals.....	27
3.1.2 Protein and enzymes .....	28
3.1.3 Buffer and reagent composition .....	28
3.1.4 Skin samples.....	29
3.2 Instruments .....	29
3.3 Biochemical Methods.....	30
3.3.1 Isolation of elastin from human samples.....	30

3.3.2	Proteolysis of tropoelastin and human elastin.....	31
3.4	Analytical methods.....	31
3.4.1	NanoHPLC-nanoESI-QqTOF mass spectrometry.....	31
3.4.2	NanoHPLC-nanoESI-Orbitrap mass spectrometry.....	32
3.4.3	NanoHPLC/nanoMALDI-TOF/TOF mass spectrometry.....	33
3.4.4	MALDI-TOF mass spectrometry.....	34
3.4.5	Scanning electron microscopy (SEM).....	34
3.4.6	Ultraviolet spectrophotometric analysis.....	34
3.5	Bioinformatics methods.....	35
3.5.1	Peptide sequencing.....	35
3.5.2	Label-free quantification of peptide digests.....	35
3.5.3	Statistical analysis.....	36
4	Results.....	38
4.1	Workflow suitability to distinguish changes in abundance of elastin hydrophobic peptides.....	38
4.2	Susceptibility of human skin elastin towards degradation by biologically relevant proteases.....	42
4.2.1	Elastase activity of NEP and its relation with previous elastic damage.....	42
4.2.2	Degradation of TE and skin elastin samples by CG and MMP-9.....	47
4.2.3	Enzymatic susceptibility of the elastin domains analysed through their degradation by CG and MMP-9.....	53
4.2.4	Age-related differences in the elastin susceptibility towards enzymatic degradation.....	58
4.2.5	Characterisation of matrikines released from elastin fibres towards enzymatic degradation.....	63
4.3	Structural changes of human elastin during skin ageing.....	65
4.3.1	Elastic fibres morphology and its susceptibility towards enzymatic degradation.....	65
4.3.2	Characterisation of elastin peptides released from elastin obtained from differential aged individuals.....	66
4.3.3	Release of potentially bioactive peptides from elastin during skin ageing.....	70
4.3.4	Classification of samples according to the sources of elastin degradation.....	71
4.4	Molecular changes of human skin elastin from Williams-Beuren Syndrome patients and healthy individuals.....	74
4.4.1	Elastin content of skin and elastic fibres morphology.....	74
4.4.2	Elastin susceptibility towards enzymatic cleavage.....	75

4.4.3	Differences between elastin peptides released from elastin isolated from skin of WBS patients and healthy individuals.....	77
4.4.4	Release of potentially bioactive peptides from elastin isolated from WBS patients and healthy donors.....	78
4.4.5	Classification of samples according to the elastin changes in WBS patients and healthy individuals .....	79
5	Discussion.....	82
5.1	Workflow suitability to distinguish changes in abundance of elastin hydrophobic peptides.....	82
5.2	Susceptibility of human skin elastin towards degradation by biologically relevant proteases .....	84
5.2.1	Elastase activity of NEP and its relation with previous elastic fibres damage .....	85
5.2.2	Degradation of TE and skin elastin samples by CG and MMP-9 .....	87
5.2.3	Enzymatic susceptibility of the elastin domains analysed through their degradation by CG and MMP-9 .....	89
5.2.4	Age-related differences in the elastin susceptibility towards enzymatic degradation.....	92
5.2.5	Peptides with bioactive sequences released from different types of skin elastin samples	95
5.3	Structural changes of human elastin during skin ageing.....	97
5.3.1	Elastic fibres morphology and its susceptibility towards enzymatic degradation.....	97
5.3.2	Characterisation of elastin peptides released from elastin obtained from differentiated aged individuals.....	98
5.3.3	Release of potentially bioactive peptides from elastin during skin ageing.....	100
5.3.4	Classification of samples according to the sources of elastin degradation.....	101
5.4	Molecular changes of human skin elastin from patients with Williams-Beuren Syndrome and healthy individuals .....	103
5.4.1	Elastin content of skin and elastic fibre morphology.....	103
5.4.2	Elastin susceptibility towards enzymatic cleavage.....	103
5.4.3	Differences between elastin peptides released from elastin isolated from skin of WBS patients and healthy individuals .....	104
5.4.4	Release of potentially bioactive peptides from elastin isolated from WBS patients and healthy donors.....	105
5.4.5	Classification of samples according to the elastin changes in WBS patients and healthy individuals .....	106
6	Conclusions .....	108
	Appendix.....	XVII

## Table of Contents

Appendix 1. Workflow suitability to distinguish changes in abundance of elastin hydrophobic peptides.....	XVII
Appendix 2. Susceptibility of human skin elastin towards degradation by biologically relevant proteases .....	XVIII
Appendix 3. Structural changes of human elastin during skin ageing.....	XXVII
Appendix 4. Molecular changes of human skin elastin from patients with Williams-Beuren Syndrome and healthy individuals .....	XXXII
Bibliography .....	XVII
Curriculum vitae .....	XXXVI
List of publications.....	XXXVII
Declaration.....	XXXIX



# List of Acronyms

a.u.	<i>Arbitrary units</i>
ACN	<i>Acetonitrile</i>
ACP	<i>Allysine aldol condensation product</i>
ADCL	<i>Autosomal dominant cutis laxa</i>
APMA	<i>p-aminophenylmercuric acetate</i>
AUC	<i>Area under the curve</i>
CE	<i>Children skin elastin</i>
CG	<i>Cathepsin G</i>
CHCA	<i>alpha-cyano-4-hydroxycinnamic acid</i>
CHO	<i>Chinese hamster ovary cells</i>
CID	<i>Collision-induced dissociation</i>
CV	<i>Coefficient of variation</i>
DDA	<i>Data-dependent acquisition</i>
ddH <sub>2</sub> O	<i>Double distilled water</i>
DEJ	<i>Dermal-epidermal junction</i>
dLNL	<i>Dehydrolysinonorleucine</i>
DMSO	<i>Dimethyl sulfoxide</i>
EBP	<i>67-kDa Elastin-binding protein</i>
ECM	<i>Extracellular matrix</i>
EDPs	<i>Elastin-derived peptides</i>
ESI	<i>Electrospray ionization</i>
FA	<i>Formic acid</i>
FC	<i>Fold change</i>
FDR	<i>False discovery rate</i>
HCA	<i>Hierarchical cluster analysis</i>
HPCA	<i>Hierarchical principal component analysis</i>
HPLC	<i>High performance liquid chromatography</i>
HUVEC	<i>Human umbilical vein endothelial cells</i>
IT	<i>Ion trap</i>
LFQ	<i>Label-free quantification</i>

LID *Laser-induced dissociation*  
LOX *Lysine-6-oxidase*  
MALDI *Matrix-assisted laser desorption/ionization*  
MMP *Matrix metalloproteinase*  
MS *Mass spectrometry*  
NEP *Neprilysin*  
OE *Old adult elastin*  
PC *Principal component*  
PCA *Principal component analysis*  
PE *Pancreatic elastase*  
PMNL *Polymorphonuclear leukocytes*  
Q *Quadrupole*  
SA *Sinapic acid*  
SEM *Scanning electron microscopy*  
SFE *Skin fibroblast-derived elastase*  
SVAS *Supravalvular aortic stenosis*  
TE *Tropoelastin*  
TFA *2,2,2-trifluoroacetic acid*  
TOF *Time-of-flight*  
Tris *2-Amino-2-hydroxymethyl-propane-1,3-diol*  
UV *Ultraviolet*  
w.a.m. *Weighted arithmetic mean*  
WBS *Williams-Beuren Syndrome*

# List of Figures

Figure 1. Skin and its cellular and extracellular matrix components.....	1
Figure 2 Elastin fibres.....	4
Figure 3. Elastic fibre assembly. ....	5
Figure 4. Schematic diagram of the domain structure of human tropoelastin.....	7
Figure 5. Model of the nanostructure of full-length and assembly of Tropoelastin. ....	10
Figure 6. Phenotype of intrinsic ageing versus photoaging.....	15
Figure 7. Principal components of a mass spectrometer.....	18
Figure 8. Label-free quantification (LFQ) methods.....	24
Figure 9. Normalised abundance of selected elastin peptides depending on the elastin concentration.....	40
Figure 10. PCA scores plot of samples with different elastin concentration .....	41
Figure 11. Variable graph of peptides quantified in samples with different elastin concentration.....	41
Figure 12. MALDI-TOF mass spectra of TE and skin elastin samples degraded by NEP..	43
Figure 13. Cleavage sites identified after digestion of TE and skin elastin samples with NEP.....	44
Figure 14. Normalised number of cleavage sites identified in samples of TE and skin elastin digested with NEP. ....	45
Figure 15. MALDI-TOF mass spectra of TE and skin elastin samples degraded by CG and MMP-9.....	47
Figure 16. Cleavage sites identified after digestion of TE and skin elastin samples with CG (A) and MMP-9 (B). ....	49
Figure 17. Sequence coverage obtained from peptides quantified after 6 h, 12 h and 48 h in CG digests. ....	50
Figure 18. Changes in normalised abundance of selected TE peptides depending on sampling point.....	51
Figure 19. Sequence coverage obtained from peptides quantified after 6 h, 12 h and 48 h in MMP-9 digests. ....	52
Figure 20. Normalised number of cleavage sites identified in samples of skin elastin digested with CG and MMP-9, respectively.....	54

Figure 21. Sum of normalised abundance by domain of elastin peptides solubilised from skin elastin digested with CG. ....	55
Figure 22. Sum of normalised abundance by domain of elastin peptides solubilised from skin elastin digested with MMP-9. ....	56
Figure 23. Degradation of different domains of elastin by CG and MMP-9, determined through a linear model. ....	58
Figure 24. Profile of quantifiable peptides obtained after digestion of TE and skin elastin samples with CG and MMP-9. ....	60
Figure 25. Amount of elastin peptides solubilised after 48 h, and quantified using an UV spectrophotometric method. ....	61
Figure 26. Modelling of elastin peptides released from mature elastin from domain 28.62	
Figure 27. Scanning electron micrographs of human skin elastin obtained from differential aged healthy individuals .....	66
Figure 28. Elastin peptides identified from PE digests of skin elastin samples from differential aged individuals. ....	67
Figure 29. Changes in normalised abundances of selected elastin peptides depending on the age of the donor. ....	68
Figure 30. First cleavage points in skin elastin isolated from differential aged individuals. ....	70
Figure 31. PCA scores plot of skin elastin samples isolated from differential aged individuals. ....	71
Figure 32 Variables graph of 55 elastin peptides with age-related changes, based on PC1 and PC2. ....	72
Figure 33. Dendrogram of skin elastin samples isolated from differential aged individuals. ....	73
Figure 34. Morphological characterisation of skin elastin isolated from healthy donors and WBS patients. ....	75
Figure 35. Cleavage sites identified after PE digestion of skin elastin samples from WBS patients and healthy donors. ....	76
Figure 36. PCA scores plot of skin elastin samples isolated from WBS patients and healthy individuals. ....	79
Figure 37 Variable graph of 64 elastin peptides with significant differences between WBS patients and healthy individuals based on PC1 and PC2. ....	80

Figure 38. Dendrogram of skin samples isolated from WBS patients and healthy individuals.....	81
---	----

### **Figures in the appendix**

Figure A-1. Normalised abundance of peptides quantified after 6 h, 12 h and 48 h in TE samples digested with CG.....	XVIII
Figure A-2. Normalised abundance of peptides quantified after 6 h, 12 h and 48 h in CE samples digested with CG.....	XIX
Figure A-3. Normalised abundance of peptides quantified after 6 h, 12 h and 48 h in OE samples digested with CG.....	XX
Figure A-4. Normalised abundance of peptides quantified after 6 h, 12 h and 48 h in TE samples digested with MMP-9. ....	XXI
Figure A-5. Normalised abundance of peptides quantified after 6 h, 12 h and 48 h in CE samples digested with MMP-9. ....	XXII
Figure A-6. Normalised abundance of peptides quantified after 6 h, 12 h and 48 h in OE samples digested with MMP-9. ....	XXIII
Figure A-7. Degradation of different domains of skin elastin determined through a linear model according to each enzyme. ....	XXIV
Figure A-8. Sum of normalised amount of peptides obtained after digestion of TE and skin elastin samples with CG and MMP-9, according to biological replicate. ....	XXV
Figure A-9. Sum of normalised amount of peptides obtained after digestion of TE and skin elastin samples with CG and MMP-9, according to instrumental replicate.....	XXV
Figure A-10. Changes in normalised abundance of elastin peptides depending on the age of the donor (part A). ....	XXVIII
Figure A-11. Changes in normalised abundance of elastin peptides depending on the age of the donor (part B). ....	XXIX

# List of Tables

Table 1. <i>In vitro</i> biological activities reported for some EDPs.....	14
Table 2. Chemicals.....	28
Table 3. Protein and Enzymes .....	28
Table 4. Buffer and reagent composition.....	29
Table 5. Instruments .....	30
Table 6. Occurrence of different amino acids at the substrate positions P1-P4 and P1'-P4' after digestion of TE and skin elastin samples with NEP.....	46

## Table in the appendix

Table A-1. Elastin peptides normalised abundance among different elastin concentrations.....	XVII
Table A-2. Most abundant peptides containing bioactive sequences that were identified and quantified after digestion of human skin elastin by CG and MMP-9.....	XXVI
Table A-3 Skin samples from differential aged healthy individuals.....	XXVII
Table A-4. Elastin peptides that showed significant differences in their normalised abundances among different elastin samples.....	XXXI
Table A-5. Skin samples from WBS patients and healthy individuals analysed by nanoHPLC-nanoESI-QqTOF MS and LFQ.....	XXXII
Table A-6 Elastin peptides that show significant differences in their normalised abundances between skin elastin samples isolated from WBS patients and healthy individuals.....	XXXIV

# Abstract

The degradation of elastin, the most abundant protein in the elastic fibres, has a pivotal role in the loss of the integrity and functionality of the skin during the ageing and some diseases such as Williams-Beuren Syndrome (WBS). Previous studies of elastin degradation have reported, which elastases are involved in this process and how they degrade elastin. The aim of this study was to investigate the degradation of skin elastin at the molecular level by evaluating the enzymatic susceptibility and age-related changes of its hydrophobic domains, and the effect of the skin ageing and WBS on their morphology and susceptibility towards enzymatic degradation.

Elastin fibres were isolated from skin biopsies of differently aged healthy individuals and WBS patients. Their morphology was characterised by scanning electron microscopy. Mass spectrometric techniques were used to investigate the molecular-level structure of elastin. For the first time, label-free quantification (LFQ) and statistical analysis were applied to study quantitative changes in the peptides released during the elastin degradation.

The analysis of the cathepsin G (CG) and matrix metalloproteinase 9 (MMP-9) digests revealed that thirteen domains in the N- and C-terminal regions of tropoelastin (TE) are particularly susceptible to enzymatic degradation. The degree of degradation of each domain was the result of the interaction of the type of enzyme, the integrity of the elastin fibre and incubation time.

The age-related loss of integrity of the fibrillar elastin favoured the elastolytic activity of neprilysin (potential skin fibroblast-derived elastase), while it decreased the efficacy of MMP-9 degradation. Elastase capacity of CG is not influenced by these changes.

Insights in the ageing process of the elastin fibres were obtained through marker peptides which showed an age-related increase or decrease in their abundances. Domains 18, 20, 24 and 26 were strongly cleaved with increasing age. The susceptibility towards enzymatic cleavage of the N-terminal and central regions of the TE was increased by the extrinsic ageing. It also stimulates the strong decomposition of elastin fibres observed in sun-exposed skin samples.

Skin elastin fibres obtained from WBS patients differed from the ones obtained from healthy individuals in three features: firstly, their high susceptibility to enzymatic cleavage, secondly, their lower proline hydroxylation degree and thirdly, the diminished total amount in the tissue. Moreover, the accelerated damage of these elastin fibres resembled the effect of extrinsic skin ageing in old adult donors.



# 1 Theoretical Background

## 1.1 Human skin and extracellular matrix

The skin is the largest organ of the human body and covers 1.6 m<sup>2</sup> of surface area [10]. It helps to maintain four essential body functions such as sensation, retention of moisture and prevention of permeation or other molecules loss, regulation of body temperature and protection of the body from external factors [11]. Additionally, the skin is a dynamic structure which involves multi-directional stretch and compression, allowing for low friction gliding movement [12].

Morphologically, human skin is composed of three distinct layers: epidermis, dermis and hypodermis [11, 13] (Figure 1). The epidermis is avascular and mainly constituted by epidermal keratinocytes and their mature cells, the cornified cells [11]. The structure beneath the epidermis, the dermis, is vascularized and relatively acellular. These two layers are united through the dermal–epidermal junction (DEJ) [4]. The last skin layer is the hypodermis, which mainly consists of loose connective tissue and it is particularly rich in proteoglycans and glycosaminoglycans [12].

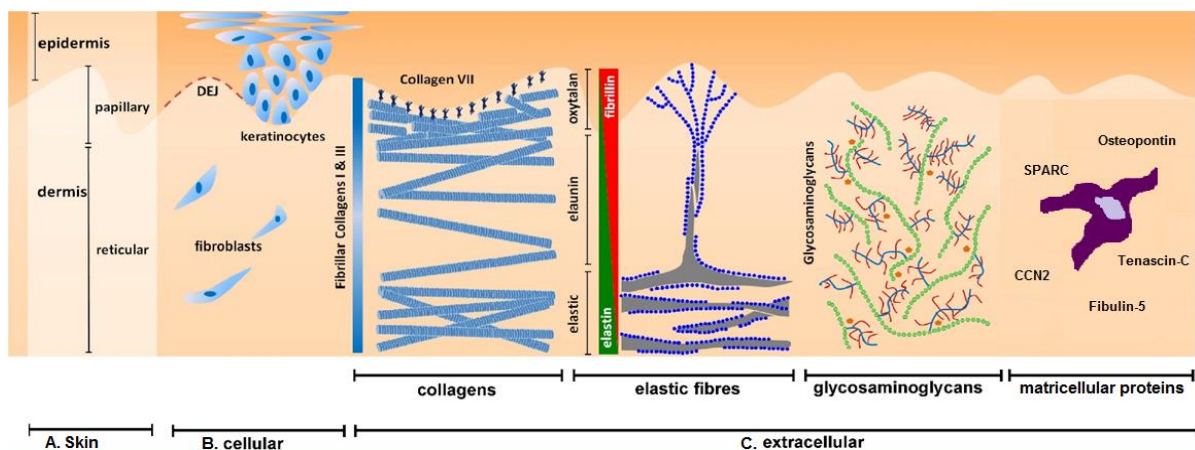


Figure 1. Skin and its cellular and extracellular matrix components.

(A). In mammalian skin, the dermis supports the epidermis. The dermis is structurally composed of the papillary and reticular layers. The deeper layer, hypodermis, is not shown in the figure. (B). Cellular components of the epidermis (keratinocytes) and dermis (fibroblasts). (C). ECM constituents. The fibre-forming structural components (collagens and elastic fibres); the non-fibre-forming molecules (proteoglycans and glycosaminoglycans); and different matricellular proteins. The figure was modified from Naylor *et al.* [4].

There are two regionally distinct areas in the dermis. The papillary layer has small diameter collagen fibres interspersed with thin elastic fibres [12], and they are richly supplied with capillaries, sensory nerve endings and cytoplasm [11]. The reticular layer, which is predominantly made up of collagen fibres, is less densely packed and organised into large interwoven fibre bundles of branching elastic fibres; these fibres, in turn, form a superstructure around the collagen fibres [12]. The majority of cells in the human dermis are fibroblasts that are thought to be responsible for synthesising the dermal extracellular matrix (ECM) proteins [4].

As in other tissues, ECM components of the skin maintain its structural integrity and participate actively in numerous aspects of cellular regulation [14]. ECM components could be sorted into three categories (Figure 1): (i) the fibre-forming structural components are made of collagens and elastic fibres. Collagens confer tensile strength to the tissue [15]. Collagens type I and III are widely distributed inside papillary and deep reticular dermis, while collagen type VII is restricted to the DEJ [4]. The elastic fibre system is fundamental in mediating tissue resilience and elasticity [15-17], and it forms a three-dimensional meshwork that spans from the papillary down to the deep dermis [18]. In the reticular dermis there are three different types of elastic fibres: oxytalan, elaunin and elastic fibres. Oxytalan fibres, which do not contain amorphous elastin, form a fine branch such as fibrillin-rich microfibrils. The elaunin fibres are arciform microfibrils with a poor elastin core. Finally, the elastic fibres are thick fibrillin-rich microfibrils with an elastin-rich core [12, 19, 20]. (ii) The non-fibre-forming molecules include proteoglycans and glycosaminoglycans, such as hyaluronic acid and chondroitin sulphate glycosaminoglycan. The function consists in hydrating the skin due to their capacity to create a charged, dynamic and osmotically active space [4, 15]. (iii) The matricellular proteins such as osteopontin, secreted protein acidic and rich in cysteine (also known as osteonectin), tenascin-C, fibulins, and the CCN family, do not have a structural function but interact in autocrine or paracrine cell-matrix signalling [15]. Tracy *et al.* reviewed the skin ECM components and their interactions [15].

## 1.2 Elastic fibres

### 1.2.1 Structure of elastic fibres

Elastic fibres are the major insoluble ECM structures that endow connective tissues subjected to repetitive distension and physical stress with resilience, permitting their low-strain mechanical response [17, 21]. These fibres are found in several tissues such as skin, lungs, alveoli, arteries, veins, the urinary tract, eye (both the cornea and suspensory ligament), fibrillar and articular cartilage, and specialised tendons such as the ligamentum nuchae [11, 13].

The assemblage of elastic fibres comprises various distinctive microfibrillar structural glycoproteins, while elastin forms an inner amorphous core of the compound elastic fibres, and one enzyme [19, 22]. Elastin-associated microfibrils include fibrillin 1-3 [20] and some associated molecules as the latent TGF- $\beta$  binding proteins (LTBPs), ADAMTS (a disintegrin and metalloproteinase with thrombospondin motifs), MAGPs (microfibril-associated glycoproteins), fibulin 2-5 and the lysyl oxidase enzyme (LOX) [17, 20, 23-26]. LOX is involved in the elastin cross-linking [27] while the elastin-associated microfibrils and fibrillin-microfibrils contribute to elastic fibre assembly and function [20], however, the last one does not play a major role in the elasticity activity [28]. For a review of microfibrillar structure, see [17, 29, 30].

Elastin is the most abundant protein in the elastic fibres; it constitutes approximately 90 % of the mature structure of them [31]. As it was mentioned previously, it provides extensibility/elastic recoil [32], and resilience [15-17] to the different tissues and it is, thus, critical for their long-term function [9, 33-35]. This protein has an entropy-based elasticity mechanism, in which the hydrophobic hydration and the release of hydration waters play the dominant role [36-39]. The dynamic nature of elastin's hydrophobic domains contributes in less extent to the elasticity [37, 40, 41].

The amount of elastin and general architecture of the mature elastic fibres have tissue-specific building arrangements that reflect different elastic requirements [14, 16, 42]. For instance, the skin contains between 2 % and 5 % of elastin, on the contrary, the aorta's composition is between 30 % and 57 % of the protein (percentages based on dry weight of the tissue) [16, 31]. Furthermore, dermal elasticity relies on integrated

networks of thick reticular elastic fibres whereas the arterial elastic fibres form concentric lamellar layers that support vascular elastic recoil [14, 20]. Although the histologic structure of elastic fibres differs among tissues, the fine detail of insoluble elastin is apparently similar regardless of location [14]. Macroscopically, elastin exhibits an amorphous appearance. At supramolecular level, the protein has a fibrillar substructure comprised of parallel-aligned  $\approx 5$  nm thick filaments, isolated or laterally aligned. They appear to be hierarchically organised as twisted-rope fibres and fibrils [18, 43, 44] (see Figure 2). For a review of the supramolecular organisation of elastin and other elastin-related compounds, see Pepe *et al.* [44].

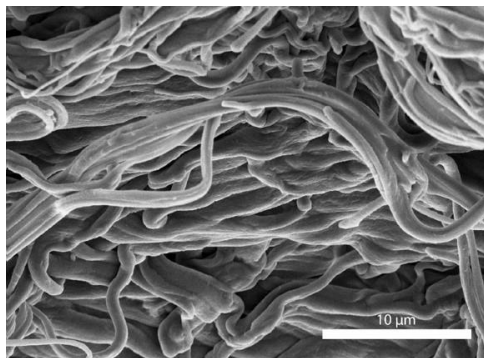


**Figure 2** Elastin fibres

The scanning electron micrographs of elastin fibres isolated from the human skin of a volunteer at the age of 6. Figure adopted from Schmelzer *et al.* [149].

### 1.2.2 Elastogenesis

In humans, the elastic fibres are formed around the time of mid-gestation and the maximum production is reached near birth and during the early neonatal period [14]. The elastin deposition is nearly complete in the first decade of life [45]. In mature organs and tissues, elastin synthesis is repressed by post-transcriptional factors [46]. The low turnover and lack of continued elastin production upon maturity reflect the extreme durability and long half-life of elastic fibres that reach the human lifespan of around 74 years [47]. However, tropoelastin (TE) expression may be reinitiated in response to wounding [47, 48] or exposure to ultraviolet (UV) radiation [49, 50]; elastin production is aberrant in these cases and does not lead to the formation of normal elastic fibres.

The *in vivo* formation of elastic fibres can be described in two independent steps: the formation of microfibrils and the arrangement of elastin core [51]. Figure 3 shows all the steps involved in the elastogenesis. A detailed description of elastogenesis can be found in Schmelzer *et al.* [3].

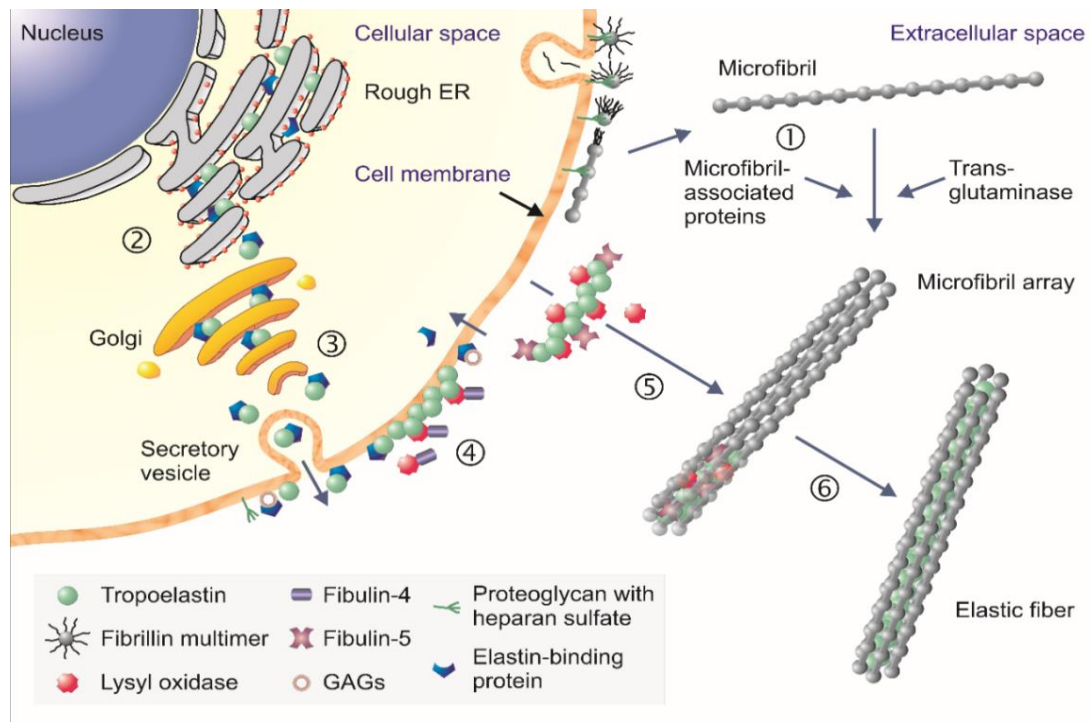


**Figure 3. Elastic fibre assembly.**

(1) Microfibrillar array in extracellular space. (2) Synthesis and binding of TE to the EBP in the rough endoplasmic reticulum (ER) (3) Transport of EBP-TE complex through the Golgi apparatus and secretion to the cell membrane. (4) The release of TE from EBP and formation of globules at the cell surface through its cross-linking mediated by lysyl oxidase or lysyl oxidase-like enzymes (5) Deposition of TE clusters onto the microfibrillar array. (6) Fusion of elastin aggregates into larger assemblies and further cross-linked to eventually form the elastic fibre. Figure and text adopted from Schmelzer [3].

During elastic fibre synthesis, the microfibrils, mainly consisting of fibrillin-1, appear before the amorphous core and are believed to act as a scaffold for the deposition of elastin [13, 24, 52]. The TE is encoded by a gene on chromosome 7q11.2 in humans. Depending on anatomical location, TE (70 kDa) is secreted by different elastogenic cells such as fibroblasts, smooth muscle cells, chondroblasts, mesothelial cell, endothelial cells, and auricular chondrocytes [3, 14, 20, 45]. After that, TE binds to a 67-kDa elastin-binding protein (EBP) to avoid its intracellular self-aggregation and degradation, and it is transported to the membrane where it is released into the extracellular space [53, 54].

Small cell surface-associated TE globules appear and increase in size with time (micro assembly) [52] through an inverse temperature transition termed coacervation. In it, the molecules are concentrated and aligned as result of multiple and specific interactions of individual hydrophobic domains of TE [55, 56]. Details of coacervation process are reviewed in Yeo *et al.* [56].

After the elastin globules reach a critical size, they are eventually transferred to pre-existing microfibrillar fibres in the ECM where they coalesce into larger structures (macro assembly) [52]. The TE molecules are covalently bound to each other through the cross-linking process [57-59]. It is initiated by the oxidative deamination of lysine side chains by the enzyme protein lysine-6-oxidase (LOX; EC 1.4.3.13) to obtain the  $\alpha$ -amino adipic  $\delta$ -semialdehyde (allysine) [60, 61]. Then, the allysine spontaneously condensates with another allysine to form allysine aldol condensation product (ACP). Another possible reaction is between allysine and the amine of an unmodified lysine side chain through a Schiff base reactions to form dehydrolysinonorleucine (dLNL). ACP and dLNL can then spontaneously condense with each other, or with other intermediates to form desmosine or its isomer, isodesmosine [58, 61, 62]. The increase in complexity of this inter- and intra-chain cross-links is thought to progress as the fibre matures and ages [63].

### 1.2.3 Tropoelastin and elastin structure

The human TE gene possesses 34 exons, but almost 30 % of them undergo alternate splicing [64] in a cassette-like fashion, in which an exon is either included or deleted, but rarely divided [65]. Splicing could be tissue-specific and developmentally regulated [51, 66]. It has been suggested that among tissues, the alternate splicing may influence the elastic fibre resilience, the fibre assembly [14, 64, 67] and the interaction of TE with other matrix molecules and cells [68]. As result of alternative splicing, TE can lose domains 22, 23, 24, 26A, 30, 32 and 33 [51, 69, 70]. However, in human skin elastin the absence of exon 26A was confirmed [71].

An additional intracellular post-translational modification that TE undergoes is the cleavage of the signal peptide in the endoplasmic reticulum [72], which apparently contributes to the correct folding of TE and its coacervation [73]; this process has to occurred before placement of the monomer at the ECM [72]. Another modification is the

hydroxylation (HyP) of some proline residues (about 1% HyP in elastin) in the endoplasmic reticulum [45, 74]. The role of hydroxylation is not completely understood [16, 75]. It seems to be related to different functions such as resistance to mechanical stresses of the organs and elastin assembly; it could also improve elastin's resistance towards proteolytic degradation [75].

Domain structure of the protein (see Figure 4) is a reflection of the exon organisation of the gene [61]. TE arrangement is made up of alternating hydrophobic regions and hydrophilic cross-link domains. Domains 1 and 36 are the signal sequence and the C-terminal domain respectively [76]. Although the amino acid compositions of all elastins have similar general characteristics, there is a variation in composition between tissues and between species [42, 69]; mammalian and avian elastins lack the amino acids histidine and methionine [61, 77].

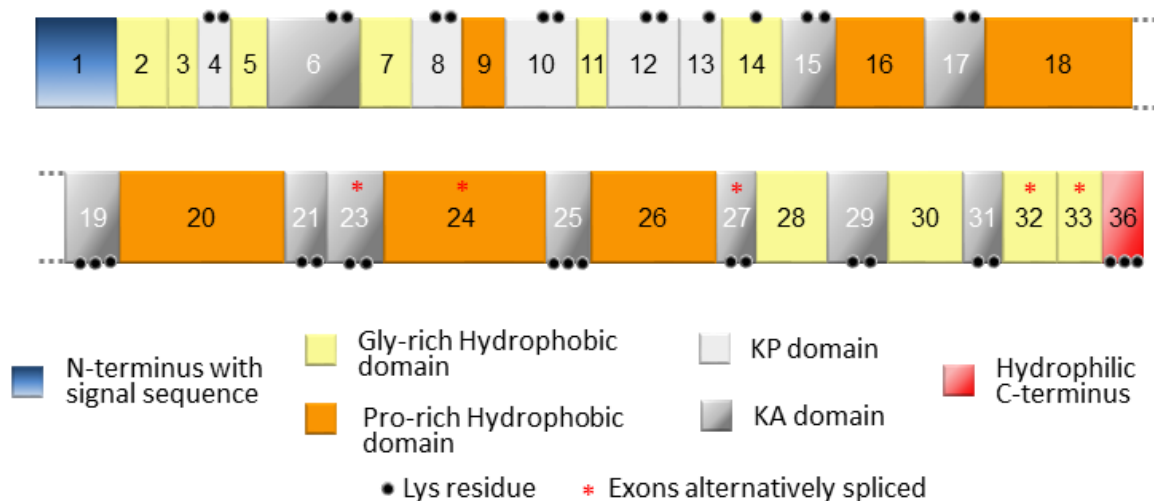


**Figure 4. Schematic diagram of the domain structure of human tropoelastin.**

The figure was adapted from Tamburro *et al.* (2003) [1].

In mammalian elastin, the hydrophobic domains are characteristically rich in glycine ( $\approx 33\%$ ), alanine ( $\approx 24\%$ ), valine ( $\approx 13\%$ ) and proline ( $\approx 10\%$ ). They have a noticeable variation in the length and composition among the mammalian elastins [61, 77]. Hydrophobic domains include many short tandem repeats and quasi-repeat sequences [78], such as PGVGVA [64, 79], which are formed by the pairwise combination of the fragments PGV, GVA, GV and GGV [80]. These domains could be classified as glycine-rich, localised mainly in the C- and N-terminal regions and proline-rich domains are found mostly in the central part of the molecule (see Figure 4). The last one is usually referred

as proline-rich domains because of their higher number of Pro residues, even if a considerable number of Gly residues are present [1]. Hydrophobic sequences are associated with the entropic mechanism of elasticity [36-41]. Moreover, they contain some interaction sites that are necessary for the aggregation of TE [56]. Furthermore, peptides derived from hydrophobic domains can interact with cell receptors, induce cell signalling and be involved in several pathologies [81].

In contrast, the cross-linking domains contain mostly polar sequences containing Ala and Lys in the form of -AlaAlaLys- and -AlaAlaAlaLys-, which are the cross-linking sequences of elastin [64, 82]. The length of cross-linking segments is highly conserved among mammalian elastins, indicative of a strong functional requirement [61]. These domains are classified into two groups: KA domains, which are rich in Ala and located in the central and C-terminal region, and the KP domains that contain Pro and are confined principally to the first third of the molecule [40]. The cross-linking process is extremely efficient. Most of the Lys residues are involved into cross-links (only  $\approx 5$  of the  $\approx 40$  Lys residues do not participate in some form of cross-link), and there are very few charged residues in elastin [65, 83]. The cross-linking of these domains confers fundamental mechanical properties to the elastin such as resistance to rupture, reversible deformation and high resilience [40].

Structural analysis of the elastin is complex due to its unique properties such as hydrophobicity, insolubility in common solvents [32, 40, 61, 79, 83], the high mobility of the elastin backbone [32, 37, 65, 84], and its lack of crystallisation [85]. Little is known about how the protein is assembled at the molecular level [37, 40, 83, 84]. The structural analysis has been focused on investigating elastin solubilized by oxalic acid ( $\alpha$ -elastin) [86-89], potassium hydroxide ( $\kappa$ -elastin) [84, 90], TE [32, 55], or elastin-like peptides [41, 73, 91]. Studying structural motifs is based on fractal properties of elastin, which indicate that the property of statistical self-similarity characterises the protein. Accordingly, short sequences show molecular and supramolecular features very similar to those of the whole protein [73, 91, 92]. The different analytical approaches used are circular dichroism [41, 73, 86, 87], Fourier transform infrared [41, 93, 94], fluorescence and nuclear magnetic resonance (NMR) spectroscopies [41, 91, 94], Raman spectroscopy [93] as well as X-ray diffraction methods [41] or molecular dynamics simulations [36, 37, 91].



As results of the different structural analysis previously mentioned, it has been suggested that elastin's sequence has a heterogeneity in its secondary structure [95]. Hydrophobic elastin-derived polypeptides show a propensity to adopt  $\beta$ - (type I, II and VIII) and  $\gamma$ -turn conformations [36, 37, 40, 73, 93, 96-98], and  $\beta$ -strand [36, 73, 84, 93], PPII [40, 41, 73, 91, 99] and unordered structures [40, 41, 84, 88, 89]. KP domains adopted similar conformations [40, 100], and the KA domains mostly show  $\alpha$ -helix conformations due to the cross-link requirement [73, 84, 89, 93, 100]. Analysis of full-length monomeric TE suggests that it contains  $\alpha$ -helix (3 % - 10 %),  $\beta$ -structures including  $\beta$ -strand and turns (45 % - 60 %), random coil secondary structures (> 40 %) [88, 90, 101] and the presence of polyproline II structure [1, 91, 102]. For a review of the structure of elastin and elastin-like polypeptides, from features of domain organisation to the supramolecular organisation of the fibre and structural flexibility see [95].

Regarding the tertiary structure adopted by TE in solution, there is not consensus either [32, 95, 103]. It has been suggested that the monomer is flexible, really dynamic [32, 95] and it has a high disordered backbone [32, 104, 105]; it looks like a transient structural form [32, 95, 103]. The structure of TE in solution has also been described as a 'thermodynamically unfolded premolten globule' state [95, 103], in which the monomer contains pockets of hydrophobic clusters, which are solvent accessible and not confined to a molecular core [32].

Taking into account the results of small-angle X-ray and neutron scattering experiments, Baldock *et al.* suggested a model for the nanostructure of full-length TE, which describes it as an asymmetric molecule with clearly distinct regions [9] (see Figure 5A). The same authors also propounded a head-to-tail model for the assembly of the TE. In it, the alignment and *n-mer* propagation of TE happen through the interaction of proximal domains 19 and 25, which are donated by one TE, and the domain 10 from a second molecule (Figure 5B). This model is based on the three cross-link domains (10, 19, and 25) and the junction with the longest molecular springs (domains 18, 20, 24 and 26) [9]. Chains of the three cross-link domains were also identified to be joined by one desmosine and two lysinonorleucine cross-links in porcine elastin [58].

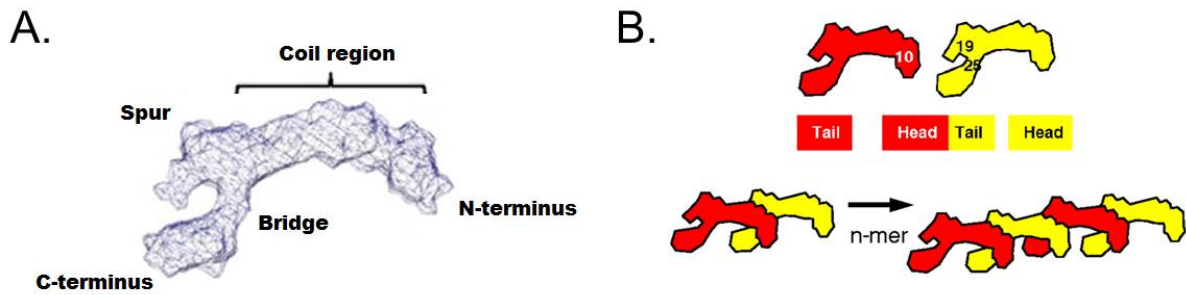


Figure 5. Model of the nanostructure of full-length and assembly of Tropoelastin.

(A) Model for full-length TE showing locations of different parts. The N-terminal region (exons 2-18) has a uniform elongated rod-shaped. It is followed by a spur region, protruding from the side of the molecule, which corresponds to a hinge region containing exons 20-24. Beyond the spur, there is a bridge to the C-terminal region that occurred at around exon 25. The molecule terminates in a more compact 'foot-like' region (exons 26-36), which includes the cell-interactive C-terminus of TE. (B) Head-to-tail model in which a molecule of TE is covalently cross-linked via domains 19 and 25 in its tail region with the domain 10 in the head part of another TE molecule. This *n-mer* propagation is an outcome of the head-to-tail mechanism. The figure was adapted from Baldock *et al.* [9].

There is no consensus about the secondary and tertiary structure of elastin either [40, 106]. Elastin-like peptides only correspond to small parts of the elastin, and their relevance to the protein structure is doubtful [3, 107, 108]. In mature elastin, hydrophobic clusters remain partially solvent accessible, to a lesser extent, though [109]. It has been hypothesised that elastin has a limited formation (if any) of a stable and buried core due to the solvent exposition and mobility of its hydrophobic domains [36, 37, 95]. It also has been hypothesised that elastin has disordered structures [39].

#### 1.2.4 Structural role of some tropoelastin domains

As result of the analysis of elastin-like peptides, some special roles of different TE domains have been suggested. Overall, the N-terminal elastic coil region has been associated with the elastic fibre assembly [110] and elasticity due to its spring-like properties [9]. Sequences from exon 2 to 7 [73] and 16 to 18 may also contribute to TE self-association [111-114]. Specific intra-molecular cross-links were confined to the region encoded by exons 6-15 [51]. Notably, domain 12 participates in cross-linking with domain 23 and could play a major role in the formation of mature elastin; domains 13 and 14 are also more exposed and available for reaction predominantly with domains 19-25 [59]. On the other hand, domains 4-6 have the high-affinity binding sites for the microfibrillar protein fibrillin-1 [115], and domains 17 and 18 were identified as critical for cell adhesion to this part of TE to human dermal fibroblast via integrin  $\alpha\beta 5$  [116]. Furthermore, a significant susceptibility of TE towards enzymatic cleavage was identified at domain 6 [83] and around domain 10 [110].

In the spur and bridge zones, it has been suggested that domains 19 and 25 are readily accessible to solvent and are enriched in intermolecular cross-links [51, 58, 59]. Domains 21/23 could be involved in the elasticity [117] and probably assist the coacervation [118] and cross-links [119]. Peptides encoded by exon 20 have a high propensity to coacervate, which could play a pivotal role in the molecular assembly of natural TE [120]. In the same way, domain 24 is also substantially solvent-exposed and could be involved in the coacervation [59]. This cross-linking enrichment could be associated with the amount of VGVAPG motif [59], which could also interact with EBP [121]. However, domains 20 and 24 played a lesser role in coacervation compared to domain 26, which has a potential role in aligning TE molecules due to a possible hydrophobic interaction with domain 18 in the intact monomer [55, 83, 112, 120]. The borders of domains 25 and 26 seem to be exposed to solvent [32] and are apparently involved in maintaining the orientation of the bridge and C-terminal region in TE during the elastic fibre assembly [122]. In particular, domain 26 is susceptible to enzymatic cleavage [83, 112].

Domains in the 'foot-like' part have been involved in three different roles: the cell adhesive activity, matrix interaction and TE assembly and cross-linking [9, 57, 83, 123, 124]. Domains 29 to 36 are critical assembly domains that mediate the interaction of TE with microfibrils in the ECM [83]. A crucial functional element is domain 30, which interacts with microfibrils [83, 94] and its deletion prevents the assembly of full-length TE [83, 125]. Domain 36 contains the C-terminal GRKRK motif that binds the integrin  $\alpha\beta 3$  during the elastin fibre assembly [123, 126-128]. It supports fibroblast adhesion [106, 128] of maturing elastin [71, 124, 129]. It is possible to find cross-linking intra- or inter-molecular between domains 6 and 36 [51, 59], and cysteine residues are disulphide bonded within the molecule, precluding their direct participation in intermolecular associations [130].

### **1.2.5 Degradation of elastic fibres**

Elastic fibres seem to undergo continuous 'physiologic' catabolism induced mainly by enzymatic proteolysis [51, 131]. Protein impairment plays a crucial function in the genesis of several diseases that involve matrix remodelling [31, 51, 132-135]. Elastases have been defined as the proteases that can degrade elastin [136], releasing peptides to

an appreciable extent [137]. Their proteolytic action is not exclusively limited to elastin and could encompass a variety of substrates [138]. It has been suggested that *in vivo*, the elastases might do a proteolytic degradation of the structural glycoprotein mantle that surrounds the elastic fibres before cleaving the elastin [137]. The enzyme activity, *in vivo*, is controlled by substrate availability, enzymes involved (type, amount and affinity), levels of their inhibitors, and the presence and function of scavenger cells [139, 140]. Aspects of the elastolysis mechanism of elastases were reviewed by Hornebeck [137].

The elastase-type proteases exhibit a broad distribution in nature [141] and have variable catalytic and substrate binding sites (For review, see [139, 142]). However, they prefer to cleave peptide bonds associated with hydrophobic or aromatic amino acids [3, 141]. Elastases are produced by different cells such as pancreatic acinar cells, polymorphonuclear leukocytes (macrophages and lymphocytes), neutrophils, mesenchymal cells, platelets, and fibroblast [134, 136, 137, 143-145]. The elastases mainly belong to three families: *serine proteases*: pancreatic elastase II [136], cathepsin G, human leukocyte elastase; myeloblastin (proteinase 3) [143, 145-149]; *matrix metalloproteinases* (MMP-2 (Gelatinase A ), -7 (Matrilysin), -9 (Gelatinase B), and -12) [149-154], and *cysteine proteases* (cathepsins K, L, V and S) [131, 134, 136, 139, 155]. Although almost all elastases are well characterised for years, only the skin fibroblast-derived elastase (SFE) remained without an undoubted identification. Recent studies indicated that SFE could correspond to the metalloprotease neprilysin (NEP) [156, 157].

### 1.2.6 Bioactive peptides

Along with its pivotal structural function, elastin plays a major role in the induction of specific responses from cells and tissues [126, 158]. Degradation (enzymatic or chemical) of elastin, especially of its hydrophobic domains [158], could lead to the production of elastin-derived peptides (EDPs), also called 'matrikines' or 'elastokines' [159-161]. These peptides have the ability to induce various intracellular signalling events that modify cell behaviour [162-165].

Elastokines have been detected in blood circulation in some physiological and pathological conditions, having significant physiological implications in the human health [138, 166-169]. In some cases, such as in ischemia/reperfusion injury [170, 171]

or tissue repair [172], EDPs might contribute to protection against damage. However, in other pathologies, EDPs seem to assist to exacerbating tissue damage. For instance, they promote emphysema [173], atherosclerosis [168, 174-177], aortic abdominal aneurysms [178], calcification of vessel walls [179], age-related macular degeneration [169], hyperplastic neointimal formation [165], melanoma [180-184] and other tumours in connective tissues [160, 185]. For reviews of the contribution of EDPs to diseases, refer to [21, 161, 186, 187].

The biological effects of EDPs have largely been attributed to their interaction with the 67-kDa elastin-binding protein (EBP). This receptor is an alternatively spliced enzymatically inactive form of the  $\beta$ -galactosidase that complexes with the 61 kDa and 55 kDa integral membrane proteins, carboxypeptidase A and sialidase, respectively [121, 159, 165, 188]. Its receptor is coupled with some intracellular signalling pathways that mediated EDPs cellular effect [165, 189]. Additional cell-surface receptors for EDPs have been identified. For instance, integrin  $\alpha\beta 3$  and  $\alpha\beta 5$  [116, 123, 128], heparin and chondroitin sulfate-containing glycosaminoglycans receptors [190] and galectin-3 receptor [191]. For elastin receptor complex review see [161] and for reviews of the interaction of cells with elastin refer to [126, 159].

It has been hypothesised that GXXP motif and a glycine residue located just after it are required for the interaction of EDPs with EBP [81, 192, 193]. These sequences are essentially inactive in the intact cross-linked protein [61]. However, elastases, even belonging to the same family, could release different peptides [137], whose biological activities are diverse and cell-specific [158]. Table 1 summarises the *in vitro* biological activities that have been reported for some EDPs. Furthermore, *in vitro*, TE has shown some cellular interactions and biological effect, which are described by Mithieux *et al.* See review [194].

SEQUENCE	BIOLOGICAL EFFECT	REFERENCE
AGLVPG; AGLVPGGPGFGPGVV	Stimulate pro-MMP-1 secretion (fibroblasts)	[147]
FGVG	Chemotaxis (monocytes)	[195]
GAIPG	Chemotaxis (M27 tumour cells)	[196]
GARPG; GAVPG	Stimulate pro-MMP-2 secretion (fibroblasts)	[152]
GFGPG; GGVLPG; GLPGVYPGGVLPGA	Stimulate pro-MMP-1 secretion (fibroblasts)	[147]
GFGVG	Chemotaxis (fibroblasts)	[197]
GLGVGAGVP	Chemotaxis (endothelial cells)	[198]

GLVPG	Chemotaxis (monocytes); stimulate pro-MMP-1 secretion (fibroblasts)	[147, 195]
GVAPG	Chemotaxis (monocytes)	[195, 199]
GVLPG; GVYPG	Stimulate pro-MMP-1 secretion (fibroblasts)	[147]
GYGPG	Stimulate pro-MMP-2 secretion (fibroblasts)	[152]
LREGDPSS	Chemotaxis (monocyte)	[200]
PGAIPG	Chemotaxis (neutrophils, M27 tumour cells); stimulate pro-MMP-1 and pro-MMP-3 expression (fibroblasts)	[81, 196]
PGFGAVPGA	Stimulate pro-MMP-2 secretion (fibroblasts)	[152]
PGFGPG	Stimulate pro-MMP-1 secretion (fibroblasts)	[147]
PGVGVA	Stimulate elastase and superoxide release; increase $[Ca^{2+}]_i$ (polymorphonuclear leukocytes - PMNL)	[201]
PGVYPG	Stimulate pro-MMP-1 secretion (fibroblasts)	[147]
VAPG	Chemotaxis (WM35 and HT168-M1 melanoma cells); stimulate of MMP-2 and MMP-3 expression (WM35 and HT168-M1 melanoma cells)	[184]
VGVA	Increase $[Ca^{2+}]_i$ and endothelium vasorelaxation (vein endothelial cells; rat aortic rings)	[202]
VGVAPG	Chemotaxis (endothelial cells; fibroblasts; keratinocytes; monocyte; neutrophils; A2058, WM35 and HT168-M1 melanoma cells; M27 lung carcinoma); enhancement of atherogenesis (monocytes in mice); increase $[Ca^{2+}]_i$ (leukocytes); induce insulin resistance associated with tissue remodeling (mice); inhibit proliferation (keratinocytes); myofibrillogenesis (smooth muscle cells); osteogenic response and increase expression of MMP-2 (smooth muscle cells); cell proliferation and downregulated elastin expression (fibroblasts); promote angiogenesis (chorio-allantoic membrane); promote superoxide production and elastase release in PMNL (leukocytes); stimulate differentiation melanocyte precursors (NNCmelb4 and NCCmelan5 cells); stimulate MT1-MMP and MMP-2 expression (melanoma cells); stimulate of MMP-2 and MMP-3 expression (WM35 and HT168-M1 melanoma cells); stimulate MMP-2 expression and activation (human fibrosarcoma HT-1080 cells); stimulate pro-MMP-1 and pro-MMP-3 expression (fibroblasts); upregulation Th-1 cytokine (T-cells); vasorelaxation - increase $[Ca^{2+}]_i$ (human umbilical vein endothelial cells-HUVEC)	[81, 164, 165, 170, 176, 178-180, 183-185, 195, 197-199, 201-213]
VGVGVA	Increase $[Ca^{2+}]_i$ ; promote superoxide production and elastase release in PMNL (leukocytes)	[201]
VGVPG	Chemotaxis (monocyte)	[199]
VPGVG	Stimulate proliferation, inhibit elastin expression (smooth muscle cells).	[214]
VVPQ	Mitogenic activity (dermal fibroblasts)	[215]
YGARPGVGVGGIP	Stimulate pro-MMP-2 secretion (fibroblasts)	[152]
YGVG	Chemotaxis (monocytes)	[195]
YTTGKLPYGYGPGG	Stimulate pro-MMP-2 secretion (fibroblasts)	[152]

**Table 1.** *In vitro* biological activities reported for some EDPs.

**Biological effects of elastin peptides derived from defined sequences of human tropoelastin.**

### 1.2.7 Elastic fibres in aging and skin diseases

Aging is understood as the gradual and progressive deterioration of integrity of multiple organ systems [216]. Loss of tissue elasticity is one of the hallmarks of aging [42, 136]. It has been associated with fragmentation and thinning of elastin structures in skin and blood vessels [42, 217], leading to loss of physiological function [218-220] and limiting the human life expectancy [221].

Cutaneous aging is a complex biological process affecting various layers of the skin [222]. It is induced by both intrinsic and extrinsic factors [223, 224]. Intrinsic (chronological) aging is genetically determined and affects the skin in a manner similar to the way various internal organs probably age. It generates fine wrinkling, increased laxity and fold accentuation, atrophy of the dermis and reduction of subcutaneous adipose tissue. Extrinsic ageing (photoaging) is induced by environmental exposure, primarily to UV radiation. Clinically it is characterised by the appearance of deep wrinkles, a sallow discoloration, telangiectasia, irregular pigmentation and furrowing and loss of elasticity [8, 131, 219, 222, 225, 226] (see Figure 6).

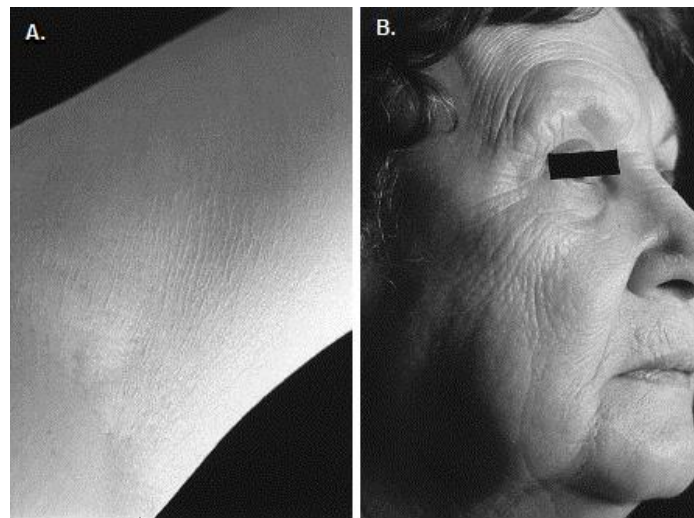


**Figure 6. Phenotype of intrinsic ageing versus photoaging.**

**(A.) Intrinsic ageing skin from arms, showing an atrophy of the skin with fine wrinkling (B.) Extrinsic ageing skin displays deep wrinkling and furrowing loss of resilience and skin tone (Figure and text adopted from [8]).**

Structural reorganisation of the dermal ECM is evident in both UV-protected and UV-exposed old skin [4]. In sun-protected areas, the number of elastic fibres decreased [138, 220, 227]. Actinically damaged skin is characterised by an accumulation of abnormal elastotic material in the reticular dermis as result of the solar elastosis process [220,

228-230]. Some biological, biochemical and molecular mechanisms of both processes are over-imposed in sun-exposed areas [220, 231-233]. They involve the upregulation of some enzymes associated with ECM degradation [136, 218, 228, 234]. For a review of the ageing mechanism see [4, 218, 235].

Regarding the role of elastin in illness, some inherited and acquired diseases have been described to alter the structure, distribution and abundance of elastic fibres. Then, elastic fibres lose functionality and increase their susceptibility to inflammatory or proteolytic damage [16]. Broad spectra of defects are related to damages to the entire fibre and the organ system affected, including from some skeletal and skin abnormalities to vascular and ocular defects [16, 236]. Although some of these syndromes do not involve elastin as the primary target, they severely affect the elastic fibre integrity [16]. For a review see [20, 69].

The genetic diseases specifically associated with mutations in elastin gene are supravalvular aortic stenosis (SVAS; OMIM #185500), autosomal dominant cutis laxa (ADCL; OMIM #123700), and Williams-Beuren Syndrome (WBS; OMIM #194050) [20, 69, 236]. In SVAS, patients present mainly translocation and a 100 kb deletion in the 5'-end and middle region of elastin gene [237-239]. This disease is characterised by morphological and functional changes in the cardiovascular system, especially in the arterial walls [236]. ADCL is related to the single nucleotide deletion in exons 30, 32 and 34 in the 3'-end of the coding region of elastin [240-242]. As a result of this frameshift, ADCL patients present reduced elastin synthesis by skin fibroblasts and deposition in the elastic fibres, fewer microfibrils and aberrant ultrastructure of dermal elastic fibres [242, 243].

WBS is a complex developmental disorder with multisystem involvement. It is a consequence of a hemizygous contiguous gene deletion, and less frequently duplication, of  $\approx 1.5$  Mb on chromosomal band 7q 11.23, which involves several genes, usually including the elastin gene [20, 238, 244, 245]. Abnormalities in connective tissues, cardiovascular and central nervous system and at the craniofacial level are characteristic in WBS patients [244, 246, 247]. In the skin, reduction of deposition of elastin in elastic fibres, a lower diameter and a less continuous appearance of them have been described [238, 248]. Skin features such as soft consistency, premature greying of



the hair, while wrinkles and abnormal scarring have been detected [238, 249]. For review see [236, 246].

Acquired elastic fibre disorders arise wherever the fibre structure and function are compromised during the natural progression of the disease [20, 250]. Examples of such diseases include elastosis and several cardiovascular and pulmonary diseases, where the elastin synthesis is reinitiated to repair damaged elastic fibres [251-255]. The newly synthesised TE could be modified for some factors, such as the presence of reactive oxygen and nitrogen species, which yields to aberrant assembly and dysfunctional fibres [256]. Furthermore, EDPs could maintain a positive feedback loop of inflammation and elastin degradation; missense variants in elastic fibre proteins may predispose them to such immune-mediated elastin destruction [257].

## 1.3 Mass spectrometry in proteomics

Mass spectrometry (MS) is an analytical technique that has been used more than one hundred years [258]. Its basic principle is to generate ions from either inorganic or organic compounds by any suitable method, to separate these ions by their mass-to-charge ratio ( $m/z$ ) and abundance [259]. Since the 1980s, MS has been applied in proteomics [258]. Currently, it is mainly used in cataloguing protein expression (molecular mass, amino acid sequence, quantitative changes), defining protein interaction and identifying sites of protein modification [260-262].

### 1.3.1 Instrumentation

By definition, a mass spectrometer consists of an ion source, a mass analyser and a detector [5] (see Figure 7). The measurements are carried out in the gas-phase ions of the analytical compound and their separation following their  $m/z$  [263]. Detailed review about mass spectrometers instrumentation is found in [263, 264] and a deep description of fundamentals and characteristic of MS and its instrumentation is presented in [259].

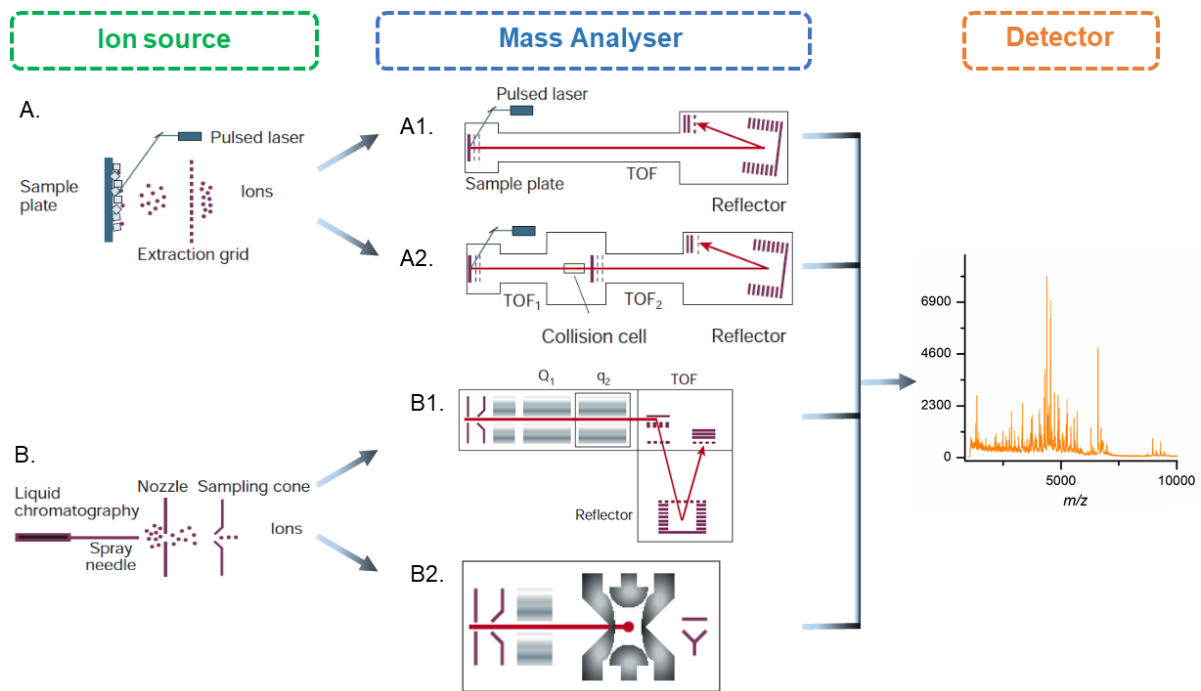


**Figure 7. Principal components of a mass spectrometer.**

The left panel depicts the ionisation and sample introduction in (A.) matrix-assisted laser desorption/ionisation (MALDI) and (B.) electro spray ionisation (ESI). The different instrumental configurations used during this thesis (A1,2; B1,2) are shown with their typical ion source: (A1) reflector time of flight (TOF) instrument, (A2) TOF-TOF instrument, (B1) the quadrupole-TOF instrument, and (B2) the (three-dimensional) ion trap. Figure and text adapted from Aebersold and Mann *et al.*[5].

Separation techniques are used to decrease sample complexity before mass analysis. Some of them are gel-based (SDS-PAGE `sodium dodecyl sulphate polyacrylamide gel electrophoresis`) and liquid-based (high performance liquid chromatography (HPLC), nanoHPLC, UltraHPLC) chromatography. As they reduce the number of ions to be analysed at the same time, they help to decrease the ion suppression effect. Furthermore, chromatographic separation allows those peptides with the same  $m/z$  to elute at different retention times, and then, more ions can be identified by the mass spectrometer [265]. HPLC devices are used as sample introduction instruments in some mass spectrometers [264].

In the ion source, the sample is volatilised and ionised to generate gas-phase ions from the molecules [263, 266]. The goal of the ion sources is to generate stable molecular ions from large, non-volatile and thermally labile compounds, such as proteins and peptides, without extensive degradation [262, 263]. The two most popular ions sources techniques in proteomics are matrix-assisted laser desorption/ionisation (MALDI) and electro spray ionisation (ESI) [263] that are called soft methods due to the fact that they generate intact molecular ions from large molecules [267, 268].

In MALDI technique the analyte is co-crystallised with an inert matrix, such as sinapinic or  $\alpha$ -cyano-hydroxycinnamic acid, which can absorb UV light [268]. When the dried solid mixture of matrix and analyte is irradiated with a pulsed laser, the matrix absorbs the energy and transfers it to the acidified analyte. The laser heating causes desorption of matrix and finally, singly-protonated analyte ions  $[M+H]^+$  are released into the gas phase [269]. In contrast, in the ESI technique, a solution of the analyte is passed through a fine needle that has a potential difference relative to a counter electrode. The high potential induces a spray of charged droplets, which are desolvated and then, the positive or negative multiply charged ions (depending on the polarity of the applied voltage) are released [267, 270].

In the mass analyser, electric or magnetic fields are applied and change the spatial trajectories, velocity or directions of the ions, which are resolved according to their  $m/z$  [266]. The currently available analysers can be classified into two categories: (i) *beam analysers*, such as quadrupole and time-of-flight analysers, in which the ions come from the ion source in a beam and pass through the analysing field to the detector and (ii) *trapping analysers*, such as ion trap, capture the ions in the analyser field where ions are formed in the analyser itself or can be injected from an external ion source [263].

In *time-of-flight* (TOF) analysers, the ions are accelerated through a fixed potential into the TOF drift tube. As the velocity of the ions is inversely proportional to their masses, they are separated according to their  $m/z$  value during the movement at a constant speed [263, 264]. On the other hand, the *quadrupole* (Q) analyser contains four hyperbolically or cylindrically shaped rod electrodes extending in the  $z$ -direction. They are mounted in a square configuration ( $xy$ -plane). When a periodic voltage (composed of a DC voltage and a radio-frequency (RF) voltage) is applied to the rods, the overall ion motion can result in a stable trajectory causing ions of a certain  $m/z$  value (range) to pass the quadrupole [259]. Ions of different  $m/z$  can be sequentially allowed to reach the detector by increasing the magnitude of the RF and DC voltages [263].

The *ion trap* (IT) analysers have the electric field in all three dimensions ( $x, y$  and  $z$ ), which can result in ions being trapped in the field [5, 263]. The ions are ejected from the trap successively in a mass-selective manner by increasing the RF voltage that is applied to the device [263, 264]. There are three ion traps available: three-dimensional (QIT), linear (LIT), and ion cyclotron resonance (ICR) ITs. The QIT is formed by three

electrodes, one ring-shaped, named annular or ring electrode, and two end cap electrodes at both sides of the ring. Inside the small cavity formed by these electrodes, the ion trapping and analysing process takes place [264]. In LIT, a trapping potential is generated by placing electrodes of slightly higher potential adjacent to the front and rear end of the multipole [263]. In ion cyclotron resonance (ICR), ions are trapped in a cell composed of four electrodes situated in a strong magnetic field, and they oscillate with a frequency (cyclotron frequency) inversely related to their  $m/z$  value [264].

The detector determines ion abundance for each corresponding ion resolved by the mass analyser according to their  $m/z$  value and generates a mass spectrum [266]. Detectors are associated with the kind of analyser used in the equipment. Some detectors used in modern mass spectrometer are the secondary electron multipliers, cryogenic detectors and the image current detection. Details about their operating mode can be found in [259].

### *Tandem mass spectrometry (MS/MS)*

Tandem mass spectrometry (MS/MS) is the experiment used to establish the identity of a compound. MS/MS involves two stages of MS. In the first stage, ions of a desired  $m/z$  are isolated from the rest of the ions emanating from the ion source. These isolated ions (termed parent ions or precursor ions) are then induced to undergo a chemical reaction to increase their internal energy, leading to their dissociation before analysis by a second MS stage. The dissociation method almost universally used is collision-induced dissociation (CID), in which the parent ion collides with a neutral target (collision) gas and some of the kinetic energy of the parent ion can be converted to internal energy, then the dissociation happens. The instruments used for MS/MS analysis are classified in tandem-in-space or tandem-in-time. Tandem-in-space instruments require distinct analysers for each stage of MS/MS such as beam-type analysers. Trapping instruments are typically tandem-in-time, in which various stages of MS/MS are performed in the same analyser, but separated in time [263]. Mass spectrometric data acquisition is done in a data-dependent manner in which information from a current mass spectrometric scan determines the parameters of subsequent scans. In most cases, full scan produces

masses of the proteins or peptides, and fragmentation scans yield their primary sequence information [262].

Some analysers can be put together to take advantage of the strengths of each one to improve the sensitivity, resolution, mass accuracy and the ability to generate MS/MS spectra from peptide fragments [5, 264]. Some of the instrument configurations most used in proteomics include triple quadrupoles (TQ), LTQ-Orbitrap hybrid instrument (Thermo Scientific), LTQ-FTICR (Thermo Scientific), TQ-FTICR hybrid instruments, Q-TOF and IT-TOF (Shimadzu) [262]. For instance, Q-QTOF instruments exhibit high resolution and mass accuracy. In the MS mode, the Q acts as an ion guide to the TOF analyser where the mass analysis takes place. In the MS/MS mode, the precursor ions (typically a multiply charged ion in ESI) are selected in the first Q and undergo fragmentation through CID in the second Q. The product ions are analysed in the TOF device [260].

### 1.3.2 Identification approaches

There is no method or instrument capable of identifying and quantifying the components of a complex protein sample in a simple, single-step operation [5]. In proteomics, the spectrometric analysis can be done following a *bottom-up* approach (analysis of proteolytic peptide mixtures), in which peptide detection is used to infer protein presence. Other options are *middle-* and *top-down* approaches (analysis of longer peptides and intact proteins, respectively), which should allow a complete characterisation of protein isoforms and post-translational modifications [261, 262]. Yates *et al.* reviewed the advantages and applications of these proteomic approaches [262].

Two main approaches are used in the identification of proteins. One strategy is the *peptide fingerprint approach*. In it, the proteins are digested with specific proteases and the resulting proteolytic peptides are analysed by MALDI-TOF MS [264]. The mass profile matches against the theoretical masses obtained from the *in silico* digest of all protein amino acid sequences in a database[5]. The proteins in the database are then ranked according to the number of peptide masses matching their sequences with a given mass error tolerance. The disadvantages of this method are that it does not give sequence information and it does not take into account all the theoretical peptide

masses expected for the given digestion conditions, then a high amount of peptides remain unidentified [264].

The second strategy to identify proteins is based on the *peptide fragmentation data*. During the MS/MS analysis, the peptide ions may decompose under various conditions (CID, metastable decay, etc), and characteristic peptide fragment ions are obtained in each decomposition process. During the CID process, the fragmentation mainly occurs at the peptide amide bonds, and one fragment preserves the N-terminus of the peptide while the other conserves the C-terminus (b and y ions, respectively) [264]. Three approaches are used: (i) peptide fragmentation fingerprint, in which un-interpreted spectra are compared to theoretical spectra produced by *in silico* digestion of the protein, using *ad hoc* search software [271, 272]; (ii) peptide sequence tag, in which the sequence and mass of the peptide are used for database searching [273]. Programs such as Mascot [272] or PEAKS [274] are used to identify peptides and proteins from uninterpreted peptide CID fragmentation spectra. They use experimental MS2 data to match against the theoretical masses obtained from *in silico*-generated fragmentation patterns at the same enzyme cleavage sites of the protein amino acid sequences in a database (e.g. SwissProt). Based on scoring functions, the proteins in the database are then ranked according to the number of peptide masses matching their sequences within a given mass error tolerance [262, 264]. (iii) The last approach that is used for the interpretation of peptide fragmentation spectra without the utilisation of any databases is the process called *de novo peptide sequencing* [275].

### 1.3.3 Quantification approaches

Due to many biological changes result from a target perturbation of a biological system rather than being absolute (on/off) changes, a new trend in protein analysis has evolved. It consists in seeking quantitative information from proteomic experiments that were previously solely qualitative [276, 277]. The classical proteomic quantification methods utilising dyes, fluorophores, or radioactivity have provided good sensitivity, linearity and dynamic range, but they are applied only to abundant and soluble proteins and do not identify the underlying protein [278]. MS-based proteomics overcome these limitations through the use of *stable isotope labelling* and *label-free* methods [266]. These methods also could be classified into two broad groups: (a) relative quantitative

proteomics methods, in which two or more samples are compared using either stable isotope labelling or label-free methods [262] and (b) absolute quantitative proteomics, in which an accuracy quantification of target molecules is provided by comparison against external or internal standards, often by use of stable isotope markers [262].

*Stable isotopic labelling* methods make use of stable isotopes such as  $^2\text{H}$ ,  $^{13}\text{C}$ ,  $^{15}\text{N}$ , and  $^{18}\text{O}$  for sample labelling [261]. This label can be introduced by (i) chemical reaction of specific amino acid residues or functional groups with an isotopically labelled reagent [279]; (ii) enzyme catalysed reactions [280]; (iii) isotopically enriched media [281-283] and (iv) using cells [284]. Analysis of these stable isotopes is typically done by creating extracted ion chromatograms (XICs) for the  $m/z$  determined for each peptide [285]. The intensity value for each peptide in one experiment can then be compared to the respective signals in one or more experiments to yield relative quantitative information [285-287]. Also, it is possible to use selected reaction monitoring (SRM) that repeatedly measures selected peptides in a highly specific and accurate manner [288]. For a review of methods of isotope-based quantifications see [277].

*Label-free quantification* (LFQ) methods [287, 289, 290] take advantage of the linear relationship between the signal and the concentration of the analyte and compare the signal intensities of the same peptide directly in different LC-MS runs of the samples to study [264]. The method overcomes the limitations of stable isotope methods. For instance, it can be applied to a high number of samples at low cost and in less time [266, 274], allowing the analysis of all peptides in one sample [278]. Although the ion suppression effect or the influence of technical variability can decrease the accuracy of LFQ methods on stable isotope methods [264], the significance of these sources of error is reduced when the samples are processed and analysed one after another and in the same way [277]. Quantification is based on two categories of measurements [291, 292]: *signal intensity (feature-based)* and *spectral counting* (see Figure 8).

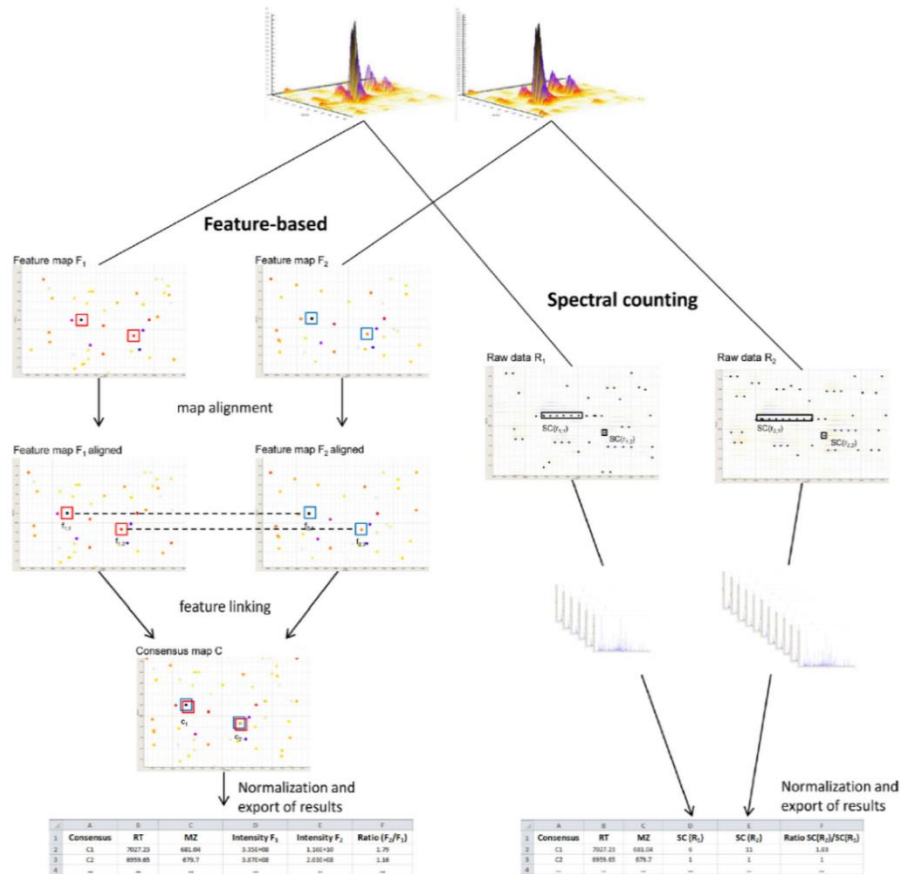


Figure 8. Label-free quantification (LFQ) methods.

Quantification of proteins can be done using two different approaches: feature-based, in which the peptides are identified in each MS run and, spectral counting, based on the number of spectra of each peptide in MS/MS. Figure adopted from Nahnsen *et al.* [6].

*Signal intensity or area under the curve (AUC)* approach measures and compares the mass spectrometric signal intensity of peptide precursor ions belonging to a particular protein. The signal intensity from ESI correlates with ion concentration [293]. The right balance between acquisition of survey and fragment spectra can be reached through two separate experiments for each sample: one MS/MS to identify as many peptides as possible, and another MS-only mode to optimise sampling of intact peptide signals. Subsequently, the integrated peak intensities are matched to determine the peptides through the comparison of their mass and retention time [278].

*Spectral counting* is based on counting the number of peptides assigned to a protein in an MS/MS analysis. The most abundant peptides will be selected for fragmentation and will produce a higher number of MS/MS spectra, and it is, therefore, proportional to the protein amount in data-dependent acquisition [294]. Hence, relative quantification can be achieved by comparing the number of such spectra between a set of analysis



[278]. This method has some disadvantages such as lack of measuring of any direct physical property of a peptide [278], inability of MS/MS to analyse all peptides, and finally, influence of the propagation of quantitative errors from technical variability over the direct measurement of peptides abundance [277]. Then, the linearity is unclear, and they have a relatively poor accuracy [295].

Some LFQ proteomic methods include the sample preparation, separation by liquid chromatography, analysis by MS, MS/MS and finally, data analysis [292]. A wide range of workflows for bioinformatic analysis of data derived from LFQ experiments has been published [292, 296-301]. In general, for every scan (mass spectrum at a given elution time), the following steps must be performed: (1) de-noising and smoothing of raw mass spectra, (2) baseline subtraction, (3) peak detection, (4) isotope deconvolution in which isotopic patterns of peptides are merged, (5) retention time shift alignment related to a previously defined reference sample or simultaneously, (6) feature extraction by grouping consecutively eluting peaks from the same peptide, taking both the  $m/z$  and the retention time window into account for peak grouping, (7) ion intensity normalisation for the entire sample, (8) identification of the corresponding amino acid sequence of each peptide by comparison to the database and then assignment of each peptide to their underlying proteins, and (10) quantification. For each peptide, the AUC is reported; the protein quantification can correspond to AUC values of the average peptide ratio for all the peptides attributed to one protein, or the ratio between the sums of the AUCs of all the peptides from the protein [289, 302].

## 2 Aim

Elastin is responsible for elasticity and resilience of the skin, and its damage plays a central role in skin ageing and diseases such as Williams-Beuren Syndrome (WBS). Furthermore, elastin-derived peptides (EDPs) released during the enzymatic degradation of the elastin have been described to induce specific responses from cells and tissues. Studying the elastin degradation previously focused on investigating the activity, cleavage preferences and role of some elastases in different pathologies. Interestingly, variations in the activity of some elastases associated to the age and quality of the fibrillar elastin have been described.

It is evident that there is a lack of information about the influence of the elastin fibre structure in the degradation process. Hence, the general goal of this thesis was contributing to the understanding of skin elastin degradation at the molecular level by evaluating four aspects; firstly, the vulnerability of the elastin hydrophobic domains and the effect of age-related changes of the fibrillary elastin on the protein susceptibility towards degradation by biologically relevant elastases; secondly, the effect of skin ageing on the morphology and susceptibility of elastin towards enzymatic degradation and thirdly, the alterations of the structure and amount of elastin present in skin samples of WBS patients. Finally, the potential role of EDPs in the tissue damage was investigated through the characterisation of the EDPs released during the analysis of the factors previously mentioned.

Studying elastin is challenging since the unique properties of the protein do not allow applying conventional techniques used in proteomics. In the last years, analysing enzymatic digests of elastin by mass spectrometry (MS) techniques has become a powerful tool to investigate elastin in a qualitative way. Due to the fact that MS has evolved to a quantitative approach, label-free quantification (LFQ) was chosen as a method to identify changes in the abundance of elastin peptides. Then, another specific goal of this thesis is to evaluate the suitability of the LFQ workflow for the quantitative analysis of the elastin.

## 3 Material and Methods

### 3.1 Materials

#### 3.1.1 Chemicals

Acetonitrile (ACN)	$C_2H_3N$	VWR Prolabo, Belgium
Acetyloxy-(4-aminophenyl)mercury; (p-aminophenylmercuric acetate (APMA))	$C_8H_9HgNO_2$	Sigma-Aldrich, USA
2-Amino-2-hydroxymethyl-propane-1,3-diol; (Tris)	$C_4H_{11}NO_3$	National diagnostics, USA
4-Aminophenylmercuric acetate	$C_8H_9HgNO_2$	Sigma-Aldrich, USA
Azanium hydrogen carbonate;(Ammonium bicarbonate)	$CH_5NO_3$	Sigma-Aldrich, USA
Calcium dichloride	$CaCl_2$	Merk, Germany
Carbononitridic bromide; (Cyanogen Bromide)	$CBrN$	Sigma-Aldrich ,USA
Chlorane; (Hydrochloric acid)	$HCl$	Grüssing, Germany
Chloroform	$CHCl_3$	Carl Roth GmbH + Co. KG, Germany
(E)-2-Cyano-3-(4-hydroxyphenyl)prop-2-enoic acid; ( $\alpha$ -cyano-4-hydroxycinnamic acid; (CHCA))	$C_{10}H_7NO_3$	Sigma-Aldrich, Switzerland
Dimethyl sulfoxide (DMSO)	$C_2H_6SO$	Carl Roth GmbH + Co. KG, Germany
Disodium hydrogen phosphate dihydrate	$H_5Na_2O_6P$	Merck, Germany
Disodium [oxido(oxoboranyloxy)boranyl]oxy-oxoboranyloxyborinate;decahydrate; (Sodium tetraborate decahydrate)	$B_4H_{20}Na_2O_{17}$	Reachim, USSR
Ethanol	$C_2H_6O$	VWR Prolabo, Belgien
Ethoxyethane	$C_4H_{10}O$	VWR Prolabo, Belgien

Formic acid; (FA)	CH <sub>2</sub> O <sub>2</sub>	Merck, Germany
(E)-3-(4-hydroxy-3,5-dimethoxyphenyl)prop-2-enoic acid; (Sinapic acid (SA))	C <sub>11</sub> H <sub>12</sub> O <sub>5</sub>	Fluka Chemie GmbH, Germany
Methanol	CH <sub>4</sub> O	VWR Prolabo, France
Potassium chloride	KCl	Merck, Germany
Potassium dihydrogen phosphate	KH <sub>2</sub> PO <sub>4</sub>	Merck, Germany
Propan-2-one	C <sub>3</sub> H <sub>6</sub> O	Merk, Germany
Propan -2-ol	C <sub>3</sub> H <sub>8</sub> O	Carl Roth GmbH + Co. KG, Germany
Sodium Azide	NaN <sub>3</sub>	Sigma-Aldrich, USA
Sodium Chloride	NaCl	Sigma-Aldrich, Switzerland
Sodium hydroxide	NaOH	Carl Roth GmbH + Co. KG, Germany
2-Sulfanylethanol; (2-Mercaptoethanol)	C <sub>2</sub> H <sub>6</sub> OS	Sigma-Aldrich, USA
2,2,2-trifluoroacetic acid; (TFA)	C <sub>2</sub> HF <sub>3</sub> O <sub>2</sub>	Sigma-Aldrich, Germany
Urea	CH <sub>4</sub> N <sub>2</sub> O	Sigma-Aldrich, Germany

Table 2. Chemicals

### 3.1.2 Protein and enzymes

Human cathepsin G	Elastin Products Company, USA
Porcine pancreatic elastase	Elastin Products Company, USA
Recombinant human MMP-9, CHO-derived	R&D Systems, USA
Recombinant human neprilysin, CHO-derived	R&D Systems, USA
Recombinant human tropoelastin, Isoform 2 (G422S)	Prof. Markus Pietzsch, Institut für Pharmazie, MLU Halle-Wittenberg, Halle
Trypsin, Type IX-S, porcine pancreas	Sigma-Aldrich, USA

Table 3. Protein and Enzymes

### 3.1.3 Buffer and reagent composition

Elastase buffer	50 mM Tris-HCl in ddH <sub>2</sub> O, pH 7.5
MMP-9 buffer	50 mM Tris, 10 mM CaCl <sub>2</sub> , 150 mM NaCl, pH 7.5
Trypsin buffer	50 mM NH <sub>4</sub> HCO <sub>3</sub> in ddH <sub>2</sub> O, pH 8.0

APMA reagent	100 mM APMA in DMSO
Chaotropic reagent	300 mM Tris, 4 M Urea, 1.5 M 2-Mercaptoethanol in ddH <sub>2</sub> O
Cleavage reagent	10 % CNBr in FA
Trypsin reagent	5333 U mL <sup>-1</sup> Trypsin in 100 mM NH <sub>4</sub> HCO <sub>3</sub>
SA matrix	10 mg mL <sup>-1</sup> SA in ACN : 0.1 % TFA (1:1 v/v)
CHCA matrix	5 mg mL <sup>-1</sup> CHCA in ACN : 0.1 % TFA (1:1 v/v)
Saline solution	1 M NaCl in ddH <sub>2</sub> O

**Table 4. Buffer and reagent composition**

### 3.1.4 Skin samples

Skin biopsies (5 mm diameter) from different healthy probands of both sexes and aged 19 - 90 were acquired postoperatively from the tumor-free border of excised skin cancer tissue from various body regions; and foreskin samples (8 mm diameter) were derived from children aged 6 – 13. Donors were caucasians with light to mild pigmentation. On the other hand, skin samples from WBS patients were obtained as punch biopsies (3 mm diameter) from donors of different sexes and ages between 19 and 46. An overview of the samples included in each study of this thesis can be found in Table A-3 and Table A-5 in the Appendixes 3 and 4. Elastin was isolated from all tissue biopsies according to the procedure described in section 3.3.1. Particularly, samples included in the study of the molecular changes of human skin elastin from patients with WBS and healthy individuals were dried in a SpeedVac and weighed before carrying out the elastin isolation procedure.

The studies were approved by the ethics committee of the Medical Faculties of the Martin Luther University Halle-Wittenberg and the Christian Albrechts University Kiel, respectively, and carried out in compliance with the Helsinki Declaration. Each participant or each subject's legally authorised representative provided full written consent.

## 3.2 Instruments

Analytical balance AG204; d = 0.01 mg	Mettler Toledo, USA
Analytical balance XA105; d = 0.01 mg	Mettler Toledo, USA
Analytical balance M2P; d = 0.001 mg	Sartorius, USA

Centrifuge MiniSpin <sup>®</sup>	Eppendorf, Germany
Centrifuge Spectrafuge TM Mini	neoLab, Germany
Magnetic Stirrer MR 1000	Heidolph, Germany
Vortex mixer Reax Top	Heidolph, Germany
Biological safety cabinet	Heraeus, Germany
pH-Meter	Mettler Toledo, USA
Pipet (2.5 µL, 10 µL, 100 µL und 1 mL)	Eppendorf, Germany
Shaker GFL 3006	GFL, Germany
Thermomixer comfort	Eppendorf, Germany
Vacuum concentrator (SpeedVac) Savant SPD 1010	Thermo Fisher Scientific, Germany

Table 5. Instruments

### 3.3 Biochemical Methods

#### 3.3.1 Isolation of elastin from human samples

Elastin samples were isolated according to the procedure described by Schmelzer *et al.* [149]. Samples were cut into smaller pieces and transferred into a 1.5 mL reaction tube, in which they remained during the whole isolation method. In each step, during the procedure, 1.5 mL of the related reagent was added, and each tube was shaken at 300 rpm for a fixed period. After that, the tubes were centrifuged for 10 min at 14.000 x g, and the supernatant was removed by pipetting. Finally, the new reagent was added.

During the first day, the samples were treated twice with saline solution by shaking them for 2 h each time. Afterwards, a mixture of ddH<sub>2</sub>O : ethanol (1:1) was added, and the samples were shaken overnight. On the second day, non-polar components such as fat were extracted using organic solvents of different polarity; the samples were shaken during 1 h with each solvent. The following solvents were used consecutively: ethanol (96 %), a mixture chloroform : methanol (2:1), ethoxyethane, propan-2-one and ethanol (96 %). The extraction step using the chloroform : methanol mixture was done twice. When the samples presented on their surface a brown or dark brown layer at the end of the extractions, this layer was removed manually. Subsequently, the cleavage solution was added, and the samples continue shaking overnight. On the third day, a new

cleavage solution was added to the samples, and they were shaken for an additional period of 6 h. Next, the samples were washed three times with a mixture of ddH<sub>2</sub>O : ethanol (1:1), by shaking them for 10 min each time. Finally, the chaotropic reagent was added, and the samples were shaken overnight. On the next day, new chaotropic reagent was added and the samples were shaken for 3 h, this step was done once more. Afterwards, the samples were washed three times in a similar way than the one described on the third day. After that, the trypsin reagent was added, and the samples were shaken overnight. On the last day, chaotropic reagent was added, and the samples were shaking for 1 h. Next, the samples were treated first, two times with ACN : 0.1 % FA in ddH<sub>2</sub>O (1:1) and second, with solutions of ddH<sub>2</sub>O : ethanol 1:1 and 3:7, by shaking the samples during 10 min each time. Then, the samples were washed with ethanol 96 %, and after 10 min of shaking, the solvent was removed, and the samples were dried for 4 h under laminar air flow. Finally, the samples were stored at -26 °C until further analysis.

### **3.3.2 Proteolysis of tropoelastin and human elastin**

Recombinant tropoelastin (TE) was dissolved at a concentration of 1 mg mL<sup>-1</sup> in elastase buffer (proteolysis with PE, CG or NEP) or MMP-9 buffer (proteolysis with MMP-9). Human skin elastin samples were dried under laminar flow box during 24 h before they were weighed and dispersed under the same conditions described for TE. All samples were incubated separately with each enzyme for 48 h at 37 °C and shaken at 300 rpm at an enzyme-to-substrate ratio of 1:100 (w/w) (CG, MMP-9) or 1:50 (w/w) (PE). Before the use of MMP-9 in the elastin digestion, the enzyme was activated through incubation with APMA reagent at a final concentration of 1 mM for 24 h at 37 °C. All digestions were stopped by addition of TFA at a final concentration of 0.5 %, which produce samples with a pH lower than 3. Digested samples were preserved at -26 °C until further analysis.

## **3.4 Analytical methods**

### **3.4.1 NanoHPLC-nanoESI-QqTOF mass spectrometry**

All digested elastin samples were analysed in a random order by nanoHPLC-nanoESI-QqTOF MS(/MS) using an UltiMate 3000 nanoHPLC system (Thermo Fisher, Germany)

coupled online to a QqTOF mass spectrometer Q-TOF-2 (Waters/Micromass, UK) following the procedure described by Heinz *et al.* [152, 303]. The mass spectrometer was equipped with a nanoESI Z-spray source and a tip adapter for PicoTips (New Objective, USA), which was used with SilicaTipemitters (10  $\mu\text{m}$ I.D.) from New Objective too.

Peptides mixtures (1.0 – 2.5  $\mu\text{L}$ ) were loaded onto the trap column (Acclaim PepMap 100 C18, 5  $\mu\text{m}$ , 100  $\text{\AA}$ , 300  $\mu\text{m}$  I.D.  $\times$  5 mm; Thermo Fisher) and washed for 10 min with a mixture of 98 % ddH<sub>2</sub>O and 2 % ACN containing 0.1 % FA at a flow rate of 6  $\mu\text{L min}^{-1}$ . Afterwards, the trapped peptides were eluted onto the separation column (Acclaim PepMap C18, 3  $\mu\text{m}$ , 100  $\text{\AA}$ , 75  $\mu\text{m}$  I.D.  $\times$  150 mm; Thermo Fisher), which was previously equilibrated with 88 % solvent A (0.1 % FA in ddH<sub>2</sub>O) and 12 % solvent B (80 % ACN and 20 % ddH<sub>2</sub>O containing 0.1% FA). The solvent system for the chromatographic separation of the peptides was: a linear gradient of solvent B up to 40 % in 51 min, followed by an increased of solvent B up to 90 % in a linear gradient during 10 min and maintaining it for 5 min; then solvent B decreased in a linear gradient until 10 % in 15 min, followed by 5 min of equilibration before starting the procedure all over again. The flow rate was 300 nL  $\text{min}^{-1}$ , and the column was maintained at 40 °C. The mass spectrometer was operated under the following conditions: positive ion mode; capillary voltage of 1.8 kV; sample cone voltage of 20 V; and source temperature of 80 °C. The  $m/z$  range evaluated in MS experiments was from 40 to 1550 and peptides were chosen for collision-induced dissociation in data-dependent acquisition (DDA) mode (Resolution 9500; mass accuracy:  $\pm$  25 ppm). The quadrupole mass filter, followed by the TOF analyser, was fit with low-mass and high-mass resolution settings of 10 a.u. (arbitrary units), and the collision energy was modified into the range of 25 eV and 60 eV depending on  $m/z$  value and charge state.

### 3.4.2 NanoHPLC-nanoESI-Orbitrap mass spectrometry

Previous to their analysis, all digested samples were desalted using Zip-Tip® U-C18 following the procedure from the supplier (EMD Millipore, USA) and re-suspended in the same initial volume using ddH<sub>2</sub>O. Samples were analysed using an UltiMate 3000 RSLCnano HPLC system (Thermo Fisher Scientific, Germany) coupled online to an



Orbitrap Q Exactive™ plus Hybrid Quadrupole-Orbitrap™ Mass Spectrometer (Thermo Fisher Scientific).

Peptides samples (300  $\mu\text{L}$ ) were loaded onto the pre-column (Acclaim PepMap 100 trap-column 75  $\mu\text{m}$  x 2 cm, nanoViper, C18), which was in line with an EASY-Spray column, (50 cm x 75  $\mu\text{m}$  ID, PepMap C18, 2  $\mu\text{m}$  ES803), both from Thermo Fisher Scientific. Peptides were eluted using a binary solvent system (0.1 % FA in ddH<sub>2</sub>O (A) and ACN containing 0.1 % FA (B)), which was applied in a linear binary gradient: first, 5 % - 40 % B in 40 min, then, up to 90 % B in the next 5 min, followed by 10 min of 90 % B, and finally from 90 % to 10 % B in 5 min. The flow rate was 300 nL min<sup>-1</sup>. In the MS analysis, the ions were produced using a NanoESI source, setting the source voltage between 1.8 – 2.5 kV. The MS/MS analysis was done using a precursor ion detection in an  $m/z$  range from 400 to 2000 with a resolution of 75000, followed by a product ion scan using HCD with the following characteristics: 28 % normalised collision energy, a resolution of 17500 and an isolation window of 2 Th. Dynamic exclusion (exclusion duration: 40 s, exclusion window:  $\pm 2$  ppm) was enabled to allow detection of less abundant ions.

### 3.4.3 NanoHPLC/nanoMALDI-TOF/TOF mass spectrometry

Skin elastin samples were analysed using an UltiMate 3000 RSLCnano system (Thermo Fisher, Germany), a Probot micro fraction collector (ThermoFisher), and a 4800 MALDI-TOF/TOF mass spectrometer (AB Sciex, Canada) as reported by Heinz *et al.* [304]

Elastin digests (1.0  $\mu\text{L}$ ) were loaded onto the trap column (Acclaim PepMap 100 C18, 5  $\mu\text{m}$ , 100  $\text{\AA}$ , 300  $\mu\text{m}$  I.D. x 5 mm; Dionex) and washed for 9 min with a mixture of 98 % of 0.1% FA in ddH<sub>2</sub>O and 2 % ACN at a flow rate of 7  $\mu\text{L}$  min<sup>-1</sup>. Afterwards, the trapped peptides were eluted onto the separation column (Acclaim PepMap RSLC C18, 2  $\mu\text{m}$ , 100  $\text{\AA}$ , 75  $\mu\text{m}$  I.D. x 150 mm; Dionex), which had already been equilibrated with 88 % solvent A (0.1 % FA in ddH<sub>2</sub>O) and 12 % solvent B (80 % ACN and 20 % ddH<sub>2</sub>O containing 0.1 % FA). The chromatographic separation of the peptides was done using the following solvent system: a linear gradient of solvent B up to 40 % in 51 min, followed by an increase of solvent B up to 90 % in 10 min using a linear gradient and it remained like that for 5 min; after, the solvent B decreased until 12 % in 15 min in a

linear gradient, followed by 5 min of re-equilibration before starting the whole process again. The flow rate was 300 nL min<sup>-1</sup>, and the column remained at 40 °C. Fractions and the CHCA matrix were blended in a 1:3.7 ratio (v/v) and the mixture was spotted in 30 s intervals onto a 384-spot MALDI plate using a Probot micro fraction collector (Dionex). The MS analysis was done in the  $m/z$  range from 600 to 5000 using a positive ionisation mode and reflectron mode by accumulating data from 1000 to 2000 laser shots per spot. Peptides with a signal-to-noise ratio above 30 were under MS/MS analysis, which was done by laser-induced dissociation (LID) and high-energy collision-induced dissociation (CID) using 1 keV as collision energy and air as the collision gas.

#### **3.4.4 MALDI-TOF mass spectrometry**

Analysis of elastin digests was done using a Voyager DE PRO time of flight mass spectrometer (SCIEX, Germany) equipped with a 337 nm nitrogen laser. Previous to the analysis, samples were mixed in a 1:9 ratio with SA matrix. Afterwards, the mixture (1 µL) was spotted onto a 100-spot MALDI target and dried before it was loaded into the instrument. Mass spectra were acquired in the positive-ion linear mode. Two  $m/z$  range were evaluated: large (10000 – 80000; Grid 90; Delay time 750) and low (1000 – 20000; Grid 93; Delay time 500). Data was displayed in Data Explorer (version 4.0; SCIEX, USA).

#### **3.4.5 Scanning electron microscopy (SEM)**

The SEM was done according to the method reported by Heinz *et al.* [304]. Prior to the analysis, elastin samples were dried under laminar flow box for 2 h, and dried samples were mounted on the aluminium support with double-sided adhesive conductive carbon tape. Afterwards, the samples were covered with a film (50 nm) of platinum-palladium in a Cressington 208HR High-Resolution Sputter Coater (Cressington Scientific Instruments, UK). The SEM images of the samples were obtained using an environmental scanning electron microscope ESEM XL 30 FEG (Philips, Netherlands), using a beam accelerating voltage between 5 kV and 20 kV, a pressure of nearly 10<sup>-4</sup> Pa and a resolution of 2 nm.

#### **3.4.6 Ultraviolet spectrophotometric analysis**

The determination of the amount of elastin peptides in TE and elastin digests was done through the adaptation of the quantification method of the peptide bond described

by Kreuzsch *et al.*, [305]. All measurements were done in a NanoDrop ND-2000c UV-Vis spectrophotometer (Thermo Scientific). Dilutions of PE digests of TE in a concentration range from 1.0 to 50.0  $\mu\text{g mL}^{-1}$  were used as standards; 1.2  $\mu\text{L}$  of each standard dilution were applied to the plate, and the absorbance was determined at 205 nm. Each sample was measured by triplicate. Elastin samples were diluted using elastase buffer and measured under the same conditions described for the TE standards. The concentration of elastin peptides in the samples was calculated by interpolation of sample absorbance on the standard curve.

## 3.5 Bioinformatics methods

### 3.5.1 Peptide sequencing

Particularly, MS/MS spectra acquired in MALDI-TOF/TOF experiments were processed into de-isotoped peak list with Mascot Distiller (Matrix Science, UK). This pre-process data and the raw data obtained in nanoESI-QqTOF MS/MS and Orbitrap MS were imported into the software Peaks Studio (version 7.5; Bioinformatics Solutions, Canada) [306], in which data processing and automated *de novo* sequencing of tandem mass spectra followed by database matching were carried out. The searches were carried out in the database SwissProt, which was taxonomically restricted to *Homo sapiens*. Enzyme specificity was set to none and hydroxyproline was adjusted as a variable modification. A peptide false discovery rate (FDR) threshold of 5 % was used for the QqTOF and MALDI-TOF/TOF data, while 1 % was accepted for Orbitrap data. The error tolerance of the precursor ion was fixed according to the calibration of the MS spectrometer: 40-50 ppm (QqTOF MS/MS data), 50 ppm (MALDI TOF/TOF MS/MS data) and 6.0 ppm (Orbitrap data). For the fragment ions, the mass error tolerance was set to 0.1 Da (QqTOF MS/MS data), 0.3 Da (MALDI TOF/TOF MS/MS data) and 0.015 Da (Orbitrap data).

### 3.5.2 Label-free quantification of peptide digests

MS raw data files obtained in different NanoHPLC-nanoESI-QqTOF MS experiments were imported into Progenesis QI for proteomics (64-bit version v2.0; Nonlinear Dynamics, UK) (<http://www.nonlinear.com/progenesis/qi>) for relative quantification between LC-MS analysis. During the data loading, a dead time correction was applied.

The peptide ion signal peak identified in the imported LC-MS analysis from the PE digests were automatically aligned to the most suitable reference mass spectra determined by the software, while the imported LC-MS analysis from the CG and MMP-9 digests were aligned using as reference the LC-MS analysis which gave the maximum number of vectors in the aligned set of samples when each LC-MS analysis was used as a reference. Furthermore, peak picking in all runs was performed using automatic sensitivity method; the maximum ion charge was set to six and the retention time range between 15 min and 65 min. All detected features were normalised based on a reference run selected by the software. Peptide identification was carried out manually by comparing the results of peptide sequencing with the  $m/z$ , charge and retention time of each peptide ion reported by Progenesis QI for proteomics. A criterion of  $m/z$  and retention time windows (50 ppm and 3 min, respectively); and unique peptides were used to deal with cases of multiple peptide identification assignments.

### 3.5.3 Statistical analysis

The elastin degradation by CG and MMP-9 was studied through a factorial design  $3^3 \times 2^1$ . Four factors were evaluated: the structural changes associated with natural ageing of the elastin (children and old adult individuals), enzyme (CG, MMP-9 and NEP), time of *in vitro* degradation (6 h, 12 h and 48 h) and the biological replicate (three individuals). The normalised abundance of peptides quantified in samples of CG and MMP-9 digests during the LFQ analysis was used to calculate the sum of the normalised abundance of the peptides obtained in each domain. Furthermore, the raw data according to the enzyme and type of elastin were analysed separately and all together in a linear model of the variance in two ways of classification to establish which domains presented a significantly different amount of peptides (p-value < 0.05). The model was validated using Bootstrapping analysis. Moreover, the influence of all factors tested during the experiment over the amount of peptides was evaluated. The domains in which peptides were obtained under all conditions (enzyme, substrate, sampling time and biological replicates) were modelled in a fourth order interaction model of fixed effects with correlated errors for the dependent variable (sum of peptides' amount). The model was validated in a normality test of the errors. The other two assumptions of the model, homoscedasticity and statistical independence of the errors were not tested

because these two assumptions were included in the model (variance structure and the correlated observations over the time).

On the other hand, normalised abundances of the peptides obtained from the LFQ analysis of samples digested with PE were analysed using ANOVA or Kruskal-Wallis tests to identify statistically significant differences ( $p$ -value  $< 0.05$ ). Peptides with  $p$ -value  $< 0.05$ , maximum fold change (FC)  $\geq 2$ , and maximum coefficient of variation (CV)  $\leq 70\%$  were selected to be analysed using principal component analysis (PCA) and hierarchical cluster analysis (HCA). The HCA was done over the first five principal components identified during the PCA.

All statistical analysis were performed with R 3.2.2 and R Commander (Rcmdr version 2.0-4; FactoMineR package) [307, 308].

## 4 Results

### 4.1 Workflow suitability to distinguish changes in abundance of elastin hydrophobic peptides

Quantitative comparison between samples evaluated under similar conditions allows identifying modifications in the amount of peptides associated with different biological or experimental conditions. Quantitative differences in elastin isolated from different donors were investigated using a workflow which involves three distinct stages: a gentle elastin isolation method, the enzymatic degradation of the protein and its MS and LFQ analysis. The isolation of the elastin from skin samples was done following the methodology described by Schmelzer *et al.* [149], which has demonstrated to preserve the morphological characteristics of the elastin fibres. PE was chosen for the complete degradation of the elastin samples, except for the evaluation of the elastolytic activity of three different enzymes (Section 4.2). All digested elastin samples were analysed under identical experimental conditions by nanoHPLC-nanoESI-QqTOF MS(/MS), and this data was subjected to LFQ analysis. The capacity of two software tools, namely PEAKS (Bioinformatics solutions) and Progenesis QIP (NonLinear Dynamics), to identify and integrate complete peaks was evaluated (data not shown). Progenesis QIP identified the higher amount of full peaks and reported less missing values; then it was chosen as LFQ software to be used during this thesis.

To characterise the variation associated with the experimental procedure, the effect of some sources of variation (biological, technical and instrumental) on the results obtained in the LFQ workflow was evaluated. The analysis was carried out with an undergraduate biochemistry student, and the results were reported in her thesis [309]. Overall, it was found that 90 % of the peptides evaluated in LFQ had a 70 % of the maximum coefficient of variation (CV) associated with the three sources studied; the biological variation is the leading cause of dispersion of results obtained with the LFQ workflow. Moreover, it was also found that after the enzymatic degradation of the elastin samples, a residual pellet, which represents maximum 8 % of the initial weight of elastin, could either be present or absent.

Taking into account that elastin could present slight variations in its dissolution, the effect of changes in the elastin concentration over the amount of peptides was studied. Five concentration levels corresponding to an elastin concentration range between 80 % and 120 % (expressed as the percentage of the initial concentration of the undigested sample) were analysed. This elastin concentration range includes the variation in total degradation of the elastin pellet previously found.

Overall, during MS/MS analysis, 157 elastin peptides were identified, which represented a 57 % of coverage of TE isoform 2 sequence. In the LFQ analysis of MS spectra, only four of the 151 quantified elastin peptides had more than 70 % of the CV. Furthermore, LFQ results showed that the variation of 20 % of the concentration of elastin induced changes in the amount of peptides from the different protein domains. However, these differences in the amount of quantified peptides were statistically significant ( $p \leq 0.05$ ) only in 69 of 151 peptides. This low variation is also reflected in the fold change (FC) calculated for the peptides. The majority of elastin peptides (137) presented an FC less than 2. Regarding the pattern of change of the elastin peptide amount, the greater part of the peptides did not present any change (for instance, peptides CEf\_32 and CEf\_46; Figure 9). Few peptides presented a slightly decreasing pattern of change in their mean (for example, peptide CEf\_35, Figure 9); however, these peptides had an FC lower than 2 and did not present significant statistical differences into the concentrations evaluated ( $p > 0.05$ ). Only ten peptides (Table A-1, Appendix 1), showed a clear increasing pattern of change with a significant difference between the amount of peptides estimated at the different concentrations ( $p \leq 0.05$ ) and an FC higher than 2, such as peptide CEf\_87 (Figure 9).

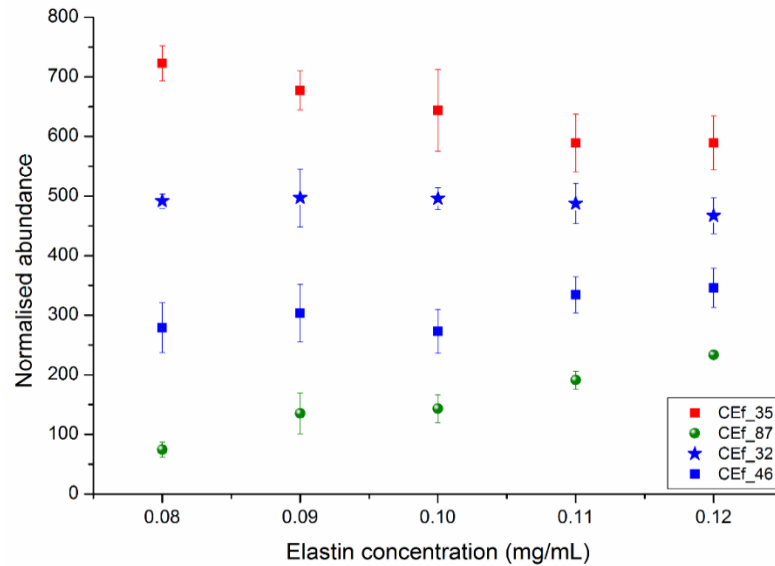


**Figure 9. Normalised abundance of selected elastin peptides depending on the elastin concentration**

The normalised abundance of the majority of peptides did not show a significant change ( $p > 0.05$ ) due to the variation of the elastin concentration (blue). Other peptides have shown a decreasing pattern of change associated to the increase of concentration of the protein, but without significant differences ( $p > 0.05$ ) (red). Only ten peptides increased their normalised abundances with the increasing elastin concentration, and they presented significant statistical differences ( $p < 0.05$ ) (green). Data shown as mean  $\pm$  s.d. (n=4).

A multivariate analysis was performed on the 151 elastin peptides to identify differences between the elastin samples. Results are shown in the principal component analysis (PCA) scores plot and variable graphic in Figure 10 and Figure 11. The first principal component (PC), which corresponds to the concentration effect, describes 40.8 % of the variation in the data set. Samples show a slight distribution along the PC 1, which could be associated with the increasing concentration. However, this variation is not enough to generate clustering of the samples according to the elastin concentration in the range of 0.09 mg/mL to 0.12 mg/mL. Only samples with a concentration of 0.08 mg/mL seem to have a slight separation. Due to the fact that samples were taken from one elastin sample, the instrumental variation could be associated with PC 2, and this explains 22.3 % of the data set variation. Apparently, it has a random effect on the normalised abundance of the peptides. It was not possible to identify a pattern in the distribution of the samples associated with this PC 2 (Figure 10).



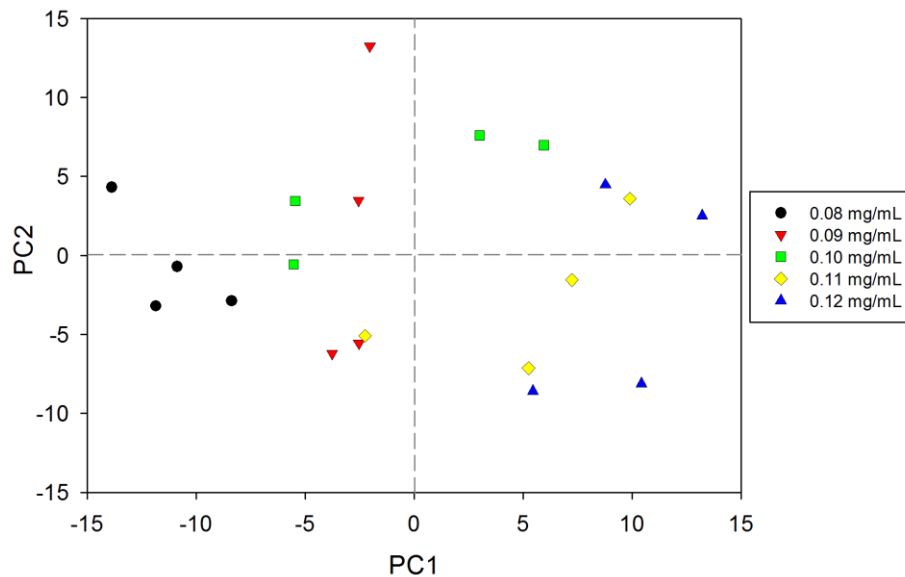


**Figure 10. PCA scores plot of samples with different elastin concentration**

The PCA reflects a few differences between the five elastin concentration levels based on the 151 elastin peptides identified after PE digestion and LFQ analysis of elastin sample.

Furthermore, a random distribution of peptides and domains was determined in variable graphic (Figure 11), which allows identifying the possible correlation of each variable (all elastin peptides are presented according to their domains) with the PCs. Then, the elastin concentration in the evaluated range and the instrumental variation do not influence the change of the normalised abundance of peptides from any domain in particular.

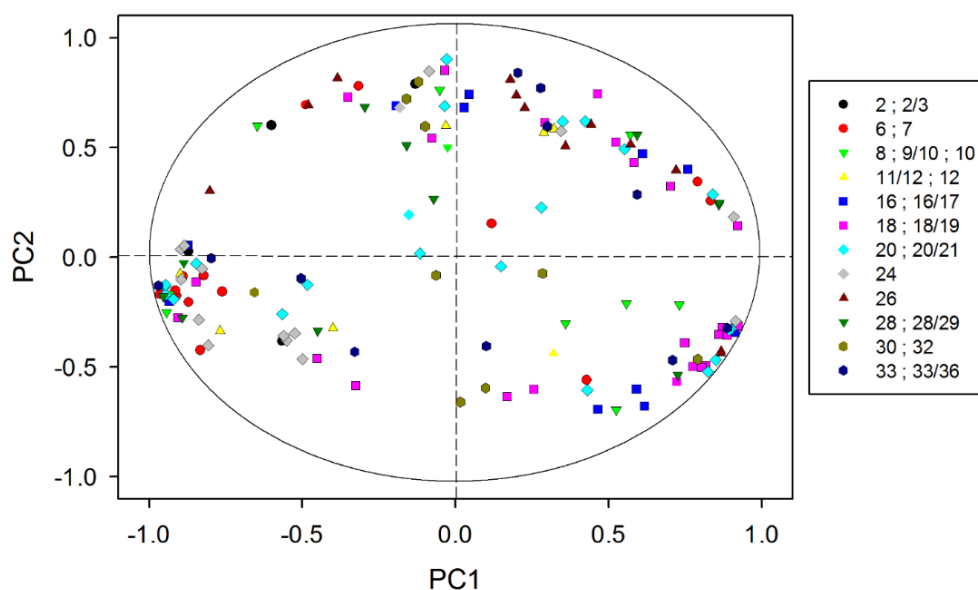


**Figure 11. Variable graph of peptides quantified in samples with different elastin concentration.**

Elastin peptides identified after PE digestion and LFQ analysis of elastin samples (151) are shown according to the domain from which they derive.

In conclusion, the LFQ workflow allows determining the changes in abundance of elastin peptides. Furthermore, each peptide must have a CV less or equal to 70 %, an FC equal or higher than 2 and statistically significant differences ( $p \leq 0.05$ ) to reflect a change in the biological condition evaluated rather than the variation associated with the experimental procedure.

## **4.2 Susceptibility of human skin elastin towards degradation by biologically relevant proteases**

The quantitative analysis of the enzymatic susceptibility of the different domains of elastin was based on the assumption that solvent-exposed domains of elastin are the first sites cleaved by the enzymes, therefore peptides found in early times and the higher amount could reflect a higher susceptibility of distinct domains to the enzymatic attack. Elastin samples were isolated from healthy donors` skin, whose ages were 10 (children skin elastin (CE); n=3), 75 and 90 (old adult skin elastin (OE); n=1; 2). Samples of TE were used as a control of the enzymes` activity. Each of the elastin and TE samples was incubated with CG, MMP-9 and NEP separately. Samples of the digests were taken after 6 h, 12 h and 48 h. Qualitative and quantitative characterisation of changes in the samples were done using MS (MALDI-TOF and nanoHPLC-nanoESI-QqTOF) techniques. In addition, an LFQ approach was used to make a quantitative comparison of nanoESI-QqTOF-MS results. Moreover, an UV spectrophotometric method was used to quantify the total peptide concentration in the supernatants of the TE and elastin digests by the absorbance of the peptide bond. At the end of the incubation time pellets of elastin remained in all CE and OE samples digested with the three enzymes.

### **4.2.1 Elastase activity of NEP and its relation with previous elastic damage**

The susceptibility of TE, CE and OE towards NEP after 48 h of digestion was qualitatively evaluated using MALDI-TOF MS. TE was completely degraded by NEP; no signal of intact TE (approximately  $m/z$  60000) was detected in samples except for the negative control, which did not contain any enzyme (Figure 12). Although the majority of peptides had  $m/z$  lower than 10000, few peptides ranging from 10000 to 20000 were detected. Replicated samples showed similar degradation patterns among them (data

not shown). Regarding the NEP digests of skin elastin samples, MALDI-TOF MS analysis only revealed few low-intensity peptide signals in OE samples. NEP digests did not show any released peptides in CE that could be identified by MALDI-TOF MS (Figure 12). Moreover, NEP digests showed a high variation between the biological replicates of CE and OE samples (data not shown).

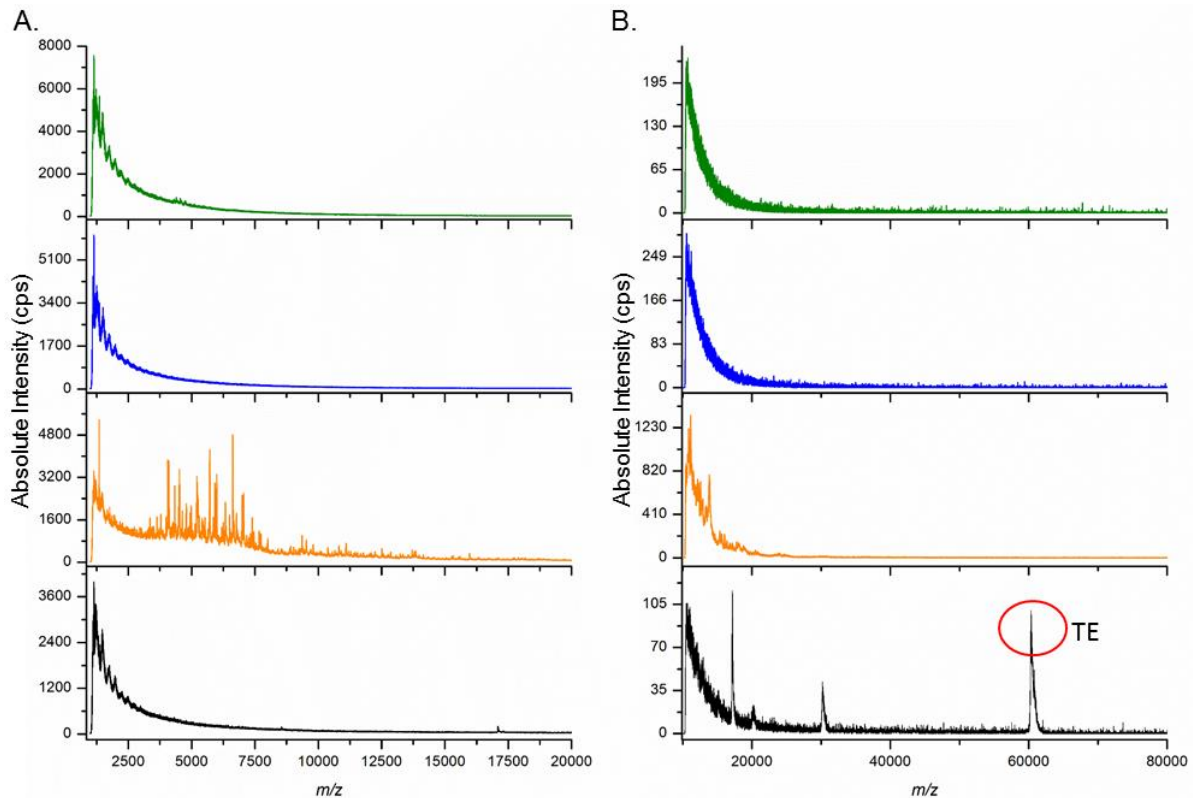


**Figure 12.** MALDI-TOF mass spectra of TE and skin elastin samples degraded by NEP.

Positive-ion MALDI-TOF mass spectra acquired in the linear mode in a low (A) and high (B)  $m/z$  range. The NEP digests of TE, CE and OE are shown in orange, blue and green, respectively. Moreover, the negative control of TE is shown in black.

Supernatants of TE, CE and OE samples digested with NEP were also evaluated using nanoHPLC separation and nanoESI-QqTOF-MS analysis. Preliminary results revealed that NEP digests had a low abundance of peptides, especially in CE and OE samples. In order to achieve a better characterisation of the cleavage pattern of elastin by NEP, these samples were studied using nanoHPLC separation followed by a more sensitive high-resolution Orbitrap MS analysis.

A significant difference between the number of cleavage sites, the number and the length of peptides obtained from TE, CE, and OE samples was found in the Orbitrap MS

analysis. Sequence coverages of 98 %, 24 % and 67 % in the TE, CE, and OE samples were determined, respectively (Figure 13).

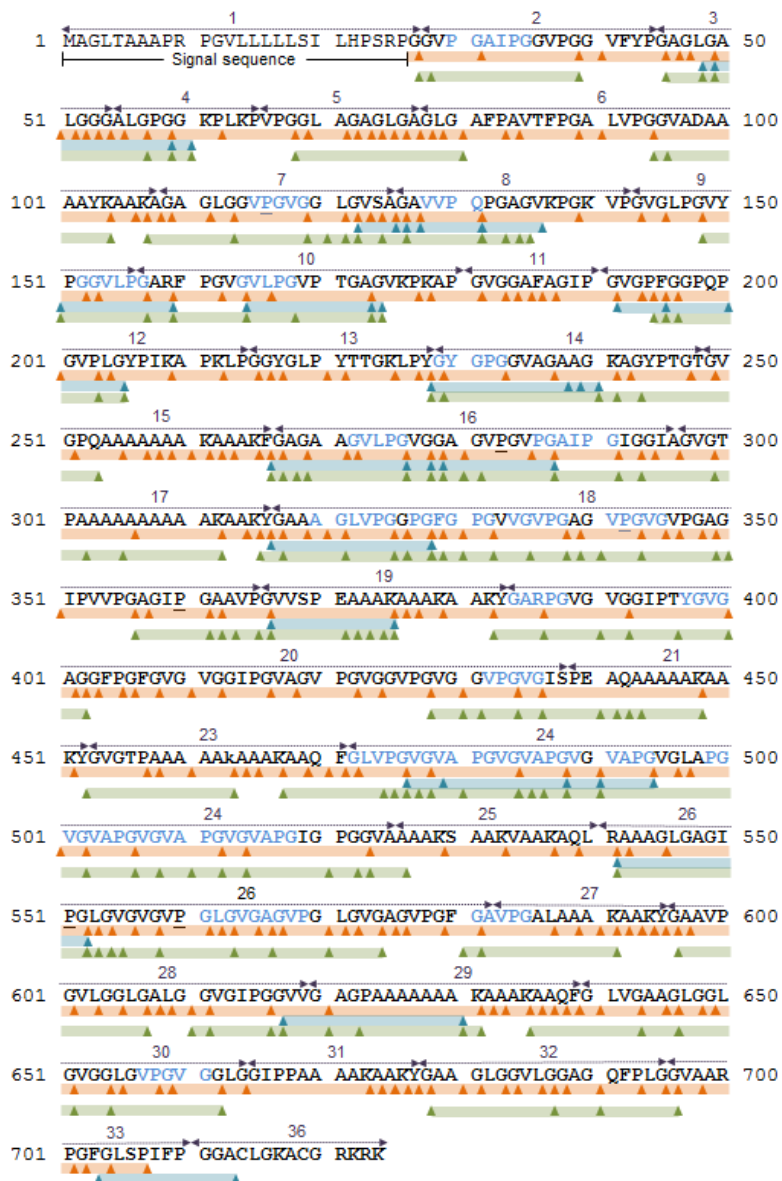


**Figure 13.** Cleavage sites identified after digestion of TE and skin elastin samples with NEP.

Cleavage sites are shown based on the sequence of human TE isoform 2 (Swiss-Prot accession number P15502-2) from Orbitrap MS/MS data. Cleavage sites are marked with triangles, and the identified sequences are represented by solid lines; orange, blue and green lines label all peptides identified in TE, CE and OE samples, respectively. Matrikines are shown in blue. Hydroxylated Pro residues have been emphasised with underline letter 'P'.

NEP produces a larger (8 to 65 amino acids; weighted arithmetic mean (w.a.m.): 26) and a higher (606 peptides) number of peptides from TE samples. In CE and OE samples, only 27 and 130 peptides were identified, respectively. Peptides' length was almost the same (CE: 9 to 15 amino acids; OE: 8 to 19 amino acids; w.a.m.: 11). Peptides from all domains (except domain 36) were identified in TE digests. In contrast, it was not

possible to identify peptides in several domains of the TE in skin elastin samples, particularly in CE samples; no peptides from domains 11, 13, 25, 31 and 36 were found in both skin samples. Additionally, no peptides were identified upon Orbitrap MS analysis in domain 36 of OE as well as in domains 2, 5, 6, 20, 21, 23, 27, 28, 30 and 32 of CE.

Overall, 290 cleavage sites were identified in TE samples, whereas in CE and OE only 44 and 164 positions were found, respectively. NEP showed a clear preference to cleave N-terminal domains in CE samples, while cleavage sites in TE and OE samples were distributed over the protein sequence. Almost all domain 2 (90 %) in TE was cleaved, while domain 21 contained the fewest amount of cleavage points (14 %). Although CE presented the lowest percentage of cleavage among the three samples, the NEP cleaved CE mainly in domains 3, 4, 8, 10, 14 and 16, which are also well cleaved in TE and OE samples. Moreover, OE samples were also well cleaved in domains 7, 18, 19, 24, 26, 28 and 29 (Figure 14). Altogether, 23 cleavage sites and three peptides (domains 10; 16 and 26) were common in all samples. Only 8 cleavage sites and 13 peptides from domains 3/4, 7-8, 9-10, 12, 14, 16, 19, 24, 26 and 28/29, were shared by both skin elastin samples.

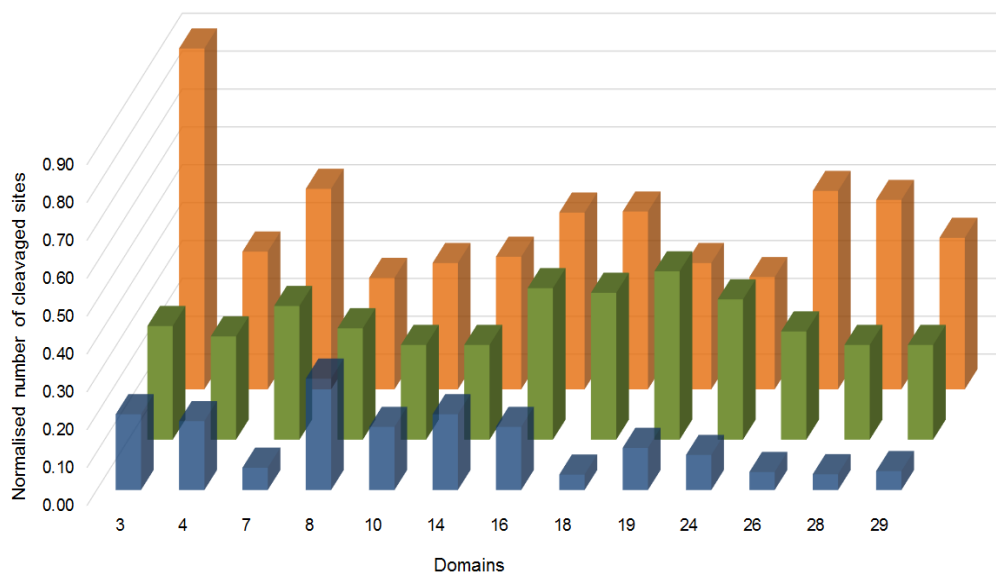


**Figure 14. Normalised number of cleavage sites identified in samples of TE and skin elastin digested with NEP.**

Number of cleavage sites identified in each domain were normalised regarding the number of a.a. of the respective domain. The graphic shows domains with  $\geq 0.25$  cleavage sites per residue in at least one of the two skin elastin samples. Results obtained from TE, CE and OE are shown in orange, blue and green, respectively.

The cleavage site specificity of NEP in TE and human skin elastin, based on the number of cleavage sites identified by MS analysis of the digests, are summarised in Table 6. In line with previous findings [310-312], NEP predominantly cleaved at the N-terminal site of the small aliphatic and/or hydrophobic amino acids Ala, Gly and Val, which are found in TE (28 %, 27 % and 17 % of all identified cleavage sites), CE (19 %, 28 % and 28 %), and OE (29 %, 23 % and 24 %). At this position, NEP also did not tolerate any amino acid with polar side chain in TE samples. Additionally, at the C-terminal position, NEP accepts Gly and Ala: TE (52 % and 21 %), CE (51 % and 16 %) and OE (62 % and 12 %). Moreover, at this position, NEP cleaved in a low percentage (7 %) the aromatic and bulky amino acids Tyr and Phe in CE samples. Throughout the second and fourth position in N-terminal sites, NEP cleaved TE and skin elastin samples following the order Gly > Ala > Val > Pro, which corresponded to the amino acids abundance in the elastin sequence. In the C-terminal residue, NEP mainly tolerated the same amino acid, but in a different order. At the P2 position, the cleavage preference in TE followed the order Ala > Pro > Gly > Val. Finally, in skin elastin samples, it was found that the cleavage in P2 follows Pro > Gly/Ala >> Val order.

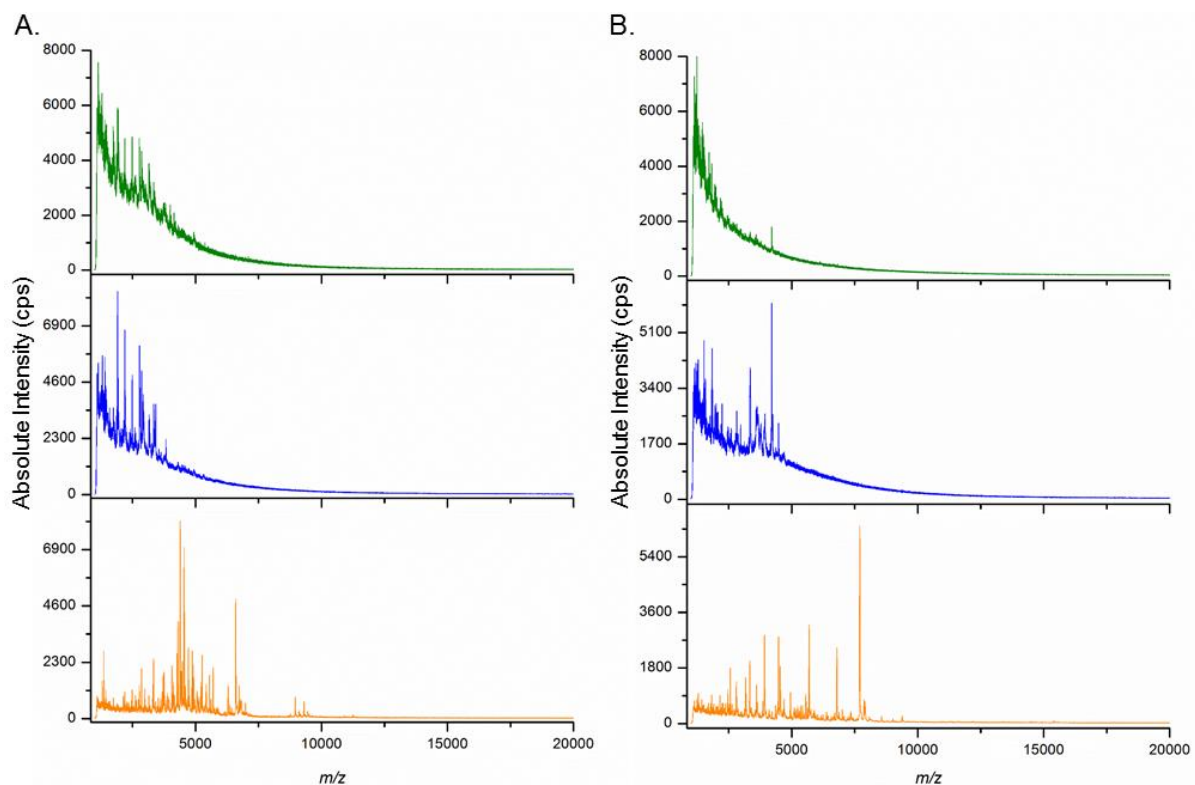
AA	P4 / %			P3 / %			P2 / %			P1 / %			P1' / %			P2' / %			P3' / %			P4' / %		
A	26	19	18	24	26	19	25	16	21	21	16	12	28	19	29	22	23	27	20	16	21	18	21	20
P	13	16	19	8	12	11	20	30	24	5	2	2	3	5	7	6	12	11	20	23	19	12	14	13
L	6	5	4	8	5	6	8	9	9	5	2	2	11	2	5	7	9	3	6	7	2	8	5	4
R	0	2	0	0	0	0	1	0	0	1	5	2	0	0	0	1	0	1	0	0	0	1	0	1
Q	0	0	1	2	2	1	1	2	1	1	2	2	1	0	1	1	0	1	1	0	2	1	5	1
S	1	2	1	0	2	2	1	2	0	0	0	1	1	0	0	1	2	1	1	5	1	1	1	0
Y	4	0	1	1	0	1	2	0	3	2	7	2	3	2	4	3	2	1	2	0	1	2	2	3
F	2	0	3	1	0	1	4	0	2	2	7	2	4	5	2	4	0	2	3	0	2	4	2	2
K	5	2	3	7	0	3	5	5	1	9	2	8	3	9	2	3	7	2	5	5	5	4	14	6
T	1	2	1	1	2	1	1	0	0	0	0	1	1	0	1	1	0	0	1	0	1	1	0	1
I	1	2	3	2	5	3	1	0	1	0	0	0	2	0	2	3	2	2	2	2	2	3	0	2
V	13	19	18	13	16	16	13	9	17	1	5	2	17	28	24	14	14	17	12	14	17	11	12	13
G	28	30	28	32	30	34	19	26	19	52	51	62	27	28	23	33	28	31	27	28	25	33	26	29
D	0	0	0	0	0	0	0	0	0	0	0	0	0	0	0	0	0	0	0	0	1	0	0	1
E	0	0	1	0	0	1	0	0	1	0	0	1	0	0	0	0	0	0	0	0	0	0	0	1
C	0	0	0	0	0	0	0	0	0	0	0	0	0	2	0	0	0	0	0	0	0	0	0	0
	TE	CE	OE	TE	CE	OE	TE	CE	OE	TE	CE	OE	TE	CE	OE	TE	CE	OE	TE	CE	OE	TE	CE	OE

Table 6. Occurrence of different amino acids at the substrate positions P1-P4 and P1'-P4' after digestion of TE and skin elastin samples with NEP.

Values are based on the number of cleavage sites identified upon MS analysis (nanoESI-Orbitrap data) of the digests.

#### 4.2.2 Degradation of TE and skin elastin samples by CG and MMP-9

MALDI-TOF MS analysis of the supernatant of the TE, CE and OE digests revealed that MMP-9 and CG cleaved the monomer comprehensively and released a high amount of peptides with  $m/z$  lower than 10000 from the three samples (Figure 15). Only in OE samples digested with CG, some low-intensity peptides with  $m/z$  between 10000 and 60000 were identified. In addition, each enzyme showed clear differences between the patterns of peptides produced with CE and OE samples. Interestingly, biological replicates of CE digested with CG and MMP-9 did not present differences among them, while OE biological replicates showed slight variations (data not shown).



**Figure 15.** MALDI-TOF mass spectra of TE and skin elastin samples degraded by CG and MMP-9.

Positive-ion MALDI-TOF mass spectra acquired in the linear mode for CG (A) and MMP-9 (B) digests of TE (orange), elastin isolated from children (blue) and old adult (green) skin samples.

Regarding the nanoESI-QqTOF results, comparable sequence coverages were obtained in TE and elastin samples digested for 48 h with both enzymes, and a smaller amount of peptides were sequenced in TE compared to the amount obtained from skin elastin samples. Based on TE isoform 2 sequence, sequence coverages of 80 % (106 peptides), 72 % (180 peptides) and 74 % (178 peptides) for CG and 78 % (130 peptides), 66 % (199 peptides) and 69 % (176 peptides) for MMP-9 were found in TE,

CE and OE digests (Figure 16A and B.). Peptides derived from domains 13, 23, 24, 25 and 32/33 were not identified in TE samples digested with CG, while peptides from domains 18, 21, 25, 28/29 and 29/30 were not determined in MMP-9 digests of TE. Interestingly, the results obtained from skin elastin samples digested with CG showed peptides derived from domains 13, 23, 24 and 32/33, as well as MMP-9 digests of the skin elastin showed peptides derived from domains 18, 28/29 and 29/30.

With respect to skin elastin samples treated with CG, they did not contain peptides from domains 4, 25 and 31 that could be identified in the nanoESI-QqTOF analysis. Particularly, peptides from domains 13, 15 and 23 were not determined in CE samples, while only peptides from domain 17 were not particularly identified in OE samples. Similarly, nanoESI-QqTOF results obtained from the skin elastin digested with MMP-9 did not show peptides derived from domains 19, 21, 25, 27 and 29; particularly, peptides derived from domains 13, 14 and 15 in CE samples and domains 4 and 11 in OE samples were not identified in the MMP-9 digests either. On the other hand, skin samples digested with each enzyme shared a high number of peptides. From all peptides identified, CG digests of CE and OE samples had nearly 66 % (119 peptides) in common, although skin elastin samples digested with MMP-9 shared 92 % (120 peptides).

On the other hand, both enzymes produced longer peptides in TE samples. These peptides contain from 5 to 63 amino acids in CG digests; and from 5 to 50 amino acids in MMP-9 digests. Additionally, their w.a.m. is 19 and 17 amino acids, respectively. In the digests of CE and OE with both enzymes, peptides had a similar length; CE and OE samples contained peptides with a length (calculated as w.a.m.) of 13 and 11 amino acids in CG digests, although 15 and 13 amino acids were found in MMP-9 digests.



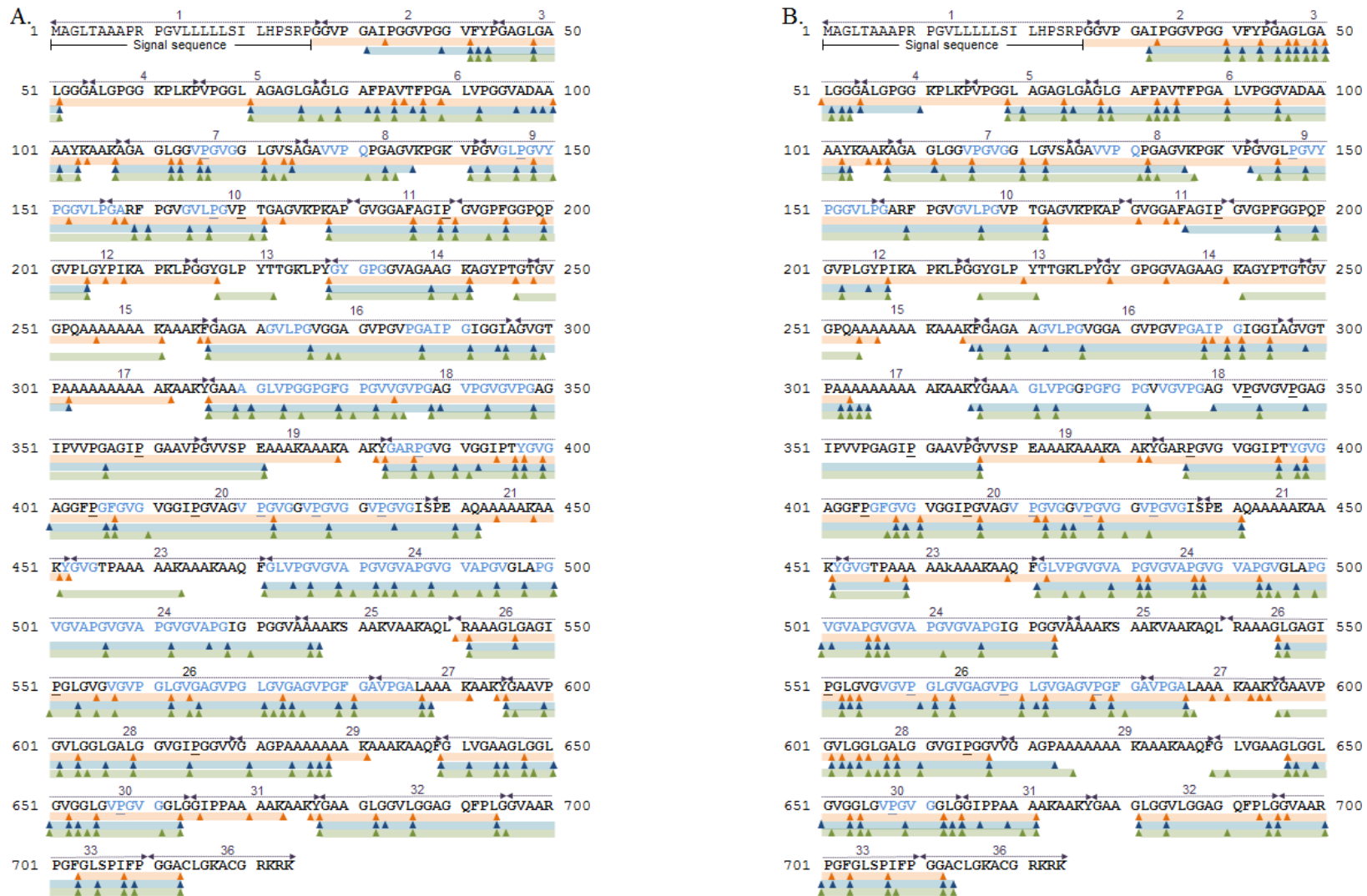
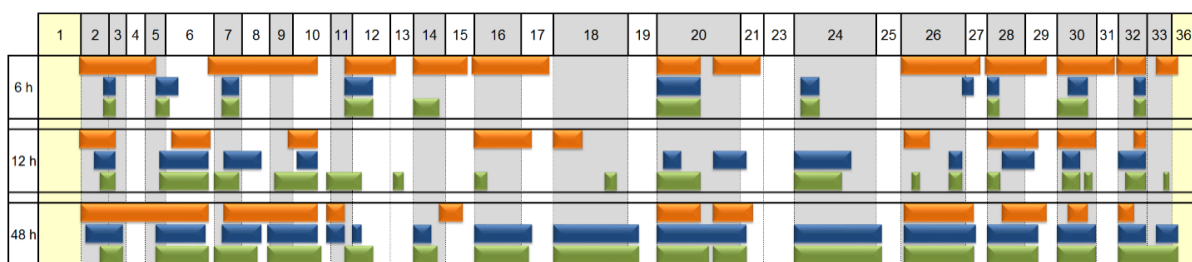


Figure 16. Cleavage sites identified after digestion of TE and skin elastin samples with CG (A) and MMP-9 (B).

Cleavage sites are shown based on the sequence of human TE isoform 2 (Swiss-Prot accession number P15502-2) from nanoESI-QqTOF-MS/MS data. Cleavage sites are marked with triangles, and the identified sequences are represented by solid lines; orange, blue and green lines label all peptides identified in TE, CE and OE samples, respectively. Matrikines identified in skin elastin samples are shown in blue. Hydroxylated Pro residues have been emphasised with underline letter 'P'.

On the other hand, LFQ analysis revealed 85, 167 and 161 quantifiable elastin peptides in TE, CE and OE samples digested with CG. A higher amount of peptides in TE and CE samples was found in MMP-9 digests. A total number of 110, 194 and 133 elastin peptides were quantified in TE, CE and OE samples digested with MMP-9, respectively. Figure 17 and Figure 19 show the sequence coverage obtained from the peptides quantified after 6 h, 12 h and 48 h. The amount of each peptide estimated at each sampling point is represented in Figure A-1 to Figure A-6 (Appendix 2).

Regarding CG digests, peptides were quantified in almost all domains of TE samples after 6 h, except domains 6, 18, 19, and 23-25. New peptides were quantified in the whole protein after 12 h and mainly after 48 h, excluding domains 11-14, 15/16, 27/28, 30 and 33/36. In contrast, quantifiable elastin peptides from skin elastin samples were measured mainly after 48 h. In CE samples, peptides from domains 2/3, 5/6, 6, 7, 11/12, 20, 24, 26/27, 28, 30 and 32 were quantified after 6 h, while peptides from domains 8/9, 10/11, 14, 16, 16/17, 18, 18/19, 24/25 and 33/36 were exclusively quantified after 48 h. Only domains 10, 20/21, 26/27 and 28/29 presented new quantifiable peptides after 12 h. Similar results were found in OE samples; peptides derived from domains 2/3, 5/6, 7, 11/12, 14, 20, 24, 28, 30 and 32 were quantified after 6 h. New peptides obtained from domains 6, 6/7, 9-11, 13, 16, 26, and 33 were measured after 12 h. The other domains (7/8, 16/17, 18, 20/21, 24/25 and 28/29) only presented quantifiable peptides at the last sampling point (48 h) (Figure 17).



**Figure 17.** Sequence coverage obtained from peptides quantified after 6 h, 12 h and 48 h in CG digests.

The domain structure of TE isoform 2 is shown true to scale. The N-terminus with the signal sequence and the hydrophilic C-terminus are shown in yellow, while hydrophobic domains are displayed in grey. The sequence coverage for TE (orange), CE (blue) and OE (green) samples digested with CG resulting from peptides quantified after 6 h, 12 h and 48 h are presented as solid bars. Data was obtained from nanoESI-QqTOF MS measurements and LFQ analysis.

Regarding peptide abundance estimated at each sampling point, the majority of peptides quantified in TE samples digested with CG, had a maximum of 7500 arbitrary units (a.u.) of average normalised abundance. Only five peptides (domains 9/10 (TC26), 11/12 (TC32), 16/17 (TC44), 28/29 (TC69) and 30/31 (TC65)) showed a higher

average abundance (until 40000 a.u. of normalised abundance) after 48 h (See Figure A-1 Appendix 2). In contrast to TE samples, a lower abundance was determined for peptides from skin elastin samples digested with CG. The majority of peptides from CE and OE samples had average intensities lower than 750 a.u. and 1500 a.u. of normalised abundance, respectively. In all three samples (TE, CE and OE), peptides quantified after 6 h presented the highest total abundance (48 h) (See Figure A-2 to Figure A-3; Appendix 2).

Overall, the peptide abundance increase had a positive correlation with the time. Peptide TC82 is an example of the positive relationship found between TE, CE and OE peptides abundance and time (Figure 18).

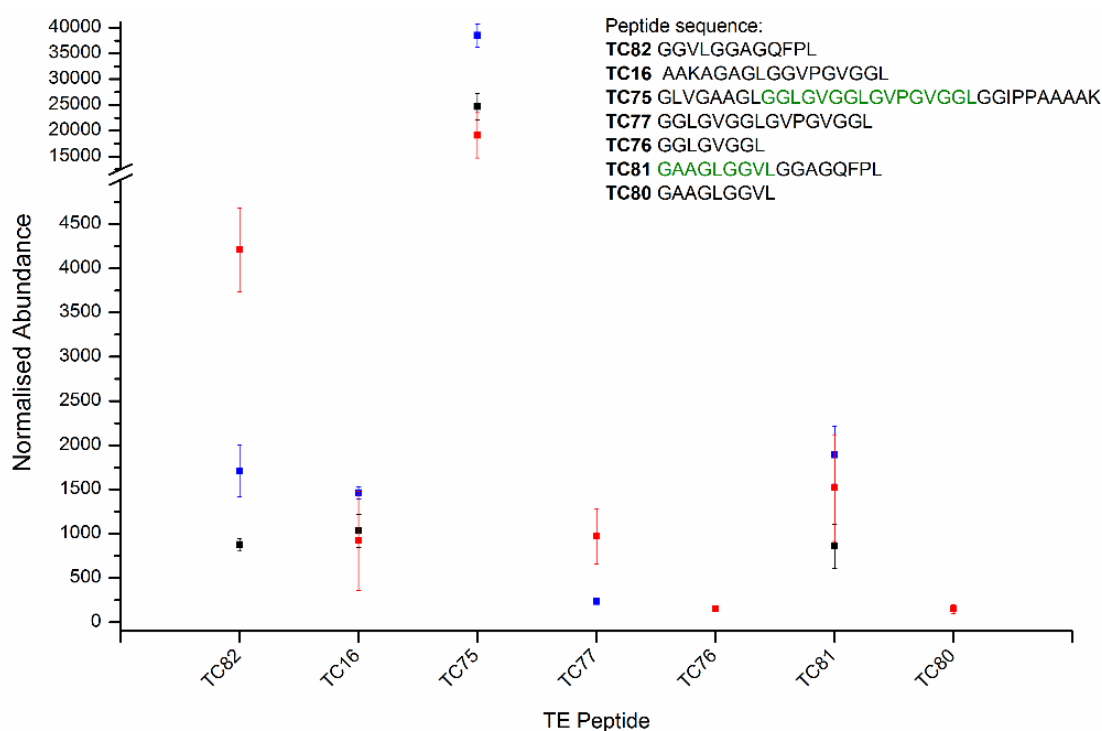


**Figure 18.** Changes in normalised abundance of selected TE peptides depending on sampling point.

The relative normalised abundance of peptides determined after 6 h (black), 12 h (blue) and 48 h (red) is shown for some peptides quantified in TE samples digested with CG. Data is presented as mean  $\pm$  s.d. (n=2).

In particular, few TE peptides did not have a positive correlation of their concentration with the time, and their amount after 48 h was lower than after 6 h or 12 h. This pattern could be associated with the dispersion of the results in some TE peptides derived from domains 6/7 such as TC16 (Figure 18) and TC17. However, other peptides from domains 12/13 (peptides TC37 and TC38), 26/27 (Peptides TC60, TC63) and 30-32 (TC75 and TC81) did not have a high variability in their replicates. Interestingly, new peptides were quantified after 12 h or 48 h, and whose sequences

were contained in the sequence of that peptide quantified after 6 h. For instance, peptide TC75 showed a lower abundance after 48 h; peptide TC77 (quantified after 12 h) and TC76 (quantified after 48 h) have sequences that are contained in the TC75 sequence (Figure 18). Other peptides (TC60, TC63 and TC81) had lower intensities than the ones determined after 12 h, as it is shown for peptide TC81; the peptide TC80, whose sequence is contained in the TC81 sequence, was quantified only after 48 h.

On the other hand, in MMP-9 digests of TE samples, the majority of quantifiable peptides were determined after 6 h in all the domains in which there were identified peptides, except for domains 8-11, 19, 20/21 and 33/36 in which peptides were quantified after 48 h. In addition, new peptides derived from domains 6-9, 11/12, 16/17, 20, 24, 26/27 and 30 were quantified after 12 h. In contrast with TE samples, CE samples digested with MMP-9 contained new quantifiable peptides derived from several domains at each sampling point. For instance, new peptides derived from domains 2/3, 5/6, 9/10, 16/17, 20, 24, 28 and 30 were quantified after 6 h, 12 h and 48 h. Domain 12 was the only domain with peptides quantified exclusively after 6 h, while peptides derived from domains 7, 8, 10, 11/12, 16, 20/21, 26 and 32-36 were quantified after 12 h and 48 h; identified peptides in other domains were quantified only after 48 h. Interestingly, OE samples showed a different pattern of quantifiable peptides. The majority of peptides in OE samples were quantified after 48 h. Only a few new peptides derived from domains 2/3, 24, 28 and 30 were measured at every sampling point. Particularly, some peptides from domains 6, 9/10, 20 and 26/27 were quantified after 12 h and 48 h (Figure 19).



**Figure 19.** Sequence coverage obtained from peptides quantified after 6 h, 12 h and 48 h in MMP-9 digests.

The domain structure of TE isoform 2 is shown true to scale. The N-terminus with the signal sequence and the hydrophilic C-terminus are shown in yellow, while hydrophobic domains are displayed in grey. The sequence coverage for TE (orange), CE (blue) and OE (green) samples digested with MMP-9 resulting from peptides quantified after 6 h, 12 h and 48 h, are presented as solid bars. Data was obtained from nanoESI-QqTOF MS measurements and LFQ analysis.

Regarding the amount of peptides, similar to the findings in samples digested with CG, MMP-9 produced the highest amount of peptides from TE samples. Overall, the TE peptides had abundances up to 8000 a.u. of normalised abundance. Only 8 peptides from domains 2/5 (TM7), 5 (TM15), 6 (TM20), 15/16 (TM45, TM46), 27/28 (TM81) and 30/31 (TM98) had higher abundances (10000 to 70000 a.u. normalised abundance) (Figure A-4, Appendix 2). Skin elastin samples presented a lower amount of peptides, especially in OE samples. Peptides in CE samples had abundances lower than 2000 a.u. of normalised abundance. However, four peptides (CM6, CM42, CM50, CM62 and CM150) had abundances between 2300 and 4500 a.u. of normalised abundance (Figure A-5 Appendix 2). The lowest normalised abundance of peptides was found in OE samples digested with MMP-9. The majority of peptides had amounts lower than 400 a.u. of normalised abundance, (Figure A-6, Appendix 2). In contrast to CG results, a high dispersion between the results of biological replicates was found for some peptides quantified in skin elastin samples digested with MMP-9 (CV over 70 %).

In addition, in the different samples digested with MMP-9, the amount of peptides obtained increased with time, in a positive correlation or in a random (increase/decrease) way such as it was previously described for TE samples digested with CG. Although a high number (17) of peptides showed a random relation between their abundance and incubation time in TE samples, only two of them had a high dispersion in the result that explains this pattern. Moreover, the other 15 peptides were quantified after 6 h along with peptides with different sequences; it was also found that part of this peptides' sequence with decreasing behaviour is the whole sequence or part of the sequence of other peptides quantified after 12 h or 48 h. On the other hand, similar to the CG results, all the peptides quantified after 6 h in CE samples digested with MMP-9 presented a positive correlation between the increase of their normalised abundance and the incubation time. Although the majority (8 of 12) of OE peptides quantified after 6 h enhanced their abundance over the time; only four peptides showed a random pattern which was related to the high variability of the results.

#### **4.2.3 Enzymatic susceptibility of the elastin domains analysed through their degradation by CG and MMP-9**

The susceptibility of the elastin domains towards enzymatic degradation was qualitatively evaluated through the number of cleavage sites per domain identified in

the nanoHPLC-nanoESI-QqTOF MS/MS analysis of the CG and MMP-9 digests. A high number of cleavage sites in the C-terminal and N-terminal regions were identified in skin elastin samples (Figure 20A and B). In these samples, both CG and MMP-9 cleaved in a large extent the domains 6, 24, 28, 30 and 33. Particularly, CG cleaved well domains 7, 10, 26 and 29, although domains 2, 3 and 5 were well cleaved by MMP-9 in both skin elastin samples.

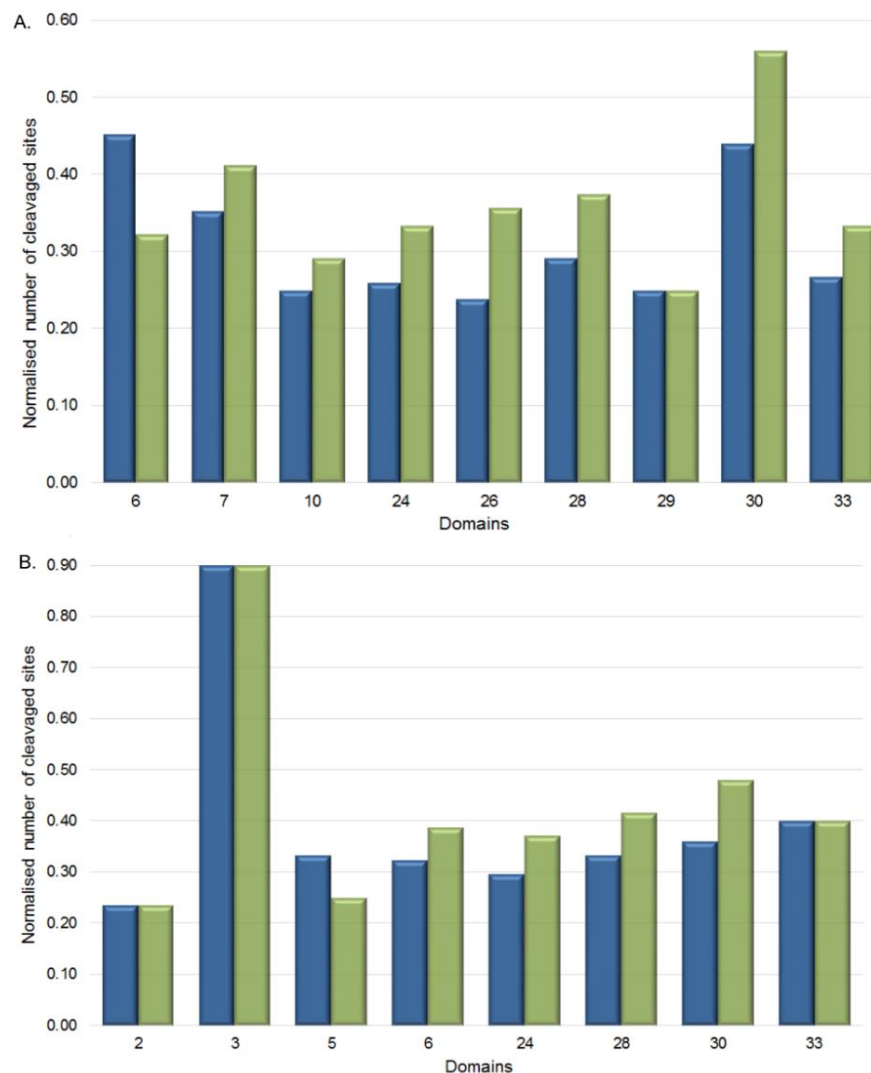


**Figure 20. Normalised number of cleavage sites identified in samples of skin elastin digested with CG and MMP-9, respectively.**

The number of cleavage sites identified in each domain was normalised with respect to the number of amino acids by domain. Graphics show domains with more than 0.25 cleavage sites per residue in the CE and OE samples digested with CG (A) or MMP-9 (B).

From a quantitative point of view, the susceptibility of the different domains of mature elastin towards the enzymatic degradation was evaluated by the sum of the normalised abundance of the quantifiable peptides by domain. This sum was calculated at each sampling point. CG could degrade the domains of the protein in CE and OE

samples similarly. As it is shown in Figure 21A for CE samples, a high amount of quantifiable peptides were mainly derived from domains 7, 11-12, 20, 20/21, 24, 26/27, 28 and 30. All these domains included peptides quantified in the three sampling points. Similar results were obtained with OE samples (Figure 21B); domains 7, 10, 11-12, 20, 24, 28 and 30 contained the highest amount of quantifiable peptides.

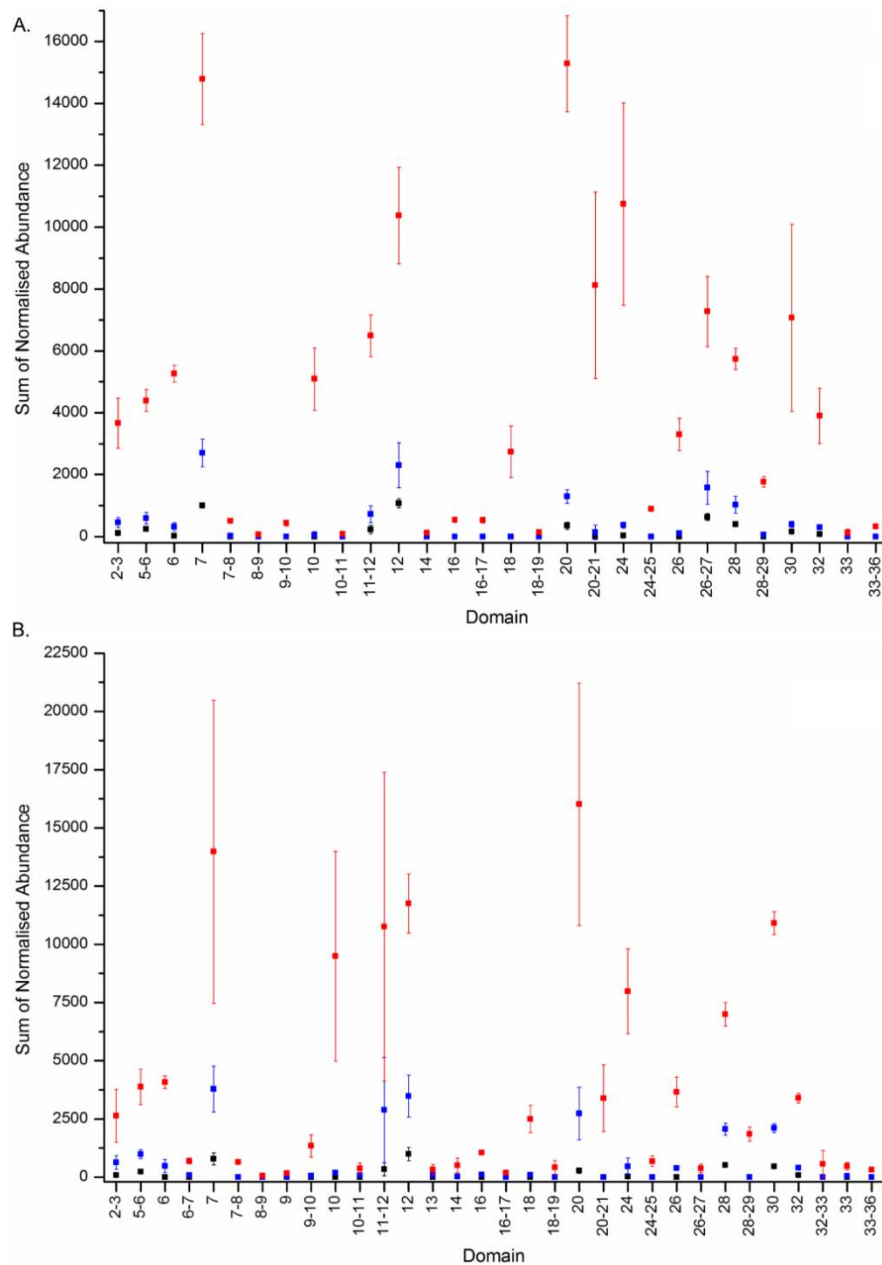


**Figure 21. Sum of normalised abundance by domain of elastin peptides solubilised from skin elastin digested with CG.**

The sum of the normalised abundance of elastin peptides in each domain, calculated after 6 h (black), 12 h (blue) and 48 h (red) in CE (A) and OE (B) samples digested with CG. Data is presented as mean  $\pm$  s.d. (n=3 biological replicates).

In the case of skin elastin samples digested with MMP-9, the profile of degradation of CE and OE samples was similar (Figure 22A and B). It was determined that the highest amount of the sum of the normalised abundance of peptides in both samples was obtained from domains 2/3, 5/6, 6, 9/10, 16/17, 20, 20/21, 24, 26, 26/27, 28 and 30. For all domains, a lower amount of peptides was estimated in OE samples than in CE samples. However, the domains with a higher amount of peptides involved peptides whose amount was determined in the three sampling points.

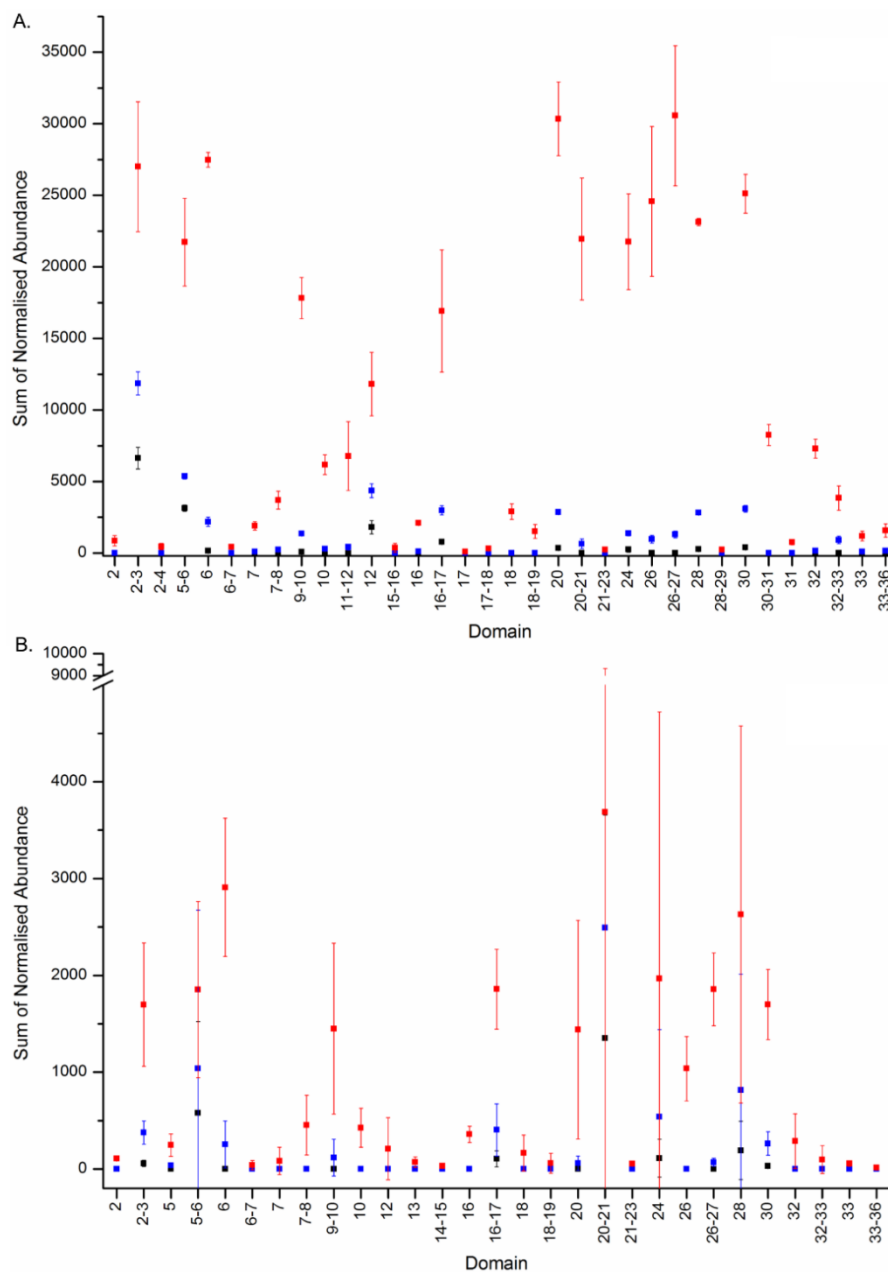


**Figure 22. Sum of normalised abundance by domain of elastin peptides solubilised from skin elastin digested with MMP-9.**

The sum of the normalised abundance of elastin peptides in each domain, calculated after 6 h (black), 12 h (blue) and 48 h (red) in CE (A) and OE (B) samples digested with MMP-9. Data is presented as mean  $\pm$  s.d. (n=3 biological replicates).



Data, for each enzyme and as a whole, was analysed using a linear model of the variance in two ways of classification to investigate which domains presented a significantly different amount of peptides. Results of the analysis according to the enzyme showed that the mean of the estimated abundance of peptides by domain (induced by CG and MMP-9 separately and both together) changed in a significant way ( $p=0.00$ ) due to the interaction between incubation time and domain. Results obtained with CG data showed that the amount of peptides by domains estimated after 6 h did not present significant differences among domains. In the second sampling point, only domain 7 showed significant difference from the other domains. The amount of peptides estimated after 48 h was clearly different among domains. After 48 h, the sum of the amount of peptides estimated in domains 2/3, 5/6, 6, 7, 10, 11/12, 12, 20, 20/21, 24, 26, 26/27, 28, 30 and 32 was significantly ( $p=0.00$ ) higher than the amount estimated in other domains (Figure A-7, Appendix 2).

These domains also showed that their abundance increased in a significant way at each sampling point ( $p=0.00$ ), except for domain 2/3, which only showed a significant difference between its abundance after 6 h and 48 h. Regarding MMP-9 results, it was not possible to identify any differences in the estimated amount of peptides by domains after 6 h and 12 h, either. Few domains have an abundance of quantifiable peptides significantly higher than the other domains at the last sampling point; domains 2/3, 6, 20, 20/21, 26, 26/27, 28 and 30 showed significant differences ( $p \leq 0.05$ ) in their abundance of quantifiable peptides with respect to other domains after 48 h. Only domains 6/7, 20, 26, 26/27 showed a significant difference ( $p \leq 0.05$ ) between their final amount of peptides, and their amount estimated after 6 h and 12 h. Domains 20/21, 28, and 30 only showed statistically significant differences ( $p \leq 0.05$ ) between the amount valued after 6 h and after 48 h.

Interestingly, the analysis of the data obtained with CG and MMP-9 all together in the linear model, as it was shown for both enzymes separately, showed a clear difference ( $p \leq 0.05$ ) in the abundance of some domains (Figure 23). Almost all domains that showed a significant difference among their abundances estimated after 6 h, 12 h and 48 h were identified in the C-terminal region of the protein (domains 20, 20/21, 24, 26, 26/27, 28 and 30 ), except for domain 6. Other domains in the N-terminal and central region of elastin showed that their abundance of quantifiable peptides after 48 h differed significantly from the estimated abundance after 6 h (domains 2/3, 5/6, 7, 12).

All the domains mentioned and domain 11/12 showed a significant statistical difference in their amount from the abundance of other domains estimated after 48 h, therefore, they could be considered as the most susceptible domains to degradation by CG and MMP-9.

Domain	2	2/3	2/4	5	5/6	6	6/7	7	7/8	8/9	9	9/10	10	10/11
6 h	0	1721	0	0	1050	43	0	446	0	0	0	20	0	0
12 h	0	3332	0	36	1998	811	28	1645	65	0	0	388	136	40
48 h	485	8749 *	451	247	7963 *	9934 **	389	7688 *	1327	65	164	5264	5296	236

Domain	11/12	12	13	14	14/15	15/16	16	16/17	17	17/18	18	18/19	20	20/21
6 h	189	970	0	16	0	0	0	222	0	0	0	0	246	338
12 h	1342	2535	44	14	0	0	55	846	0	0	23	0	1736	820
48 h	8007	8536 *	201	313	31	368	1016	4875	106	317	2074	534	15770 **	9288 **

Domain	21/23	24	24/25	26	26/27	28	28/29	30	30/31	31	32	32/33	33	33/36
6 h	0	106	0	0	157	347	0	258	0	0	40	0	0	0
12 h	0	688	0	367	738	1678	19	1466	0	0	216	308	38	38
48 h	140	10614 **	788	8145 **	10018 **	9625 **	1284	11200 **	8242	749	3721	1504	461	561

Figure 23. Degradation of different domains of elastin by CG and MMP-9, determined through a linear model.

Amount of peptides expressed as the effect calculated in a linear model, using the normalised abundance of peptides quantified in skin elastin samples digested with CG and MMP-9. Statistically significant differences between the amount of peptides estimated after 48 h and 6 h are shown as \* while differences between 48 h and 12 h are represented by \*\*. Domains with a significantly high amount of normalised abundance of peptides after 48 h are shown as !.

#### 4.2.4 Age-related differences in the elastin susceptibility towards enzymatic degradation

As mentioned previously, the number of cleavage sites was used to compare the degradation of the elastin qualitatively. Overall, OE showed the highest number of cleavage sites identified in the samples digested with both enzymes. In total, 170 and 155 (CG; MMP-9) cleavage sites were identified in OE digests while 146, 148 (CG, MMP-9) sites were found in the CE samples (Figure 16). Regarding the similarities in cleavage sites between different substrates, CG cleaved TE, CE and OE in 53 sites in common; almost half of the cleavage sites found in CE samples (72 of 146) were also identified in OE samples. On the other hand, the MMP-9 digests of the three substrates shared 71 cleavage sites, while one-third of the cleavage sites identified in CE (50 of 148) was also found in OE samples. Comparison of the domain whose peptides were identified by nanoESI-QqTOF MS/MS analysis, CG and MMP9 digests showed substantial similarity in their cleavage sites accessibility; both enzymes cleaved domains 3, 6, 7 and 26 in the three substrates. Additionally, CG and MMP-9 cleaved well domains 9, 16, 20, 24, 30 and

33 in skin elastin samples but not necessarily in TE samples. Particularly, 3 domains (13, 15 and 23) in CG digests, and 5 domains (4, 11, 13, 14 and 15) from the total domains identified in MMP-9 samples showed to be cleaved in CE but not in OE or vice versa (Figure 16A and B).

Regarding the quantitative differences between CE and OE samples digested with CG during 48 h, a higher amount of total normalised abundance of quantifiable peptides derived from domain 6, 16/17, 20/21 and 26/27 was found in CE than in OE samples. In contrast, domains 6/7, 9, 9/10, 10/11, 13, 14, 16, 28 and 30 had a higher amount of total normalised abundance of quantifiable peptides in OE samples than in CE samples (Figure 21A and B). Interestingly, MMP-9 differs from CG in the capacity of cleavage OE samples. For all the domains in which peptides from OE digests were quantified, the sum of the normalised abundance of peptides by each domain was lower than the sum of quantifiable peptides in the related domain in CE samples. Furthermore, domains with the highest intensity in OE samples, only reached almost 20 % of the sum of the normalised abundance calculated in the related domain in CE samples.

In order to study if the whole amount of quantifiable peptides obtained from CE and OE samples differ when both substrates are digested with the same enzyme, the whole amount of quantifiable peptides obtained after digestion of TE, CE and OE with CG and MMP-9 was calculated as the sum of the normalised abundance of all peptides quantified at each sampling point. Figure 24 shows the profile of the sum of the normalised amount of all quantifiable peptides determined by LFQ in each sample. Both enzymes produced a higher amount of peptides in TE than in skin elastin samples at each sampling point. A final quantity of  $912677 \pm 115201$  a.u. and  $1044983 \pm 318671$  a.u. of normalised abundance was calculated after 48 h in TE samples digested with CG and MMP-9 respectively. It is likely that the high amount of peptides in TE samples is a result of their solubility in water and their low resistance to the enzymatic cleavage. Interestingly, skin elastin samples digested with CG showed a similar increasing tendency and a similar total amount of peptides in each sampling time. After 48 h,  $119806 \pm 10841$  a.u. and  $121498 \pm 7420$  a.u. of the normalised amount of peptides were calculated for CE and OE samples digested with CG, respectively. In contrast, for MMP-9 digests, CE samples presented a higher amount of peptides ( $351168 \pm 15366$  a.u. of normalised amount) than OE samples ( $26854 \pm 15477$  a.u. of normalised amount). Although MMP-9 induced

a strong change of CE peptides concentration over the time, only a slow variation was found for OE (Figure 24).

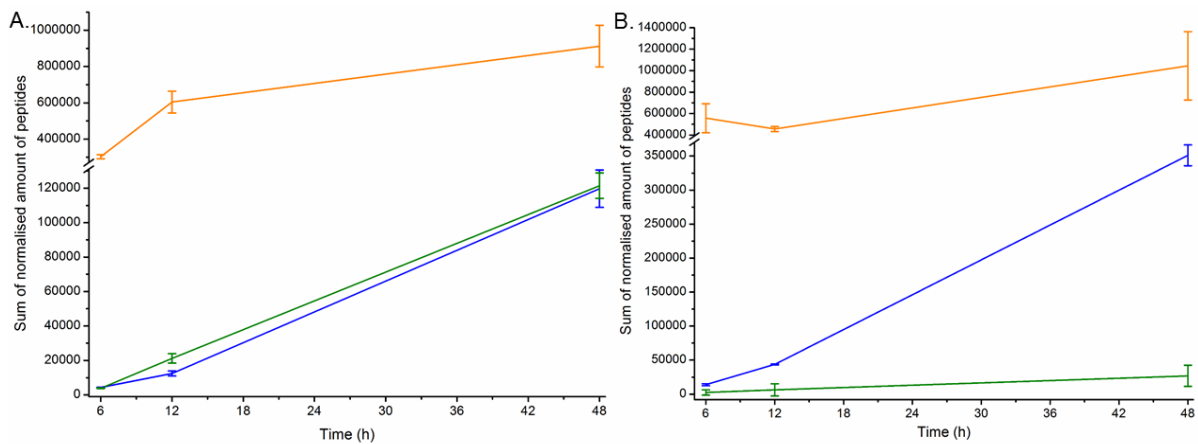


**Figure 24. Profile of quantifiable peptides obtained after digestion of TE and skin elastin samples with CG and MMP-9.**

**Sum of the normalised amount of quantifiable peptides determined after digestion of TE (orange), CE (blue) and OE (green) with CG (A) and MMP-9 (B) after 6 h, 12 h and 48 h, according to LFQ results. Data is shown as mean ± s.d. (n=3).**

Particularly, MMP-9 results showed a higher dispersion related to biological variability than CG results. Furthermore, CE results did not show considerable variation between biological replicates, but OE results presented a higher dispersion with both enzymes (Figure A-8; Appendix 2). It was associated with the difference between the results obtained from the sample belonging to the 75-year-old donor, and the results belonging to the 90-year-old donors. Previous reports showed that after 70 years, the elastic fibres are highly degraded [313], then, the elastins isolated from 90-year-old donors underwent a high damage. The instrumental replicates did not induce a significant variation of the results obtained with both enzymes (Figure A-9; Appendix 2).

To determine the full amount of peptides that the enzymes released from the skin elastin samples after 48 h of incubation, the total amount of solubilised elastin peptides was quantified through the absorption of the peptide bond in solution, using an UV spectrophotometric method. At the end of the incubation time, the two enzymes generated a significant ( $p < 0.05$ ) higher amount of peptides from the TE compared to the CE and OE samples digested with the respective enzyme (Figure 25). In addition, samples of skin elastin digested with CG and MMP-9 showed a different statistical amount of peptides compared to the negative control ( $p < 0.05$ ). Only CE samples digested with MMP-9 showed a significant higher amount of peptides than OE samples digested with the same enzyme.

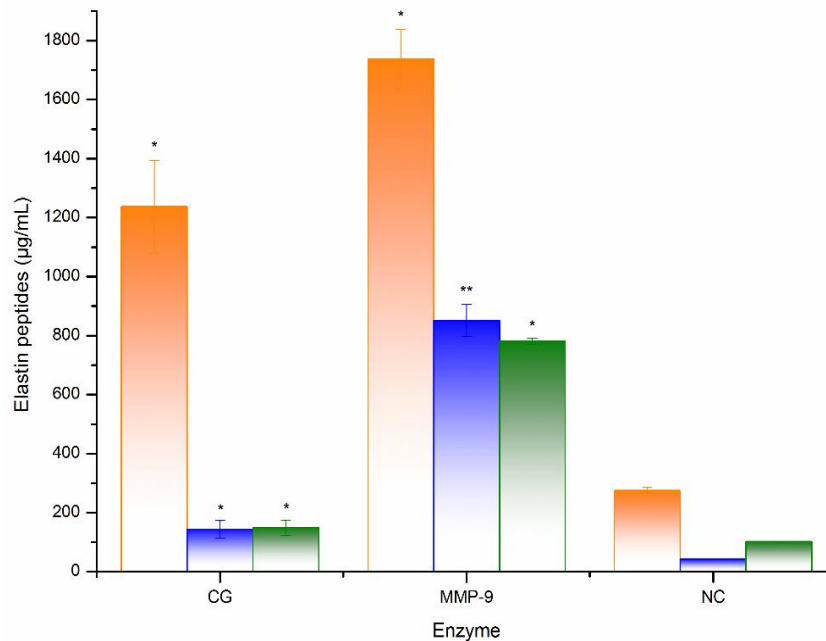


**Figure 25. Amount of elastin peptides solubilised after 48 h, and quantified using an UV spectrophotometric method.**

The amount of peptides released by CG and MMP-9 after 48 h of digestion of TE, CE and OE samples are shown in orange, blue and green, respectively. Negative controls (NC) correspond to samples without enzyme added. Significant difference ( $p < 0.05$ ) between the sample and related negative control are labelled as \*, and significant difference ( $p < 0.05$ ) between CE and OE samples digested with the same enzyme are shown as \*\*.

Moreover, the influence of all factors tested during the experiment over the amount of peptides obtained by domain during the enzymatic degradation of the elastin was evaluated in a fourth order interaction model of fixed effects with correlated errors for the dependent variable sum of peptides' amount. The results of the model are estimated coefficients (slopes) that represent the influence of each factor separately or the influence of the interaction among two or more factor over the amount of peptides determined in each domain. If the influence of the factor or the interaction of factors is significant, it is reflected as a variation of the slope. The interpretation of the results of the model was done in a hierarchical way in reference to the interactions among all factors. For instance, if the interaction among all the factors (type of elastin, enzyme, incubation time and biological variability) is significant, this interaction would be the responsible for the sum of peptides observed in a domain. When the interaction among the four factors is not significant, the biological variability factor is excluded. Then, the interaction among the other three factors is evaluated. In all the cases, this interaction was significant and was established as the responsible for the amount of peptides observed in the domains.

It was determined that the sum of peptides derived from domains 2/3, 5-8, 9/10, 10, 12, 16, 16/17, 18-21, 24, 26, 26/27, 28, 30, 32, 33 and 33/36 fulfilled the balance information proportion criteria of the model. Analysis of normal distribution showed that only domains 5/6, 10, 16, 16/17, 18, 24, 28, 33/36 had a normal distribution of their errors with a mean equal to zero ( $p \leq 0.05$ ), which allowed their modelling. The results showed that variation of peptides was influenced ( $p = 0.00$ ) by the interaction of incubation time, substrate (type of elastin), enzyme, and biological variability for the domains 5/6, 10, 16/17 and 33/36. In addition, the biological replicate did not influence the change of peptides found in domains 16, 18, 24 and 28. However, the interaction of incubation time, substrate and enzyme ( $p = 0.00$ ) generated the variation of the amount of peptides in these domains. As an example, the differences found by the model for the interaction of three factors (enzyme, type of elastin and incubation time) are shown in the effect plot for the domain 28 (Figure 26A). Significant changes in the slope (differences) in all the conditions were observed. The results of the model described the experimental findings for domain 28 (Figure 26B).

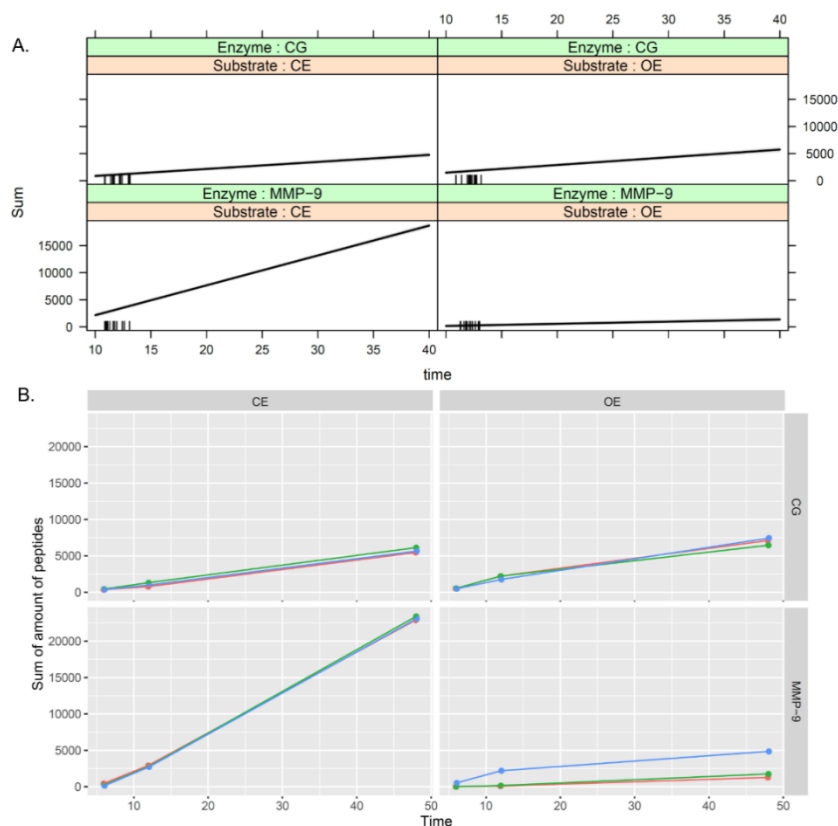


**Figure 26. Modelling of elastin peptides released from mature elastin from domain 28.**

**A. Effect plot for results of the model for the interaction of three factors (enzyme, type of elastin and time) for domain 28. B. Results observed for domain 28 in LFQ analysis; the three biological replicates are shown in red, green and blue.**

In conclusion, the model allows indicating that interaction between the factors related to the enzyme (type of enzyme and incubation time), and the substrate (type of elastin) defines the amount of peptides obtained during the degradation of all the different elastin domains evaluated in the model. Interestingly, the biological variability only has effect over the amount of peptides obtained in some domains.

#### **4.2.5 Characterisation of matrikines released from elastin fibres towards enzymatic degradation**

Overall, CG, MMP-9 and NEP showed a different capacity to release EDPs from the human skin elastin. Skin elastin samples digested with CG contained the highest number of EDPs (29 bioactive sequences, of which 14 were non-repetitive), although MMP-9 and NEP released the lowest amount of matrikines; 25 and 22 sequences were found in these samples, of which 11 and 10 were non-repetitive respectively. The bioactive sequences most frequently found in all skin samples (taking all peptides together) were VPGVG (108 peptides), VGVA (100 peptides), VAPG (99 peptides), GVAPG / VGVAPG (97 peptides) and PGVGVA (84 peptides). In contrast, the sequences GLPGVYPGGVLPGA, AGLVPGGPGFGPGVV, PGVYYPG and GARPG were the least identified in the elastin peptides released by the three enzymes. In the skin samples digested with MMP-9, a high number of peptides containing the sequences GAVPG, FGVG, GFGVG, GLGVGAGVP and PGFGAVPGA was also identified. Additionally, CG produced a large amount of peptides containing GAVPG and AGLVPG sequences, and they were the only digests in which the sequences AGLVPGGPGFGPGVV and GLPGVYPGGVLPGA were identified. Finally, the bioactive sequences YGARPGVGVGGIP and YTTGKLPYGYGPGG were not found in any peptide obtained from the skin elastin digested with the three enzymes, although these sequences were identified in TE samples digested with MMP-9 and NEP (data non shown). For all these motifs some *in vitro* biological activities have been reported (see Table 1. *In vitro* biological activities reported for some EDPs. , Chapter 1).

Regarding the number of peptides released which contained bioactive sequences, a total of 175 (MMP-9) and 149 (CG) peptides were found, which correspond to 47 % and 42 % of the total amount of peptides identified. Only eight peptides with matrikines were found in common in the skin samples digested with CG and MMP-9. The 56 % of the total peptides identified in the NEP digests of skin elastin samples (88 peptides) contained EDPs. Six peptides were shared between CG or MMP-9 and NEP; moreover,

the peptides VYPGGVLPGAR (residues 149-159) and APGVGVAPGVGVAPG (480-494) were found in all samples digested with the three enzymes. On the other hand, a similar amount of matrikines were identified in CE and OE samples digested with CG (76 and 73 peptides); MMP-9 digests showed a higher release of peptides with matrikines from CE than from OE samples (95 and 80 peptides). In contrast, OE digested by NEP showed a significantly higher amount of peptides with matrikines (74 peptides) than CE samples (14 peptides).

The majority of EDPs from the skin samples digested with CG and NEP were found in the central region of the protein, between domains 16 and 24 although in MMP-9 digests, the highest amount of peptides was found between domains 20 and 30 (Figure 14 and Figure 16A, B). The three enzymes produced a significant number of matrikines from domain 24; the skin elastin samples contained 36 (CG), 39 (MMP-9) and 20 (NEP) peptides derived from this domain. CG and NEP also produced a higher amount of matrikines from domain 18 (21 and 12 peptides). Furthermore, CG and MMP-9 generated several peptides between domains 20 and 21 (22 and 39 peptides respectively). Particularly, MMP-9 also released a higher amount of matrikines from domains 26 and 26/27 (26 and 19 peptides respectively).

Matrikines found in skin elastin samples digested with CG and MMP-9, which had the 15 % top abundance among all peptides from the same sample quantified after 48 h, are presented in Table A-2 (Appendix 2). These peptides are derived mainly from domains in the N- and C-terminal regions of the elastin and contained 18 bioactive sequences. The sequence VPGVG was the most frequently identified. Particularly, skin elastin samples digested with MMP-9 contained a high amount of peptides that included the sequences PGFGAVPGA and GAVPG. In addition, peptides with high abundance found in CE samples digested with CG and OE samples digested with NEP contained especially the sequences GLVPG, GVAPG, PGVGVA, VAPG, VGVA, and VGVAPG. These sequences have several biological reported effects (see Table 1. *In vitro* biological activities reported for some EDPs. , Chapter 1).



## **4.3 Structural changes of human elastin during skin ageing**

Skin ageing is characterised by different features including wrinkling, atrophy of the dermis and loss of elasticity associated with damage of the elastin [8, 138, 313]. Some studies about morphological changes of the elastic fibres have been reported [4, 229, 230, 314]. However, the molecular change of elastin remains not well characterised. In this section, elastin samples isolated from the sun-protected or sun-exposed skin of differently aged donors (Table A-3; Appendix 3) were analysed to get molecular-level insights into the degradation of the protein during ageing. Morphological changes were characterised using SEM. Afterwards, elastin samples were enzymatically degraded and analysed using MS analysis and LFQ quantification. Multivariate analysis was used to identify differences between cleavage patterns and to determine the contribution of extrinsic and intrinsic ageing to the proteolytic susceptibility of elastin. Additionally, the release of matrikines during the skin ageing was also evaluated.

### **4.3.1 Elastic fibres morphology and its susceptibility towards enzymatic degradation**

Clear differences were found between elastin fibres obtained from young and old donors. In Figure 27, the scanning electron micrographs of elastin fibres isolated from the skin of children (2 samples), adults (2 samples) and old adults (2 samples) are shown, which exemplify the characteristic features found in all analysed samples. Elastin arranged in intact fibres with smooth surfaces and diameters of about 0.5  $\mu\text{m}$  - 2.0  $\mu\text{m}$  were typical in elastin derived from sun-protected skin biopsies of young donors (Figure 27A, B). Taking young individual's fibres as a reference, elastin from the sun-protected skin of a 43-year-old individual showed a slightly damaged surface (it became rougher); no notable changes in the diameter or arrangement of the fibres were determined (Figure 27C, D). In contrast, significant changes were found in elastin fibres derived from the sun-exposed upper chest of the 90-year-old individuals. These fibres presented an entire rough surface and are partly fragmented or broken (Figure 27E, F). Additionally, the fibres were slightly disintegrated into fibrils. These fibrils have diameters below 1  $\mu\text{m}$ , but they were still organised in larger fibres.

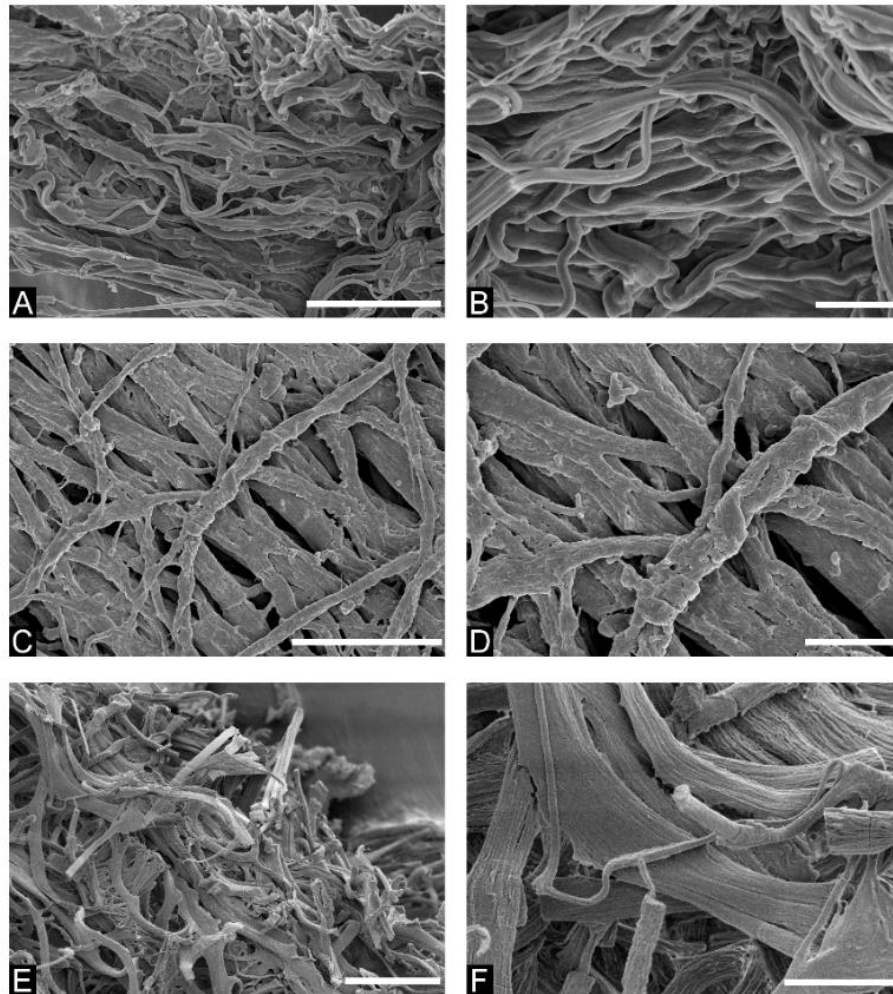


**Figure 27. Scanning electron micrographs of human skin elastin obtained from differential aged healthy individuals**

Representative micrographs of human skin elastin isolated from the skin of a 6-year-old individual (A, B), a 43-year-old individual (C, D) and a 90-year-old individual (E, F). The white bars represent either 20  $\mu\text{m}$  (A, C, E) or 6  $\mu\text{m}$  (B, D, F). Figure adopted from Mora *et al.* [2]

The morphological changes of the fibres are reflected in the susceptibility of the elastin fibres towards enzymatic attack. Although isolated elastin from skin samples was totally degraded by PE, differences in the degradability of the samples were identified. In general, the older the elastin fibres are, the more susceptible the protein is to the cleavage. The pellet of the elastin from older donors (90 years) was no longer visible after 24 h, while some elastin pellets of children (6 years) stayed intact much longer and needed around 24 h more to be fully digested.

#### **4.3.2 Characterisation of elastin peptides released from elastin obtained from differential aged individuals**

Overall, MS analysis of the digested samples allowed sequencing of 303 peptides in total, which corresponds to a sequence coverage of 67 % based on TE isoform 2 (Figure

28), which agrees with previous work in the research group [129, 149]. The extensive cross-linking of KA and KP domains lead to a lack of the identification of peptides from this domains.

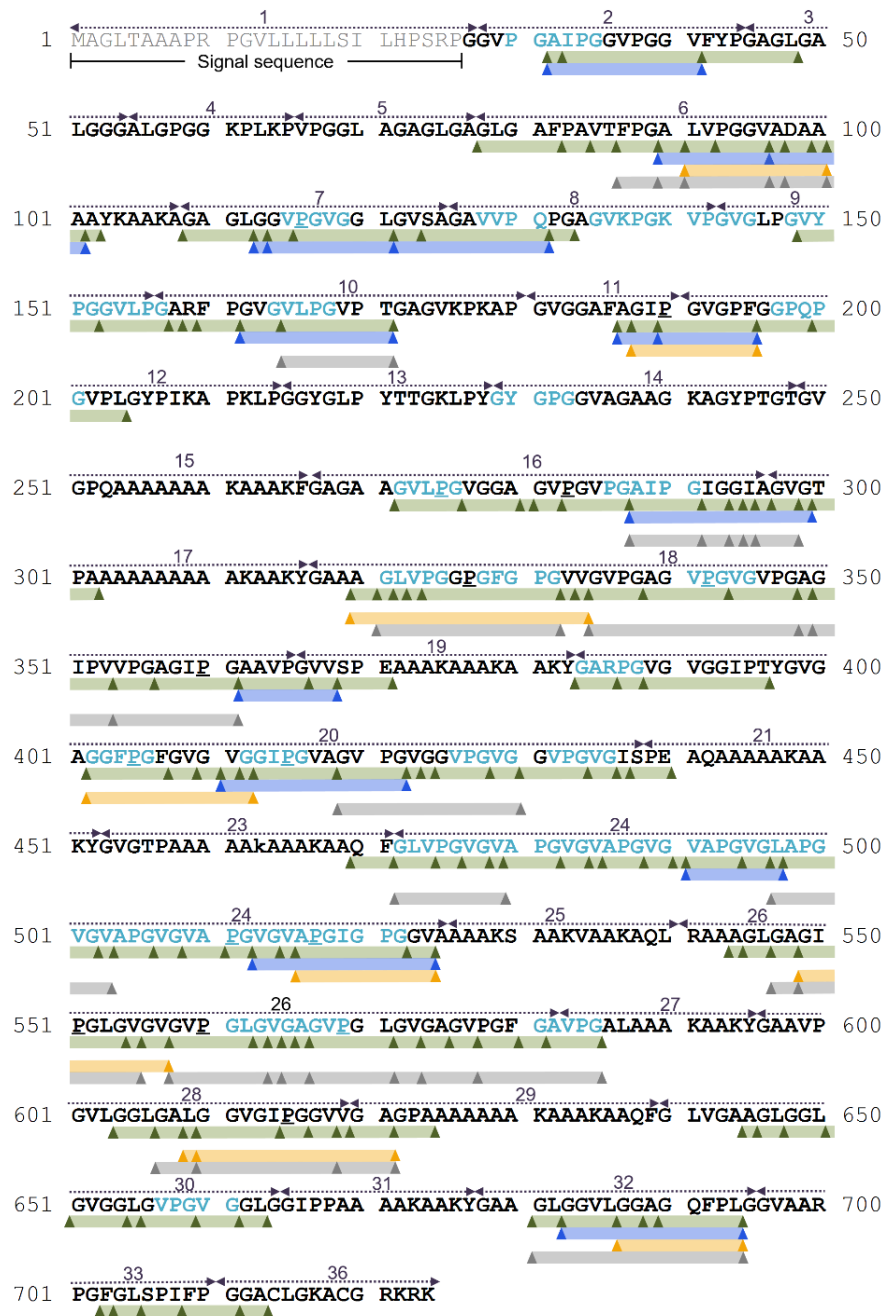


**Figure 28.** Elastin peptides identified from PE digests of skin elastin samples from differential aged individuals.

Cleavage sites are marked with triangles. Sequence coverage resulting from elastin peptides in the PE digests is shown by solid lines. Blue and orange lines comprise 16 and 9 peptides that showed a significant age-related increase and decrease in their normalised abundances, respectively. Grey lines represent the 30 peptides that showed significant differences in their abundances among different elastin samples. However, no age-related increase or decrease was displayed. Bioactive sequences are highlighted in light blue. Data based on the sequence of TE isoform 2 (Swiss-Prot accession number P15502-2). Figure adopted from Mora *et al.* [2].

The normalised abundance of each peptide contained in the elastin samples digested with PE was determined using LFQ (Figure A-10 and Figure A-11; Appendix 3). The data was unsuitable for ANOVA since its studentized residuals do not fulfil a normal distribution. Kruskal-Wallis test was performed to evaluate significant differences among peptides classified according to the donors' age; children (6-19 years), adults (43-70 years) and old adults (80-90 years). The normalised abundance of 55 of these elastin peptides showed significant differences ( $p < 0.05$ ) and an  $FC \geq 2$  among the different groups evaluated (Table A-4; Appendix 3).

Sixteen of the peptides with significant changes showed an age-related increase in their normalised abundances, while 9 exhibited an age-related decrease concerning the amount of the peptide in the children group (Table A-4; Appendix 3). Some peptides showed a stronger age-related increase in their abundances, such as peptides from domain 6 (Figure 29A), whereas others showed a weaker increase, for instance, peptides from domain 24 (Figure 29B).

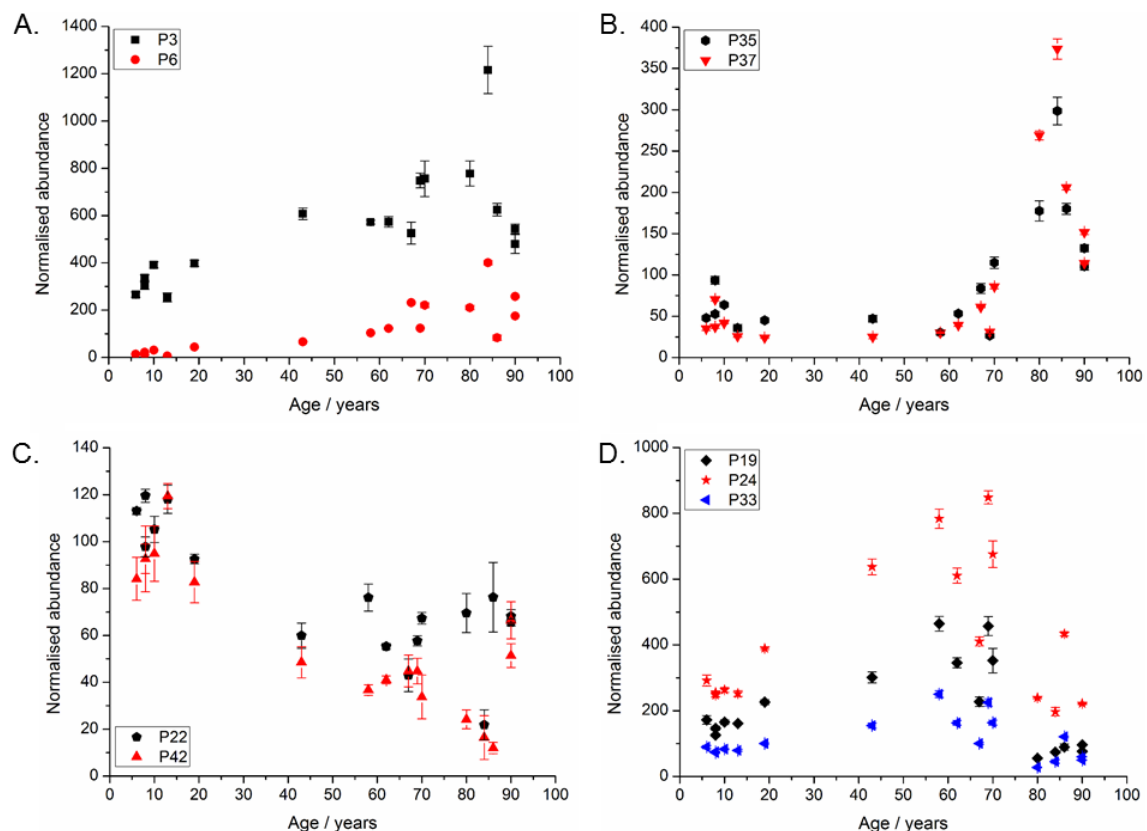


**Figure 29.** Changes in normalised abundances of selected elastin peptides depending on the age of the donor.

An age-related increase of the normalised abundances is shown for peptides derived from (A) domain 6 and (B) domain 24 of TE isoform 2. (C) depicted an age-related decrease of peptides derived from domains 18 and 26, and (D) showed peptides from domains 16, 18 and 20, whose normalised abundances increased up to donor ages of 70 and decreased at ages > 70. Data is presented as mean  $\pm$  s.d. ( $n = 4$ ). Figure adopted from Mora *et al.* [2].

In addition, the decrease in the abundance of the nine peptides with increasing age (Figure 29C) was found to be much less pronounced than the changes in the case of peptides that showed an increase in their abundances (Figure 29A, B). The normalised abundances of the other 30 peptides did not show a direct correlation with age ( $p > 0.05$ ). They are released in higher quantities from young and adult elastin samples (6 – 70 years), and their abundances drop in old elastin samples from donors between 80 and 90 years (Table A-4 (Appendix 3); Figure 29D).

The 55 peptides with significant changes in their abundance are derived from domains distributed throughout the sequence of TE (Figure 28). Few peptides derived from domain 6, 10, 11/12, 18, 18/19, 26, 26/27 and 32 displayed a higher normalised abundance in comparison with the majority of other peptides (Figure A-10 and Figure A-11; Appendix 3). The largest number of peptides with significant changes were derived from domains 18, 24 and 26. Interestingly, the majority of the peptides from these domains (P23-P29, P34, P36, P39-P41, P44 and P46; Table A-4 (Appendix 3)) showed a fluctuating pattern of change with age. They are released in higher quantities from young and adult elastin samples (6 – 70 years), whereas abundances dropped in old elastin samples from donors between 80 and 90 years, such as it is shown in Figure 29D. The majority of the peptides which showed an age-related decrease in their normalised abundances were derived from the central and C-terminal parts, while only three peptides were derived from the N-terminal domains of the TE molecule (Table A-4 (Appendix 3); Figure 30). However, the N-terminal region (from domains 2 to 11/12) of the protein mainly contained peptides which increased their abundance with the age of the donor (Table A-4 (Appendix 3); Figure 30). Finally, it is noteworthy that some of the 303 identified peptides did not show significant age-related changes in their abundances according to LFQ (Figure 28), for instance, peptides from the domains 30 and 33.

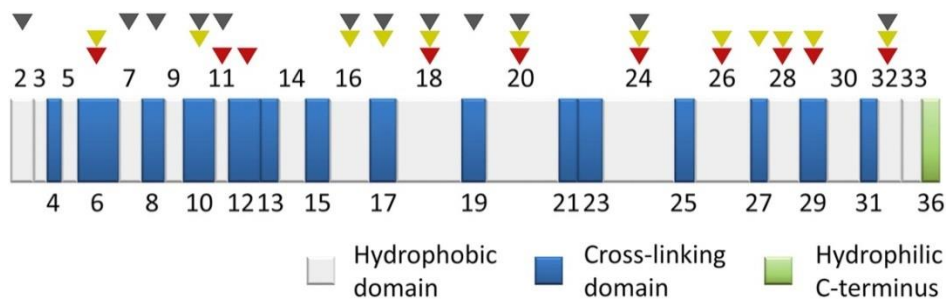


Figure 30. First cleavage points in skin elastin isolated from differential aged individuals.

Domain structure of TE isoform 2. The length of each domain regarding amino acid residues is shown true to scale. First cleavage points in skin elastin based on peptides that showed an age-related decrease in their normalised abundances is marked with red triangles. Cleavage points that occurred with increasing age of the individual are shown as yellow triangles. Cleavage points that occurred mainly in old individuals and show an age-related increase in their abundances are marked with grey triangles. Figure adopted from Mora *et al.* [2].

### 4.3.3 Release of potentially bioactive peptides from elastin during skin ageing

Regarding the release of bioactive sequences in peptides during enzymatic degradation of elastin, it was found that 20 of the 55 peptides contained potentially bioactive motifs including various GXXPG motifs, FGVG, GFGVG, VAPG, VGVA, VGVPG, VPGVG and VVPQ (Table A-4, Appendix 3). Three of these peptides displayed an age-related decrease in their abundances, whereas 8 peptides showed an age-related increase in their abundances (Table A-4, Appendix 3). Two of the 3 peptides with an age-related decrease in their abundance included multiple bioactive motifs overlapped in their sequences; P31 contains FGVG and GFGVG, while P22 contains AGLVPG, GFPG, GLVPG and PGFGPG. Interestingly, peptide P22 has also been found in CG and HLE digests of human skin elastin [147]. The third peptide, P38, only contains the GXXPG motif GIGPG which does not have reports of bioactivity. The peptides that display an age-related increase contain the motifs GGVP (P1, P8), GVLPG (P11), GGIPG (P32); GVAPG and VGVAPG (P37) as well as VPGVG (P8, P9), VVPQ (P10), VAPG (P35, P37) and VGVA (P37). Further potentially bioactive motifs were identified in peptides whose abundances showed an increase up to the age of 70 and dropped at ages > 70 including GFGPG, PGGPG (P23), GLVPG (P23, P34), GAVPG (P47, P48), VGVPG and VPGVG (P24-27). The biological activity determined in *in vitro* studies for these motifs is summarised in Table 1. *In vitro* biological activities reported for some EDPs. (Chapter 1).

#### 4.3.4 Classification of samples according to the sources of elastin degradation

Principal component analysis (PCA) and hierarchical cluster analysis (HCA) were carried out based on the 55 peptides that displayed significant differences in their normalised abundances among the groups, to identify the differences between elastin samples associated with the age of the donor and the sun exposure condition of the body region. PCA scores plot showed that elastin samples were clustering according to their age and the degree of sun exposure (Figure 31).

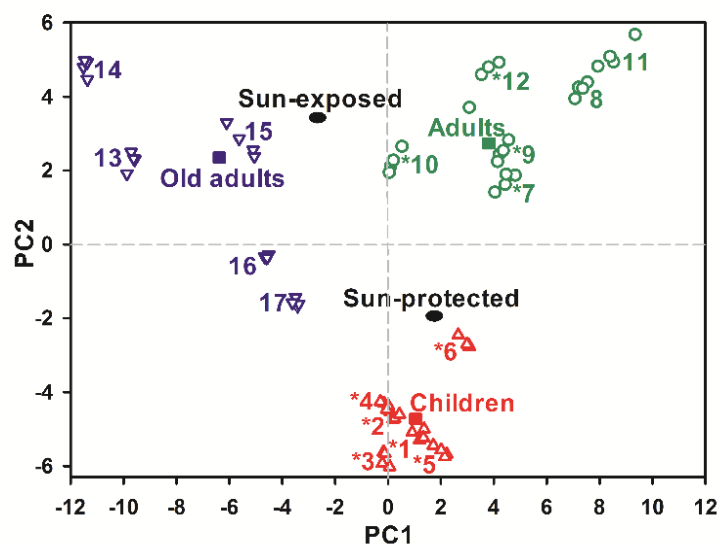


Figure 31. PCA scores plot of skin elastin samples isolated from differential aged individuals.

The PCA scores plot shows the separation of the samples derived from children (red triangles), adults (green circles) and old adults (purple inverted triangles), based on the 55 elastin peptides that resulted from enzymatic degradation of elastin; they displayed significant changes in their normalised abundances. Figure adopted from Mora *et al.* [2].

Due to the fact that in the skin, intrinsic ageing is always superimposed on extrinsic ageing [313], the PC1 and PC2 could not be assigned independently to each one of these two sources of variation. The first PC, which describes 51.4 % of the variation in the data set, not only does it explain age-related changes in the peptide pattern (intrinsic ageing) but it also explains minor extent changes in the samples related to sun exposure (extrinsic ageing). The second PC, which describes 27.5 % of the variation between the samples, explains predominantly the effects of sun exposure on the samples. However, PC2 is also connected to intrinsic ageing. It is interesting that the higher the age of the sample donor, the more the samples spread out into their clusters. Samples obtained from children (6 to 13 years) clustered very close together, and they did not show a significant dispersion associated to the PC2, except for the sample S6 of a 19-year-old

subject that was found a little bit further apart from the other children samples. The adult samples and old adult samples displayed a high dispersion associated with the sun exposure, but they remained clustered by the age of the donors. Particularly, the samples from the faces of both old adults ( $\geq 80$  years; S13-S15), and adults (S8, S11) showed the strongest effects of photoaging in their respective clusters.

The variables graph showed that each variable, i.e. each peptide was more correlated with one of the principal components (PCs) and, thus, with the effects of intrinsic and extrinsic ageing (Figure 33). For instance, in particular, P3, P6, P10, P18, P23, P30 and P32 were positively correlated with PC2, which means that they are released predominantly during enzymatic degradation of sun-exposed elastin samples from adults and old adults. In contrast, peptides P5, P7, P22, P42, P50 and P52 were negatively correlated with sun exposure and were mainly released upon proteolysis of children sun-protected elastin samples. With the exception of P5, the peptides negatively correlated with the PC2 also showed an age-related decreasing pattern of change in their normalised abundances (Table A-4; Figure A-10 and Figure A-11 in Appendix 3).

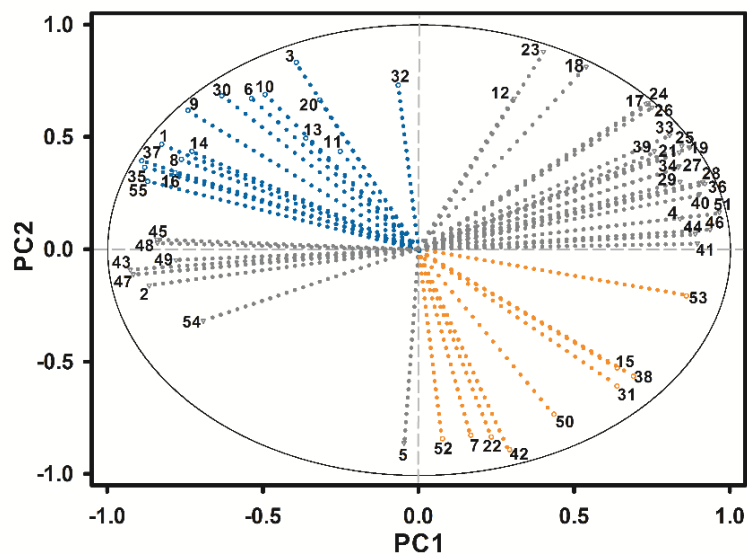


Figure 32 Variables graph of 55 elastin peptides with age-related changes, based on PC1 and PC2.

Peptides that showed an age-related increase in the normalised abundances are highlighted in blue. Peptides that presented an age-related decrease in their normalised abundances are highlighted in orange, and peptides that did not exhibit a clear age-related pattern of change are shown in grey. Figure adopted from Mora *et al.* [2].

Furthermore, the peptides associated with the PC1 showed a fluctuating change of their normalised abundances with age, and they could not be related to sun-exposed or sun-protected elastin samples. Peptides P4, P41, P44, P46, P51 and P53 were positively



correlated with PC1 and were predominantly released from samples of the adult group (ages 43 -70). In addition, they decreased their normalised abundance in old adults (ages 80 - 90). Peptides P2, P43, P45, P47-P49 and P54 were negatively correlated with PC1; their normalised abundance dropped in adult group, and they were released in higher quantities from samples of the old adult group.

Differences and similarities among the samples were subsequently compared by hierarchical clustering analysis (hierarchical principal component analysis, HPCA) over the first five PCs identified in PCA. The plot of HPCA (Figure 32) shows all samples classified into two statistically significant clusters. Cluster I contained samples from the sun-exposed skin of donors from ages between 80 and 90. Cluster II split into two sub-clusters. Samples of elastin of non-sun exposed skin from children (6 -19 years) constituted sub-cluster IIa, whereas sub-cluster IIb contained samples from donors with ages between 43 and 70. Moreover, it is noteworthy that in sub-cluster IIb, sun-exposed samples (S8 and S11) were differentiated from samples of body regions that were not sun-exposed (S7, S9, S10 and S12).

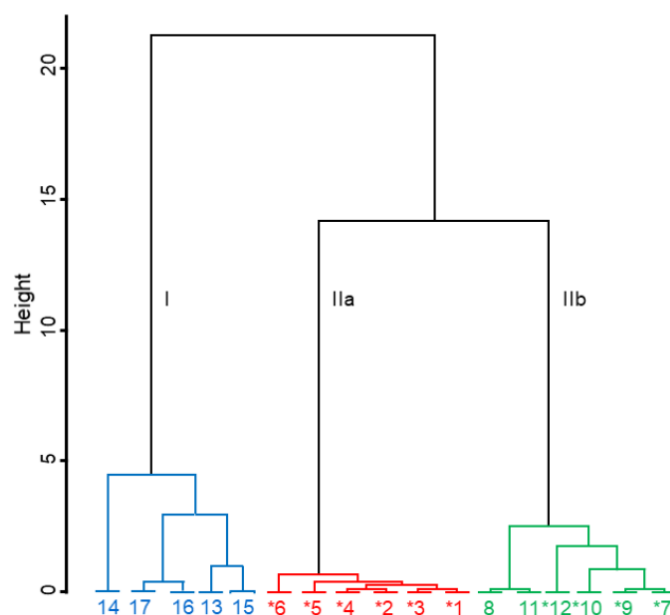


**Figure 33. Dendrogram of skin elastin samples isolated from differential aged individuals.**

**Dendrogram showing hierarchical clustering of the 17 samples over the first five PCs identified by PCA. Samples derived from children, adults and old adults are shown in red, green and blue, respectively. Asterisks denote elastin samples derived from sun-protected skin. Figure adopted from Mora *et al.* [2]**

## 4.4 Molecular changes of human skin elastin from Williams-Beuren Syndrome patients and healthy individuals

Premature skin ageing, the *in vitro* alteration of elastin deposition in the elastic fibres and the reduction of the diameter of these fibres have been previously described in patients with Williams-Beuren Syndrome (WBS) [238, 244, 248]. However, the molecular basis of structural abnormalities in the skin elastin of WBS patients is not entirely understood. This section deals with the structural characterisation of human skin from WBS patients in comparison with human elastin from healthy individuals. The elastin content of skin samples of WBS patients ( $n = 10$ ; age  $38.9 \pm 5.9$  years old) and healthy individuals ( $n = 10$ ; age  $44.1 \pm 12.7$  years old) was determined. Afterwards, all elastin samples were morphologically characterised using SEM, and their susceptibility to enzymatic degradation was studied using nanoHPLC-MALDI-TOF/TOF MS technique. Furthermore, digests of new elastin samples of healthy donors and WBS patients (Table A-5; Appendix 4) were analysed by nanoHPLC-nanoESI-QqTOF MS(/MS), and the normalised abundance of each elastin peptide in the samples was determined using LFQ. Multivariate analysis was applied to identify differences between enzymatic digests of skin elastin samples.

### 4.4.1 Elastin content of skin and elastic fibres morphology

Skin samples from WBS patients contained significantly less elastin compared to the skin of healthy individuals ( $n = 10$ ,  $p \leq 0.05$ ). It was found that skin samples from WBS patients and healthy donors have an elastin content of  $1.6 \% \pm 0.4 \%$  and  $6.0 \% \pm 2.4 \%$  (% on a dry basis), respectively. In addition to the differences in the elastin content, elastin samples obtained from WBS patients presented particular morphological characteristics. Representative images displaying typical features found in the elastin samples analysed by SEM are shown in Figure 34. Elastin fibres isolated from healthy donors showed the similar morphological characteristic of the samples investigated in the previous section (4.3.2). The skin elastin fibres from young individuals (around 35 years) showed smooth surfaces and consisted mainly of intact larger fibre bundles of diameter above  $1 \mu\text{m}$  (Figure 34A and B). In contrast, the elastin fibres isolated from the skin of healthy old individuals (around 90 years) appeared broken and fragmented; the

larger fibre bundles were not completely disintegrated, and it is still possible to identify many smaller fibres (diameter below  $1\mu\text{m}$ ) arranged in these larger bundles (Figure 34E and F). Interestingly, skin elastin fibres from WBS patients (19 years old) resembled the characteristics described for elastic fibres isolated from healthy old individuals. The WBS elastic fibres were fragmented and damaged, and the larger fibre bundles appeared disintegrated into smaller fibres with diameters below  $1\mu\text{m}$  (Figure 34C and D).

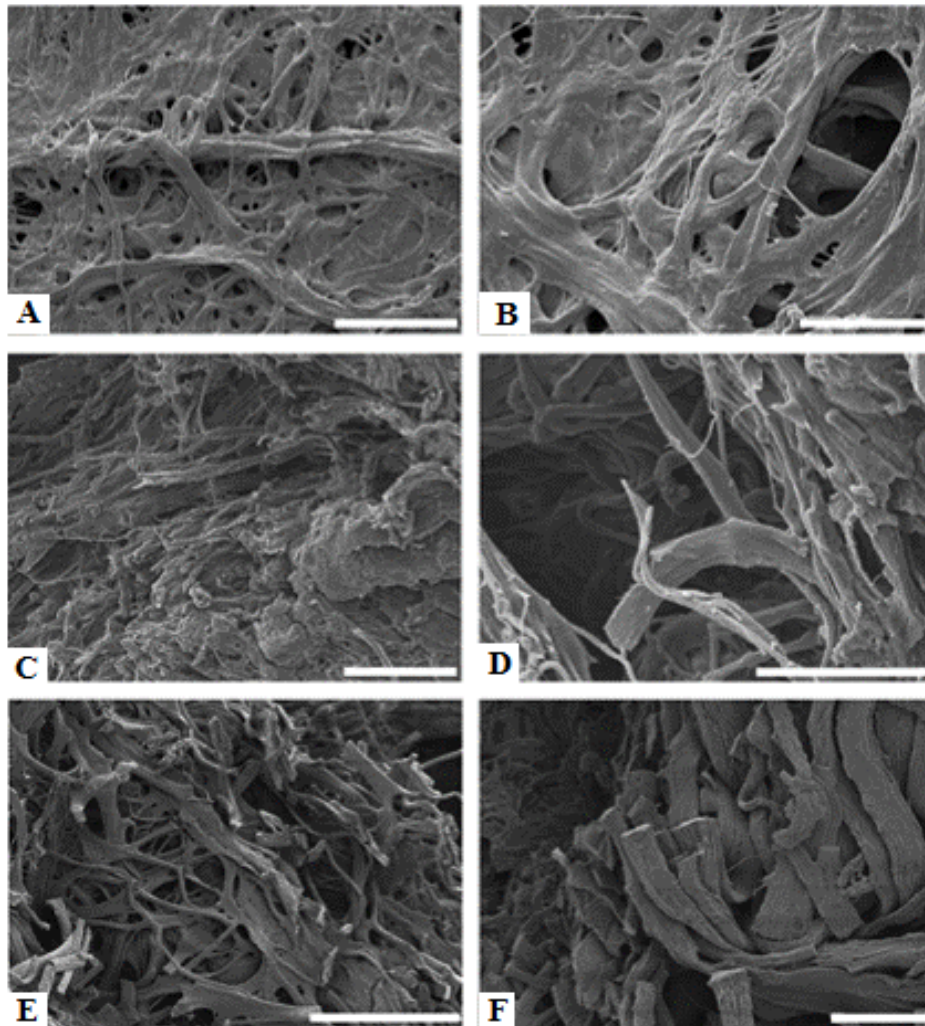


Figure 34. Morphological characterisation of skin elastin isolated from healthy donors and WBS patients.

Scanning electron micrographs of skin elastin obtained from a 40-year-old healthy individual (A and B), a 19-year-old WBS patient (C and D), and a 90-year-old healthy individual (E and F). The white bars represent either  $30\mu\text{m}$  (A, C and E) or  $10\mu\text{m}$  (B, D and F). Figure and text adapted from Heinz *et al.* [7].

#### 4.4.2 Elastin susceptibility towards enzymatic cleavage

Elastin fibres isolated from both WBS patients and healthy individuals were well cleaved by PE (Figure 35); no difference in the degradability of the samples was observed. Samples pellets from WBS patients and old adult healthy individuals were no

longer visible almost at the same time (after 24h). Overall, in the MS analysis, all the identified peptides were derived from non-cross linked regions of the elastin (Figure 35).

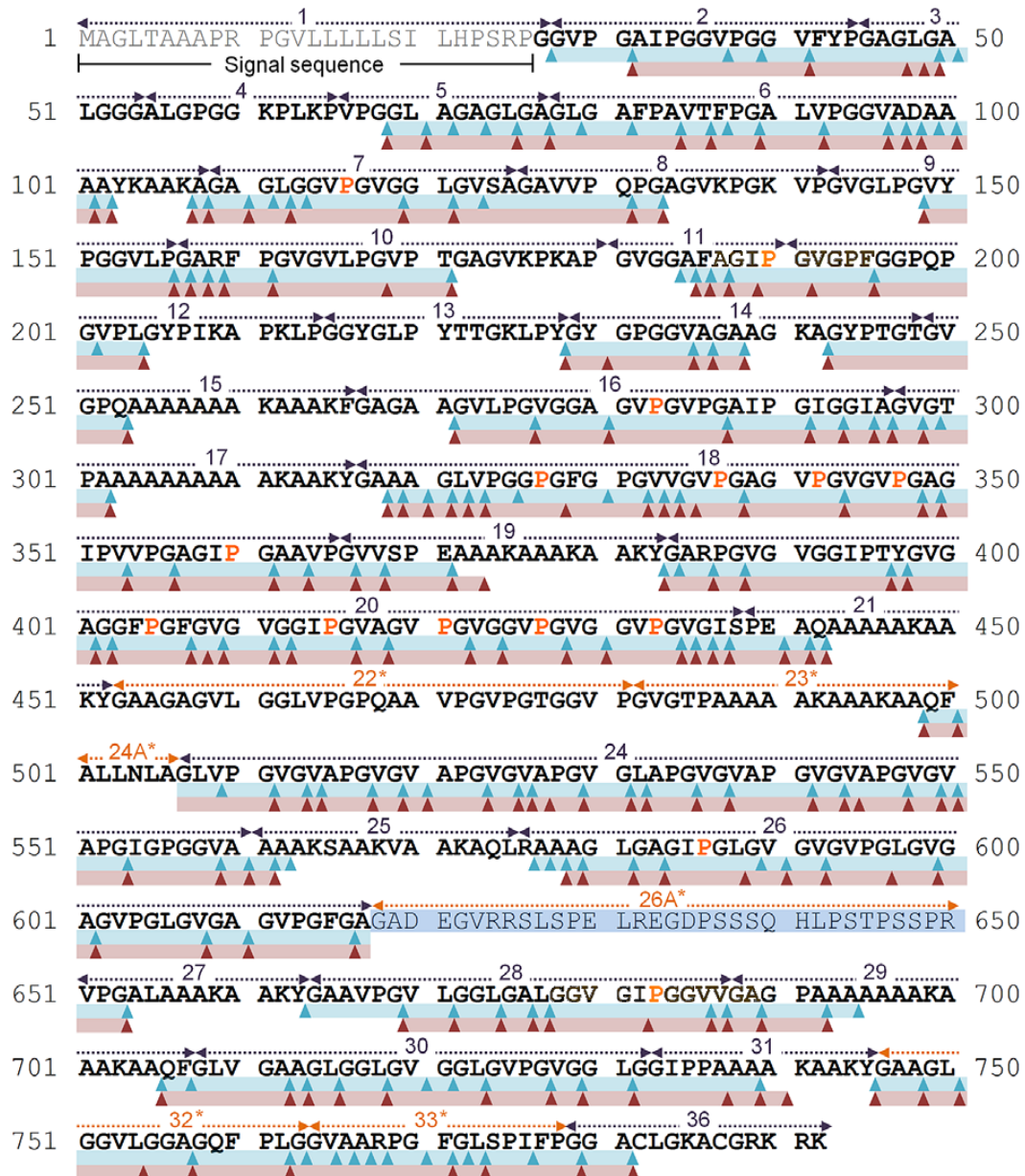


Figure 35. Cleavage sites identified after PE digestion of skin elastin samples from WBS patients and healthy donors.

Cleavage sites in elastin from WBS patients are marked with blue triangles, and sequenced regions are labelled with solid blue lines. For elastin from healthy donors, cleavage sites are indicated with red triangles, and sequenced regions are labelled with solid red lines. Hydroxyproline residues identified in elastin from healthy individuals are shown as capital letter P in orange. Exons that are subject to alternative splicing are labelled with an asterisk. Exon 26A whose existence has been the subject of debate for many years as it has never been identified on protein level is labelled with a solid blue line. Data is shown based on TE isoform 9 (Swiss-Prot accession number P15502-9). Figure and text adapted from Heinz *et al.*, [7].

Similar sequence coverages were obtained upon linear peptide sequencing from enzymatic digests of skin elastin from WBS patients (71 %) and healthy donors (69 %). Interestingly, more than 75 % of the cleavage sites found in skin elastin were shared between samples of healthy donors and WBS patients. Although it is a direct consequence of the broad cleavage specificity of PE, it also indicates that elastin from healthy donors and WBS patients are structurally similar and the K residues seem to be mainly comprised in cross-links. This assumption is also supported by the results of other experiments using trypsin (TR), which cleaves C-terminal to K and R residues, and it could not cleave the elastin isolated from the skin of healthy donors or WBS patients (data non shown). Regarding the presence or absence of certain domains, elastin digests did not contain peptides derived from exons 24A and 26A. However, it was possible to identify peptides derived from domains 26 and 27 as well as 23 and 24, which indicates that exons 24A and 26A are spliced out from skin elastin of WBS patients and healthy donors. Additionally, linear peptides derived from domain 22 were not identified in the enzymatic digest either. Overall, these results agree with previous studies over elastin isolated skin samples derived from healthy donors [71, 129, 315, 316].

#### **4.4.3 Differences between elastin peptides released from elastin isolated from skin of WBS patients and healthy individuals**

To determine differences between the abundance of peptides in elastin derived from healthy donors and WBS patients, elastin skin samples isolated from individuals of each condition (Table A-5; Appendix 4) were simultaneously digested and analysed with a MS technique. Overall, 181 elastin peptides were quantified using LFQ analysis; 64 of them displayed differences statistically significant between the samples obtained from WBS patients and healthy donors ( $p < 0.05$ ;  $FC \geq 2$  and a  $CV \leq 70\%$ ) (Table A-6; Appendix 4). The majority of peptides with significant differences are derived from domains 16, 18, 24 and 26 and occurred with higher abundances in elastin from healthy probands. However, 28 peptides showed a higher abundance in elastin digests of WBS patients, and interestingly, some of them constituted almost all the peptides with significant differences identified from domains 10, 11/12, 26, 26/27 and 28/29. On the other hand, it is worth mentioning that all the peptides containing HyP residues had higher abundances in elastin from healthy donors (Table A-6).

Interestingly, 35 of the 64 peptides, which showed significant changes in their normalised abundance in healthy individuals and WBS patients, also showed a significant age-related change of their abundance estimated in samples obtained from other healthy donors (Section 4.2). For instance, 8 and 3 peptides determined in elastin samples derived from healthy donors and WBS patients matched with peptides which presented an age-related increase in elastin samples obtained from differential aged healthy individuals (Section 4.2). Similarly, 2 and 3 peptides identified in healthy and WBS elastin samples are equal to peptides with age-related decrease and 13 and 6 peptides correlate with peptides with a fluctuating age-related change on their abundances.

#### **4.4.4 Release of potentially bioactive peptides from elastin isolated from WBS patients and healthy donors.**

Regarding the release of potentially bioactive peptides, it was found that some matrikines were identified in 30 peptides from the 64 peptides which showed significant differences in their normalised abundances between the samples of WBS patients and healthy donors (Table A-6; Appendix 4). The bioactive sequences identified included FGVG, GFGVG, PGVGVA, VGVA, VAPG and VPGVG, as well as various GXXPG motifs. The VPGVG and VAPG sequences were the most frequently found (10 and 8 peptides, respectively), and together with the GLVPG, GVLPG and VGVPG sequences, they were identified in peptides whose normalised abundance presented higher values in samples from both healthy individuals and WBS patients. Interestingly, the majority of the remaining sequences identified (namely FGVG, GAVPG, GVAPG, GFGVG, PGAIPG, GAIPG, PGVGVA and VGVAPG) were found in peptides with higher normalised abundance in elastin isolated from WBS patients. On the other hand, only two bioactive sequences, GFGPG and PGFGPG, were exclusively found in peptides whose normalised abundance is higher in elastin isolated from healthy donors. As it has been mentioned in previous sections, these motifs displayed a variety of bioactivities (see Table 1. *In vitro* biological activities reported for some EDPs. , Chapter 1). Finally, other identified GXXPG motifs were GGFPG, GPQPG, GLAPG and GGIPG, which do not have reports of biological activity yet, but in particular, GLAPG and GPQPG adopt the type VIII beta-turn conformation which has been hypothesised to facilitate the interaction of the peptide with the EBP [193].

#### 4.4.5 Classification of samples according to the elastin changes in WBS patients and healthy individuals

PCA and HPCA analysis were carried out using the normalised abundance of the 64 peptides with significant differences between elastin isolated from WBS patients and healthy individuals. The PCA scores plot showed a clear separation of WBS elastin samples and the healthy elastin samples based on the PC1, which described 68.4 % of the variation in the dataset (Figure 36). Furthermore, samples presented a low dispersion along the PC2, which explained 10.3 % of the total variation of the data. This PC could be associated with changes in the age of the donors, since samples obtained from the older donors in WBS patients and healthy individuals were found to be further apart from the other samples in the PC2 axes but they remain into the respective cluster.

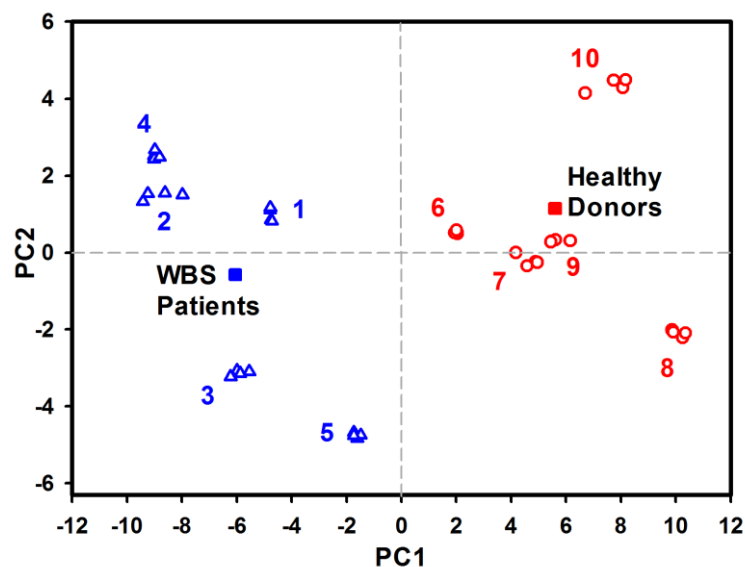
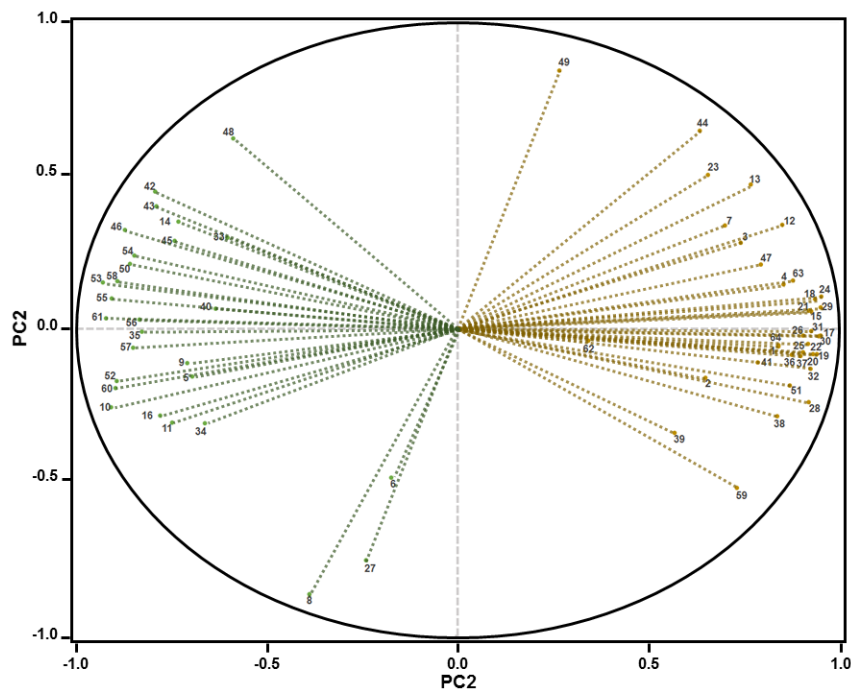


Figure 36. PCA scores plot of skin elastin samples isolated from WBS patients and healthy individuals.

The PCA scores plot shows the separation of the samples derived from WBS patients (blue triangles) and healthy donors (red circles), based on the 64 elastin peptides that resulted from enzymatic degradation of elastin and displayed significant changes in their normalised abundances between healthy individuals and WBS patients.

In the variables graph, peptides are clearly distinguished between elastin peptides whose normalised abundance is higher in healthy individuals (positive position in the PC1) and WBS patients (negative position in PC1) (Figure 37). Moreover, peptides P15, P17-19, P21, P22, P24-26, P28-32 and P37 are strongly and positively correlated with the PC1 (healthy donors elastin), while peptides P10, P52, P53, P55, P58, P60 and P61 showed the opposite effect; they were the most negatively correlated with PC1 (WBS patients elastin). Additionally, the peptides P49, P44, P23, P13, P7 and P12 (healthy donors); and P14, P42, P43, P45 and P48 (WBS patients) were positively correlated with

the age (PC2) while P59 and 39 (healthy donors); and P11, P34, P6, P8 and P27 (WBS patients) were negatively correlated with PC2.



**Figure 37** Variable graph of 64 elastin peptides with significant differences between WBS patients and healthy individuals based on PC1 and PC2.

Peptides found in higher amounts in elastin isolated from WBS patients or healthy individuals are shown in green and yellow, respectively.

Finally, the analysis of the HCA over the first five PCs identified in PCA showed that samples were split into two main clusters that contained elastin isolated from healthy individuals (cluster I) and WBS patients (cluster II) (Figure 38). Samples in each cluster seemed to be divided into two subclusters which could be associated with the age-related changes of the elastin in healthy donors' samples. Elastin samples isolated from healthy individuals of 19 (S6), 43 (S7) and 62 (S9) years old were split from samples of individuals of 58 (S8) and 70 (S10) years old. Interestingly, S8 corresponded to a sample from a sun-exposed region of the body and seemed to be more damaged than a sample from a sun-protected region (S9), which agrees with our finding of the upper damage of elastin samples from sun-exposed body regions (Section 4.2). On the other hand, WBS patients had a smaller age range than healthy donors, and age-related changes of samples were not so clearly identified. In cluster II, samples obtained from WBS patients of 25 and 28 years old (S4 and S2, respectively) split from samples of patients of 24 (S1), 40 (S5) and 27 (S3) years old. It seems that samples S4 and S2 show the effect of other factors additional to the age such as the extrinsic ageing.



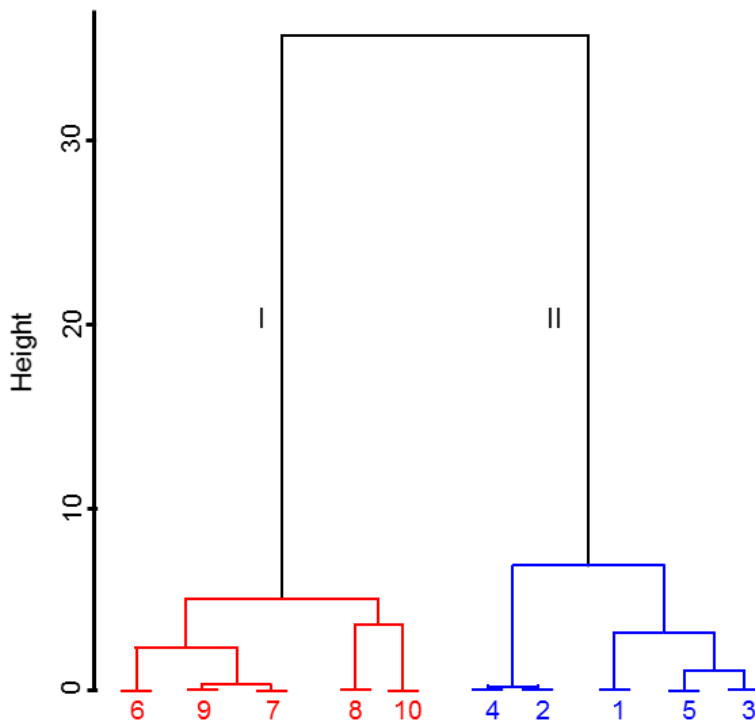


**Figure 38. Dendrogram of skin samples isolated from WBS patients and healthy individuals.**

**Dendrogram showing hierarchical clustering of the 10 samples over the first five PCs identified by PCA. Samples isolated from WBS patients are shown in blue; samples isolated from healthy donors are shown in red.**

# 5 Discussion

## 5.1 Workflow suitability to distinguish changes in abundance of elastin hydrophobic peptides.

In order to contribute to the understanding of the degradation of the elastin, during this thesis, the modifications of the protein under normal and pathological conditions were studied through a quantitative approach using LFQ in addition to the qualitative characterisation. Since it is the first time that LFQ is used to analyse the changes in elastin, the reliability of the workflow was tested. Overall, LFQ has shown to be a trusty method for doing the relative quantification of peptides and proteins, thereby giving rise to reliable estimates of the change in elastin peptides under different conditions. Among the diverse MS quantitative approaches available, LFQ was chosen because of its capacity to do a simultaneous comparison of the majority of peptides among samples [317]. An important step in the LFQ workflow design is to select the software to be used. In fact, the software has a major impact on the precision and accuracy during the quantification [318, 319]. Some software is available, with a specific algorithm for each one [292, 300]. Progenesis QI for proteomics (Progenesis QIP) (64-bit version v2.0; Nonlinear Dynamics, Newcastle Upon Tyne, UK) identified the highest number of complete peaks and reported the lowest amount of missing data, indicating that this software has the best performance in the data set evaluated. Although missing data could be associated with low abundance of the peptides, the capacity of the software to identify and quantify the peaks could impact the amount of data obtained [317].

It is important to mention that the quantifiable peptides reported in this thesis are restricted to the peptides identified during the sequencing analysis (MS/MS data) done in the software PEAKS Studio [274], which are aligned in time and  $m/z$  with the peptide ions quantified in MS raw data by Progenesis QIP. As a result, these quantifiable peptides are less than the peptides identified in MS analysis or sequenced during the MS/MS analysis. In fact, low abundance peptides could remain unidentified due to the fact that their individual precursors do not reach an acceptable intensity to be analysed in the MS/MS analysis [320]. Similar to previous reports [129, 149], the protein coverage obtained in the MS/MS analysis of the mature elastin after its complete

degradation with PE ranged between 50 % and 60 %, as a consequence of the impossibility to sequence peptides involved in cross-linking using the current sequencing tools [147, 315, 316].

The reproducibility of the LFQ workflow is a key condition to get reliable results since the relative quantification requires comparison of identical proteolytic peptides in each of the two samples to accurately determine relative ratio of the protein or peptide [321]. Since it is not possible to control all the variability sources that influence an analytical methodology, the knowledge of the variability allows establishing thresholds to distinguish the variability related to the experimental performance from the biological condition evaluated. Few reports are found about the variability associated with a bottom-up LFQ MS approach. Some studies showed a CV between 27 % and 66 % [322-324]. The study of the impact of variability sources over the LFQ workflow results [309] showed that the three sources of variation (biological, technical and instrumental) could induce up to 70 % of variability (expressed as CV). This CV is slightly higher compared to the maximum CV reported in the other studies. It could be explained by the differences in the analysed matrix, sample preparation and instrument performance. Particularly, the elastin solubilisation has a high influence on the technical variation. Residual pellets were randomly identified in samples, which could indicate that the incomplete degradation of the elastin pellet is more associated with the elastin sample than to an enzyme issue. PE was chosen to completely degrade the mature elastin due to its broad specificity, which has shown a preference for the C-terminal residues of Gly, Val, Leu, Ala and Ile [129, 325]. Furthermore, PE has shown its high efficiency to degrade the mature elastin in previous studies [129, 149, 326]. Because of the residual elastin pellet is PE resistant, it was not possible to confirm its composition using MS techniques. However, the residual elastin pellet could correspond to epidermis that was not completely degraded during the elastin isolation procedure. This assumption is based on the finding that the elastin pellets were completely solubilised by PE when the epidermis is removed mechanically from the samples during their isolation procedure.

Due to the variation possibility of the total elastin concentration in the samples as a result of the digestion and preparation of the samples, the effect of the amount of protein over the normalised abundance of quantifiable elastin peptides was also analysed. As expected, peaks with different intensity were observed at each concentration. Moreover, the majority of elastin peptides did not have a significant

change ( $p > 0.05$ ) in their normalised abundance when the elastin concentration was modified in the evaluated range (80 % and 120 %; 1.25 FC). Only ten peptides seem to have changed linearly with the elastin concentration. Consequently, the normalised abundance of every elastin peptide does not reflect the total concentration of the protein in the sample. In ESI-MS, the relationship between the amount of analyte present and measured signal intensity is complex and incompletely understood [5]. The intensity of the fragment ions is dependent on the collision energy and specific composition of the peptide [327]. In addition, the differential ionisation and charged droplet desolvation efficiency of each peptide also have an effect over the intensities obtained [328, 329]. Furthermore, it is relevant the finding that the current data does not show any cluster and pattern in the PCA and variable graphic respectively. It indicates that elastin concentration and the instrumental variation under the conditions evaluated do not induce significant changes in the normalised abundance of elastin peptides that could be identified through the multivariate analysis. Overall, our results show that the LFQ workflow could be applied to compare the abundance of peptides among samples, but it does not have a good accuracy for the absolute protein quantification.

## **5.2 Susceptibility of human skin elastin towards degradation by biologically relevant proteases**

The degradation of fibrillar elastin by elastases is influenced particularly by three factors: the peptide bond specificity of the elastases, differences in available sequences on the elastin surface that could be recognised by the elastase catalytic domain and the presence of remote site contacts between enzyme and substrate [141]. The elastases and their cleavage pattern have been described previously. To gain insights in the available sequences in the fibrillary elastin, the susceptibility of hydrophobic domains of the protein towards enzymatic degradation was analysed. Elastin samples were digested with three different enzymes, cathepsin G (CG), matrix metalloproteinase-9 (MMP-9) and neprilysin (NEP). The peptides released during the digestion of mature elastin with each enzyme reflect the elastin domains susceptibility since the protease cleavage relies on direct interactions between the enzyme and individual peptide bonds in its target protein [330, 331]. Additionally, during this section also the influence of the donor's age on the susceptibility of the protein towards the enzymatic degradation was analysed.

Samples isolated from children donors (CE) represent a mature elastin without significant damage to its structure, although elastin samples obtained from old donors (OE) show elastin partially degraded in some way by intrinsic and extrinsic factors that *in vivo* affect the skin. Since all elastin samples were isolated simultaneously, the impairment of the elastin structure associated with the isolation process is similar in all samples and does not influence the results obtained with each enzyme.

### **5.2.1 Elastase activity of NEP and its relation with previous elastic fibres damage**

From the three enzymes included in this study, NEP is the only one for which elastase activity has not been fully characterised. Neprilysin (EC 3.4.24.11, CD10, enkephalinase, and CALLA) is a type-II integral membrane glycoprotein, member of the M13 subgroup of zinc-dependent endopeptidases [332]. It has been reported to be the skin fibroblast-derived elastase (SFE) [156, 157]. The up-regulated expression and activity of NEP during mouse ageing skin and UVB-repetitively exposed skin seem to be associated with the impairment of elastic fibre network surrounding the fibroblast and the subsequent loss of skin elasticity and wrinkle formation [156, 157, 333].

MS (MALDI-TOF, nanoESI-QqTOF and Orbitrap) analysis of NEP digests showed a high number of peptides in TE samples, while a low amount of peptides was identified in the skin elastin digests. Moreover, analysis using a UV spectrophotometric method for the quantification of total peptides bond in the samples confirm that CE and OE samples do not contain a high concentration of peptides in solution (data not shown). Consequently, elastase activity of NEP on mature elastin could be considered inefficient. This finding is consistent with previous studies that report that SFE has a limited elastolytic activity towards bovine [3H]ligamentum nuchae elastin [334], or human skin elastic fibres [335]. Nevertheless, it is also reported that SFE extensively degrades skin elastic fibres [334, 336] and that NEP displays elastase activity over human elastin [157]. This discrepancy among the reports about the elastolytic activity of the enzyme could be linked to the variation in the morphological characteristic of elastin samples. It has been indicated that structural organisation of elastic fibres in the tissue [134] and the damage that the protein undergoes in the *in vivo* ageing and during the isolation process affect the efficacy of some elastases [149, 326, 337].

Regarding the cleavage analysis based on nanoHPLC-Orbitrap MS/MS data, a higher number of cleavage sites obtained in TE samples than in skin elastin samples agree with the fact that cross-linking increase the resistance of the mature elastin against enzymatic degradation [16, 159, 338]. The cleavage of TE and elastin is particularly interesting due to the fact that substrates previously reported for NEP are proteins with a low size (about 3000 Da) [339]. The cleavage of proteins with larger sizes is restricted by the structural characteristics of the enzyme. NEP structure is constituted by a short N-terminal cytoplasmic domain, followed by a single transmembrane helix, and a large C-terminal extracellular domain that contains the active site [339]. The active site of NEP, which is located in a central and roughly spherical cavity (diameter of approximately 20Å), is only accessible via a small, circular opening formed primarily by charged residues [339]. The entry of large substrates into the active site of the enzyme could be related to two possible conformational changes: the first one is a localised loop shift that allows substrate access and the second one is a hinge-mediated opening of domain 1 and 2 [340]. Therefore, in the case of proteins with large size and complex tertiary structures, it is necessary that they have permissive structures that allow the contact between the enzyme active site and the protein, such as the case of the outer edge of the structure of the fibroblast growth factor-2 [341]. TE has a smaller size and a less complex structure than the mature elastin, which could promote their better cleavage by NEP. In addition, some hydrophobic domains seem to be hidden in the core of the elastin fibres as a result of the cross-linking [32, 109, 342], therefore NEP has lower probability of interaction with the elastin fibre, because the mature protein has less contact sites than the TE.

Particularly, OE samples were better cleaved than CE samples. A possible explanation for this might be that the fibres that undergo age-related damage are disintegrated and broken [343, 344], consequently, they could interact better with the NEP active site than the intact elastin fibres. In addition, the age-related changes could also make accessible to the enzyme some domains that were hidden in intact fibres, generating new contact sites that could promote the interaction of EO with NEP. The hypothesis of new cleavage sites in OE fibres is supported by the finding that NEP increased its cleavage preference at the N-terminal site of Ala (19 % in CE; 29 % in OE) and the C-terminal position of Gly (51 % in CE; 62 % in OE).

On the cleavage site specificity of NEP, it is known that the enzyme has a preference to cleave N-terminal peptide bonds at hydrophobic aliphatic or aromatic residues [312]. The NEP active site contains at S1' position the Phe563 which could impart the preference for hydrophobic/aromatic P1' residue [311, 339]. In contrast, the S1 site has a broad specificity, and Gly is the best-accepted residue in the P1 position [312]. In line with these previous reports, at the N-terminal site, NEP predominantly cleaves both the small aliphatic and hydrophobic amino acids Ala, Gly and Val. It is interesting the high tolerance found for Ala, although it has been reported as uncommon for NEP to cleave on the amino terminal side of this amino acid [340]; this is explained because Ala and Gly are the most common amino acid residue in TE. At the C-terminal position, NEP also tolerates Gly and Ala. In contrast to the relatively well-defined S1' specificity, other subsite preferences are less obvious. For example, the S2' subsite, which is necessary for the stabilisation of enzyme/substrate interactions [345], has reduced specificity and can interact with bulky side-chains more than hydrophobic and negatively charged residues [312, 345, 346]. It is also reported that S2' interacts efficiently with the C-terminal free carboxyl group of the substrates [312]. Throughout the second and fourth position in N-terminal sites, NEP cleaves TE and skin elastin samples following the order Gly>Ala>Val>Pro, which corresponds to the amino acid abundance in the elastin sequence. In the C-terminal site, NEP mainly tolerates the same amino acid but with a different order, as a consequence of differences in the accessibility of the cleavage sites. Overall, the nature of the amino acid residue held at positions 2 to 4 in C- and N-terminals residues of NEP has been influenced by three factors. First, the amino acid cleavage preferences of the enzyme, second, the proportion of each amino acid into the elastin sequence and third, the accessibility of the cleavage sites. Similar findings were previously reported for the cleavage preferences of other elastases such as PR3, HLE and CG [147].

### **5.2.2 Degradation of TE and skin elastin samples by CG and MMP-9**

Qualitative analysis through MALDI-TOF MS and nanoHPLC-nanoESI-QqTOF MS techniques showed that TE was readily and comprehensively degraded by CG and MMP-9, indicating their enzymatic activity under the current experimental conditions. The degradation of TE by CG and MMP-9 has been demonstrated in previous studies [147, 149, 152]. In contrast to the current results, peptides in all domains and a coverage of nearly 100 % were determined for the TE digested with CG in a similar enzyme-

substrate ratio (1:100 w/w) but with an incubation time of 24 h [147]. Also, a coverage of 60 % was determined for digested TE with MMP-9 at an enzyme-substrate ratio (1:500 w/w) during 4 h [152]. The differences between previous studies and our current results regarding the percentage of coverage could be attributed to methodological differences among the studies. The contact time between the enzyme and the elastin, as well as the amount of the proteolytic enzyme, could induce the modification of the pattern of peptides obtained at the end of the enzymatic digestion [347].

Interestingly, a lower number of peptides and cleavage sites were found in TE samples digested with CG and MMP-9 than in skin elastin samples digested with the respective enzyme. This result could be attributed to the incubation time used during the experiment; the longest time of incubation allows further degradation of TE peptides, so they could not be identified by nanoHPLC-nanoESI-QqTOF MS analysis because they have an abundance under the detection limit. It is also possible that their sequences contain less than 5 amino acids, which is the minimum number of amino acids requested to be sequenced. Previous studies have suggested that TE could be degraded by longer intermediate peptides that undergo a further degradation [348-350]. In the current experiment, the successive cleavage of peptides in TE samples is supported by three findings. First, MALDI-TOF MS spectra do not show the signal of the monomer or peptides with  $m/z$  higher than 5000 in TE samples; this indicates that the molecule was completely cleaved. Second, skin elastin samples digested with the respective enzymes showed peptides in some of the domains in which no peptides were identified in TE samples; this demonstrates the capacity of the enzyme to cleave these domains. Since the cross-linking increased the resistance of the protein against enzymatic cleavage [16, 159, 338], lack of peptides in these domains in TE samples could show that they are well degraded in the monomer. Consequently, they could not be detected by the reasons previously mentioned. Furthermore, peptides in these domains were found in previous studies in which a short incubation time was used for the digestion of the TE with CG and MMP-9 [147, 152]. Third, during the LFQ analysis, some peptides from TE samples were mainly quantified in all domains after 6 h of incubation, and particularly, the abundance of some of them decreased after 12 h or 48 h. It indicates that peptides could undergo further degradation after 6 h. The same pattern was described for the digestion of peptides from exon 24 with HLE, in which the longest



fragments increased first, and then decreased, which indicates that they are further hydrolyzed by the enzyme [351].

Regarding skin elastin digests, CG and MMP-9 degraded both the CE and OE samples. This finding agrees with previous reports of the elastolytic activity of CG [147, 149, 326, 352-354] and MMP - 9 [141, 355]. However, MMP-9 has also reports of its null or low activity to cleave insoluble elastin [347, 356]. As it was mentioned in the NEP results, this discrepancy among the reports of elastolytic activity of some enzyme could be related to the morphological characteristic and the integrity of the fibres of the elastin samples used in each one [134, 149, 326, 337].

On the other hand, the domains not identified from the elastin samples digested with both enzymes, except for domain 14, contain Lys residues which could be involved in cross-linking. As a consequence, these domains could not be sequenced using the current techniques. In contrast with the results obtained in TE in which the majority of peptides are detected after 6 h, and undergo further degradation, the peptides in elastin samples do not show this behaviour. Few elastin peptides were detected after 6 h, and their amount had a positive correlation with the time. As it was previously mentioned, the proteolytic resistance of the mature elastin lies in its cross-linking [16, 159, 338]. Furthermore, the degradation of the peptides after their release from TE and not from elastin could be related to differences in the elastolytic mechanism too. It has been suggested that in mature elastin, the elastases such as CG and MMP-9 are adsorbed on the protein surface through a slow initial complex followed by isomerization to a tightly bound complex. The enzyme cannot freely diffuse from its substrate, but it can move along it; hence, the elastin is preferentially hydrolyzed by the preadsorbed elastase. In contrast, TE is rapidly and directly bound in a catalytically productive manner [134, 136, 137].

### **5.2.3 Enzymatic susceptibility of the elastin domains analysed through their degradation by CG and MMP-9**

In order to compare the vulnerability of the elastin domains towards the enzymatic attack, from a qualitative point of view, the number of cleavage sites per domain determined in the CG and MMP- 9 digests was taken as a reference. Moreover, a quantitative evaluation of the degradation of each elastin domain was obtained through the LFQ analysis. To include all the peptides quantified in the samples in the estimation

of the most labile domains, the sum of the normalised abundance of the peptides was calculated by domain for each one of the skin elastin samples digested with CG and MMP-9, respectively. Although the sum of the normalised abundance of the quantifiable peptides does not correspond to the total amount of peptides obtained by the digestion of the samples, they could depict the tendency in the degradation of each domain of the mature elastin by each enzyme. The most susceptible domains are identified by their early detection time and their highest amount of the sum of the normalised abundance of the peptides.

Hydrophobic domains through the whole molecule were cleaved by both enzymes, despite the differences in the cleavage preference between CG and MMP-9 [147, 152]. Particularly, from the different domains identified in the current nanoHPLC-nanoESI-QqTOF MS analysis, the skin elastin samples digested with CG and MMP-9 showed a high number of cleavage sites in domains 6, 7, 24, 26, 28, 30 and 33. Interestingly, NEP cleaved both substrates in the domains 3, 7, 16, 24 and 26 despite its low elastase activity. This finding is in line with previous reports in which similar access to scissile peptide bonds in elastin and comparable energy requirements for the elastosis for some enzymes were determined [136, 141, 357]. Quantitative results obtained with both CG and MMP-9 show that domains with a higher amount of the sum of normalised abundance at 48 h correspond to the domains in which peptides were identified after 6 h and 12 h. This result suggests that these domains are more exposed on the surface of the elastin and they might need to be degraded before the enzyme gets access to the other domains in the elastin fibre. In addition, statistically significant differences were found among the sum of the normalised abundance of the domains, especially in the N- and C-terminal regions of elastin. In particular, domains 2/3, 5/6, 6, 7, 11/12, 12, 20, 20/21, 24, 26, 26/27, 28 and 30 are the domains with a significant high abundance of quantifiable peptides after 48 h of incubation with the enzymes. Except for the border between the two domains, the majority of these domains also have a large number of cleavage sites; hence, it is possible to hypothesise that these thirteen domains are the most susceptible to the CG and MMP-9 degradation in the samples analysed. These results agree with previous reports that show that the C- and N-terminal regions of the elastin are more labile to degradation by MMP-7; MMP-12 and MMP-9 [315, 316].

Furthermore, the thirteen domains reported here are showing that nearly 60 % of the hydrophobic domains in the mature elastin are highly susceptible to the enzymatic

cleavage. It agrees with two previous reports in which it was suggested (through experimental data and simulations) that the elastin's hydrophobic domains have limited exposure [32, 109] and that some hydrophobic residues are buried in the elastin structure [342]. Particularly, the higher susceptibility of domains 6, 20, 24 and 26 could be associated with their length. Since these domains are four of the longest domains in the TE sequence (up to 30 residues in length), this high amount of amino acids lead to a higher probability to be cleaved. Interestingly, KA or KP domains follow all the solvent-exposed domains identified, except for domain 2/3. It has been suggested that the cross-linking found among domains 10, 19 and 25 [58], could lead the 19 to 25 area to be more available to solvents [59]. Similarly, other domains that are involved in cross-linking could also contribute to explain the enzymatic susceptibility of the hydrophobic domains. For instance, the allysine residues in domains 21 and 23 could participate in inter-domain cross-link [304, 358], which could lead to the high enzymatic susceptibility of the domains 20, 20/21 and 24. In addition, specific intra-molecular cross-links were suggested to happen in the region encoded by exons 6-15 [51]. Thus, it could be related to the high susceptibility found in domains 5/6, 7, 11/12 and 12. On the other hand, the high protease susceptibility of domains 20, 24, 26 and 30 could also be related to their solvent-exposed condition that was linked to a potential role in the alignment of TE molecules during coacervation [55, 59, 83, 84, 112, 120]. Interestingly, a preponderant role in the alignment of molecules of TE has also been described for the domains 18 and 32 [55, 112] but they were not identified such as solvent exposed domains in the mature elastin. It could indicate that these two domains are buried in the non-exposed region of the elastin fibres as a result of the TE molecules cross-linking. In addition, the high susceptibility of domains 6 and 26 is also in line with the finding that these domains in TE are susceptible to proteolytic cleavage [83, 112, 120]. Interestingly, the hypersensitive protease sequence of TE on the boundary of domain 25 and 26 [32, 83] was not identified in the elastin samples digested with CG and MMP-9; nevertheless, it was found that in mature elastin the border of domains 26 and 27 is highly susceptible to enzymatic degradation. A possible explanation for this might be that the border 25/26 is involved in the cross-link and then, it is not more solvent exposed in the mature elastin. Furthermore, the structural changes associated to the cross-link could expose the border 26/27 to the enzymatic attack.

#### **5.2.4 Age-related differences in the elastin susceptibility towards enzymatic degradation**

A higher number of cleavage sites were identified in OE samples than in CE samples after 48 h of digestion with each one of the three enzymes studied. It is known that the ageing process induces disruption and fragmentation of the skin elastic fibres by the action of elastases and other factors such as UV radiation [132, 133, 138, 359-362]. It has also been reported that new sites for the activity of enzymes such as PR3 were created when elastolysis proceeded [145], and limited elastolysis could extensively modify elastin structure, favouring higher interaction with PE [137]. Therefore, the larger number of cleavage sites identified here in OE samples could indicate new elastin areas exposed to enzymatic attack in OE compared to CE samples. It is also indicated by the finding that peptides derived from domain 13 and 14/15 only were identified in OE samples digested with CG and MMP-9. On the other hand, the high number of cleavage sites could also be related to the previous damage that the elastin undergoes during the ageing process. Since the elastic fibres are age-related damaged, fragments of the domains with different length could remain in these fibres. Thus, when the enzyme cleaves the OE, new cleaved sites are originated due to the previous fragmentation and the cleavage by the enzyme under study. It could also be supported by the finding that some domains with a high amount of cleavage sites determined in OE samples were also identified such as a high susceptible to enzymatic attack; for instance, domains 24, 28 and 30.

Interestingly, comparison results of the sum of the normalised abundance of quantifiable peptides per domain showed that in MMP-9 digests, all domains from the OE samples had a lower amount of this sum than the respective domain in CE samples digested with the same enzyme. Taking into account that the degradation profile of CE and OE samples digested by MMP-9 was similar, this finding suggest that elastolytic activity of MMP-9 is mainly related to the solvent-exposed domains in the intact fibres. In contrast, results obtained from the CG digests showed a different behaviour. The domains 6, 16/17, 20/21 and 26/27 were found in a higher amount in CE samples digested with CG. These domains were also identified as solvent exposed domains susceptible to degradation by CG and MMP-9, except for domain 16/17. In addition, domains 6/7, 9, 9/10, 10/11, 13, 14, 16, 28 and 30 had a higher amount of normalised abundance of total quantifiable peptides in OE than in CE samples digested with CG.

None of these domains was determined as solvent exposed, excluding domains 28 and 30. Moreover, the number of cleavage sites identified in the majority of these domains was higher in the OE samples digested with both enzymes. It is possible to hypothesise that the low solvent exposure of these domains could be associated with their arrangement inside the structure of the fibres since the intra-molecular cross-links could be present in the region encoded by exons 6 to 15 [51, 83]. Nonetheless, it is necessary to confirm the differences between CE and OE samples through further studies.

Most notably CG digests of CE and OE contained a similar amount of peptides, while MMP-9 produced a higher amount of peptides from CE than from OE samples. These results were determined by using the sum of quantifiable peptides (LFQ data) and confirmed by quantification of the total amount of bond peptides in the digests by an UV spectrophotometric method. Similar results for CG were reported in a previous qualitative study [149]. Additionally, the findings reported here agree with the report that in an *ex vivo* study of skin elastic fibres degradation, MMP-9 is an efficient elastase. However, its elastolysis reached a plateau phase with only 50 % hydrolysis; while this behaviour was not described for CG [137, 355]. The MMP-9 plateau phase could show that the damage to the elastin fibres might reach a similar state to the one observed in OE. Consequently, the enzyme will not continue cleaving the fibres with the same efficacy. On the other hand, the qualitative results obtained for NEP suggest that this enzyme has an opposite behaviour to MMP-9, and requires a previous elastic fibre damage to degrade elastin, similar to the one previously reported for HLE [149]. Overall, our results showed that the age-related damage of the fibrillar elastin seems to expose new sites that could or not favour the interaction and elastolytic activity of some enzymes. Hence, it is not possible to conclude that in general, CE or OE are more or less susceptible towards the enzymatic degradation.

Variation in the elastolytic activity of some enzyme over fibrillar elastin has been previously described. As mentioned earlier, the discrepancies among the studies were related to the fact that structural organisation of the elastic fibres is different among the tissues and from the structural damage associated with the isolation process [134, 149, 326, 337]. However, these sources of variation do not apply to the results obtained in the current study. Through the modeling of the sum of the normalized abundance of quantifiable peptides data in a fourth order interaction model of fixed effects with

correlated errors, it was possible to determine that the observed timeframe of peptide generation in each domain depends on the interaction of factors such as enzyme, incubation time, integrity of the elastin structure (CE or OE), and in some cases, the biological variability. As expected, contact time between the enzyme and the elastin substrate induces higher concentrations of peptides as it has been previously reported [363]. Particularly, the biological variability affected domains that were not identified as solvent exposed in the elastin fibres. It seems possible that the amount of these domains quantified during this analysis is under the influence of the previous damage to the fibres. Consequently, the influence of the biological variability could be associated with the significant age-related differences observed between the replicates of old adult donors.

On the other hand, it is possible to hypothesise that the preponderance of the interaction between the integrity of the elastin fibre and type of enzyme could be associated with the accessibility of the active site and the binding requirements of each enzyme. For instance, CG has an extensive and flexible binding site at S1 [147, 364], its active site does not impose strict structural requirements to the residues at P2-P4 and P1'-P4' [147], and it interacts avidly with elastin compared to PE or HLE [353]. Therefore, modifications in OE, which are related to the fibres breakdown and different hydrophobic domains available to enzymatic cleavage, could not influence the elastolytic activity of CG on fibrillar elastin. On the contrary, MMP-9 possesses a deep S1' pocket [365] and requires the binding of its fibronectin type II module [142, 366, 367] and its OG domain (another secondary substrate binding exosites outside the active site) [142, 368, 369] with the elastic fibre to display its elastolytic activity. As a consequence, changes in the domains exposed in the fibrillary elastin could impair the interaction between this enzyme and the protein. In fact, gelatinase binding through the fibronectin type II-like domain was suggested to be rate-limiting for catalysis of elastin [366]. In addition, inhibition of the elastolytic activity of the MMP-9 through the restriction of its binding through FN-II module has been previously reported [365]. Further investigation must be done to support the influence of these two factors over the variability of the enzymes' elastolytic activity.

Importantly, the degradation of the elastic fibres with the enzymes studied here suggests that there are three types of elastases; first, elastases as MMP-9, that preferentially degrade intact elastin fibres; second, enzymes that mainly degrade elastin

in already disintegrated fibres as NEP and finally, elastases as CG which have similar elastolytic activity in both kinds of fibres. Then, it is interesting to evaluate the elastolytic activity of other enzymes to determine its category. This is important due to the fact that the majority of the elastases have been evaluated over elastin isolated through harsh procedures, and the elastolytic activity of some enzymes, such as cathepsin V, has shown a high dependence on their exosites that bind the elastin [370].

Finally, the relation between the previous protein structure damage and the elastolytic activity of the enzymes is relevant for the understanding of the elastic fibres degradation. NEP and MMP-9 require elastin with particular characteristics for their elastolytic activity. In both cases, once the protein with the specific feature is depleted, their elastase activity would be limited. In contrast, the elastase activity of CG seems not to be influenced by the damage in the elastic fibres. These findings suggest that the degradation of the elastic fibres by elastases could happen in a coordinated and synergic mechanism. Some elastases such as MMP-9 and CG could promote the initial damage of the fibrillary elastin that would lead to the breakdown of some elastin fibres; these damaged elastin fibres undergo further proteolysis by CG, NEP or other proteases, leading to a higher tissue damage. This hypothesis is also supported by previous reports that in sun-exposed skin areas, CG acts conjointly with neutrophil elastase to damage elastic fibres [140, 352]. It is also interesting that the degradation of elastin by the monocyte-derived macrophages could be a consequence of the MMPs' activity (especially MMP-9) and another cysteine protease [371]. In addition, MMP-9 and CG seem to be overexpressed in older adult skin [132, 372], which could produce the initial elastin fibre damage and increase the elastic fibre susceptibility towards other enzymes. Thus, it could partially explain the high degradation of elastic fibres found in old age skin.

#### **5.2.5 Peptides with bioactive sequences released from different types of skin elastin samples**

An important consequence of the elastin degradation is the generation of matrikines. Similarly to previous reports for the CG [147] and MMP-9 [152], several matrikines from the fibrillar elastin were released during the present study. Few peptides with bioactive sequences were found in common in the skin elastin samples digested with each one of the three enzymes, which could be explained by the differences in their cleavage

preferences. In addition, MMP-9 and NEP released more matrikines from CE and OE samples, respectively, due to the fact that they degrade CE and OE differently. In contrast, CG, which degrades CE and OE with comparable efficacy, generates a similar number of peptides with bioactive sequences. Thus, the impairment in the structure of elastin seems not to influence the released matrikines by this enzyme.

The EDP with the highest abundance in the skin elastin digests by CG and MMP-9 are mainly derived from domains 7, 7/8, 9/10, 10, 20, 20/21, 24, 26/27 and 30. Except for the domains 7/8, 9/10 and 10, the other domains were identified as very vulnerable to the enzymatic degradation. Hence, peptides derived from these domains were found in a higher amount in the CG and MMP-9 digests. Particularly, a large number of EDPs derived from domain 24 is explained by the fact that this domain contains multiple GxxPG sequences; GxxP sequences (in which x  $\neq$  Gly) could be bioactive since they may adopt a type VIII  $\beta$ -turn conformation and interact with EBP [192, 193]. Interestingly, the sequence VPGVG was the most frequently identified and it presented the highest abundance regarding other sequences found in the peptides from elastin skin samples digested with CG and MMP-9. This sequence has proven to induce the proliferation of smooth muscle cells and reduction of elastin expression in chick VSMC [214]. On the other hand, the sequences PGFGAVPGA and GAVPG were also identified in several of the most abundant peptides found in skin samples digested with MMP-9. These sequences have shown to stimulate the pro-MMP-2 secretion in human dermal fibroblasts [152]. Furthermore, CG has proved to release some peptides containing multiple times the motifs VGVAPG and GVAPGV [147]. In addition to these two motifs, GLVPG, PGVGVA, VAPG and VGVA were also released by CG and NEP. These sequences have several biological reported effects (See Table 1. *In vitro* biological activities reported for some EDPs, Chapter 1). It is interesting that some of these activities are related to the chemotaxis of monocytes and release of some enzymes, such as pro-MMP-1, -2, -3 and elastase [147, 184, 195, 201], and they foster superoxide production [201]. It is also interesting that some of these motifs are found several times in one peptide sequence, which could help overall bioactivity [159]. Additionally, about half of the peptides released by each enzyme contained one or more bioactive motifs, which may enhance the probability of an interaction of the matrikines with the EBP. Taking into account that CG, MMP-9 and NEP are overexpressed in the photodamaged human skin [156, 157, 372, 373], it is possible to speculate that they contribute to exacerbating the local tissue



damage in the skin due to their elastase activity and through the stimulation of the activity of other enzymes that degrade the ECM.

## **5.3 Structural changes of human elastin during skin ageing**

Cutaneous ageing is a complex biological process that happens as intrinsic and extrinsic ageing and influences mainly the dermis. Intrinsic or innate ageing is the physiological process observed in the sun protected skin, while extrinsic ageing or photoaging is induced and accelerated by environmental influences such as UV radiation, smoking and air pollution, and whose effects are superimposed on those of innate ageing [4, 222, 313, 374, 375]. At molecular level, both ageing processes are connected by phenotypic alterations in cutaneous cells; and structural and functional changes of ECM components. These components produce significant variations in the mechanical properties of the skin [4]. In this section, the effect of intrinsic and extrinsic ageing over the degradation of human skin elastin samples was studied by SEM, LFQ and multivariate analysis.

### **5.3.1 Elastic fibres morphology and its susceptibility towards enzymatic degradation**

Skin ageing leads to changes in the morphology of elastin fibres. An evident deterioration of the fibres is observed when derived samples from old adult donors are compared with samples from young and adult donors, as it has been described in a previous study for young and aged rat elastin [343]. In fact, intrinsic ageing comprises the degeneration of the elastic fibre arrangement; this degeneration can involve three elements, the separation of elastin fibrils from each other; the formation of cystic spaces and eventually pronounced fragmentation of elastic fibres in individuals over 70 years [4, 313, 314]. Furthermore, the extrinsic ageing is superimposed on these effects and is linked with the infiltration of inflammatory cells, macrophages and mast cells, which could prompt an increased expression of unspecific proteases including MMPs and NSPs. These enzymes could further degrade elastin and other ECM components [360, 376-378]. Thus, the fragmentation and disintegration into fibrils, which were identified as particular features in samples derived from old adult donors, indicate the deleterious

effect of the intrinsic and extrinsic ageing. In line with this result, an age-related increase in the susceptibility of the elastin fibres towards PE attack was observed. This increase in the elastin susceptibility agreed with the results described in the previous section for NEP and with the activity reported for HLE; HLE cleaves elastin fibres isolated from older donors (90 years), whereas young, intact fibres are resistant towards this protease [149]. Overall, these results support the statement that intrinsic and extrinsic ageing produce a constant damage to elastin fibres that enhances the protein's susceptibility towards enzymatic degradation [313, 362].

### **5.3.2 Characterisation of elastin peptides released from elastin obtained from differentiated aged individuals**

LFQ and statistical analysis indicate that some peptides have a normalised abundance that differs significantly between samples from children, adults and old adults. Three different age-related patterns of change of the peptide's abundance were identified: decrease, increase and fluctuation (increase-decrease). Interestingly, about half of the peptides with significant age-related differences in their normalised abundance are released from domains 18, 24 and 26, which are the largest hydrophobic domains in TE. Furthermore, these domains seem to have a relevant role in the coacervation of the TE molecules and have been reported as the first contact points between different TE molecules. Hence they could be considered such as solvent-exposed [55, 112]. As a consequence, these domains could be better cleaved by the elastases and released in great extent from elastin during the ageing process. In line with the results reported in the previous section (4.2), some of the domains which contain peptides with age-related patterns of change (namely domains 6, 7, 11/12, 20, 24, 26, 26/27 and 28) also showed a high susceptibility to the enzymatic degradation by CG and MMP-9.

The nine peptides with a decreasing abundance over age could indicate that they are the first to be released from elastin through enzymatic degradation at ages below 20. Hence, they are involved in the early cleavage sites in previously intact elastin. Also, it can be presumed that these first cleavages impair the stability of elastin and make it more susceptible to further cleavage, which for example fosters the release of peptides with an age-related increase in their abundances. This inference is based on the finding that the 9 elastin peptides decrease their abundances to their minimum level at ages

around 70, while the normalised abundances of other elastin peptides increase significantly.

Furthermore, the resistance of young elastin (from donors below 20 years) towards enzymatic degradation is also revealed in the relatively low quantities of peptides that were released in these samples. The decrease in the peptide abundances with increasing age was determined to be much less pronounced than the changes in the case of peptides that show an age-related increase in their abundance. On the other hand, the nine peptides with the age-related decrease in their normalised abundance are found mainly in domains 18, 20, 24 and 26, which are solvent-exposed and, thus, highly susceptible to enzymatic cleavage [55, 112]. Particularly, the N-terminal part of TE seems to contain some early cleavage points in domains 6, 11 and 12 (peptides showing decreasing abundances over the age). Nevertheless, in general, this part of the molecule predominantly contains peptides with an age-related increase in their normalised abundance (domains 2 to 11/12), which suggests that this region of the molecule could be less accessible to immediate cleavage and it is exposed to enzymatic cleavage after the pre-damage to elastin has occurred. It is interesting to note that some peptides display a stronger age-related increase in their abundances, whereas others show a weaker increase. This opposite pattern may be related to the differing accessibility of different parts of TE associated with pre-damage to elastin and elastin fibre components such as fibrillins; as a result of intrinsic and extrinsic ageing as was described in detail previously [313, 314, 379].

Furthermore, 30 peptides showed significant differences in their abundances between distinct elastin samples, however, they displayed a fluctuating change with age. The finding, that the shift point of the normalised abundance of these peptides is near the age of 70, correlates with previous observations in which the elastic fibres degradation starts at the age around 30, and it dramatically increases at ages older than 70 during the intrinsic skin ageing [313]. The decrease in the abundance of peptides in samples from old adults (80-90 years) may be related to the fact that peptides from these domains, especially domains 18, 24 and 26, may have already been released to almost full extent by proteases such as MMPs or NSP *in vivo* at ages below 80. Another reason for this behaviour may be the progressive damage to elastin in elderly individuals that may generate other preferable and more accessible cleavage sites for the enzyme, which leads to the release of other peptides.

Finally, it is interesting that some of the 303 identified peptides in the LFQ analysis do not show significant age-related changes in their abundance, for instance, peptides from the domains 30 and 33. This result may be related to the fact that some regions of TE do not become more accessible for cleavage with increasing age, for instance, some highly cross-linked regions of the protein. Moreover, some domains in the C-terminal part of TE plays a critical role in elastin function, for instance in the cell adhesive activity, and it influences matrix interactions; as well as fibre formation and cross-linking [124, 128, 136].

### **5.3.3 Release of potentially bioactive peptides from elastin during skin ageing**

A high number of peptides with an age-related variation of their amount contain motifs into their sequences. Undoubtedly, the release of the EDPs corresponds with the resistance of elastin towards enzymatic cleavage. Few amount of peptides with matrikines are released in the first 20 years of life time, whereas a significantly higher amount of them is liberated at ages older than 40. In addition, this reflects the effects of acute or chronic sun exposure and continuous innate tissue ageing that increase enzymatic degradation of elastin over time either slowly (intrinsic ageing) or rapidly (extrinsic ageing). Interestingly, peptides with an age-related decrease in their abundance included multiple motifs overlapped in their sequences, which could favour their interaction with the elastin receptor. In *in vitro* studies, these bioactive sequences have shown to be chemotactic for monocytes (FGVG, GLVPG [195]) and fibroblast (GFGVG [197]). They also stimulate pro-MMP-1 secretion in human dermal fibroblast (AGLVPG, GLVPG and PGFGPG [147]). Similarly, the peptides, that displayed an age-related increase in their abundance, contain motifs which have shown to induce the expression of some enzymes, such as pro-MMP-1 (GVAPGV [81]), MMP-2 (VAPG [184]) and pro-MMP-3 (GVAPGV; VAPG [81, 184]). Moreover, they contain VVPQ that has shown mitogenic activity on dermal fibroblast [215], as well as the GXXPG motif VGVAPG which displays a variety of biological activities due to its strong interaction with EPB [121]. These activities include, for instance, chemotaxis of monocytes and fibroblasts [203] and induction of the expression of pro-MMP-1 in fibroblasts [81]. Furthermore, the same motifs were identified in peptides with an age-related increase-decrease pattern in their abundances; particularly, the sequences VPGVG, GAVPG and VGVPG were also found in these peptides. These motifs could increase cell proliferation

and autoregulation of elastin expression (VPGVG) [214], increase of the pro-MMP-2 secretion in human dermal fibroblast (GAVPG)[152] , and be chemotactic for monocytes (VGVPG) [199]. As a consequence of the release of peptides containing bioactive motifs, an exacerbation of local tissue damage may occur through their negative effects, for instance, the upregulation of further ECM-degrading proteases, as it has been previously suggested [81].

#### **5.3.4 Classification of samples according to the sources of elastin degradation**

The PCA scores plot and the HCA dendrogram showed that the skin elastin samples are clustered according to the age and the degree of sun exposure. Almost half percentage of variation in the data is described by PC1. This PC is related to the intrinsic ageing, indicating that the release of elastin peptides reflects mainly the age of the donor, which is consistent with the previous report focusing on the degradation of skin elastin by HLE [149]. However, a minor extent of the variation in the data explained by PC1 is also related to the extrinsic ageing, since it is always superimposed on intrinsic ageing in sun-exposed areas [313]. Hence, the development of skin ageing involves processes that are concomitant and influences the turnover of the elastin, for instance, the up-regulation of several elastases. Similarly, the PC2, which explained 30 % of the variation among the samples by the effects of sun exposure on the skin, is also related to the intrinsic ageing. Interestingly, the two main clusters identified in HCA analysis separated the samples of ages  $\geq 80$  from those  $< 80$ , which agrees with the dramatic increase in the elastin degradation at ages above 70 [313].

Furthermore, the clusters and subclusters in the HCA dendrogram reveal that the damage of the elastin fibre along the life time could be described in three stages according to the growing incidence of the intrinsic and extrinsic ageing. The sun-protected skin of children, which clustered very close together in the PCA, shows that almost no damage to elastin associated with intrinsic and extrinsic ageing happened, since the mature elastin has just been fully deposited at this age [380]. With increasing age, the effects of the extrinsic and intrinsic ageing are overlapped in a different amount in the individuals, and a higher dispersion of the samples is obtained. As a consequence, the sample of the 19 years old individual is found a little far apart from the young samples, indicating the beginning effects of innate ageing on elastin. As a result of this

low amount of damage in the elastin, the samples from donors aged between 6 and 19 are found together in the same cluster. The next stage includes the changes observed in samples obtained from sun-protected and sun-exposed skin areas of adults aged between 43 and 70. During this period, elastin degradation starts to progress considerably and leads to morphological changes previously described [313]. Interestingly, the samples from sun-protected and sun-exposed body regions are found in different subclusters, indicating that there is an overlap between the effect of both ageing processes. In addition, there is a clear difference in the enzymatic susceptibility of elastin samples, most likely due to an acceleration of elastin degradation in the sun-exposed areas [360, 376]. Finally, the last stage includes the changes described for the samples of donors aged over 80. These samples showed the highest damage in the elastin fibre, which agrees with the previous finding that the structures present in ECM considerably change at ages above 70, even in sun-protected areas of the skin [313].

Finally, the variables graph describes a correlation between the sun exposure condition of the skin and the release of peptides. Overall, peptides derived from the N-terminal and central regions of the TE molecule (domains 6-16) are mainly degraded in samples from sun-exposed parts of the body and older donors, also indicating their low exposition to the enzymatic cleavage in intact elastin. In contrast, the peptides derived from the C-terminal region of TE (domains 26-32) are derived from samples of non-sun-exposed skin from young or adult donors. Hence, its peptides are correlated with the intrinsic ageing; it seems like this region is solvent exposed, and the peptides of the protein are released earlier than peptides from the N- or central region of the TE. Particularly, the age-related increase in the abundance of some peptides, which are derived from domain 6 (P3 and P6), is also strongly correlated with UV exposure. This finding agrees with the hypothesis that extrinsic ageing, which is superimposed on intrinsic ageing, fosters the ageing process, for instance, elastin becomes more susceptible towards the cleavage by some elastases leading to the decomposition of fibrillar elastin [4, 313, 314].

## **5.4 Molecular changes of human skin elastin from patients with Williams-Beuren Syndrome and healthy individuals**

### **5.4.1 Elastin content of skin and elastic fibre morphology**

One of the most visible symptoms of Williams-Beuren Syndrome (WBS) patients is the premature skin ageing [244]. This symptom could be related to the findings of some previous studies, which have shown a significantly reduced diameter of the dermal elastic fibres and an *in vitro* reduced deposition of elastin in these fibres [238, 248]. In line with these previous studies, a small amount of elastin in WBS patients' skin was identified in comparison with healthy individuals' skin. Furthermore, the smaller amounts of damaged elastin fibres found in skin samples of WBS patients could be related with a decreased elastic modulus and a reduced viscoelasticity of WBS patients' skin versus healthy subjects [249]. Overall, it seems as if the hemizyosity of the elastin gene in WBS patients induces the phenotypic features described here.

Particularly, the SEM results showed a clear similarity between the elastin obtained from healthy old adult individuals and the elastin isolated from the WBS patients. This finding suggests that elastin fibres from WBS patients undergo a higher damage than elastin from healthy donors of similar age, which correlates with the premature skin ageing observed in them.

### **5.4.2 Elastin susceptibility towards enzymatic cleavage**

MS analysis of the enzymatic elastin digests suggests that skin samples from both healthy individuals and WBS patients contain TE isoform 2, since peptides derived from exons 22, 24A and 26A were not identified. This finding is in agreement with previous results obtained from skin elastin isolated from healthy donors [71, 129, 147, 315]. Moreover, all peptides identified are derived from non-cross-linked regions of elastin, since the peptides from the cross-linked KA and KP domains cannot be sequenced with commercially available bioinformatic tools. Interestingly, identical number and position of the cleavage sites were found in skin elastin from WBS patients and healthy donors. These results are a direct consequence of the broad cleavage specificity of PE. Additionally, it also indicates that elastin from WBS patients and healthy individuals are

structurally similar; and the Lys residues are predominantly involved in cross-linking in both samples.

#### **5.4.3 Differences between elastin peptides released from elastin isolated from skin of WBS patients and healthy individuals**

During the LFQ and statistical analysis, 35 % of peptides identified showed statistically significant differences ( $p < 0.05$ ) between the skin elastin samples obtained from WBS patients and healthy donors. It is interesting to note that the majority of peptides with higher abundance in elastin digests of WBS patients are derived from the C-terminal domains 26, 26/27 and 28/29 and the N-terminal domains 10, 11/12. This result may suggest that the C-terminal region of TE in elastin from WBS patients is more susceptible towards enzymatic cleavage. Particularly, these domains were identified such as susceptible to enzymatic degradation in elastin samples isolated from healthy individuals and degraded by CG and MMP-9 (Section 4.2.3). Furthermore, it was found that these domains contained cleavage sites that appear with the age increase of healthy individuals; these domains also contained peptides whose abundance increase with the ageing in elastin fibres (Section 4.3.2). Therefore, a high amount of normalised abundance of peptides from these domains in elastin samples isolated from WBS patients could be attributed to the high effect of the ageing that these fibres undergo, increasing their susceptibility to enzymatic degradation.

It is worth mentioning that peptides with the highest abundance in skin elastin digests from healthy individuals are derived from domains 16, 18 and 20. Domains 16 and 18 were found not to be highly susceptible to degradation in elastin samples from healthy individuals digested with CG and MMP-9. Moreover, it was found that these domains mainly contained peptides, whose normalised abundance increased over time and stopped at the age of 70, afterward they decreased at the period between 70 and 90 years, which could indicate a higher susceptibility to enzymatic cleavage at ages over 70 than in lower ages (section 4.3.2). Taking into account the differences between the age range of the groups included in this study (healthy individuals (19-70 years) and WBS patients (24 – 40 years)), the skin of healthy donors has undergone age-related changes due to its higher age range. The high normalised abundance of peptides from these domains could indicate that the ageing process of the elastic fibres in healthy individuals is lower than the observed in the WBS patients, which resembled age-related changes of



healthy individuals aged over 70. As a consequence, the extreme ageing of the elastin fibres isolated from WBS patients could have promoted the *in vivo* release of these peptides in a high amount.

It is also interesting that peptides containing HyP residues had higher abundances in elastin from healthy individuals, suggesting that maybe the skin elastin has an overall lower hydroxylation degree in samples from WBS patients, which leads to an overall lower number of peptides with HyP residues. The role of HyP in elastin is not understood completely. However, it was suggested that prolyl hydroxylation might contribute to the adaptation of the elastin properties in different tissues [381] and could increase the elastin's resistance towards proteolytic degradation [75]. Therefore, one possible implication of the lower amount of these residues is that it could contribute to the loss of elasticity, functionality and resistance towards enzymatic degradation of WBS patients' skin. However, further studies must be done to confirm this hypothesis.

#### **5.4.4 Release of potentially bioactive peptides from elastin isolated from WBS patients and healthy donors.**

Concerning the release of peptides containing matrikines, about half of the peptides that showed significant differences in their normalised abundances contained bioactive sequences. Interestingly, digests from WBS patients and healthy individuals have almost the same number of potentially bioactive peptides; nevertheless, WBS patient samples contained more matrikine diversity. In particular, the peptides found in samples from healthy individuals and WBS patients contained sequences that have shown *in vitro* activities which could promote the tissue damage. For instance, they could be chemotactic for monocytes (GLVPG and VGVPG [195, 199]), stimulate the expression and/or secretion of some enzymes such as MMP-1 (GLVPG, GVLPG [147]), MMP-2 and MMP-3 (VAPG [184]) and enhance the proliferation of smooth cells and decreasing the elastin expression in VSMC (VPGVG [214]). Especially, the VGVAPG motif was found mainly in peptides released in a higher amount from WBS elastin. As mentioned in previous sections, this motif displayed a variety of bioactivities (See Table 1. *In vitro* biological activities reported for some EDPs., Chapter 1), for instance, chemotaxis of monocytes and fibroblasts [203], and induction of the expression of pro-MMP-1 in fibroblasts [81]. On the other hand, samples derived from WBS patients also contained a high amount of peptides with bioactive sequences that have been described to be

chemotactic for monocytes (FGVG and GVAPG [195, 199]), fibroblast (GFGVG [197]) or neutrophils (PGAIPG and GAIPG [196]), while GAVPG, GVAPGV and PGAIPG have been found to induce the pro-MMP-1, -2 and/or -3 secretion [81, 152]. In addition, PGVGVA stimulates the superoxide production and elastase release in PMNL [201]. Overall, the release of potentially bioactive peptides could stimulate some enzymes that may accelerate elastin degradation in the skin of WBS patients' skin and contribute to the premature skin ageing that is observed in these individuals. Due to the fact that other peptides, which contain matrikines, also foster the degradation of the elastin in skin samples from healthy donors; our results do not allow to distinguish that enhanced degradation of elastin fibres induced by matrikines happens exclusively in WBS samples.

#### **5.4.5 Classification of samples according to the elastin changes in WBS patients and healthy individuals**

The PCA scores plot showed a clear separation of the WBS elastin and the healthy elastin based on the PC1, which described nearly 69 % of the variation in the data set. Furthermore, the two main clusters in the HCA dendrogram split the samples from healthy donors and WBS patients. Thus, these results demonstrated that skin elastin samples obtained from WBS patients and healthy donors have significant differences in their enzymatic susceptibility. Interestingly, the PC2 described only 10 % of the variation in the data. This PC could be associated with the intrinsic and extrinsic skin ageing. In healthy individuals, the samples from donors aged between 19 and 62 did not present a high dispersion in the PC2. In contrast, the samples S10 and S8, which were obtained from the sun-protected body region of a 70 year donor and the sun-exposed body region of a 58 year individual, were found in opposite positions in the PC2; nonetheless, these samples were found in the same sub-cluster in the HCA dendrogram. These results indicate that these samples present similar enzymatic susceptibility. Moreover, the highest damage of the S10 and S8 samples could be associated with the effects of intrinsic and extrinsic ageing, respectively. This finding agrees with our results in the preceding section (4.2) and with the previous report that at ages above 70 the elastin degradation strongly increases [313] and in sun-exposed body areas it is accelerated by the UV radiation [360, 382].

Despite the short age range of WBS patients and the fact that all samples were obtained from the forearm; in the PCA the samples S3 and S5 are parallel to the sun-

exposed samples obtained from a healthy donor (S8), and they were split from the other WBS samples in a different cluster in the HCA analysis; it could be possible to speculate that these samples from WBS patients present a higher damage in the elastin structure compared to other WBS samples, which resembles the one produced by the extrinsic ageing in healthy old individuals.

On the other hand, the variables graph also showed a clear differentiation between the peptides related to samples derived from WBS patients and healthy individuals, which explain the high percentage of variation described by PC1. The high abundance of peptides derived from domains 26, 26/27 and 28/29 in WBS elastin and domains 16 and 18 in healthy elastin have the highest impact on the differentiation of the samples in the PC1. As previously mentioned, the C-terminal region seems to be more susceptible towards enzymatic cleavage in elastin isolated from WBS patients, as a possible consequence of the high ageing that the samples undergo.

It is also interesting that high abundant peptides derived from domain 24 presented a positive correlation with PC2 in both WBS and healthy elastin samples. This could indicate an *in vivo* lower enzymatic degradation of this domain compared to the other elastin domains. It seems possible that these results are due to the intrinsic ageing effect, since these peptides are correlated to the samples S4 and S10; these two samples are derived from the non-exposed body regions of the oldest donors in each group. Furthermore, some peptides derived from domains 20 and 28 are negatively correlated with PC2 in healthy elastin, while peptides derived from domains 10, 11/12, 18 and 20 are the ones that have a negative correlation with the PC2 in WBS elastin samples. As mentioned previously, a possible explanation for this might be that premature ageing in WBS skin induce the highest enzymatic susceptibility of these domains. These results support the assumption that elastin samples S3 and S5 show a similar pattern of degradation to the one obtained from the sun-exposed skin of healthy old individuals.

## 6 Conclusions

The damage of elastin plays a critical role in the loss of the tissue integrity and functionality, which serves as the fundamental motivation for the analysis of the molecular basis of the degradation of fibrillar elastin. For the first time, an LFQ workflow was applied to quantitatively analyse the degradation of elastin. As the discussion part of this thesis has shown, this method in combination with some statistic tests allows identifying changes in the amount of peptides released from fibrillar elastin. Thus, this methodology was applied to the analysis of the degradation of elastin isolated from the skin obtained from different healthy donors and WBS patients. However, future works may involve further improvements to handle the effect of the biological variability on the results, for instance, increasing the number of donors included in the studies. In addition, it is also important to reduce the gap between the number of peptides identified and quantified, through the use of mass spectrometers that are capable of doing simultaneous MS and MS/MS analysis (Orbitrap MS).

In this study, the statistical analysis of the LFQ results showed that not all hydrophobic domains in intact fibrillar elastin have a similar enzymatic susceptibility. Thirteen domains from the N- and C-terminal regions of TE are most vulnerable to enzymatic attack by cathepsin G (CG) and matrix metalloproteinase 9 (MMP-9). Interestingly, the susceptibility of these hydrophobic domains appears to be the result of the solvent exposure points generated by the cross-linking of the KA or KP domains in mature elastin, but further investigation is necessary to prove this hypothesis. On the other hand, the current results suggest that the susceptibility of different hydrophobic domains in fibrillar skin elastin towards enzymatic degradation is the product of the interaction of the enzyme type, the integrity of the elastin fibre and incubation time. Furthermore, the ageing process affects the integrity of the fibrillar elastin but does not increase their susceptibility towards CG and MMP-9 degradation. Neprilysin (NEP), which has been postulated to be the skin fibroblast-derived elastase, cleaved TE well, but the degradation of the mature elastin was not complete, consequently, the elastase activity of NEP could be considered as deficient. Remarkably, the elastolytic activity of NEP is improved in already disintegrated elastin. Taken together, these results suggest that elastases could be classified into three categories: first, elastases that preferentially

degrade intact elastin fibres, second, enzymes that mainly degrade elastin in already disintegrated fibres and finally, elastases which have similar elastolytic activity in both kinds of fibres. Further studies may be done to determine which category each elastase belongs to, which could help to explain the role of each enzyme in the accelerated damage of the elastin during ageing and some pathologies such as WBS. Moreover, these findings reinforce the importance to evaluate the action of elastases on fibrillar elastin of different integrities.

Regarding the effect of skin ageing on the elastin degradation, the intrinsic skin ageing seems to be related to the first cleavage points of the TE in its large hydrophobic domains of central and C-terminal regions. It is thought that these first cleavage sites make the protein more susceptible to further cleavage. In addition, the N-terminal and central parts of TE are the most cleaved domains in elderly individuals, and their cleavage seems to be enhanced by extrinsic ageing. In general, the decomposition of elastin fibres correlates with an increasing susceptibility of the fibres towards PE degradation. One possible implication of these findings is that the elastic fibres are more susceptible to different enzymes in old individuals *in vivo*. That could explain the severe structural damage of elastin at ages above 70. This strong damage has been previously described in the literature and confirmed by the results presented in this thesis. An interesting question that remains to be answered by future research is the role of the enzymes that are overexpressed in sun-exposed body regions and old adult individuals with respect to the degradation of the elastin. In addition, the methodology described here could be applied to study solar elastosis (deposition of elastolytic material in the dermis) to identify if it is a consequence of the degradation of elastin or the result of abnormal synthesis of elastin in the skin.

On the other hand, the results described here indicate that elastins derived from WBS patients and healthy donors differ in the proline hydroxylation degree and the susceptibility towards enzymatic cleavage. The higher susceptibility of the elastin from WBS patients may be associated with structural changes that happen during an altered elastogenesis. Further research about the impact of other proteins involved in the elastogenesis would be useful to support this hypothesis. Interestingly, the damage of elastin in these patients seems to correspond to an accelerated ageing process which in some cases resembles the effect of extrinsic ageing in the skin of healthy old adult individuals. Particularly, a significantly lower amount of elastin was observed in skin

samples derived from WBS patients, which could be the result of the premature ageing that the elastic fibres have undergone. Further research with elastases involved in extrinsic ageing will provide a better understanding of the high degradation observed in the skin elastin of WBS patients.

Finally, EDPs released during the elastin degradation in the skin of WBS patients and healthy donors as well as skin ageing of healthy individuals suggest that matrikines could prompt the damage of the tissue through the induction of the other enzymes. Then, it could be interesting to study the effect of the most abundant EDPs released in each condition analysed during this thesis with respect to the stimulation of the production of other enzymes that degrade the ECM.

## Appendix

### Appendix 1. Workflow suitability to distinguish changes in abundance of elastin hydrophobic peptides

Code	Residue	Peptide sequence	Normalised abundance (mg/mL)					FC	CV
			0.08	0.09	1.00	1.10	1.20		
43	281-293	GVPGVPGAIPGIG	14.30 ±1.63	18.65 ±2.27	19.07 ±2.78	24.43 ±2.65	27.95 ±1.01	2.0	15
62	335-353	GVPGAGVPGVGVPGAGIPV	87.54 ±15.43	120.96 ±33.05	112.41 ±15.95	144.78 ±15.23	170.88 ±5.59	2.0	27
65	339-356	AGVPGVGVPGAGIPVVPG	24.84 ±7.49	36.63 ±10.03	38.85 ±12.58	55.67 ±9.10	71.52 ±1.92	2.9	32
67	344-361	VGVPGAGIPVVPGAGIPG	12.50 ±2.17	19.94 ±3.27	22.70 ±4.79	31.25 ±4.56	35.43 ±3.37	2.8	21
87	419-440	GVPGVGGVPGVGGVPGVGSPE	74.42 ±12.64	135.31 ±33.79	143.23 ±23.35	191.17 ±15.12	233.60 ±5.63	3.1	25
90	423-437	VGGVPGVGGVPGVGI	24.54 ±1.80	31.91 ±5.07	33.64 ±7.84	47.05 ±6.35	55.67 ±1.59	2.3	23
95	472-484	GLVPGVGVAPGVG	9.30 ±1.32	13.73 ±2.33	17.81 ±2.28	18.51 ±2.49	19.84 ±2.58	2.1	17
96	472-488	GLVPGVGVAPGVGVAPG	22.74 ±1.86	29.72 ±4.47	33.72 ±6.82	44.96 ±6.17	52.21 ±1.55	2.3	20
109	544-557	AGLGAGIPGLGVGV	21.14 ±7.15	31.29 ±8.39	29.77 ±7.51	43.31 ±5.11	53.83 ±2.61	2.5	34
110	545-557	GLGAGIPGLGVGV	18.43 ±5.12	24.10 ±5.27	23.27 ±4.85	33.60 ±4.42	38.72 ±2.65	2.1	28

**Table A-1. Elastin peptides normalised abundance among different elastin concentrations.**

**Elastin peptides that show significant differences in their normalised abundances among samples with different elastin concentration. Data shown as mean ± s.d. (n=4).**

## Appendix 2. Susceptibility of human skin elastin towards degradation by biologically relevant proteases

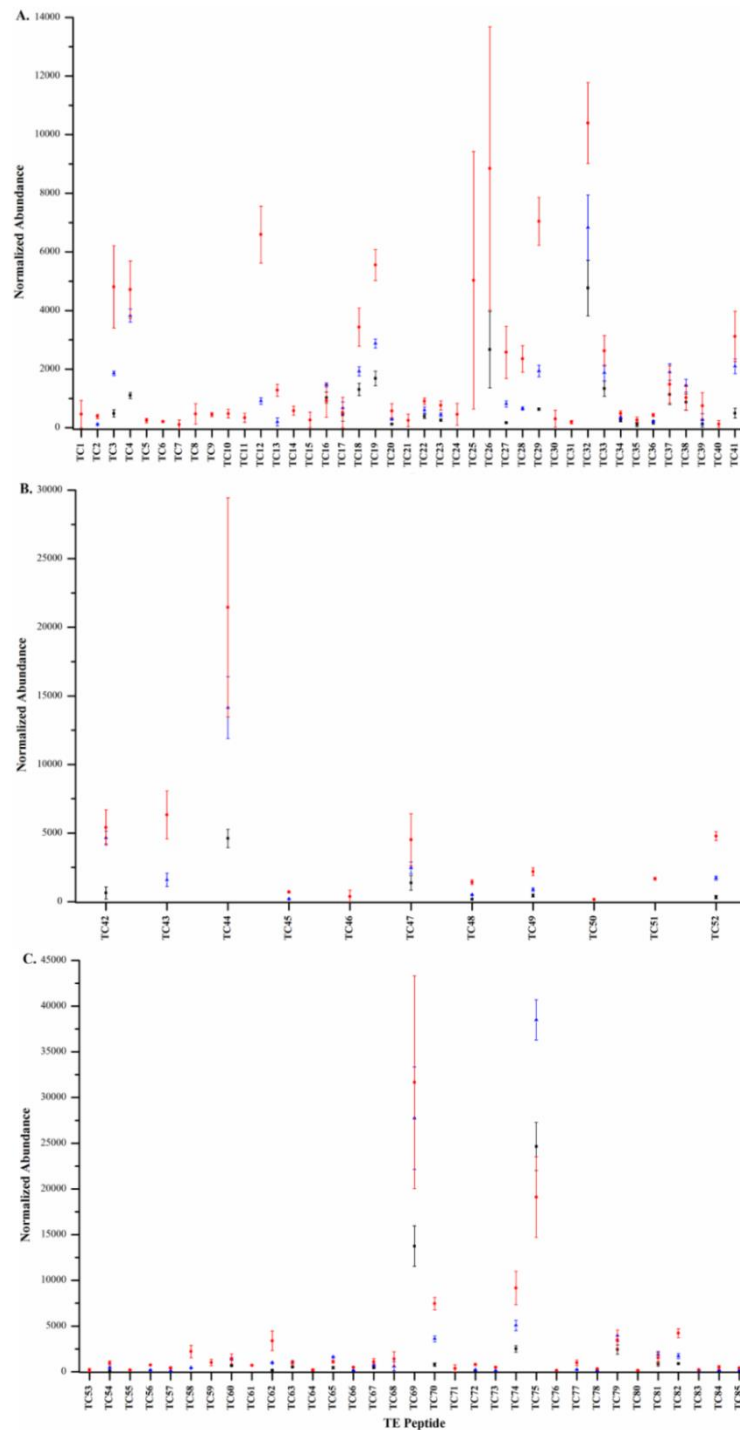


**Figure A-1. Normalised abundance of peptides quantified after 6 h, 12 h and 48 h in TE samples digested with CG.**

Normalised abundance of peptides found in TE samples digested by CG derived from (A) domains 2 to 14, (B) domains 15 to 23 and (C) domains 24 to 36. Measurements were done after 6 h (black), 12 h (blue) and 48 h (red). Data is presented as mean  $\pm$  s.d. (n=2).



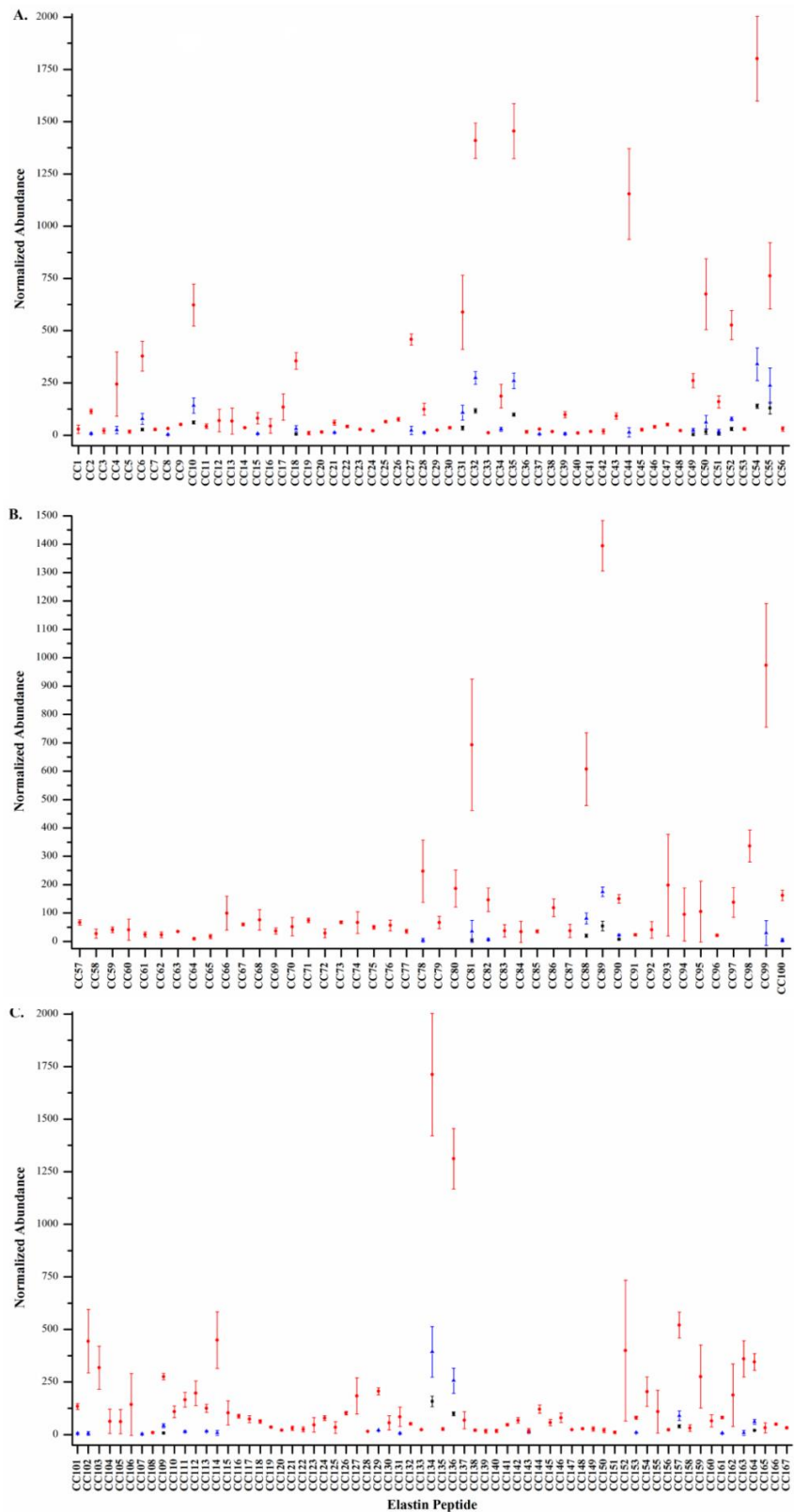


**Figure A-2. Normalised abundance of peptides quantified after 6 h, 12 h and 48 h in CE samples digested with CG.**

Normalised abundance of peptides found in CE samples digested by CG derived from (A) domains 2 to 14, (B) domains 15 to 23 and (C) domains 24 to 36. Measurements were done after 6 h (black), 12 h (blue) and 48 h (red). Data is presented as mean  $\pm$  s.d. (n=3).

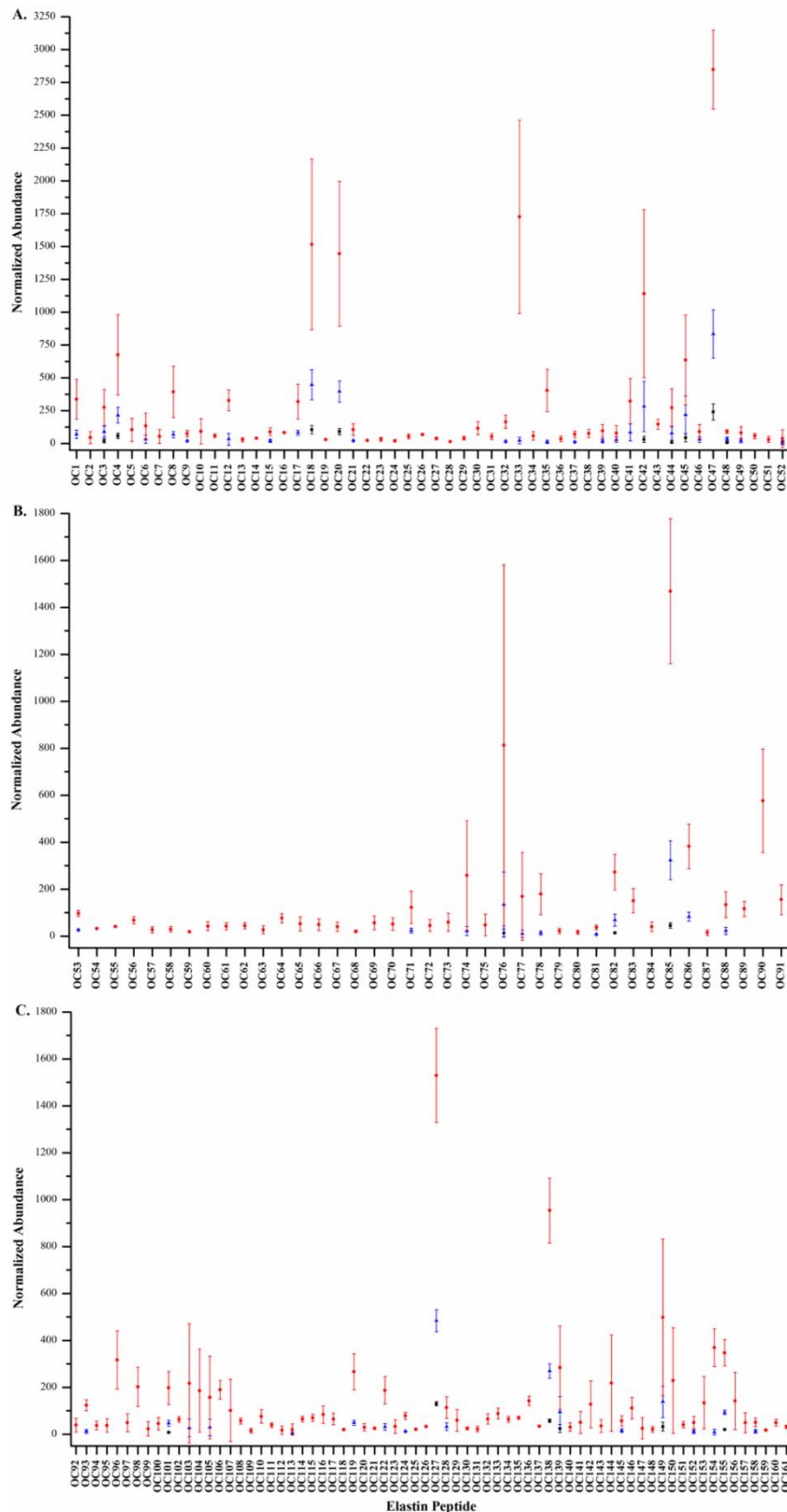


**Figure A-3. Normalised abundance of peptides quantified after 6 h, 12 h and 48 h in OE samples digested with CG.**

Normalised abundance of peptides found in OE samples digested by CG derived from (A) domains 2 to 14, (B) domains 15 to 23 and (C) domains 24 to 36. Measurements were done after 6 h (black), 12 h (blue) and 48 h (red). Data is presented as mean  $\pm$  s.d. (n=3).

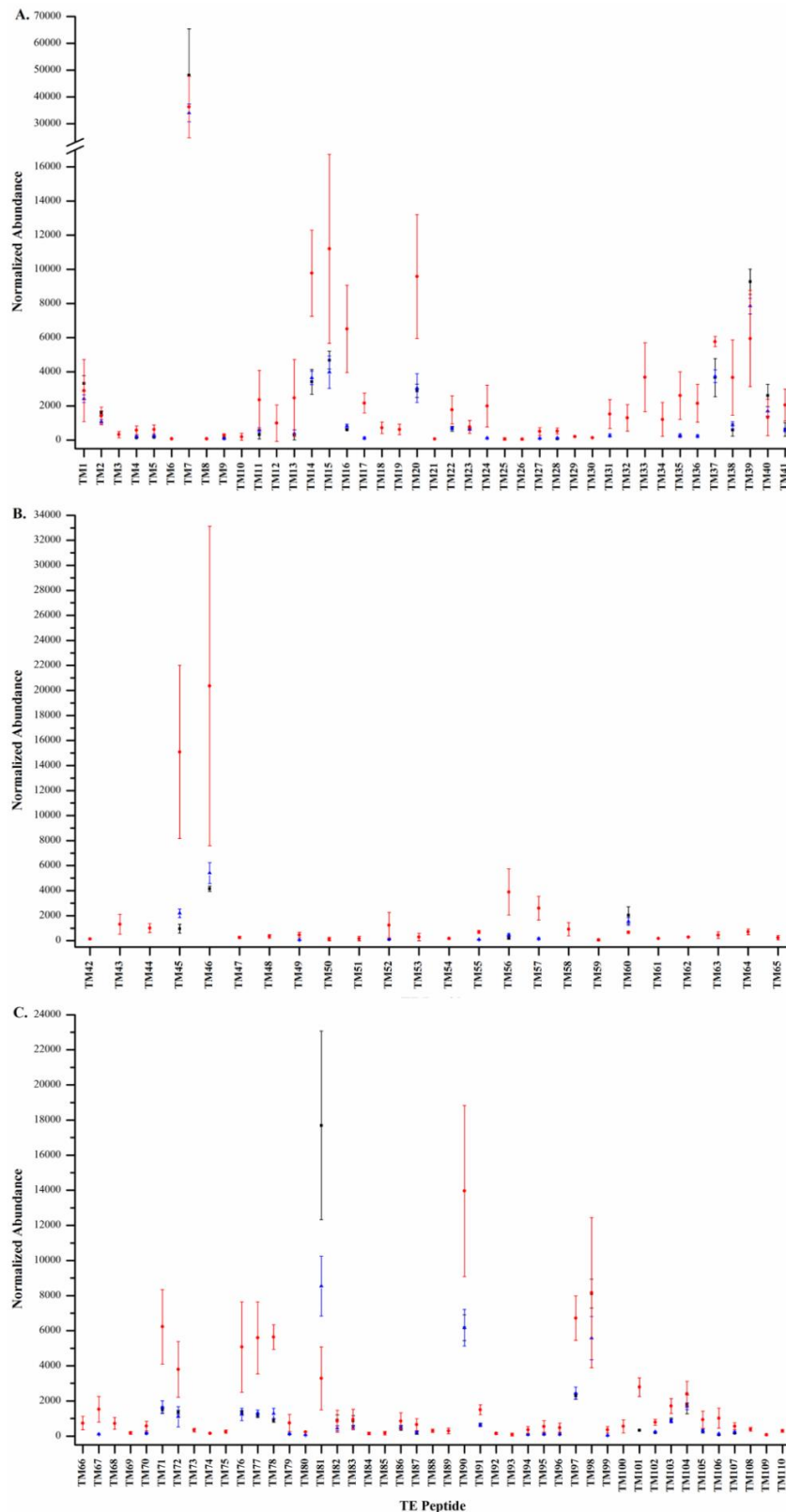


**Figure A-4. Normalised abundance of peptides quantified after 6 h, 12 h and 48 h in**

**TE samples digested with MMP-9.**

Normalised abundance of peptides found in TE samples digested by MMP-9 derived from (A) domains 2 to 14, (B) domains 15 to 23 and (C) domains 24 to 36. Measurements were done after 6 h (black), 12 h (blue) and 48 h (red). Data is presented as mean  $\pm$  s.d. (n=2).

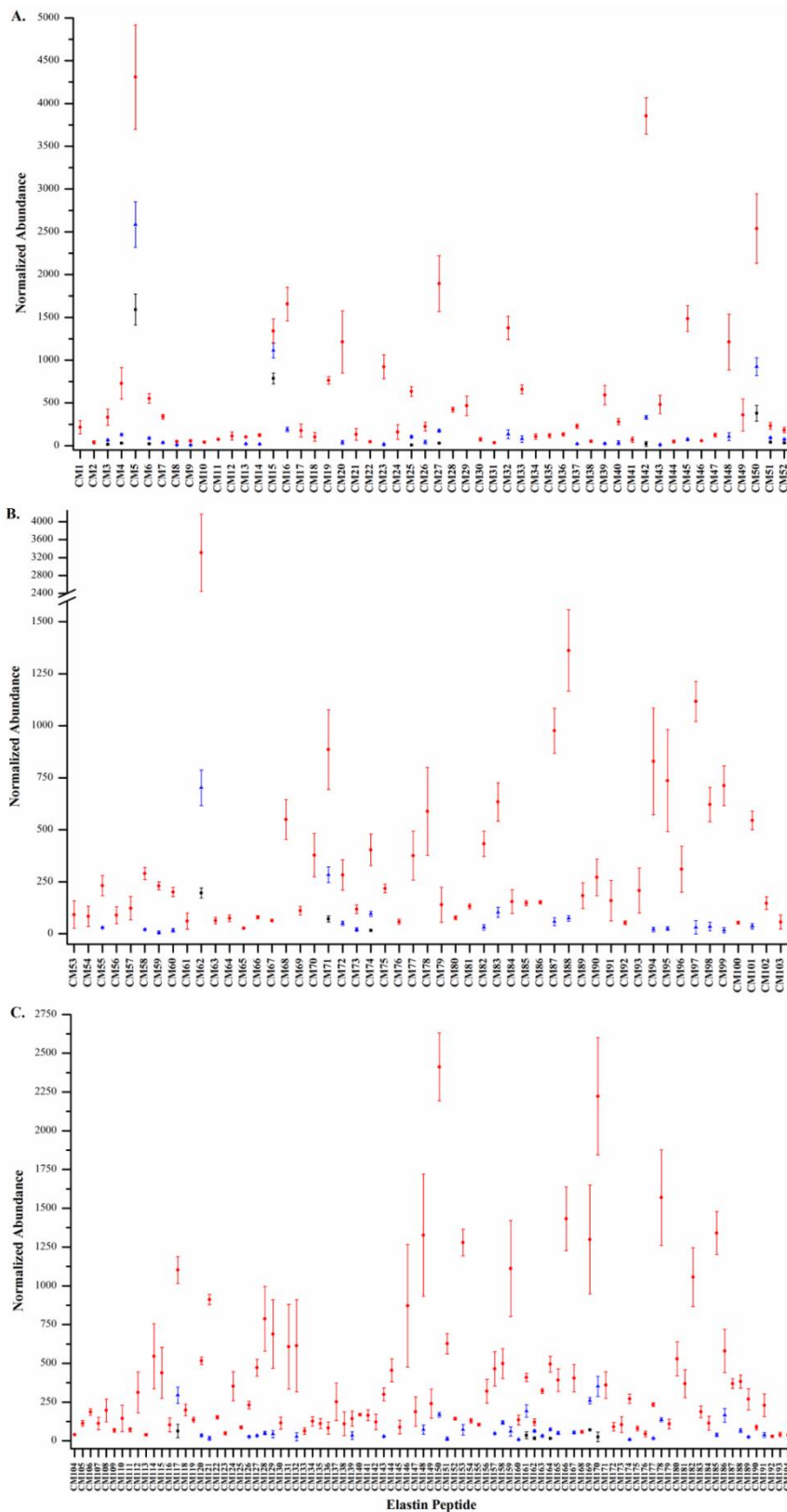


**Figure A-5. Normalised abundance of peptides quantified after 6 h, 12 h and 48 h in**

**CE samples digested with MMP-9.**

Normalised abundance of peptides found in CE samples digested by MMP-9 derived from (A) domains 2 to 14, (B) domains 15 to 23 and (C) domains 24 to 36. Measurements were done after 6 h (black), 12 h (blue) and 48 h (red). Data is presented as mean  $\pm$  s.d. (n=3).

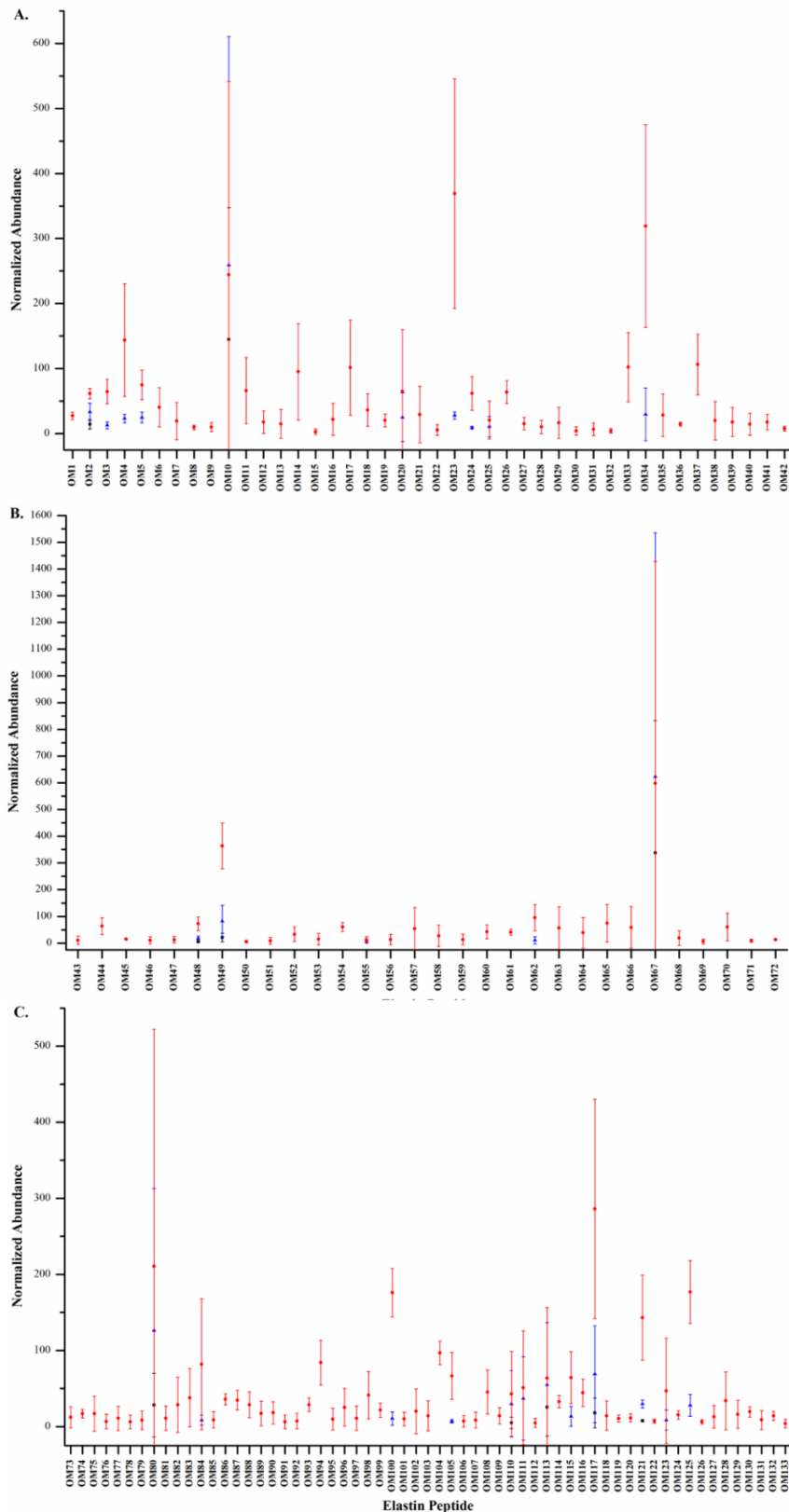


**Figure A-6. Normalised abundance of peptides quantified after 6 h, 12 h and 48 h in OE samples digested with MMP-9.**

Normalised abundance of peptides found in OE samples digested by MMP-9 derived from (A) domains 2 to 14, (B) domains 15 to 23 and (C) domains 24 to 36. Measurements were done after 6 h (black), 12 h (blue) and 48 h (red). Data is presented as mean  $\pm$  s.d. (n=3).

Domain	CG 6h	CG 12h	CG 48h	MMP-9 6h	MMP-9 12h	MMP-9 48h
2	0	0	0	0	0	485
2-3	96	548	3151 *!	3346	6116	14348 !
2-4	0	0	0	0	0	451
5	0	0	0	0	36	247
5-6	241	793	4136 *!	1860	3202	11789
6	11	401	4672 *!	74	1221	15195 *!
6-7	0	83	696	0	0	236
7	892	3245 !	14381 *!	0	46	994
7-8	0	13	578	0	118	2076
8-9	0	0	65	0	0	0
9	0	0	164	0	0	0
9-10	0	32	893	40	744	9636
10	0	125	7290 *!	0	146	3301
10-11	0	40	236	0	0	0
11-12	283	1804	8622 *!	0	419	6778
12	1034	2892	11063 *!	907	2178	6009
13	0	87	330	0	0	72
14	16	14	313	0	0	0
14-15	0	0	0	0	0	31
15-16	0	0	0	0	0	368
16	0	53	800	0	58	1233
16-17	0	0	363	444	1691	9387
17	0	0	0	0	0	106
17-18	0	0	0	0	0	317
18	0	47	2619	0	0	1529
18-19	0	0	281	0	0	787
20	318	2013	15649 *!	174	1459	15892 *!
20-21	0	68	5754 *!	676	1572	12822 *!
21-23	0	0	0	0	0	140
24	30	413	9365 *!	183	962	11864
24-25	0	0	788	0	0	0
26	0	246	3483 *!	0	489	12807 *!
26-27	315	788	3826 *!	0	688	16210 *!
28	458	1543	6370 *!	235	1813	12879 *!
28-29	0	29	1809	0	0	234
30	306	1254	8991 *!	209	1677	13408 *!
30-31	0	0	0	0	0	8242
31	0	0	0	0	0	749
32	81	353	3649 *!	0	78	3792
32-33	0	0	565	0	462	1973
33	0	25	298	0	51	623
33-36	0	0	325	0	76	797

**Figure A-7. Degradation of different domains of skin elastin determined through a linear model according to each enzyme.**

Amount of peptides expressed as the effect calculated in a linear model according to the enzyme. Differences statistically significant among the amount of peptides estimated after 48 h and 6 h are showed as \* while differences among 48 h and 12 h are represented by . Differences between domains at each sampling point are showed as !.

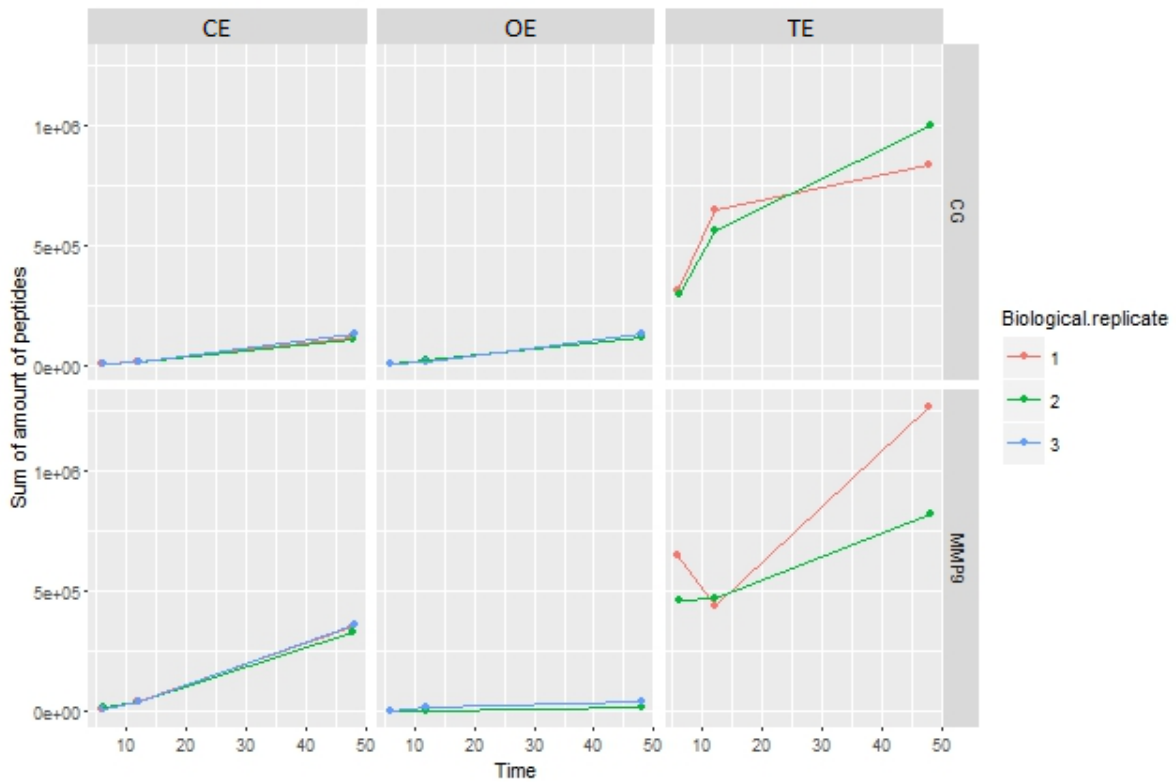


**Figure A-8. Sum of normalised amount of peptides obtained after digestion of TE and skin elastin samples with CG and MMP-9, according to biological replicate.**

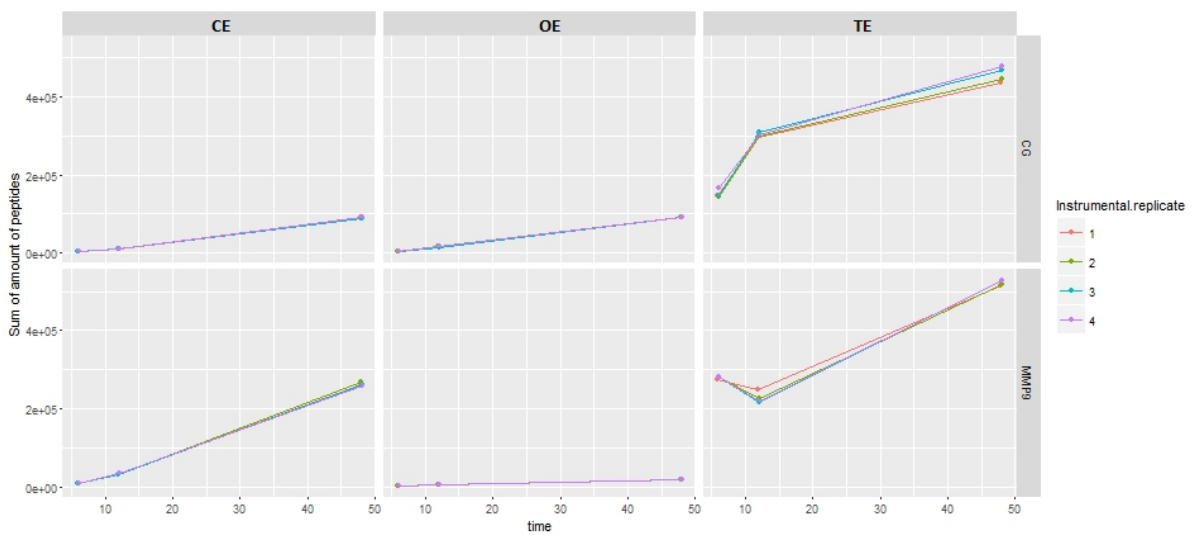


**Figure A-9. Sum of normalised amount of peptides obtained after digestion of TE and skin elastin samples with CG and MMP-9, according to instrumental replicate.**

Residue	Sequence identified	Mass (Da)	CE CG	OE CG	CE_MP9	OE_MP9
113-121	GGVPGVGGGL	711.39	<b>1409±84</b>	<b>1516±651</b>		
114-121	GVPVGGGL	654.37	<b>1455±131</b>	<b>1445±552</b>		
123-132	VSAGAVVPQP	923.51			593±114	<b>102±53</b>
146-159	<b>L</b> PGVYPGGVLPGAR	1367.76			<b>3855±213</b>	<b>319±156</b>
160-171	FPGVGVLPGVPT	1138.64	<b>1154±217</b>	<b>1726±735</b>		
160-172	FPGVGVLPGVPTG	1195.66			<b>1486±152</b>	<b>106±47</b>
161-170	PGVGVLPGVVP	922.51		<b>404±161</b>		
384-397	<b>G</b> ARPGVGVGGIPTY	1299.69	<b>693±232</b>	813±769		
399-416	VGAGGF <b>P</b> GFGVGVGG <b>I</b> PG	1532.76			<b>976±108</b>	x
399-416	VGAGGF <b>P</b> GFGVGVGG <b>I</b> PG	1516.77			<b>1362±196</b>	43±26
410-425	GVG <b>G</b> IPGVAGV <b>P</b> GVGG	1264.68			x	<b>95±49</b>
417-441	VAGV <b>P</b> GVGGV <b>P</b> GVGGVPGV <b>G</b> ISPEA	2084.13			<b>829±256</b>	57±79
423-441	VGGV <b>P</b> GVGGV <b>P</b> GV <b>G</b> ISPEA	1619.85			<b>1117±96</b>	59±78
423-442	VGGV <b>P</b> GVGGV <b>P</b> GV <b>G</b> ISPEAQ	1747.91	<b>336±56</b>	x		
423-442	VGGV <b>P</b> GVGGV <b>P</b> GV <b>G</b> ISPEAQ	1731.92	<b>973±217</b>	<b>576±220</b>		
472-488	<b>GL</b> VPGVGVAPGV <b>G</b> VAPG	1401.80	<b>444±151</b>	<b>316±124</b>	186±21	12±14
472-494	<b>GL</b> VPGVGVAPGV <b>G</b> VAPGVVAPG	1882.07	<b>318±102</b>	202±84		
477-488	<b>V</b> GVAPGVVAPG(a)	978.55	<b>276±15</b>	197±71		
489-506	<b>V</b> GVAPGVGLAPGV <b>G</b> VAPG	1472.84	<b>450±135</b>	189±40		
498-523	APGVGVAPGVGVVAPGVVAPGIGPGG	2065.13			<b>1102±86</b>	211±311
507-523	VG <b>V</b> APGVGVAPGIGPGG	1359.75			<b>912±33</b>	82±86
562-586	LG <b>V</b> GAGV <b>P</b> GLGV <b>G</b> AGV <b>P</b> GFGAV <b>P</b> GA	2032.11			<b>871±395</b>	25±25
564-586	VGAGV <b>P</b> GLGV <b>G</b> AGV <b>P</b> GFGAV <b>P</b> GA	1862.01			<b>1326±394</b>	41±31
571-586	LG <b>V</b> GAGV <b>P</b> GFGAV <b>P</b> GA	1324.71			<b>2412±219</b>	<b>176±32</b>
573-586	VGAGV <b>P</b> GFGAV <b>P</b> GA	1154.61			<b>1279±87</b>	<b>97±15</b>
580-586	FGAV <b>P</b> GA	617.32			320±77	<b>67±31</b>
581-587	<b>G</b> AV <b>P</b> GAL	583.33	<b>1712±291</b>			
647-662	LG <b>L</b> GVGG <b>L</b> GV <b>P</b> GVGG	1264.71			<b>2223±379</b>	x
655-662	LG <b>V</b> PGVGG	654.37			<b>1569±309</b>	<b>177±41</b>

**Table A-2. Most abundant peptides containing bioactive sequences that were identified and quantified after digestion of human skin elastin by CG and MMP-9.**

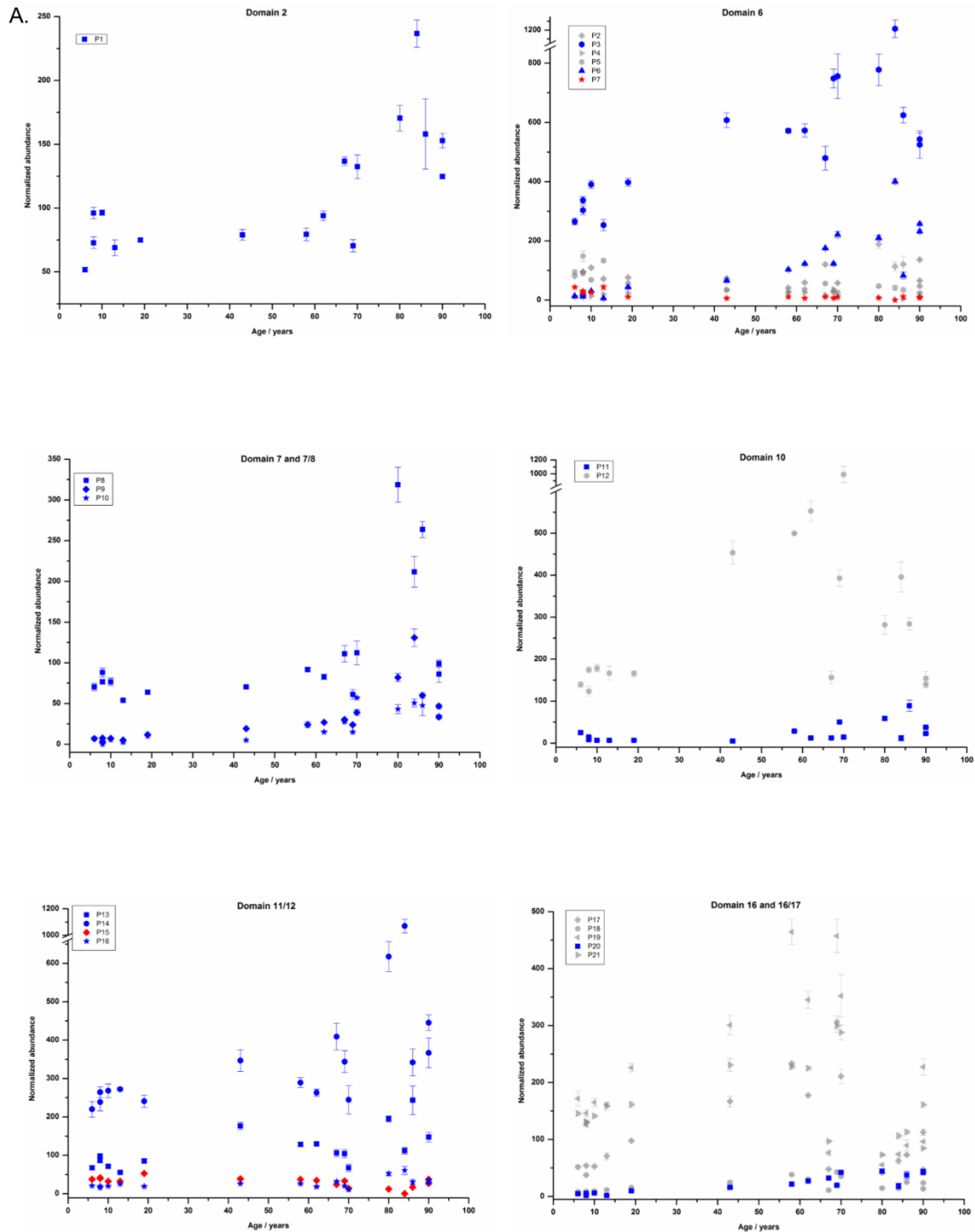
Peptides, which were only identified but not quantified, are shown with “x”. The sequence of peptides also identified in OE samples digested with NEP are indicated with (a). Hydroxylated proline residues are denoted as **P**. Potentially bioactive motifs are shown in blue. Data is presented as mean ± s.d. (n=3).



### Appendix 3. Structural changes of human elastin during skin ageing

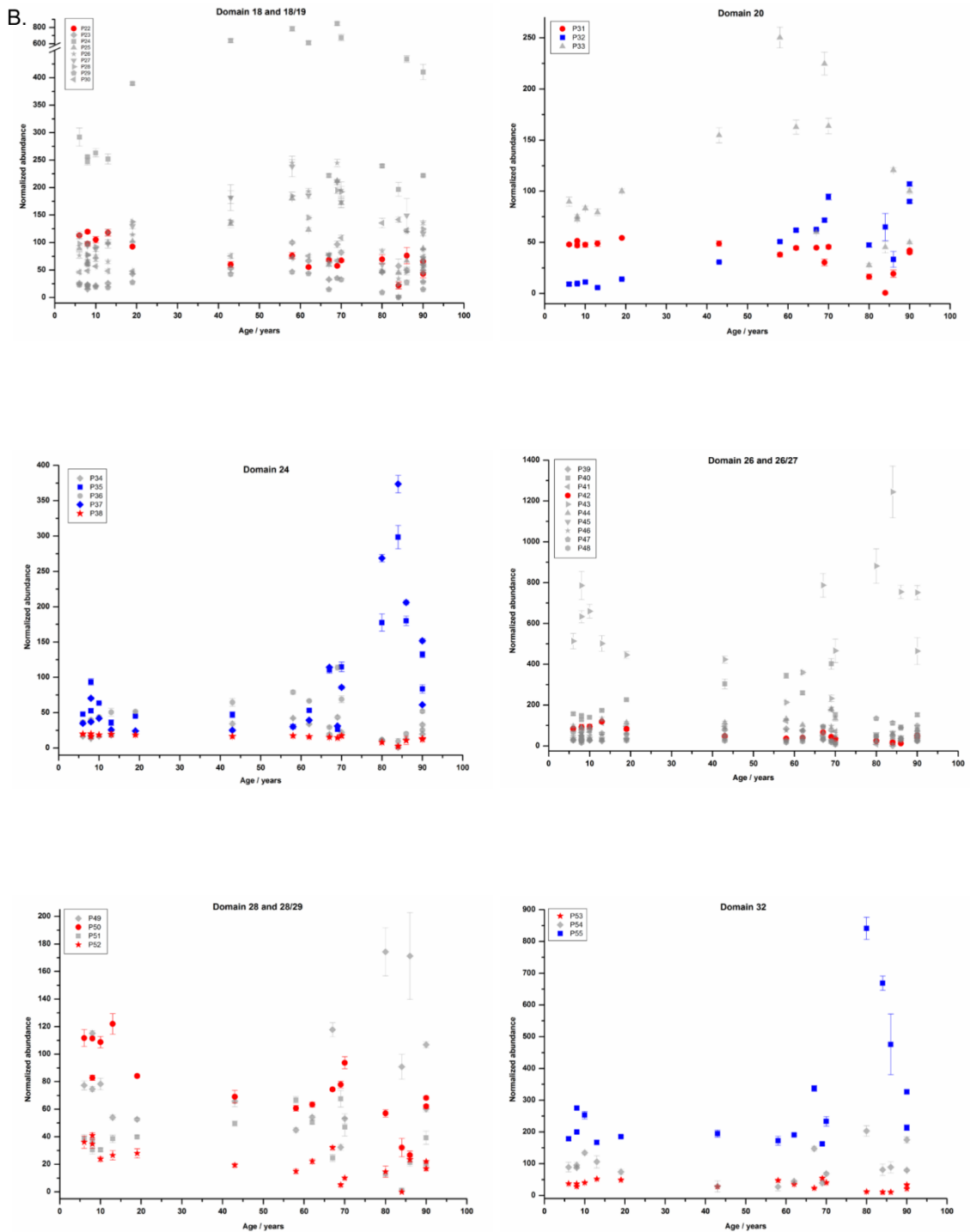
Sample number	Age of individuals upon sample taking in years	Region of body	Sun exposure
S1	6	Foreskin	Sun-protected
S2	8	Foreskin	Sun-protected
S3	8	Foreskin	Sun-protected
S4	10	Foreskin	Sun-protected
S5	13	Foreskin	Sun-protected
S6	19	Foot	Sun-protected
S7	43	Hip	Sun-protected
S8	58	Face	Sun-exposed
S9	62	Foot	Sun-protected
S10	67	Hip	Sun-protected
S11	69	Face	Sun-exposed
S12	70	Foot	Sun-protected
S13	80	Face	Sun-exposed
S14	84	Face	Sun-exposed
S15	86	Face	Sun-exposed
S16	90	Chest	Sun-exposed
S17	90	Chest	Sun-exposed

Table A-3 Skin samples from differential aged healthy individuals.



**Figure A-10. Changes in normalised abundance of elastin peptides depending on the age of the donor (part A).**

Elastin peptides derived from domains 2 to 16/17 (A) and 18 to 32 (B), which showed a significant age-related increase (blue) and decrease (red) in their normalised abundances. Peptides that showed significant differences in their abundances among different elastin samples, despite the lack of no age-related increase or decrease pattern, are shown in grey. Data is presented as mean  $\pm$  s.d. (n = 4)



**Figure A-11. Changes in normalised abundance of elastin peptides depending on the age of the donor (part B).**

Elastin peptides derived from domains 2 to 16/17 (A) and 18 to 32 (B), which showed a significant age-related increase (blue) and decrease (red) in their normalised abundances. Peptides that showed significant differences in their abundances among different elastin samples, despite the lack of no age-related increase or decrease pattern, are shown in grey. Data is presented as mean  $\pm$  s.d. (n = 4)

Code	Peptide sequence	Monoisotopic mass / Da	Residues	Domain	Ratio normalised abundances		Change with age
					Adults/Children	Old adults/Children	
P1	AIPGGVPGGV	822.46	32- 41	2	1.28	2.19	Increase
P2	FPGALVPGGV	912.51	87- 96	6	0.72	1.42	Fluctuating
P3	ALVPGGV	611.36	90- 96	6	1.92	2.27	Increase
P4	ALVPGGVA	682.40	90- 97	6	1.57	0.50	Fluctuating
P5	ALVPGGVADAA	939.50	90-100	6	0.34	0.39	Fluctuating
P6	ALVPGGVADAAA	1010.54	90-101	6	6.34	11.08	Increase
P7	LVPGGVADAA	868.46	91-100	6	0.30	0.25	Decrease
P8	GGVPGVGGL	711.39	113-121	7	1.23	2.73	Increase
P9	GVPVGGL	654.37	114-121	7	3.89	10.08	Increase
P10	GVSAGAVVPQ	883.48	122-131	7/8	4.30	7.93	Increase
P11	GVGVLPGVPT	894.52	162-171	10	1.83	3.96	Increase
P12	VLPGVPT	681.41	165-171	10	3.22	1.59	Fluctuating
P13	AGIPGVGPF	813.44	187-195	11/12	1.53	2.19	Increase
P14	AGIPGVGPF	829.43	187-195	11/12	1.26	2.27	Increase
P15	GIPGVGPF	742.40	188-195	11/12	0.77	0.48	Decrease
P16	P <sub>u</sub> GVGPF	588.29	190-195	11/12	1.12	2.04	Increase
P17	AIPGIG	526.31	288-293	16	3.14	1.11	Fluctuating
P18	AIPGIGG	583.33	288-294	16	3.17	1.92	Fluctuating
P19	AIPGIGGI	696.42	288-295	16	2.00	0.65	Fluctuating
P20	AIPGIGGIAGVG	980.57	288-299	16/17	5.42	7.62	Increase
P21	IGGIAGV	585.35	292-298	16/17	1.58	0.74	Fluctuating
P22	AGLVPGGPGFGPGVV	1279.69	320-334	18	0.60	0.51	Decrease
P23	GLVPGGPGFGPG	1010.52	321-332	18	2.80	2.02	Fluctuating
P24	GVPGAGVPGVGVPG	1118.61	335-348	18	2.22	1.06	Fluctuating
P25	GVPGAGVPGVGVPG	1134.60	335-348	18	1.79	0.73	Fluctuating
P26	GVPGAGVPGVGVPGA	1189.65	335-349	18	2.52	1.22	Fluctuating
P27	GVPGAGVPGVGVPGAGIPV	1555.87	335-353	18	1.72	0.77	Fluctuating
P28	AGIPVVPAGAGIPG	1119.63	349-361	18	1.53	0.60	Fluctuating
P29	GIPVVPAGAGIPG	1032.60	350-361	18	1.65	0.74	Fluctuating
P30	AAVPGVV	611.36	362-368	18/19	1.54	2.11	Increase
P31	GGFPGFGVGVG	949.47	402-412	20	0.85	0.48	Decrease
P32	VGGIPGVAGVPG	978.55	411-422	20	6.24	6.90	Increase
P33	GVPGVGGVPGVG	950.52	419-430	20	2.03	0.82	Fluctuating
P34	GLVPGVGV	696.42	472-479	24	1.86	0.89	Fluctuating
P35	VAPGVGL	611.36	491-497	24	1.13	3.09	Increase
P36	LAPGVGV	611.36	497-503	24	1.63	0.55	Fluctuating
P37	VGVAPGIGPGGV	978.55	513-524	24	1.39	5.43	Increase
P38	APGIGPGGV	723.39	516-524	24	0.86	0.50	Decrease
P39	GAGIPGLGV	739.42	547-555	26	2.20	0.96	Fluctuating
P40	GIPGLGV	611.36	549-555	26	1.60	0.49	Fluctuating
P41	GIPGLGV	627.36	549-555	26	1.26	0.34	Fluctuating
P42	GIPGLGVGV	783.45	549-557	26	0.48	0.32	Decrease
P43	GVPGLGVGA	725.41	558-566	26	0.70	1.39	Fluctuating
P44	GV <sub>u</sub> PGLGVGA	741.40	558-566	26	1.19	0.49	Fluctuating
P45	VGAGV <sub>u</sub> PGL	684.38	564-571	26	0.79	1.49	Fluctuating
P46	GAGVPGLVG	725.41	565-573	26	1.36	0.52	Fluctuating
P47	GAGVPGFGAVPG	984.50	574-585	26/27	0.68	1.55	Fluctuating
P48	PGFGAVPG	700.35	578-585	26/27	0.79	1.48	Fluctuating
P49	GALGGVGI <sub>u</sub> PGGVVGA	1179.66	607-621	28/29	0.81	1.60	Fluctuating
P50	LGGVGI <sub>u</sub> PGGVVGA	1067.60	609-621	28/29	0.71	0.48	Decrease
P51	GGVGI <sub>u</sub> PGGV	711.39	610-618	28	1.42	0.53	Fluctuating
P52	GGVGI <sub>u</sub> PGGVVGA	938.52	610-621	28/29	0.55	0.49	Decrease
P53	GLGGVL	514.31	681-686	32	0.94	0.44	Decrease

<b>P54</b>	GLGGVLGGAGQFPL	1241.68	681-694	32	0.61	1.28	Fluctuating
<b>P55</b>	GGVLGGAGQFPL	1071.57	683-694	32	1.03	2.41	Increase

**Table A-4. Elastin peptides that showed significant differences in their normalised abundances among different elastin samples.**

**Fold changes were calculated based on the average normalised abundance of each peptide in the children group. Hydroxylated proline residues are denoted as P. Potentially bioactive motifs are highlighted in bold blue. Data is shown based on TE isoform 2 (SwissProt accession number 15502-2).**

## Appendix 4. Molecular changes of human skin elastin from patients with Williams-Beuren Syndrome and healthy individuals

Code sample	Age of individuals upon sample taking in years	Region of body	Condition
S1	24	Forearm	WBS patient
S2	25	Forearm	WBS patient
S3	27	Forearm	WBS patient
S4	28	Forearm	WBS patient
S5	40	Forearm	WBS patient
S6	19	Plantar	Healthy proband
S7	43	Hip	Healthy proband
S8	58	Cheek	Healthy proband
S9	62	Toe	Healthy proband
S10	70	Foot	Healthy proband

Table A-5. Skin samples from WBS patients and healthy individuals analysed by nanoHPLC-nanoESI-QqTOF MS and LFQ.

Peptide Number	Peptide Sequence	Monoisotopic mass/Da	Residues	Domain	Ratio normalised abundances WBS/Healthy
P1	AIPGGVPG	666.37	32-39	2	0.60
P2	ALVPGGVA	682.40	90-97	6	0.55
P3	GAGLGGVPGVGGGL	1025.55	109-121	7	0.47
P4	GVPGVGGGL	654.37	114-121	7	0.65
P5	FPGVGVLPGVPT	1138.64	160-171	10	1.99
P6	GVGVLPGVPT	894.52	162-171	10	1.61
P7	VLPGVPT	681.41	165-171	10	0.48
P8	FAGIPG	560.30	186-191	11/12	1.65
P9	AGIPGVGPF	813.44	187-195	11/12	1.68
P10	GIPGVGPF	742.40	188-195	11/12	2.64
P11	VGPFGGPQPGVPL	1220.66	192-204	11/12	2.11
P12	GVLPGVGGA	725.41	272-280	16	0.67
P13	GVLPGVGGAGVPGVPG	1304.71	272-287	16	0.39
P14	GVLPGVGGAGVPGVPGAIPG	1626.91	272-291	16	2.88
P15	VGGAGVPGVPG	881.46	277-287	16	0.29
P16	VGGAGVPGVPGAIPG	1203.66	277-291	16	1.95
P17	AIPGIG	526.31	288-293	16	0.41
P18	AIPGIGG	583.33	288-294	16	0.34
P19	AIPGIGGI	696.42	288-295	16	0.48
P20	AIPGIGGIA	767.45	288-296	16	0.39
P21	GLVPGGPGFGPG	1010.52	321-332	18	0.42
P22	GLVPGGPGFGPGV	1109.59	321-333	18	0.21
P23	GLVPGGPGFGPGVV	1224.65	321-334	18	0.56
P24	GPGVGVPGAGVPG	1134.60	330-343	18	0.31
P25	GVPGAGVPGVGVPG	1118.61	335-348	18	0.63
P26	GVPGAGVPGVGVPGA	1189.65	335-349	18	0.58
P27	AGVPGVGVPGAGIPVVPG	1498.85	339-356	18	1.76
P28	VGVPGAGIPVVPG	1117.65	344-356	18	0.51
P29	AGIPVVPGAGIPG	1119.63	349-361	18	0.39
P30	GIPVVPG	637.38	350-356	18	0.33
P31	GIPVVPGAGIPG	1048.59	350-361	18	0.30
P32	AAVPGVV	611.36	362-368	18/19	0.66
P33	PGVGVGGIPT	852.47	387-396	20	1.56
P34	GGFPGF	580.26	402-407	20	1.60
P35	GGFPGFGVGVGGIPG	1273.65	402-416	20	3.38
P36	GVGVGGIPGVA	897.4919	408-418	20	0.42
P37	GVGGIPGVA	741.4021	410-418	20	0.55
P38	GVPGVGGVPGVGV	950.5185	419-430	20	0.63
P39	VGGVPGVG	640.3544	423-430	20	0.67
P40	GVPGVGGVPGVGVISPE	1376.73	425-440	20/21	2.82

P41	<b>GLVPGVGV</b>	696.417	472-479	24	0.54
P42	<b>GLVPGVGVAPGVG</b>	1077.6182	472-484	24	3.84
P43	<b>GLVPGVGVAPGVGVAPG</b>	1401.798	472-488	24	3.98
P44	<b>VAPGVGL</b>	611.3643	491-497	24	0.64
P45	<b>VGLAPGVGVAPG</b>	992.5654	495-506	24	1.76
P46	<b>LAPGVGVAPGVGVAPG</b>	1316.7451	497-512	24	6.40
P47	<b>PGVGVAPGIGPG</b>	992.5291	511-522	24	0.39
P48	<b>VG VAPGIGPGGV</b>	978.5498	513-524	24	1.87
P49	<b>VAPGIGPGGV</b>	822.4599	515-524	24	0.64
P50	GAGIPGLGVGV	895.5127	547-557	26	2.20
P51	GIPGLGV	627.3591	549-555	26	0.38
P52	GIPGLGVGV	767.4541	549-557	26	2.03
P53	<b>GVGVPLGVGA</b>	881.497	556-566	26	3.00
P54	GVPGLGVGA	725.4072	558-566	26	2.06
P55	GAGVPGF <b>GAVPG</b>	984.5028	574-585	26/27	2.41
P56	GVPGF <b>GAVPG</b>	856.4443	576-585	26/27	1.66
P57	PGF <b>GAVPG</b>	700.3544	578-585	26/27	1.85
P58	GALGGVGI <b>PGGVVGA</b>	1179.6611	607-621	28/29	2.11
P59	LGGVGIPG	668.3857	609-616	28	0.62
P60	LGGVGIPGGV <b>VGA</b>	1051.6025	609-621	28/29	2.08
P61	GGVGIPGGV <b>VGA</b>	938.5185	610-621	28/29	2.55
P62	GLGGLGV	571.3329	646-652	30	0.65
P63	GGLGVGGL	628.3544	648-655	30	0.66
P64	GLSPIFPG	786.4276	704-711	33	0.56

Table A-6 Elastin peptides that show significant differences in their normalised abundances between skin elastin samples isolated from WBS patients and healthy individuals.

Ratios were calculated based on the average normalised abundance of each peptide in the five samples of WBS and healthy individuals. Hydroxylated proline residues are denoted as P. Potentially bioactive motifs are highlighted in bold blue. Data is shown based on TE isoform 2 (SwissProt accession number 15502-2).



# Bibliography

1. Tamburro, A.M., B. Bochicchio, and A. Pepe, *Dissection of human tropoelastin: exon-by-exon chemical synthesis and related conformational studies*. *Biochemistry*, 2003. **42**(45): p. 13347-62.
2. Mora Huertas, A.C., et al., *Molecular-level insights into aging processes of skin elastin*. *Biochimie*, 2016. **128-129**: p. 163-73.
3. Schmelzer, C., *Assembly and Properties of Elastic Fibers*, in *Elastic Fiber Matrices*. 2016, CRC Press. p. 1-30.
4. Naylor, E.C., R.E.B. Watson, and M.J. Sherratt, *Molecular aspects of skin ageing*. *Maturitas*, 2011. **69**(3): p. 249-256.
5. Aebersold, R. and M. Mann, *Mass spectrometry-based proteomics*. *Nature*, 2003. **422**(6928): p. 198-207.
6. Nahnsen, S., et al., *Tools for label-free peptide quantification*. *Mol Cell Proteomics*, 2013. **12**(3): p. 549-56.
7. Heinz, A., et al., *Elastins from patients with Williams-Beuren syndrome and healthy individuals differ on the molecular level*. *Am J Med Genet A*, 2016. **170**(7): p. 1832-42.
8. Scharffetter-Kochanek, K., et al., *Photoaging of the skin from phenotype to mechanisms*. *Exp Gerontol*, 2000. **35**(3): p. 307-16.
9. Baldock, C., et al., *Shape of tropoelastin, the highly extensible protein that controls human tissue elasticity*. *Proc Natl Acad Sci U S A*, 2011. **108**(11): p. 4322-4327.
10. Hagsiwa, S. and T. Shimada, *Skin Morphology and Its Mechanical Properties Associated with Loading*, in *Pressure Ulcer Research: Current and Future Perspectives*, D.L. Bader, et al., Editors. 2005, Springer Berlin Heidelberg: Berlin, Heidelberg. p. 161-185.
11. Shimizu, H., *Shimizu's textbook of dermatology / Hiroshi Shimizu*. 2007, Japan: Hokkaido University Press. 547.
12. Wong, R., et al., *The dynamic anatomy and patterning of skin*. *Exp Dermatol*, 2016. **25**(2): p. 92-8.
13. McGrath, J.A. and J. Uitto, *Anatomy and Organization of Human Skin*, in *Rook's Textbook of Dermatology*. 2010, Wiley-Blackwell. p. 1-53.
14. Parks, W.C., et al., *Elastin*, in *Advances in Molecular and Cell Biology*, E.E. Bittar, Editor. 1993, Elsevier. p. 133-181.
15. Tracy, L.E., R.A. Minasian, and E.J. Caterson, *Extracellular Matrix and Dermal Fibroblast Function in the Healing Wound*. *Adv Wound Care (New Rochelle)*, 2016. **5**(3): p. 119-136.
16. Vrhovski, B. and A.S. Weiss, *Biochemistry of tropoelastin*. *Eur J Biochem*, 1998. **258**(1): p. 1-18.
17. Kielty, C.M., M.J. Sherratt, and C.A. Shuttleworth, *Elastic fibres*. *J Cell Sci*, 2002. **115**(Pt 14): p. 2817-28.
18. Pasquali Ronchetti, I., et al., *Study of elastic fiber organization by scanning force microscopy*. *Matrix Biol*, 1998. **17**(1): p. 75-83.
19. Cotta-Pereira, G., F. Guerra Rodrigo, and S. Bittencourt-Sampaio, *Oxytalan, elaunin, and elastic fibers in the human skin*. *J Invest Dermatol*, 1976. **66**(3): p. 143-8.
20. Baldwin, A.K., et al., *Elastic fibres in health and disease*. *Expert Rev Mol Med*, 2013. **15**: p. e8.
21. Baud, S., et al., *Elastin peptides in aging and pathological conditions*. *Biomol Concepts*, 2013. **4**(1): p. 65-76.

22. Robert, B., et al., *Studies on the nature of the "microfibrillar" component of elastic fibers*. Eur J Biochem, 1971. **21**(4): p. 507-16.
23. Hunzelmann, N., et al., *Increased deposition of fibulin-2 in solar elastosis and its colocalization with elastic fibres*. Br J Dermatol, 2001. **145**(2): p. 217-22.
24. Jensen, S.A., et al., *Protein interaction studies of MAGP-1 with tropoelastin and fibrillin-1*. J Biol Chem, 2001. **276**(43): p. 39661-6.
25. Katsuta, Y., et al., *Fibulin-5 accelerates elastic fibre assembly in human skin fibroblasts*. Exp Dermatol, 2008. **17**(10): p. 837-42.
26. Choi, J., et al., *Analysis of dermal elastic fibers in the absence of fibulin-5 reveals potential roles for fibulin-5 in elastic fiber assembly*. Matrix Biol, 2009. **28**(4): p. 211-20.
27. Kagan, H.M. and P. Cai, *Isolation of active site peptides of lysyl oxidase*. Methods Enzymol, 1995. **258**: p. 122-32.
28. Koenders, M.M., et al., *Microscale mechanical properties of single elastic fibers: the role of fibrillin-microfibrils*. Biomaterials, 2009. **30**(13): p. 2425-32.
29. Wagenseil, J.E. and R.P. Mecham, *New insights into elastic fiber assembly*. Birth Defects Res C Embryo Today, 2007. **81**(4): p. 229-40.
30. Mecham, R.P. and M.A. Gibson, *The microfibril-associated glycoproteins (MAGPs) and the microfibrillar niche*. Matrix Biol, 2015. **47**: p. 13-33.
31. Uitto, J., *Biochemistry of the elastic fibers in normal connective tissues and its alterations in diseases*. J Invest Dermatol, 1979. **72**(1): p. 1-10.
32. Muiznieks, L.D. and A.S. Weiss, *Flexibility in the solution structure of human tropoelastin*. Biochemistry, 2007. **46**(27): p. 8196-205.
33. Mithieux, S.M. and A.S. Weiss, *Elastin*. Advances in Protein Chemistry, 2005. **70**: p. 437-61.
34. Parks, W.C., et al., *Elastin*, in *Advances in Molecular and Cell Biology*, H.K. Kleinman, Editor. 1993, JAI Press: Greenwich, CT. p. 133-182.
35. Dorrington, K.L. and N.G. McCrum, *Elastin as a rubber*. Biopolymers, 1977. **16**(6): p. 1201-22.
36. Li, B., et al., *Hydrophobic hydration is an important source of elasticity in elastin-based biopolymers*. J Am Chem Soc, 2001. **123**(48): p. 11991-8.
37. Li, B. and V. Daggett, *Molecular basis for the extensibility of elastin*. J Muscle Res Cell Motil, 2002. **23**(5-6): p. 561-73.
38. Gosline, J.M., *Hydrophobic interaction and a model for the elasticity of elastin*. Biopolymers, 1978. **17**(3): p. 677-95.
39. Perticaroli, S., et al., *Elasticity and Inverse Temperature Transition in Elastin*. J Phys Chem Lett, 2015. **6**(20): p. 4018-25.
40. Bochicchio, B. and A. Pepe, *Role of polyproline II conformation in human tropoelastin structure*. Chirality, 2011. **23**(9): p. 694-702.
41. Martino, M., et al., *On the occurrence of polyproline II structure in elastin*. Journal of Molecular Structure, 2000. **519**(1-3): p. 173-189.
42. Green, E.M., et al., *The structure and micromechanics of elastic tissue*. Interface Focus, 2014. **4**(2): p. 20130058.
43. Gotte, L., et al., *The ultrastructural organization of elastin*. J Ultrastruct Res, 1974. **46**(1): p. 23-33.
44. Pepe, A., B. Bochicchio, and A.M. Tamburro, *Supramolecular organization of elastin and elastin-related nanostructured biopolymers*. Nanomedicine (Lond), 2007. **2**(2): p. 203-18.
45. Mecham, R.P., *Elastin synthesis and fiber assembly*. Ann N Y Acad Sci, 1991. **624**: p. 137-46.

46. Rucker, R.B. and M.A. Dubick, *Elastin metabolism and chemistry: potential roles in lung development and structure*. Environ Health Perspect, 1984. **55**: p. 179-91.
47. Shapiro, S.D., et al., *Marked longevity of human lung parenchymal elastic fibers deduced from prevalence of D-aspartate and nuclear weapons-related radiocarbon*. J Clin Invest, 1991. **87**(5): p. 1828-34.
48. Amadeu, T.P., et al., *Fibrillin-1 and elastin are differentially expressed in hypertrophic scars and keloids*. Wound Repair Regen, 2004. **12**(2): p. 169-74.
49. Seo, J.Y., et al., *Ultraviolet radiation increases tropoelastin mRNA expression in the epidermis of human skin in vivo*. J Invest Dermatol, 2001. **116**(6): p. 915-9.
50. Bernstein, E.F., et al., *Enhanced elastin and fibrillin gene expression in chronically photodamaged skin*. J Invest Dermatol, 1994. **103**(2): p. 182-6.
51. Mithieux, S.M. and A.S. Weiss, *Elastin*. Adv Protein Chem, 2005. **70**: p. 437-61.
52. Kozel, B.A., et al., *Elastic fiber formation: a dynamic view of extracellular matrix assembly using timer reporters*. J Cell Physiol, 2006. **207**(1): p. 87-96.
53. Hinek, A. and M. Rabinovitch, *67-kD elastin-binding protein is a protective "companion" of extracellular insoluble elastin and intracellular tropoelastin*. J Cell Biol, 1994. **126**(2): p. 563-74.
54. Hinek, A., et al., *Retrovirally Mediated Overexpression of Versican V3 Reverses Impaired Elastogenesis and Heightened Proliferation Exhibited by Fibroblasts from Costello Syndrome and Hurler Disease Patients*. Am J Pathol, 2004. **164**(1): p. 119-31.
55. Toonkool, P., et al., *Hydrophobic domains of human tropoelastin interact in a context-dependent manner*. J Biol Chem, 2001. **276**(48): p. 44575-80.
56. Yeo, G.C., F.W. Keeley, and A.S. Weiss, *Coacervation of tropoelastin*. Adv Colloid Interface Sci, 2011. **167**(1-2): p. 94-103.
57. Brown-Augsburger, P., et al., *Functional domains on elastin and microfibril-associated glycoprotein involved in elastic fibre assembly*. Biochem J, 1996. **318**(Pt 1): p. 149-55.
58. Brown-Augsburger, P., et al., *Identification of an elastin cross-linking domain that joins three peptide chains. Possible role in nucleated assembly*. J Biol Chem, 1995. **270**(30): p. 17778-83.
59. Wise, S.G., et al., *Specificity in the coacervation of tropoelastin: solvent exposed lysines*. J Struct Biol, 2005. **149**(3): p. 273-81.
60. Lent, R.W., et al., *Studies on the reduction of elastin. II. Evidence for the presence of alpha-amino adipic acid delta-semialdehyde and its aldol condensation product*. Biochemistry, 1969. **8**(7): p. 2837-45.
61. Kozel, B.A., R.P. Mecham, and J. Rosenbloom, *Elastin*, in *The Extracellular Matrix: an Overview*, R.P. Mecham, Editor. 2011, Springer Berlin Heidelberg: Berlin, Heidelberg. p. 267-301.
62. Anwar, R.A. and G. Oda, *Structure of Desmosine and Isodesmosine*. Nature, 1966. **210**(5042): p. 1254-1255.
63. Partridge, S.M., et al., *Biosynthesis of the desmosine and isodesmosine cross-bridges in elastin*. Biochem J, 1964. **93**(3): p. 30c-33c.
64. Boyd, C.D., et al., *Mammalian tropoelastin: multiple domains of the protein define an evolutionarily divergent amino acid sequence*. Matrix, 1991. **11**(4): p. 235-41.
65. Rosenbloom, J., W.R. Abrams, and R. Mecham, *Extracellular matrix 4: the elastic fiber*. Faseb j, 1993. **7**(13): p. 1208-18.
66. Heim, R.A., et al., *Alternative splicing of rat tropoelastin mRNA is tissue-specific and developmentally regulated*. Matrix, 1991. **11**(5): p. 359-66.

67. Sugitani, H., et al., *Alternative splicing and tissue-specific elastin misassembly act as biological modifiers of human elastin gene frameshift mutations associated with dominant cutis laxa*. J Biol Chem, 2012. **287**(26): p. 22055-67.
68. Parks, W.C., et al., *Cellular expression of tropoelastin mRNA splice variants*. Matrix, 1992. **12**(2): p. 156-62.
69. Christiano, A.M. and J. Uitto, *Molecular pathology of the elastic fibers*. J Invest Dermatol, 1994. **103**(5 Suppl): p. 53s-57s.
70. Indik, Z., et al., *Alternative splicing of human elastin mRNA indicated by sequence analysis of cloned genomic and complementary DNA*. Proc Natl Acad Sci U S A, 1987. **84**(16): p. 5680-4.
71. Schmelzer, C.E., M. Getie, and R.H. Neubert, *Mass spectrometric characterization of human skin elastin peptides produced by proteolytic digestion with pepsin and thermitase*. J Chromatogr A, 2005. **1083**(1-2): p. 120-6.
72. Sandberg, L.B., N.T. Soskel, and T.B. Wolt, *Structure of the elastic fiber: an overview*. J Invest Dermatol, 1982. **79 Suppl 1**: p. 128s-132s.
73. Ostuni, A., et al., *Molecular and supramolecular structural studies on human tropoelastin sequences*. Biophys J, 2007. **93**(10): p. 3640-51.
74. Uitto, J., H.P. Hoffmann, and D.J. Prockop, *Synthesis of elastin and procollagen by cells from embryonic aorta. Differences in the role of hydroxyproline and the effects of proline analogs on the secretion of the two proteins*. Arch Biochem Biophys, 1976. **173**(1): p. 187-200.
75. Bochicchio, B., et al., *Investigating the role of (2S,4R)-4-hydroxyproline in elastin model peptides*. Biomacromolecules, 2013. **14**(12): p. 4278-88.
76. Tamburro, A.M., *A never-ending love story with elastin: a scientific autobiography*. Nanomedicine (Lond), 2009. **4**(4): p. 469-87.
77. Sage, H., *The evolution of elastin: correlation of functional properties with protein structure and phylogenetic distribution*. Comp Biochem Physiol B, 1983. **74**(3): p. 373-80.
78. Miao, M., et al., *Structural determinants of cross-linking and hydrophobic domains for self-assembly of elastin-like polypeptides*. Biochemistry, 2005. **44**(43): p. 14367-75.
79. Debelle, L. and A.M. Tamburro, *Elastin: molecular description and function*. Int J Biochem Cell Biol, 1999. **31**(2): p. 261-72.
80. Rauscher, S., et al., *Proline and Glycine Control Protein Self-Organization into Elastomeric or Amyloid Fibrils*. Structure, 2006. **14**(11): p. 1667-1676.
81. Brassart, B., et al., *Conformational dependence of collagenase (matrix metalloproteinase-1) up-regulation by elastin peptides in cultured fibroblasts*. J Biol Chem, 2001. **276**(7): p. 5222-7.
82. Eyre, D.R., M.A. Paz, and P.M. Gallop, *Cross-linking in collagen and elastin*. Annu Rev Biochem, 1984. **53**: p. 717-48.
83. Kozel, B.A., et al., *Domains in tropoelastin that mediate elastin deposition in vitro and in vivo*. J Biol Chem, 2003. **278**(20): p. 18491-8.
84. Debelle, L., et al., *The secondary structure and architecture of human elastin*. Eur J Biochem, 1998. **258**(2): p. 533-9.
85. Tamburro, A.M., B. Bochicchio, and A. Pepe, *The dissection of human tropoelastin: from the molecular structure to the self-assembly to the elasticity mechanism*. Pathol Biol (Paris), 2005. **53**(7): p. 383-9.
86. Mammi, M., L. Gotte, and G. Pezzin, *Evidence for order in the structure of alpha-elastin*. Nature, 1968. **220**(5165): p. 371-3.
87. Urry, D.W., B. Starcher, and S.M. Partridge, *Coacervation of solubilized elastin effects a notable conformational change*. Nature, 1969. **222**(5195): p. 795-6.

88. Vrhovski, B., S. Jensen, and A.S. Weiss, *Coacervation characteristics of recombinant human tropoelastin*. Eur J Biochem, 1997. **250**(1): p. 92-8.
89. Muiznieks, L.D., S.A. Jensen, and A.S. Weiss, *Structural changes and facilitated association of tropoelastin*. Arch Biochem Biophys, 2003. **410**(2): p. 317-23.
90. Debelle, L., et al., *Bovine elastin and kappa-elastin secondary structure determination by optical spectroscopies*. J Biol Chem, 1995. **270**(44): p. 26099-103.
91. Bochicchio, B., et al., *Dissection of human tropoelastin: solution structure, dynamics and self-assembly of the exon 5 peptide*. Chemistry, 2004. **10**(13): p. 3166-76.
92. Tamburro, A.M., A. De Stradis, and L. D'Alessio, *Fractal aspects of elastin supramolecular organization*. J Biomol Struct Dyn, 1995. **12**(6): p. 1161-72.
93. Debelle, L. and A.J. Alix, *The structures of elastins and their function*. Biochimie, 1999. **81**(10): p. 981-94.
94. Tamburro, A.M., et al., *Supramolecular amyloid-like assembly of the polypeptide sequence coded by exon 30 of human tropoelastin*. J Biol Chem, 2005. **280**(4): p. 2682-90.
95. Muiznieks, L.D., A.S. Weiss, and F.W. Keeley, *Structural disorder and dynamics of elastin*. Biochem Cell Biol, 2010. **88**(2): p. 239-50.
96. Urry, D.W., *Entropic elastic processes in protein mechanisms. II. Simple (passive) and coupled (active) development of elastic forces*. J Protein Chem, 1988. **7**(2): p. 81-114.
97. Urry, D.W., *What is elastin; what is not*. Ultrastruct Pathol, 1983. **4**(2-3): p. 227-51.
98. Castiglione-Morelli, A., et al., *Spectroscopic studies on elastin-like synthetic polypeptides*. Int J Biol Macromol, 1990. **12**(6): p. 363-8.
99. Tiffany, M.L. and S. Krimm, *Circular dichroism of poly-L-proline in an unordered conformation*. Biopolymers, 1968. **6**(12): p. 1767-70.
100. Reichheld, S.E., et al., *Conformational transitions of the cross-linking domains of elastin during self-assembly*. J Biol Chem, 2014. **289**(14): p. 10057-68.
101. Debelle, L., Alix A.J.P., *Optical spectroscopic determination of bovine tropoelastin molecular model*. Journal of Molecular Structure, 1995. **348**: p. 321-324.
102. Bochicchio, B., et al., *Spectroscopic evidence revealing polyproline II structure in hydrophobic, putatively elastomeric sequences encoded by specific exons of human tropoelastin*. Biopolymers, 2004. **73**(4): p. 484-93.
103. Dyksterhuis, L.B., et al., *Tropoelastin as a thermodynamically unfolded premolten globule protein: The effect of trimethylamine N-oxide on structure and coacervation*. Arch Biochem Biophys, 2009. **487**(2): p. 79-84.
104. Perry, A., et al., *Observation of the glycines in elastin using (13)C and (15)N solid-state NMR spectroscopy and isotopic labeling*. J Am Chem Soc, 2002. **124**(24): p. 6832-3.
105. Pometun, M.S., E.Y. Chekmenev, and R.J. Wittebort, *Quantitative observation of backbone disorder in native elastin*. J Biol Chem, 2004. **279**(9): p. 7982-7.
106. Le Brun, A.P., et al., *Molecular orientation of tropoelastin is determined by surface hydrophobicity*. Biomacromolecules, 2012. **13**(2): p. 379-86.
107. Flamia, R., et al., *Transformation of amyloid-like fibers, formed from an elastin-based biopolymer, into a hydrogel: an X-ray photoelectron spectroscopy and atomic force microscopy study*. Biomacromolecules, 2007. **8**(1): p. 128-38.
108. Flamia, R., et al., *AFM study of the elastin-like biopolymer poly(ValGlyGlyValGly)*. Biomacromolecules, 2004. **5**(4): p. 1511-8.
109. Gosline, J.M., Yew, F.F., Weis-Fogh, T., *Reversible structural changes in a hydrophobic protein, elastin, as indicated by fluorescence probe analysis*. Biopolymers, 1975. **14**(9): p. 1811-1826.

110. Yeo, G.C., et al., *A negatively charged residue stabilizes the tropoelastin N-terminal region for elastic fiber assembly*. J Biol Chem, 2014. **289**(50): p. 34815-26.
111. Gowda, D.C., et al., *Synthesis and characterization of the human elastin W4 sequence*. Int J Pept Protein Res, 1995. **46**(6): p. 453-63.
112. Jensen, S.A., B. Vrhovski, and A.S. Weiss, *Domain 26 of tropoelastin plays a dominant role in association by coacervation*. J Biol Chem, 2000. **275**(37): p. 28449-54.
113. Sato, F., et al., *Distinct steps of cross-linking, self-association, and maturation of tropoelastin are necessary for elastic fiber formation*. J Mol Biol, 2007. **369**(3): p. 841-51.
114. Wachi, H., et al., *Domains 16 and 17 of tropoelastin in elastic fibre formation*. Biochem J, 2007. **402**(1): p. 63-70.
115. Clarke, A.W., et al., *Coacervation is promoted by molecular interactions between the PF2 segment of fibrillin-1 and the domain 4 region of tropoelastin*. Biochemistry, 2005. **44**(30): p. 10271-81.
116. Lee, P., et al., *A novel cell adhesion region in tropoelastin mediates attachment to integrin alphaVbeta5*. J Biol Chem, 2014. **289**(3): p. 1467-77.
117. Wise, S.G., et al., *Tropoelastin: a versatile, bioactive assembly module*. Acta Biomater, 2014. **10**(4): p. 1532-41.
118. Kumashiro, K.K., et al., *Cooperativity between the hydrophobic and cross-linking domains of elastin*. J Biol Chem, 2006. **281**(33): p. 23757-65.
119. Dyksterhuis, L.B. and A.S. Weiss, *Homology models for domains 21-23 of human tropoelastin shed light on lysine crosslinking*. Biochem Biophys Res Commun, 2010. **396**(4): p. 870-3.
120. Pepe, A., et al., *Dissection of human tropoelastin: supramolecular organization of polypeptide sequences coded by particular exons*. Matrix Biol, 2005. **24**(2): p. 96-109.
121. Mecham, R.P., et al., *Elastin binds to a multifunctional 67-kilodalton peripheral membrane protein*. Biochemistry, 1989. **28**(9): p. 3716-22.
122. Yeo, G.C., et al., *Tropoelastin bridge region positions the cell-interactive C terminus and contributes to elastic fiber assembly*. Proc Natl Acad Sci U S A, 2012. **109**(8): p. 2878-83.
123. Rodgers, U.R. and A.S. Weiss, *Integrin alpha v beta 3 binds a unique non-RGD site near the C-terminus of human tropoelastin*. Biochimie, 2004. **86**(3): p. 173-8.
124. Broekelmann, T.J., et al., *Modification and functional inactivation of the tropoelastin carboxy-terminal domain in cross-linked elastin*. Matrix Biol, 2008. **27**(7): p. 631-9.
125. Muiznieks, L.D., et al., *Contribution of domain 30 of tropoelastin to elastic fiber formation and material elasticity*. Biopolymers, 2016. **105**(5): p. 267-75.
126. Rodgers, U.R. and A.S. Weiss, *Cellular interactions with elastin*. Pathol Biol (Paris), 2005. **53**(7): p. 390-8.
127. Nonaka, R., F. Sato, and H. Wachi, *Domain 36 of tropoelastin in elastic fiber formation*. Biol Pharm Bull, 2014. **37**(4): p. 698-702.
128. Bax, D.V., et al., *Cell adhesion to tropoelastin is mediated via the C-terminal GRKRK motif and integrin alphaVbeta3*. J Biol Chem, 2009. **284**(42): p. 28616-23.
129. Getie, M., C.E. Schmelzer, and R.H. Neubert, *Characterization of peptides resulting from digestion of human skin elastin with elastase*. Proteins, 2005. **61**(3): p. 649-57.
130. Brown, P.L., et al., *The cysteine residues in the carboxy terminal domain of tropoelastin form an intrachain disulfide bond that stabilizes a loop structure and positively charged pocket*. Biochem Biophys Res Commun, 1992. **186**(1): p. 549-55.
131. Codriansky, K.A., et al., *Intracellular degradation of elastin by cathepsin K in skin fibroblasts--a possible role in photoaging*. Photochem Photobiol, 2009. **85**(6): p. 1356-63.

132. Chung, J.H., et al., *Ultraviolet modulation of human macrophage metalloelastase in human skin in vivo*. J Invest Dermatol, 2002. **119**(2): p. 507-12.
133. Kahari, V.M. and U. Saarialho-Kere, *Matrix metalloproteinases in skin*. Exp Dermatol, 1997. **6**(5): p. 199-213.
134. Novinec, M., et al., *Interaction between human cathepsins K, L, and S and elastins: mechanism of elastinolysis and inhibition by macromolecular inhibitors*. J Biol Chem, 2007. **282**(11): p. 7893-902.
135. Samouillan, V., et al., *Alterations in the chain dynamics of insoluble elastin upon proteolysis by serine elastases*. Biopolymers, 2001. **58**(2): p. 175-85.
136. Antonicelli, F., et al., *Elastin-elastases and inflamm-aging*. Curr Top Dev Biol, 2007. **79**: p. 99-155.
137. Hornebeck, W. and H. Emonard, *The cell-elastin-elastase(s) interacting triade directs elastolysis*. Front Biosci (Landmark Ed), 2011. **16**: p. 707-22.
138. Frances, C. and L. Robert, *Elastin and elastic fibers in normal and pathologic skin*. Int J Dermatol, 1984. **23**(3): p. 166-79.
139. Brömme, D. and S. Wilson, *Role of Cysteine Cathepsins in Extracellular Proteolysis*, in *Extracellular Matrix Degradation*, W.C. Parks and R.P. Mecham, Editors. 2011, Springer Berlin Heidelberg: Berlin, Heidelberg. p. 23-51.
140. Cavarra, E., et al., *UVA light stimulates the production of cathepsin G and elastase-like enzymes by dermal fibroblasts: a possible contribution to the remodeling of elastotic areas in sun-damaged skin*. Biol Chem, 2002. **383**(1): p. 199-206.
141. Mecham, R.P., et al., *Elastin degradation by matrix metalloproteinases. Cleavage site specificity and mechanisms of elastolysis*. J Biol Chem, 1997. **272**(29): p. 18071-6.
142. Mannello, F. and V. Medda, *Nuclear localization of matrix metalloproteinases*. Prog Histochem Cytochem, 2012. **47**(1): p. 27-58.
143. Fruh, H., et al., *Human myeloblastin (leukocyte proteinase 3): reactions with substrates, inactivators and activators in comparison with leukocyte elastase*. Biol Chem, 1996. **377**(9): p. 579-86.
144. Shapiro, S.D., *Neutrophil elastase: path clearer, pathogen killer, or just pathologic?* Am J Respir Cell Mol Biol, 2002. **26**(3): p. 266-8.
145. Ying, Q.L. and S.R. Simon, *Elastolysis by proteinase 3 and its inhibition by alpha(1)-proteinase inhibitor: a mechanism for the incomplete inhibition of ongoing elastolysis*. Am J Respir Cell Mol Biol, 2002. **26**(3): p. 356-61.
146. Hajjar, E., et al., *Structures of human proteinase 3 and neutrophil elastase--so similar yet so different*. Febs j, 2010. **277**(10): p. 2238-54.
147. Heinz, A., et al., *The action of neutrophil serine proteases on elastin and its precursor*. Biochimie, 2012. **94**(1): p. 192-202.
148. Owen, C.A. and E.J. Campbell, *Extracellular proteolysis: new paradigms for an old paradox*. J Lab Clin Med, 1999. **134**(4): p. 341-51.
149. Schmelzer, C.E., et al., *Does human leukocyte elastase degrade intact skin elastin?* Febs j, 2012. **279**(22): p. 4191-200.
150. Collier, I.E., et al., *On the structure and chromosome location of the 72- and 92-kDa human type IV collagenase genes*. Genomics, 1991. **9**(3): p. 429-34.
151. Fridman, R., et al., *Activation of progelatinase B (MMP-9) by gelatinase A (MMP-2)*. Cancer Res, 1995. **55**(12): p. 2548-55.
152. Heinz, A., et al., *Degradation of tropoelastin by matrix metalloproteinases--cleavage site specificities and release of matrikines*. Febs j, 2010. **277**(8): p. 1939-56.
153. Opdenakker, G., et al., *Gelatinase B functions as regulator and effector in leukocyte biology*. J Leukoc Biol, 2001. **69**(6): p. 851-9.
154. Wilson, C.L. and L.M. Matrisian, *Matrilysin: an epithelial matrix metalloproteinase with potentially novel functions*. Int J Biochem Cell Biol, 1996. **28**(2): p. 123-36.

155. Punturieri, A., et al., *Regulation of elastolytic cysteine proteinase activity in normal and cathepsin K-deficient human macrophages*. J Exp Med, 2000. **192**(6): p. 789-99.
156. Imokawa, G. and K. Ishida, *Biological Mechanisms Underlying the Ultraviolet Radiation-Induced Formation of Skin Wrinkling and Sagging I: Reduced Skin Elasticity, Highly Associated with Enhanced Dermal Elastase Activity, Triggers Wrinkling and Sagging*. Int J Mol Sci, 2015. **16**(4): p. 7753-7775.
157. Morisaki, N., et al., *Neprilysin is identical to skin fibroblast elastase: its role in skin aging and UV responses*. J Biol Chem, 2010. **285**(51): p. 39819-27.
158. Almine, J.F., et al., *Elastin-based materials*. Chem Soc Rev, 2010. **39**(9): p. 3371-9.
159. Duca, L., et al., *Elastin as a matrikine*. Crit Rev Oncol Hematol, 2004. **49**(3): p. 235-44.
160. Maquart, F.-X., et al., *An introduction to matrikines: extracellular matrix-derived peptides which regulate cell activity: Implication in tumor invasion*. Crit Rev Oncol Hematol, 2004. **49**(3): p. 199-202.
161. Scandolera, A., et al., *The Elastin Receptor Complex: A Unique Matricellular Receptor with High Anti-tumoral Potential*. Front Pharmacol, 2016. **7**: p. 32.
162. Duca, L., et al., *The elastin receptor complex transduces signals through the catalytic activity of its Neu-1 subunit*. J Biol Chem, 2007. **282**(17): p. 12484-91.
163. Duca, L., et al., *Elastin peptides activate extracellular signal-regulated kinase 1/2 via a Ras-independent mechanism requiring both p110gamma/Raf-1 and protein kinase A/B-Raf signaling in human skin fibroblasts*. Mol Pharmacol, 2005. **67**(4): p. 1315-24.
164. Karnik, S.K., et al., *Elastin induces myofibrillogenesis via a specific domain, VGVAPG*. Matrix Biol, 2003. **22**(5): p. 409-25.
165. Mochizuki, S., B. Brassart, and A. Hinek, *Signaling pathways transduced through the elastin receptor facilitate proliferation of arterial smooth muscle cells*. J Biol Chem, 2002. **277**(47): p. 44854-63.
166. Fulop, T., Jr., et al., *Determination of elastin peptides in normal and arteriosclerotic human sera by ELISA*. Clin Physiol Biochem, 1990. **8**(6): p. 273-82.
167. Nikolov, A., et al., *Abnormal levels of age-elastin derived peptides in sera of diabetic patients with arterial hypertension*. Central-European Journal of Immunology, 2014. **39**(3): p. 345-351.
168. Petersen, E., F. Wagberg, and K.A. Angquist, *Serum concentrations of elastin-derived peptides in patients with specific manifestations of atherosclerotic disease*. Eur J Vasc Endovasc Surg, 2002. **24**(5): p. 440-4.
169. Sivaprasad, S., N.V. Chong, and T.A. Bailey, *Serum elastin-derived peptides in age-related macular degeneration*. Invest Ophthalmol Vis Sci, 2005. **46**(9): p. 3046-51.
170. Robinet, A., et al., *Elastin-derived peptides enhance angiogenesis by promoting endothelial cell migration and tubulogenesis through upregulation of MT1-MMP*. J Cell Sci, 2005. **118**(Pt 2): p. 343-56.
171. Robinet, A., et al., *Binding of elastin peptides to S-Gal protects the heart against ischemia/reperfusion injury by triggering the RISK pathway*. Faseb j, 2007. **21**(9): p. 1968-78.
172. Antonicelli, F., et al., *Role of the elastin receptor complex (S-Gal/Cath-A/Neu-1) in skin repair and regeneration*. Wound Repair Regen, 2009. **17**(5): p. 631-8.
173. Houghton, A.M., et al., *Elastin fragments drive disease progression in a murine model of emphysema*. J Clin Invest, 2006. **116**(3): p. 753-9.
174. Bizbiz, L., A. Alperovitch, and L. Robert, *Aging of the vascular wall: serum concentration of elastin peptides and elastase inhibitors in relation to cardiovascular risk factors. The EVA study*. Atherosclerosis, 1997. **131**(1): p. 73-8.
175. Fulop, T., Jr., et al., *Elastin peptides induced oxidation of LDL by phagocytic cells*. Pathol Biol (Paris), 2005. **53**(7): p. 416-23.



176. Gayral, S., et al., *Elastin-derived peptides potentiate atherosclerosis through the immune Neu1-PI3Kgamma pathway*. Cardiovasc Res, 2014. **102**(1): p. 118-27.
177. Robert, L., *Aging of the vascular wall and atherogenesis: role of the elastin-laminin receptor*. Atherosclerosis, 1996. **123**(1-2): p. 169-79.
178. Hance, K.A., et al., *Monocyte chemotactic activity in human abdominal aortic aneurysms: role of elastin degradation peptides and the 67-kD cell surface elastin receptor*. J Vasc Surg, 2002. **35**(2): p. 254-61.
179. Simionescu, A., K. Philips, and N. Vyavahare, *Elastin-derived peptides and TGF-beta1 induce osteogenic responses in smooth muscle cells*. Biochem Biophys Res Commun, 2005. **334**(2): p. 524-32.
180. Debret, R., et al., *Elastin-Derived Peptides Induce a T-Helper Type 1 Polarization of Human Blood Lymphocytes*. Arteriosclerosis, Thrombosis, and Vascular Biology, 2005. **25**(7): p. 1353-1358.
181. Debret, R., et al., *Elastin fragments induce IL-1beta upregulation via NF-kappaB pathway in melanoma cells*. J Invest Dermatol, 2006. **126**(8): p. 1860-8.
182. Devy, J., et al., *Elastin-derived peptides enhance melanoma growth in vivo by upregulating the activation of Mcol-A (MMP-1) collagenase*. Br J Cancer, 2010. **103**(10): p. 1562-70.
183. Ntayi, C., et al., *Elastin-derived peptides upregulate matrix metalloproteinase-2-mediated melanoma cell invasion through elastin-binding protein*. J Invest Dermatol, 2004. **122**(2): p. 256-65.
184. Pocza, P., et al., *Locally generated VGVAPG and VAPG elastin-derived peptides amplify melanoma invasion via the galectin-3 receptor*. Int J Cancer, 2008. **122**(9): p. 1972-80.
185. Brassart, B., et al., *Regulation of matrix metalloproteinase-2(gelatinase A, MMP-2), membrane-type matrixmetalloproteinase-1 (MT1-MMP) and tissue inhibitor of metalloproteinases-2 (TIMP-2) expression by elastin-derived peptides in human HT-1080 fibrosarcoma cell line*. Clinical & Experimental Metastasis, 1998. **16**(6): p. 489-500.
186. Fulop, T., A. Khalil, and A. Larbi, *The role of elastin peptides in modulating the immune response in aging and age-related diseases*. Pathol Biol (Paris), 2012. **60**(1): p. 28-33.
187. Qin, Z., *Soluble elastin peptides in cardiovascular homeostasis: Foe or ally*. Peptides, 2015. **67**: p. 64-73.
188. Hinek, A., et al., *The 67-kD elastin/laminin-binding protein is related to an enzymatically inactive, alternatively spliced form of beta-galactosidase*. Journal of Clinical Investigation, 1993. **91**(3): p. 1198-1205.
189. Jacob, M.P., et al., *Effect of elastin peptides on ion fluxes in mononuclear cells, fibroblasts, and smooth muscle cells*. Proc Natl Acad Sci U S A, 1987. **84**(4): p. 995-9.
190. Broekelmann, T.J., et al., *Tropoelastin interacts with cell-surface glycosaminoglycans via its COOH-terminal domain*. J Biol Chem, 2005. **280**(49): p. 40939-47.
191. Ochieng, J., et al., *Galectin-3 regulates the adhesive interaction between breast carcinoma cells and elastin*. J Cell Biochem, 1999. **75**(3): p. 505-14.
192. Fuchs, P., L. Debelle, and A.J.P. Alix, *Structural study of some specific elastin hexapeptides activating MMP1*. Journal of Molecular Structure, 2001. **565-566**: p. 335-339.
193. Moroy, G., A.J. Alix, and S. Hery-Huynh, *Structural characterization of human elastin derived peptides containing the GXXP sequence*. Biopolymers, 2005. **78**(4): p. 206-20.
194. Mithieux, S.M., S.G. Wise, and A.S. Weiss, *Tropoelastin--a multifaceted naturally smart material*. Adv Drug Deliv Rev, 2013. **65**(4): p. 421-8.

195. Bisaccia, F., et al., *Migration of monocytes in the presence of elastolytic fragments of elastin and in synthetic derivatives. Structure-activity relationships.* Int J Pept Protein Res, 1994. **44**(4): p. 332-41.
196. Grosso, L.E. and M. Scott, *PGAIPG, a repeated hexapeptide of bovine and human tropoelastin, is chemotactic for neutrophils and Lewis lung carcinoma cells.* Arch Biochem Biophys, 1993. **305**(2): p. 401-4.
197. Long, M.M., et al., *Chemotaxis of fibroblasts toward nonapeptide of elastin.* Biochim Biophys Acta, 1988. **968**(3): p. 300-11.
198. Long, M.M., et al., *Elastin repeat peptides as chemoattractants for bovine aortic endothelial cells.* J Cell Physiol, 1989. **140**(3): p. 512-8.
199. Castiglione Morelli, M.A., et al., *Structure-activity relationships for some elastin-derived peptide chemoattractants.* J Pept Res, 1997. **49**(6): p. 492-9.
200. Bisaccia, F., et al., *The amino acid sequence coded by the rarely expressed exon 26A of human elastin contains a stable beta-turn with chemotactic activity for monocytes.* Biochemistry, 1998. **37**(31): p. 11128-35.
201. Hauck, M., et al., *Effects of synthesized elastin peptides on human leukocytes.* Biochem Mol Biol Int, 1995. **37**(1): p. 45-55.
202. Faury, G., et al., *Action of tropoelastin and synthetic elastin sequences on vascular tone and on free Ca<sup>2+</sup> level in human vascular endothelial cells.* Circ Res, 1998. **82**(3): p. 328-36.
203. Senior, R.M., et al., *Val-Gly-Val-Ala-Pro-Gly, a repeating peptide in elastin, is chemotactic for fibroblasts and monocytes.* J Cell Biol, 1984. **99**(3): p. 870-4.
204. Fujimoto, N., S. Tajima, and A. Ishibashi, *Elastin peptides induce migration and terminal differentiation of cultured keratinocytes via 67 kDa elastin receptor in vitro: 67 kDa elastin receptor is expressed in the keratinocytes eliminating elastic materials in elastosis perforans serpiginosa.* J Invest Dermatol, 2000. **115**(4): p. 633-9.
205. Blaise, S., et al., *Elastin-derived peptides are new regulators of insulin resistance development in mice.* Diabetes, 2013. **62**(11): p. 3807-16.
206. Chang, C.H., et al., *Melanocyte precursors express elastin binding protein and elastin-derived peptide (VGVAPG) stimulates their melanogenesis and dendrite formation.* J Dermatol Sci, 2008. **51**(3): p. 158-70.
207. Kamoun, A., et al., *Growth stimulation of human skin fibroblasts by elastin-derived peptides.* Cell Adhes Commun, 1995. **3**(4): p. 273-81.
208. Tajima, S., et al., *Modulation by elastin peptide VGVAPG of cell proliferation and elastin expression in human skin fibroblasts.* Archives of Dermatological Research, 1997. **289**(8): p. 489-492.
209. Blood, C.H., et al., *Identification of a tumor cell receptor for VGVAPG, an elastin-derived chemotactic peptide.* J Cell Biol, 1988. **107**(5): p. 1987-93.
210. Blood, C.H. and B.R. Zetter, *Membrane-bound protein kinase C modulates receptor affinity and chemotactic responsiveness of Lewis lung carcinoma sublines to an elastin-derived peptide.* J Biol Chem, 1989. **264**(18): p. 10614-20.
211. Mecham, R.P., et al., *The elastin receptor shows structural and functional similarities to the 67-kDa tumor cell laminin receptor.* J Biol Chem, 1989. **264**(28): p. 16652-7.
212. Sarfati, I., et al., *Inhibition by protease inhibitors of chemotaxis induced by elastin-derived peptides.* J Surg Res, 1996. **61**(1): p. 84-8.
213. Yusa, T., C.H. Blood, and B.R. Zetter, *Tumor cell interactions with elastin: implications for pulmonary metastasis.* Am Rev Respir Dis, 1989. **140**(5): p. 1458-62.
214. Wachi, H., et al., *Stimulation of cell proliferation and autoregulation of elastin expression by elastin peptide VPGVG in cultured chick vascular smooth muscle cells.* FEBS Lett, 1995. **368**(2): p. 215-9.

215. Spezzacatena, C., et al., *Synthesis, Solution Structure and Biological Activity of Val-Val-Pro-Gln,a Bioactive Elastin Peptide*. European Journal of Organic Chemistry, 2005. **2005**(8): p. 1644-1651.
216. Belsky, D.W., et al., *Quantification of biological aging in young adults*. Proc Natl Acad Sci U S A, 2015. **112**(30): p. E4104-E4110.
217. Robert, L., *Longevity and aging, genetic and post-genetic mechanisms. Which target to choose for postponing and treating age-related diseases*. European Geriatric Medicine, 2012. **3**(1): p. 61-66.
218. Kammeyer, A. and R.M. Luiten, *Oxidation events and skin aging*. Ageing Res Rev, 2015. **21**: p. 16-29.
219. Landau, M., *Exogenous factors in skin aging*. Curr Probl Dermatol, 2007. **35**: p. 1-13.
220. Seite, S., et al., *Elastin changes during chronological and photo-ageing: the important role of lysozyme*. J Eur Acad Dermatol Venereol, 2006. **20**(8): p. 980-7.
221. Robert, L., A.M. Robert, and T. Fulop, *Rapid increase in human life expectancy: will it soon be limited by the aging of elastin?* Biogerontology, 2008. **9**(2): p. 119-33.
222. Uitto, J. and E.F. Bernstein, *Molecular mechanisms of cutaneous aging: connective tissue alterations in the dermis*. J Investig Dermatol Symp Proc, 1998. **3**(1): p. 41-4.
223. Koehler, M.J., et al., *Intrinsic, solar and sunbed-induced skin aging measured in vivo by multiphoton laser tomography and biophysical methods*. Skin Res Technol, 2009. **15**(3): p. 357-63.
224. Suwabe, H., et al., *Degenerative processes of elastic fibers in sun-protected and sun-exposed skin: immunoelectron microscopic observation of elastin, fibrillin-1, amyloid P component, lysozyme and alpha1-antitrypsin*. Pathol Int, 1999. **49**(5): p. 391-402.
225. Sakura, M., Chiba, Y. , Kamiya, E. , Furukawa, A. , Kawamura, N. , Niwa, M. , Takeuchi, M. , Enokido, Y. and Hosokawa, M., *Differences in the Histopathology and Cytokine Expression Pattern between Chronological Aging and Photoaging of Hairless Mice Skin*. Modern Research in Inflammation, 2014. **3**: p. 82-89.
226. Sakuraoka, K., et al., *Analysis of connective tissue macromolecular components in Ishibashi rat skin: role of collagen and elastin in cutaneous aging*. J Dermatol Sci, 1996. **12**(3): p. 232-7.
227. Oikarinen, A., et al., *Connective tissue alterations in skin exposed to natural and therapeutic UV-radiation*. Photodermatol, 1985. **2**(1): p. 15-26.
228. Chen, Z., et al., *Heat modulation of tropoelastin, fibrillin-1, and matrix metalloproteinase-12 in human skin in vivo*. J Invest Dermatol, 2005. **124**(1): p. 70-8.
229. Mera, S.L., et al., *Elastic fibres in normal and sun-damaged skin: an immunohistochemical study*. Br J Dermatol, 1987. **117**(1): p. 21-7.
230. Montagna, W., S. Kirchner, and K. Carlisle, *Histology of sun-damaged human skin*. J Am Acad Dermatol, 1989. **21**(5 Pt 1): p. 907-18.
231. Berneburg, M., H. Plettenberg, and J. Krutmann, *Photoaging of human skin*. Photodermatol Photoimmunol Photomed, 2000. **16**(6): p. 239-44.
232. Fisher, G.J., et al., *Mechanisms of photoaging and chronological skin aging*. Arch Dermatol, 2002. **138**(11): p. 1462-70.
233. Gilchrist, B.A., *A review of skin ageing and its medical therapy*. Br J Dermatol, 1996. **135**(6): p. 867-75.
234. Robert, L., J. Labat-Robert, and A.M. Robert, *Physiology of skin aging*. Pathol Biol (Paris), 2009. **57**(4): p. 336-41.
235. Makrantonaki, E., et al., *Skin aging*. Der Hautarzt, 2015. **66**(10): p. 730-737.
236. Milewicz, D.M., Z. Urban, and C. Boyd, *Genetic disorders of the elastic fiber system*. Matrix Biol, 2000. **19**(6): p. 471-80.

237. Micale, L., et al., *Identification and characterization of seven novel mutations of elastin gene in a cohort of patients affected by supravalvular aortic stenosis*. Eur J Hum Genet, 2010. **18**(3): p. 317-23.
238. Urban, Z., et al., *Elastin gene deletions in Williams syndrome patients result in altered deposition of elastic fibers in skin and a subclinical dermal phenotype*. Pediatr Dermatol, 2000. **17**(1): p. 12-20.
239. Urban, Z., et al., *Supravalvular aortic stenosis: genetic and molecular dissection of a complex mutation in the elastin gene*. Hum Genet, 2001. **109**(5): p. 512-20.
240. Callewaert, B., et al., *New insights into the pathogenesis of autosomal-dominant cutis laxa with report of five ELN mutations*. Hum Mutat, 2011. **32**(4): p. 445-55.
241. Hadj-Rabia, S., et al., *Twenty patients including 7 probands with autosomal dominant cutis laxa confirm clinical and molecular homogeneity*. Orphanet J Rare Dis, 2013. **8**: p. 36.
242. Tassabehji, M., et al., *An elastin gene mutation producing abnormal tropoelastin and abnormal elastic fibres in a patient with autosomal dominant cutis laxa*. Hum Mol Genet, 1998. **7**(6): p. 1021-8.
243. Olsen, D.R., et al., *Cutis laxa: reduced elastin gene expression in skin fibroblast cultures as determined by hybridizations with a homologous cDNA and an exon 1-specific oligonucleotide*. J Biol Chem, 1988. **263**(14): p. 6465-7.
244. Ewart, A.K., et al., *Hemizyosity at the elastin locus in a developmental disorder, Williams syndrome*. Nat Genet, 1993. **5**(1): p. 11-6.
245. Schubert, C., *The genomic basis of the Williams-Beuren syndrome*. Cell Mol Life Sci, 2009. **66**(7): p. 1178-97.
246. Morris, C.A. and C.B. Mervis, *Williams syndrome and related disorders*. Annu Rev Genomics Hum Genet, 2000. **1**: p. 461-84.
247. Pober, B.R., *Williams-Beuren syndrome*. N Engl J Med, 2010. **362**(3): p. 239-52.
248. Dridi, S.M., et al., *Skin elastic fibers in Williams syndrome*. Am J Med Genet, 1999. **87**(2): p. 134-8.
249. Kozel, B.A., et al., *Skin findings in Williams syndrome*. Am J Med Genet A, 2014. **164a**(9): p. 2217-25.
250. Robb, B.W., et al., *Characterization of an in vitro model of elastic fiber assembly*. Mol Biol Cell, 1999. **10**(11): p. 3595-605.
251. Deslee, G., et al., *Elastin expression in very severe human COPD*. European Respiratory Journal, 2009. **34**(2): p. 324-331.
252. Krettek, A., G.K. Sukhova, and P. Libby, *Elastogenesis in Human Arterial Disease. A Role for Macrophages in Disordered Elastin Synthesis*, 2003. **23**(4): p. 582-587.
253. Maeda, I., et al., *Immunochemical and immunohistochemical studies on distribution of elastin fibres in human atherosclerotic lesions using a polyclonal antibody to elastin-derived hexapeptide repeat*. J Biochem, 2007. **142**(5): p. 627-31.
254. Pierce, R.A., et al., *Chronic lung injury in preterm lambs: disordered pulmonary elastin deposition*. Am J Physiol, 1997. **272**(3 Pt 1): p. L452-60.
255. Rongioletti, F. and A. Rebora, *Fibroelastolytic patterns of intrinsic skin aging: pseudoxanthoma-elasticum-like papillary dermal elastolysis and white fibrous papulosis of the neck*. Dermatology, 1995. **191**(1): p. 19-24.
256. Akhtar, K., et al., *Oxidative and nitrosative modifications of tropoelastin prevent elastic fiber assembly in vitro*. J Biol Chem, 2010. **285**(48): p. 37396-404.
257. Hu, Q., et al., *Inflammatory destruction of elastic fibers in acquired cutis laxa is associated with missense alleles in the elastin and fibulin-5 genes*. J Invest Dermatol, 2006. **126**(2): p. 283-90.
258. Yates Iii, J.R., *A century of mass spectrometry: from atoms to proteomes*. Nat Meth, 2011. **8**(8): p. 633-637.

259. Gross, J.H., *Mass Spectrometry A textbook*. 2nd ed. 2011, Heidelberg, Germany: Springer Berlin Heidelberg. 753.
260. Domb, B. and R. Aebersold, *Mass spectrometry and protein analysis*. Science, 2006. **312**(5771): p. 212-7.
261. Han, X., A. Aslanian, and J.R. Yates, 3rd, *Mass spectrometry for proteomics*. Curr Opin Chem Biol, 2008. **12**(5): p. 483-90.
262. Yates, J.R., C.I. Ruse, and A. Nakorchevsky, *Proteomics by mass spectrometry: approaches, advances, and applications*. Annu Rev Biomed Eng, 2009. **11**: p. 49-79.
263. Glish, G.L. and R.W. Vachet, *The basics of mass spectrometry in the twenty-first century*. Nat Rev Drug Discov, 2003. **2**(2): p. 140-50.
264. Canas, B., et al., *Mass spectrometry technologies for proteomics*. Brief Funct Genomic Proteomic, 2006. **4**(4): p. 295-320.
265. Annesley, T.M., *Ion suppression in mass spectrometry*. Clin Chem, 2003. **49**(7): p. 1041-4.
266. Micallef, J., et al., *Applying mass spectrometry based proteomic technology to advance the understanding of multiple myeloma*. J Hematol Oncol, 2010. **3**: p. 13.
267. Ho, C., et al., *Electrospray Ionisation Mass Spectrometry: Principles and Clinical Applications*. Clin Biochem Rev, 2003. **24**(1): p. 3-12.
268. Lewis, J.K., J. Wei, and G. Siuzdak, *Matrix-Assisted Laser Desorption/Ionization Mass Spectrometry in Peptide and Protein Analysis*, in *Encyclopedia of Analytical Chemistry*. 2006, John Wiley & Sons, Ltd.
269. Karas, M., M. Gluckmann, and J. Schafer, *Ionization in matrix-assisted laser desorption/ionization: singly charged molecular ions are the lucky survivors*. J Mass Spectrom, 2000. **35**(1): p. 1-12.
270. Whitehouse, C.M., et al., *Electrospray interface for liquid chromatographs and mass spectrometers*. Anal Chem, 1985. **57**(3): p. 675-9.
271. Eng, J.K., A.L. McCormack, and J.R. Yates, *An approach to correlate tandem mass spectral data of peptides with amino acid sequences in a protein database*. J Am Soc Mass Spectrom, 1994. **5**(11): p. 976-89.
272. Perkins, D.N., et al., *Probability-based protein identification by searching sequence databases using mass spectrometry data*. Electrophoresis, 1999. **20**(18): p. 3551-67.
273. Mann, M. and M. Wilm, *Error-tolerant identification of peptides in sequence databases by peptide sequence tags*. Anal Chem, 1994. **66**(24): p. 4390-9.
274. Zhang, J., et al., *PEAKS DB: de novo sequencing assisted database search for sensitive and accurate peptide identification*. Mol Cell Proteomics, 2012. **11**(4): p. M111.010587.
275. Papayannopoulos, I.A., *The interpretation of collision-induced dissociation tandem mass spectra of peptides*. Mass Spectrometry Reviews, 1995. **14**(1): p. 49-73.
276. Eliuk, S. and A. Makarov, *Evolution of Orbitrap Mass Spectrometry Instrumentation*. Annu Rev Anal Chem (Palo Alto Calif), 2015. **8**: p. 61-80.
277. Ong, S.E. and M. Mann, *Mass spectrometry-based proteomics turns quantitative*. Nat Chem Biol, 2005. **1**(5): p. 252-62.
278. Bantscheff, M., et al., *Quantitative mass spectrometry in proteomics: a critical review*. Anal Bioanal Chem, 2007. **389**(4): p. 1017-31.
279. Ross, P.L., et al., *Multiplexed protein quantitation in Saccharomyces cerevisiae using amine-reactive isobaric tagging reagents*. Mol Cell Proteomics, 2004. **3**(12): p. 1154-69.
280. Yao, X., C. Afonso, and C. Fenselau, *Dissection of Proteolytic 18O Labeling: Endoprotease-Catalyzed 16O-to-18O Exchange of Truncated Peptide Substrates*. Journal of Proteome Research, 2003. **2**(2): p. 147-152.

281. Brun, V., et al., *Isotope dilution strategies for absolute quantitative proteomics*. Journal of Proteomics, 2009. **72**(5): p. 740-749.
282. Gerber, S.A., et al., *Absolute quantification of proteins and phosphoproteins from cell lysates by tandem MS*. Proc Natl Acad Sci U S A, 2003. **100**(12): p. 6940-5.
283. Kirkpatrick, D.S., S.A. Gerber, and S.P. Gygi, *The absolute quantification strategy: a general procedure for the quantification of proteins and post-translational modifications*. Methods, 2005. **35**(3): p. 265-73.
284. Ong, S.E., et al., *Stable isotope labeling by amino acids in cell culture, SILAC, as a simple and accurate approach to expression proteomics*. Mol Cell Proteomics, 2002. **1**(5): p. 376-86.
285. Bondarenko, P.V., D. Chelius, and T.A. Shaler, *Identification and relative quantitation of protein mixtures by enzymatic digestion followed by capillary reversed-phase liquid chromatography-tandem mass spectrometry*. Anal Chem, 2002. **74**(18): p. 4741-9.
286. Chelius, D. and P.V. Bondarenko, *Quantitative profiling of proteins in complex mixtures using liquid chromatography and mass spectrometry*. J Proteome Res, 2002. **1**(4): p. 317-23.
287. Wang, G., et al., *Label-free protein quantification using LC-coupled ion trap or FT mass spectrometry: Reproducibility, linearity, and application with complex proteomes*. J Proteome Res, 2006. **5**(5): p. 1214-23.
288. Sandin, M., et al., *Data processing methods and quality control strategies for label-free LC-MS protein quantification*. Biochim Biophys Acta, 2014. **1844**(1 Pt A): p. 29-41.
289. Wang, W., et al., *Quantification of proteins and metabolites by mass spectrometry without isotopic labeling or spiked standards*. Anal Chem, 2003. **75**(18): p. 4818-26.
290. Wiener, M.C., et al., *Differential mass spectrometry: a label-free LC-MS method for finding significant differences in complex peptide and protein mixtures*. Anal Chem, 2004. **76**(20): p. 6085-96.
291. Neilson, K.A., et al., *Less label, more free: approaches in label-free quantitative mass spectrometry*. Proteomics, 2011. **11**(4): p. 535-53.
292. Zhu, W., J.W. Smith, and C.-M. Huang, *Mass Spectrometry-Based Label-Free Quantitative Proteomics*. Journal of Biomedicine and Biotechnology, 2010. **2010**: p. 6.
293. Voyksner, R.D. and H. Lee, *Investigating the use of an octupole ion guide for ion storage and high-pass mass filtering to improve the quantitative performance of electrospray ion trap mass spectrometry*. Rapid Commun Mass Spectrom, 1999. **13**(14): p. 1427-37.
294. Liu, H., R.G. Sadygov, and J.R. Yates, 3rd, *A model for random sampling and estimation of relative protein abundance in shotgun proteomics*. Anal Chem, 2004. **76**(14): p. 4193-201.
295. Old, W.M., et al., *Comparison of label-free methods for quantifying human proteins by shotgun proteomics*. Mol Cell Proteomics, 2005. **4**(10): p. 1487-502.
296. Deng, N., et al., *freeQuant: A Mass Spectrometry Label-Free Quantification Software Tool for Complex Proteome Analysis*. ScientificWorldJournal, 2015. **2015**: p. 137076.
297. Lai, X., et al., *A novel alignment method and multiple filters for exclusion of unqualified peptides to enhance label-free quantification using peptide intensity in LC-MS/MS*. J Proteome Res, 2011. **10**(10): p. 4799-812.
298. Mueller, L.N., et al., *An assessment of software solutions for the analysis of mass spectrometry based quantitative proteomics data*. J Proteome Res, 2008. **7**(1): p. 51-61.

299. Wong, J.W., A.B. Schwahn, and K.M. Downard, *ETISEQ--an algorithm for automated elution time ion sequencing of concurrently fragmented peptides for mass spectrometry-based proteomics*. BMC Bioinformatics, 2009. **10**: p. 244.
300. Wong, J.W., M.J. Sullivan, and G. Cagney, *Computational methods for the comparative quantification of proteins in label-free LCn-MS experiments*. Brief Bioinform, 2008. **9**(2): p. 156-65.
301. Griffin, N.M., et al., *Label-free, normalized quantification of complex mass spectrometry data for proteomic analysis*. Nat Biotechnol, 2010. **28**(1): p. 83-9.
302. Benk, A.S. and C. Roesli, *Label-free quantification using MALDI mass spectrometry: considerations and perspectives*. Anal Bioanal Chem, 2012. **404**(4): p. 1039-56.
303. Heinz, A., et al., *Molecular-level characterization of elastin-like constructs and human aortic elastin*. Matrix Biology, 2014. **38**: p. 12-21.
304. Heinz, A., et al., *In vitro cross-linking of elastin peptides and molecular characterization of the resultant biomaterials*. Biochim Biophys Acta, 2013. **1830**(4): p. 2994-3004.
305. Kreuzsch, S., et al., *UV measurements in microplates suitable for high-throughput protein determination*. Anal Biochem, 2003. **313**(2): p. 208-15.
306. Zhang, G., et al., *Protein Quantitation Using Mass Spectrometry*. Methods in molecular biology (Clifton, N.J.), 2010. **673**: p. 211-222.
307. Fox, J., *The R Commander: A Basic-Statistics Graphical User Interface to R*. J Stat Softw, 2005. **14**(9): p. 42.
308. Team, R.C., *R: A language and Environment for Statistical Computing*. 2013.
309. Avila Castillo, A., *Untersuchung möglicher Einflussgrößen bei der komparativen massenspektrometrischen Analyse von Elastinverdauen*, in *Institut für Biochemie und Biotechnologie*. 2012, Martin-Luther-Universität Halle-Wittenberg: Halle (Saale), Deutschland. p. 50.
310. Sexton, T., et al., *Active site mutations change the cleavage specificity of neprilysin*. PLoS One, 2012. **7**(2): p. e32343.
311. Tiraboschi, G., et al., *A three-dimensional construction of the active site (region 507-749) of human neutral endopeptidase (EC.3.4.24.11)*. Protein Eng, 1999. **12**(2): p. 141-9.
312. Barros, N.M., et al., *Neprilysin carboxydipeptidase specificity studies and improvement in its detection with fluorescence energy transfer peptides*. Biol Chem, 2007. **388**(4): p. 447-55.
313. Braverman, I.M. and E. Fonferko, *Studies in cutaneous aging: I. The elastic fiber network*. J Invest Dermatol, 1982. **78**(5): p. 434-43.
314. Uitto, J., *The role of elastin and collagen in cutaneous aging: intrinsic aging versus photoexposure*. J Drugs Dermatol, 2008. **7**(2 Suppl): p. s12-6.
315. Heinz, A., et al., *Insights into the degradation of human elastin by matrilysin-I*. Biochimie, 2011. **93**(2): p. 187-94.
316. Taddese, S., et al., *Mapping of macrophage elastase cleavage sites in insoluble human skin elastin*. Matrix Biol, 2008. **27**(5): p. 420-8.
317. Bantscheff, M., et al., *Quantitative mass spectrometry in proteomics: critical review update from 2007 to the present*. Analytical and Bioanalytical Chemistry, 2012. **404**(4): p. 939-965.
318. Al Shweiki, M.H.D.R., et al., *Assessment of Label-Free Quantification in Discovery Proteomics and Impact of Technological Factors and Natural Variability of Protein Abundance*. Journal of Proteome Research, 2017. **16**(4): p. 1410-1424.
319. Shalit, T., et al., *MS1-Based Label-Free Proteomics Using a Quadrupole Orbitrap Mass Spectrometer*. Journal of Proteome Research, 2015. **14**(4): p. 1979-1986.

320. Geromanos, S.J., et al., *The detection, correlation, and comparison of peptide precursor and product ions from data independent LC-MS with data dependant LC-MS/MS*. Proteomics, 2009. **9**(6): p. 1683-95.
321. Silva, J.C., et al., *Absolute quantification of proteins by LCMSE: a virtue of parallel MS acquisition*. Mol Cell Proteomics, 2006. **5**(1): p. 144-56.
322. Clair, G., et al., *Spatially-Resolved Proteomics: Rapid Quantitative Analysis of Laser Capture Microdissected Alveolar Tissue Samples*. Sci Rep, 2016. **6**: p. 39223.
323. Nagaraj, N. and M. Mann, *Quantitative analysis of the intra- and inter-individual variability of the normal urinary proteome*. J Proteome Res, 2011. **10**(2): p. 637-45.
324. Piehowski, P.D., et al., *Sources of Technical Variability in Quantitative LC-MS Proteomics: Human Brain Tissue Sample Analysis*. Journal of proteome research, 2013. **12**(5): p. 2128-2137.
325. Narayanan, A.S. and R.A. Anwar, *The specificity of purified porcine pancreatic elastase*. Biochem J, 1969. **114**(1): p. 11-7.
326. Reilly, C.F. and J. Travis, *The degradation of human lung elastin by neutrophil proteinases*. Biochim Biophys Acta, 1980. **621**(1): p. 147-57.
327. Shadforth, I., D. Crowther, and C. Bessant, *Protein and peptide identification algorithms using MS for use in high-throughput, automated pipelines*. Proteomics, 2005. **5**(16): p. 4082-95.
328. Cox, J.T., et al., *On the Ionization and Ion Transmission Efficiencies of Different ESI-MS Interfaces*. Journal of the American Society for Mass Spectrometry, 2015. **26**(1): p. 55-62.
329. Tang, L. and P. Kebarle, *Dependence of ion intensity in electrospray mass spectrometry on the concentration of the analytes in the electrosprayed solution*. Analytical Chemistry, 1993. **65**(24): p. 3654-3668.
330. Alonso, M.C., et al., *Proteolytic mapping of kinesin/ncd-microtubule interface: nucleotide-dependent conformational changes in the loops L8 and L12*. The EMBO Journal, 1998. **17**(4): p. 945-951.
331. Gomes, X.V., L.A. Henricksen, and M.S. Wold, *Proteolytic Mapping of Human Replication Protein A: Evidence for Multiple Structural Domains and a Conformational Change upon Interaction with Single-Stranded DNA*. Biochemistry, 1996. **35**(17): p. 5586-5595.
332. Turner, A.J., R.E. Isaac, and D. Coates, *The neprilysin (NEP) family of zinc metalloendopeptidases: genomics and function*. Bioessays, 2001. **23**(3): p. 261-9.
333. Nakajima, H., et al., *Epithelial-mesenchymal interaction during UVB-induced up-regulation of neutral endopeptidase*. Biochem J, 2012. **443**(1): p. 297-305.
334. Homsy, R., et al., *Characterization of human skin fibroblasts elastase activity*. J Invest Dermatol, 1988. **91**(5): p. 472-7.
335. Szendroi, M., et al., *On the presence of a metalloprotease in human skin fibroblasts that degrades the human skin elastic fiber system*. J Invest Dermatol, 1984. **83**(3): p. 224-9.
336. Schwartz, E., F.A. Cruickshank, and M.G. Lebowitz, *Elastase-like protease and elastolytic activities expressed in cultured dermal fibroblasts derived from lesional skin of patients with pseudoxanthoma elasticum, actinic elastosis, and cutis laxa*. Clin Chim Acta, 1988. **176**(2): p. 219-24.
337. Mecham, R.P., *Methods in elastic tissue biology: elastin isolation and purification*. Methods, 2008. **45**(1): p. 32-41.
338. Christner, P., et al., *Degradation of tropoelastin by proteases*. Analytical Biochemistry, 1978. **88**(2): p. 682-688.
339. Oefner, C., et al., *Structure of human neutral endopeptidase (Neprilysin) complexed with phosphoramidon*. J Mol Biol, 2000. **296**(2): p. 341-9.



340. Webster, C.I., et al., *Engineering neprilysin activity and specificity to create a novel therapeutic for Alzheimer's disease*. PLoS One, 2014. **9**(8): p. e104001.
341. Goodman, O.B., Jr., et al., *Neprilysin inhibits angiogenesis via proteolysis of fibroblast growth factor-2*. J Biol Chem, 2006. **281**(44): p. 33597-605.
342. Li, B., D.O.V. Alonso, and V. Daggett, *The molecular basis for the inverse temperature transition of elastin1*. Journal of Molecular Biology, 2001. **305**(3): p. 581-592.
343. Imayama, S. and I.M. Braverman, *A hypothetical explanation for the aging of skin. Chronologic alteration of the three-dimensional arrangement of collagen and elastic fibers in connective tissue*. Am J Pathol, 1989. **134**(5): p. 1019-25.
344. Ritz-Timme, S., I. Laumeier, and M.J. Collins, *Aspartic acid racemization: evidence for marked longevity of elastin in human skin*. Br J Dermatol, 2003. **149**(5): p. 951-9.
345. Dion, N., et al., *Characterisation of neprilysin (EC 3.4.24.11) S2' subsite*. FEBS Lett, 1997. **411**(1): p. 140-4.
346. Kim, Y.A., et al., *Analysis of the importance of arginine 102 in neutral endopeptidase (enkephalinase) catalysis*. J Biol Chem, 1992. **267**(17): p. 12330-5.
347. Barroso, B., N. Abello, and R. Bischoff, *Study of human lung elastin degradation by different elastases using high-performance liquid chromatography/mass spectrometry*. Anal Biochem, 2006. **358**(2): p. 216-24.
348. Hayashi, A., H. Wachi, and S. Tajima, *Presence of elastin-related 45-kDa fragment in culture medium: specific cleavage product of tropoelastin in vascular smooth muscle cell culture*. Biochim Biophys Acta, 1995. **1244**(2-3): p. 325-30.
349. Romero, N., et al., *Role of plasma and serum proteases in the degradation of elastin*. Arch Biochem Biophys, 1986. **244**(1): p. 161-8.
350. Taddese, S., et al., *In vitro degradation of human tropoelastin by MMP-12 and the generation of matrikines from domain 24*. Matrix Biol, 2009. **28**.
351. Lombard, C., et al., *Human leukocyte elastase hydrolysis of peptides derived from human elastin exon 24*. Biochimie, 2006. **88**(12): p. 1915-21.
352. Boudier, C., et al., *The elastolytic activity of cathepsin G: an ex vivo study with dermal elastin*. Am J Respir Cell Mol Biol, 1991. **4**(6): p. 497-503.
353. Boudier, C., C. Holle, and J.G. Bieth, *Stimulation of the elastolytic activity of leukocyte elastase by leukocyte cathepsin G*. J Biol Chem, 1981. **256**(20): p. 10256-8.
354. Desfontaines, L., et al., *Susceptibility of baboon aorta elastin to proteolysis*. Biol Chem Hoppe Seyler, 1990. **371**(5): p. 441-6.
355. Berton, A., et al., *Analysis of the ex vivo specificity of human gelatinases A and B towards skin collagen and elastic fibers by computerized morphometry*. Matrix Biol, 2000. **19**(2): p. 139-48.
356. Skjøt-Arkil, H., et al., *Measurement of MMP-9 and -12 degraded elastin (ELM) provides unique information on lung tissue degradation*. BMC Pulmonary Medicine, 2012. **12**(1): p. 34.
357. Hornebeck, W., B. Robert, and L. Robert, *[Kinetic and thermodynamic study of the alkaline dispersion of elastin]*. C R Acad Sci Hebd Seances Acad Sci D, 1972. **275**(25): p. 2981-4.
358. Dyksterhuis, L.B., et al., *Domains 17-27 of tropoelastin contain key regions of contact for coacervation and contain an unusual turn-containing crosslinking domain*. Matrix Biol, 2007. **26**(2): p. 125-35.
359. Pillai, S., C. Oresajo, and J. Hayward, *Ultraviolet radiation and skin aging: roles of reactive oxygen species, inflammation and protease activation, and strategies for prevention of inflammation-induced matrix degradation - a review*. Int J Cosmet Sci, 2005. **27**(1): p. 17-34.

360. Rijken, F., R.C. Kiekens, and P.L. Bruijnzeel, *Skin-infiltrating neutrophils following exposure to solar-simulated radiation could play an important role in photoageing of human skin*. *Br J Dermatol*, 2005. **152**(2): p. 321-8.
361. Saarialho-Kere, U., et al., *Accumulation of matrilysin (MMP-7) and macrophage metalloelastase (MMP-12) in actinic damage*. *J Invest Dermatol*, 1999. **113**(4): p. 664-72.
362. Sherratt, M.J., *Tissue elasticity and the ageing elastic fibre*. *Age (Dordr)*, 2009. **31**(4): p. 305-25.
363. Barroso, B., N. Abello, and R. Bischoff, *Study of human lung elastin degradation by different elastases using high-performance liquid chromatography/mass spectrometry*. *Anal Biochem*, 2006. **358**.
364. Hof, P., et al., *The 1.8 Å crystal structure of human cathepsin G in complex with Suc-Val-Pro-PheP-(OPh)<sub>2</sub>: a Janus-faced proteinase with two opposite specificities*. *Embo j*, 1996. **15**(20): p. 5481-91.
365. Berton, A., et al., *Involvement of fibronectin type II repeats in the efficient inhibition of gelatinases A and B by long-chain unsaturated fatty acids*. *J Biol Chem*, 2001. **276**(23): p. 20458-65.
366. Shipley, J.M., et al., *The structural basis for the elastolytic activity of the 92-kDa and 72-kDa gelatinases. Role of the fibronectin type II-like repeats*. *J Biol Chem*, 1996. **271**(8): p. 4335-41.
367. Xi, L., et al., *A combined molecular modeling study on gelatinases and their potent inhibitors*. *Journal of Computational Chemistry*, 2010. **31**(1): p. 24-42.
368. Overall, C.M., *Matrix metalloproteinase substrate binding domains, modules and exosites. Overview and experimental strategies*. *Methods Mol Biol*, 2001. **151**: p. 79-120.
369. Rosenblum, G., et al., *Insights into the Structure and Domain Flexibility of Full-Length Pro-Matrix Metalloproteinase-9/Gelatinase B*. *Structure*, 2007. **15**(10): p. 1227-1236.
370. Du, X., et al., *Elastin degradation by cathepsin V requires two exosites*. *J Biol Chem*, 2013. **288**(48): p. 34871-81.
371. Filippov, S., et al., *Matrilysin-dependent elastolysis by human macrophages*. *J Exp Med*, 2003. **198**.
372. Zheng, Y., et al., *Expression of cathepsins in human skin photoaging*. *Skin Pharmacol Physiol*, 2011. **24**(1): p. 10-21.
373. Quan, T., et al., *Elevated matrix metalloproteinases and collagen fragmentation in photodamaged human skin: impact of altered extracellular matrix microenvironment on dermal fibroblast function*. *J Invest Dermatol*, 2013. **133**(5): p. 1362-6.
374. Vierkötter, A. and J. Krutmann, *Environmental influences on skin aging and ethnic-specific manifestations*. *Dermato-endocrinology*, 2012. **4**(3): p. 227-231.
375. Watson, R.E., et al., *Damage to skin extracellular matrix induced by UV exposure*. *Antioxid Redox Signal*, 2014. **21**(7): p. 1063-77.
376. Fisher, G.J., et al., *Molecular basis of sun-induced premature skin ageing and retinoid antagonism*. *Nature*, 1996. **379**(6563): p. 335-9.
377. Pasquali-Ronchetti, I. and M. Baccarani-Contri, *Elastic fiber during development and aging*. *Microsc Res Tech*, 1997. **38**(4): p. 428-35.
378. Rijken, F. and C.A. Bruijnzeel-Koomen, *Photoaged skin: the role of neutrophils, preventive measures, and potential pharmacological targets*. *Clin Pharmacol Ther*, 2011. **89**(1): p. 120-4.
379. Hibbert, S.A., et al., *A potential role for endogenous proteins as sacrificial sunscreens and antioxidants in human tissues*. *Redox Biol*, 2015. **5**: p. 101-13.

380. Bilac, C., M.T. Sahin, and S. Ozturkcan, *Chronic actinic damage of facial skin*. Clin Dermatol, 2014. **32**(6): p. 752-62.
381. Schmelzer, C.E., et al., *Prolyl hydroxylation in elastin is not random*. Biochim Biophys Acta, 2016. **1860**(10): p. 2169-77.
382. Fisher, G.J. and J.J. Voorhees, *Molecular mechanisms of photoaging and its prevention by retinoic acid: ultraviolet irradiation induces MAP kinase signal transduction cascades that induce Ap-1-regulated matrix metalloproteinases that degrade human skin in vivo*. J Investig Dermatol Symp Proc, 1998. **3**(1): p. 61-8.

# Curriculum vitae

## Personal information

Name **Angela Cristina Mora Huertas**  
Born/date Guateque (Boyacá) / 04.03.1980  
Country Colombia

## Education background

2006 – 2008 **MSc on Pharmaceutical Sciences.** Universidad Nacional de Colombia. Bogotá. Colombia  
1997 – 2003 **Pharmaceutical Chemist.** Universidad Nacional de Colombia. Bogotá. Colombia  
1991 – 1996 **High school education.** Colegio Nacionalizado Valle de Tenza. Guateque. Colombia.

## Professional experience

February 2010 – Current **Auxiliary Lecturer and Researcher.** *Universidad Nacional de Colombia. Department of Pharmacy. Faculty of Sciences, Colombia*  
September 2007 – July 2009 **Junior Account Manager.** *Ciba S.A., Colombia*  
February 2006 – August 2007 **Assistant Research.** *Universidad Nacional de Colombia. Department of Pharmacy. Faculty of Sciences, Colombia*  
June 2005 - January 2006 **Quality Control and Chemical Analyst.** *Fresenius Medical Care, Colombia*  
July 2004 - May 2005 **Instrumental Lab Chemistry Analyst.** *Laboratory Genfar SA., Colombia*  
November 2002 - May 2004 **R&D Pharmaceutical Chemist.** *Laboratory JGB S.A., Colombia*

# List of publications

- **Mora Huertas, A.C.**, Schmelzer, C.E., Hoehenwarter, W., Heyroth, F., Heinz, A. Molecular-level insights into aging processes of skin elastin. *Biochimie* 128-129 (2016): 163-173.
- Heinz, A., **Mora Huertas, A. C.**, Schröder C.U., Pankau, R., Gosch, A., Schmelzer, C.E.H. Elastins from patients of the Williams-Beuren syndrome and healthy individuals differ on the molecular level. *American Journal of Medical Genetics Part A* 170 (2016): 1832-1842.
- **Mora, A.C.**; Aragón, D.M.; Ospina, L.F. Effects of *Physalis peruviana* fruit extract on stress oxidative parameters in streptozotocin-diabetic rats. *Lat. Am. J. Pharm.* 29(7) (2010): 1132-6.
- **Mora H., A.C.**; Aragón N., D.M.; Ospina G., L.F. Characterization of oxidative stress on Wistar diabetics rats. *Vitae* 16(3) (2009):311-319.
- Colombian Handbook of Medicinal plants. Ministerio de la Protección Social. República de Colombia. Made by the Department of Pharmacy. Faculty of Science. Universidad Nacional de Colombia. Principal Researcher: Roberto Pinzón. Assistant Researchers: Diana Liévano, **Angela Mora**, Diana Rueda, Angélica Sandoval. ISBN 978958701997-1 (2008)
- **Mora-Huertas A.C.**, Schmelzer C.E., Hoehenwater, W., Heinz, A. Degradation of elastin by Neprelysin. *Manuscript in preparation.*

## Poster presentations

- A. Heinz, **A.C. Mora Huertas**, W. Hoehenwarter, C.E.H. Schmelzer: Investigating the effects of intrinsic and extrinsic aging on human skin elastin, *Annual Meeting of the German Society for Matrix Biology*, Freiburg, Germany, March 03 – 05, 2016.
- **A.C. Mora Huertas**, C.E.H. Schmelzer, C.U. Schröder, A. Heinz: Insights into the age-related changes in elastic fibers from skin, *5th Symposium on Structural Proteomics*, Halle, Germany, November 19/20, 2015.

- **A. C. Mora Huertas**, C.E.H. Schmelzer, C.U. Schröder, R.H.H. Neubert, A. Heinz: Seeking marker peptides for tracking age-related changes in elastic tissues, *48th annual conference of the German Society for Mass Spectrometry*, Wuppertal, Germany, March 01 - 04, 2015.

# Declaration

I hereby declare that I have composed the present dissertation independently and without unauthorised third-party help. No other people directly or indirectly were involved in the intellectual production, selection and evaluation of the material here enclosed. All the texts and illustrations used in this work, which were taken literally or meaningfully from published or unpublished text belonging to other authors, are without exception marked as such in both the text and the references. All people who were significant facilitators of the work were duly acknowledged. Furthermore, I hereby certify that the present doctoral thesis has not been submitted to other Universities or Higher Learning Institutions in the same or similar version as a thesis or examination procedure. I have not done any previous unsuccessful promotions. The work submitted in written form corresponds to that on the electronic storage medium.

---

Angela Cristina Mora Huertas

Halle (Saale), 14.06.2017